Viral lysis of marine microbes in relation to vertical stratification

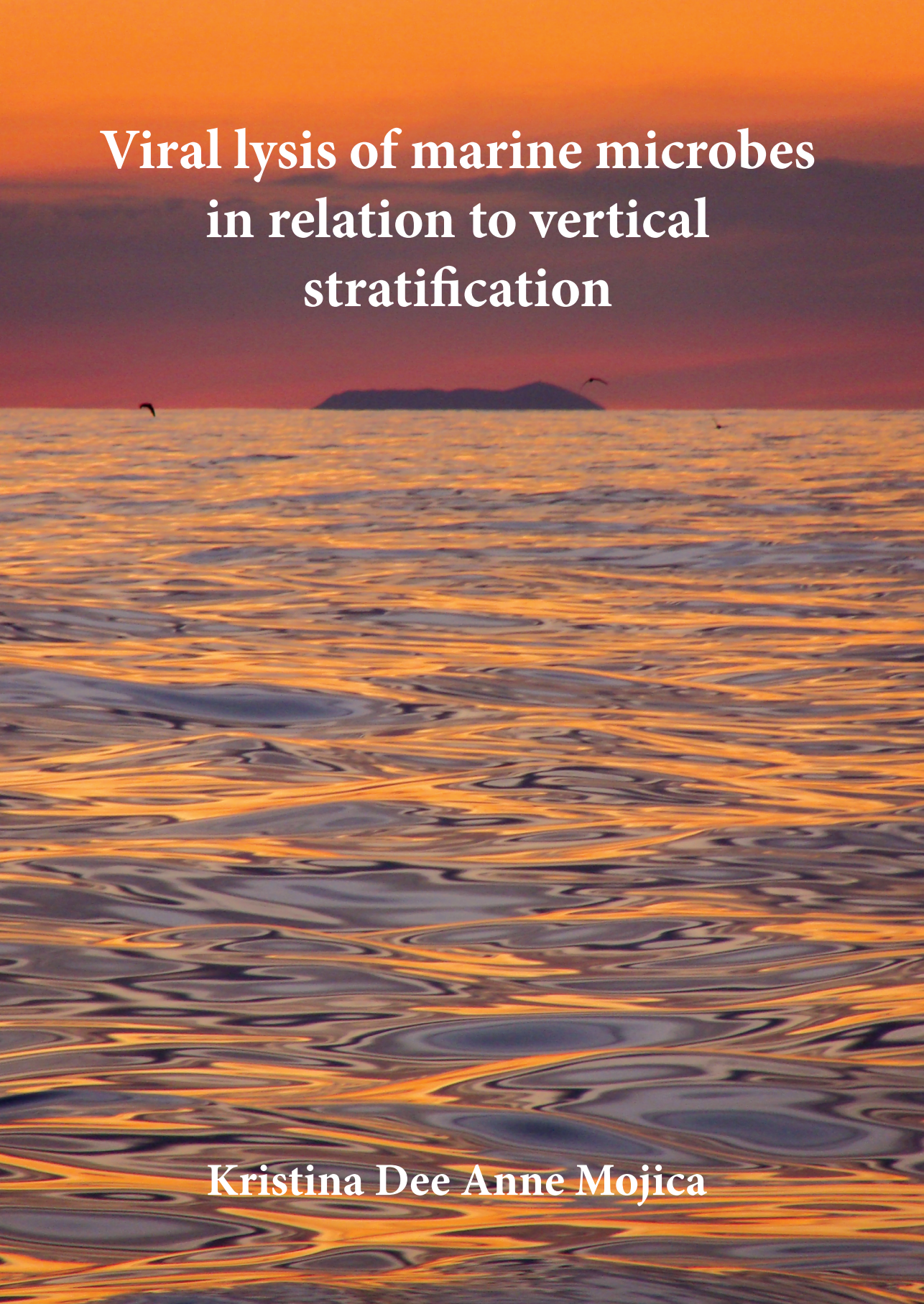

Kristina Dee Anne Mojica

VIRAL LYSIS OF MARINE MICROBES IN RELATION TO VERTICAL STRATIFICATION

Kristina Dee Anne Mojica

Promotor:	Prof. dr. C. P. D. Brussaard	NIOZ, Texel & IBED/UvA, Amsterdam
Overige leden:	Prof. dr. J. Huisman	IBED/UvA, Amsterdam
	Prof. dr. ir. H. A. Dijkstra	IMAU, Utrecht
	Prof. dr. L. J. Stal	NIOZ, Yerseke & IBED/UvA, Amsterdam
	Prof. dr. P. H. van Tienderen	IBED/UvA, Amsterdam
	Prof. dr. S. W. Wilhelm	University of Tennessee, Knoxville, USA

Faculteit: Faculteit der Natuurwetenschappen, Wiskunde en Informatica

VIRAL LYSIS OF MARINE MICROBES IN RELATION TO VERTICAL STRATIFICATION

ACADEMISCH PROEFSCHRIFT

ter verkrijging van de graad van doctor
aan de University of Amsterdam
op gezag van de Rector Magnificus
prof. dr. D.C. van den Boom
ten overstaan van een door het college voor promoties ingestelde
commissie, in het openbaar te verdedigen in de Aula der Universiteit
op woensdag dag 16 September 2015, te 11 uur

door

Kristina Dee Anne Mojica
geboren te Texas, Verenigde Staten van Amerika

Viral lysis of marine microbes in relation to vertical stratification

PhD thesis, University of Amsterdam, IBED, The Netherlands

The research described in this thesis was supported by the Earth and Life Sciences Foundation (ALW), which is subsidized by the Netherlands Organization for Scientific Research (NWO). Research was conducted at the Royal Netherlands Institute for Sea Research (NIOZ, Texel)

Publication of this thesis was financially supported by the Royal Netherlands Institute for Sea Research (NIOZ, Texel)

Author: Kristina D. A. Mojica

ISBN: 978-94-91407-20-8

Cover photo:	Kristina D. A. Mojica
Cover and Lay-out:	Ferdinand van Nispen, Citroenvlinder-dtp.nl, Bilthoven, the Netherlands
Printed by:	GVO drukkers & vormgevers, Ede, the Netherlands

Contents

Dedicated to my parents, Kurt and Janey Dustin

Chapter 1

General Introduction

Viruses are the most abundant biological entities in the oceans and are important mortality agents of heterotrophic and autotrophic microbial populations. These microbial hosts are numerically dominant and constitute the largest percentage (>90%) of living biomass in the ocean. Collectively microorganisms manage the pools and fluxes of energy and nutrients in the ocean. Loss factors play an essential role in controlling the activity and production of marine microbial communities and thus ocean ecosystem net productivity. Different mortality pathways influence the cycling of energy and biogeochemical elements very differently. Yet, little is known about how physicochemical factors regulate the partitioning of mortality amongst viral lysis and grazing, limiting our ability to predict how the ocean will respond to global climate change. This chapter provides a brief introduction to the different ecological and biogeochemical roles that autotrophic microorganisms, heterotrophic prokaryotes and viruses play in the marine environment, with special focus on the cycling of carbon. In addition, it provides a short overview of how global warming is expected to alter ocean stratification and what we currently know about how this will affect the structure and functioning of microbial populations. This all sets the stage for the overall aim of this thesis which is to mechanistically understand the ecological relevance of stratification in structuring microbial populations, with particular focus on losses due to viral lysis and grazing.

1.1. Phytoplankton

Marine photoautotrophic microorganisms are predominately eukaryotic and prokaryotic phytoplankton. As primary producers, phytoplankton synthesize organic compounds from aqueous carbon dioxide (CO_2) through the process of photosynthesis. Consequently, factors which regulate light and inorganic nutrient availability (e.g., nitrogen, phosphorus and iron) strongly influence the nature and activity of phytoplankton communities. Marine phytoplankton take up large amounts carbon dioxide annually (~50 Pg C y^{-1}; Falkowski 2002) and contribute almost half of the global net primary production occurring on the planet (Field et al. 1998). Approximately 5-10 Pg C y^{-1} of this photosynthetically fixed carbon is exported from the surface into the deep ocean, via the biological pump, reducing the surface partial pressure of CO_2 which governs air-sea CO_2 exchange and therefore plays an essential role in the long term regulation of atmospheric CO_2 and climate (Ducklow et al. 2001; Jiao et al. 2010; Henson et al. 2011). As the base of most marine food chains, phytoplankton provide a significant fraction of the total organic matter (OM) available to higher trophic levels. Phytoplankton production

thus sets upper limits to both the overall activity of the pelagic food web and the quantity of organic carbon exported downwards. Accordingly, the quantification of rates, patterns and mechanisms that control uptake of CO_2 by phytoplankton and the fate of the resultant organic carbon is an important central theme in ecological and biogeochemical research.

Cell size affects many of the processes determining the growth of phytoplankton, including metabolic rates (e.g. internal metabolic transport), nutrient diffusion, uptake and requirements, excretion and light absorption (Malinsky-Rushansky and Legrand 1996; Bricaud et al. 2004; Mei et al. 2009; Finkel et al. 2010). Due to these physiological restrains of size, small cells with larger surface to volume ratios have a competitive advantage in stable and oligotrophic (nutrient poor) waters (Agawin et al. 2000). Due the ecological relevance of size, phytoplankton are often separated based on cell size into micro- (200-20 μm), nano- (20-2 μm) and pico-phytoplankton (<2 μm). In general, the largest size classes are dominated by diatoms and dinoflagellates while the smallest size classes consist of cyanobacteria, prasinophytes and prymnesiophytes (Gibb et al. 2000; Cuvelier et al. 2010; Not et al. 2012).

Cell size also governs grazing and sinking rates, as well as the likelihood of viral infection (Murray and Jackson 1992; Kiorboe 1993; Chen and Liu 2010). Consequently, phytoplankton size largely determines trophic organization and the efficiency with which photosynthetic OM is transferred to higher trophic levels or exported to the deep ocean (Legendre and Rivkin 2002; Falkowski and Oliver 2007; Finkel et al. 2010). Biomass and production dominated by small phytoplankton is associated with high numerical abundance, slow sedimentation rates, and rapid cycling of OM through the microbial food web (e.g. dominated by bacteria and smaller zooplankton such as cililates and flagellates), which results in low potential carbon export to the deep sea (Azam et al. 1983; Legendre and Rassoulzadegan 1996; Finkel et al. 2010). In contrast, larger phytoplankton allow for a more efficient transfer of OM through short food chains (dominated by copepods and larger zooplankton), higher sedimentation rates and therefore enhanced downward export and biological CO_2 drawdown. How environmental conditions and size affect the relative contribution of grazing and viral lysis to phytoplankton mortality remains largely unknown due to the scarcity of reports for viral induced mortality of marine phytoplankton populations, as well as direct comparisons between these different mortality pathways across broad ocean regions. As grazing and loss due to viral infection (section 1.3) affect the fate of photosynthetically fixed carbon

very differently, understanding the underlying factors regulating the division of morality amongst these pathways is equally important for understanding ocean ecosystem productivity and biogeochemical cycles.

1.2 Heterotrophic prokaryotes

The term 'heterotroph' is generally applied to refer to chemoorganoheterotrophs. Heterotrophic prokaryotes are comprised of members from two domains of life - Archaea and Bacteria. Traditionally, Archaea were thought to only contribute a significant fraction of the prokaryotic community within extreme environments, however, it is now known that they can comprise greater than 30% of total microbial abundance in surface waters of the ocean (Delong 1992; Pernthaler et al. 2002; Pernthaler and Amann 2005). Thus, throughout the remainder of this thesis, 'bacteria' or 'prokaryotes' will be used synonymously, referring to Bacteria and Archaea. Heterotrophic prokaryotes have the ability to utilize organic compounds as a source of both energy and carbon, which can be incorporated directly as low molecular weight (LMW; <600 Da) or indirectly through the use of extracellular enzymes which cleave high molecular weight (HMW) molecules to LMW molecules (Gasol et al. 2008). Heterotrophic prokaryotes thus play an essential role in marine environments by remineralizing organic matter and thereby maintain the bioavailability of potential growth limiting nutrients (e.g. nitrogen, phosphorus, and carbon), as well as provide transfer mechanism of this material to higher trophic levels (i.e., microbial loop, Azam et al. 1983; Figure 1). In addition, through the mineralization of dead particulate matter (POM) and DOM, and the dissolution of sinking POM, heterotrophic prokaryotes affect the magnitude of the vertical organic fluxes and thus represent an integral part of the oceanic biological pump (Nagata et al. 2000; Ducklow et al. 2001; Jiao et al. 2010).

The relevance of heterotrophic bacteria to biogeochemical cycling of organic matter are largely determined by fluxes of bacterial production (BP) and respiration (BR) (Ducklow et al. 2010). These two fluxes are related to bacterial growth efficiency (BGE), the fraction of the total organic carbon assimilated to build up biomass. Substrate supply and complexity and inorganic nutrient availability appear to be most important factors regulating BGE in aquatic systems (del Giorgio and Cole 1998; Reche et al. 1998; Cuevas et al. 2011). However, there still remains a large amount of uncertainty in regards to what controls the magnitude and variation in BGE of ocean systems.

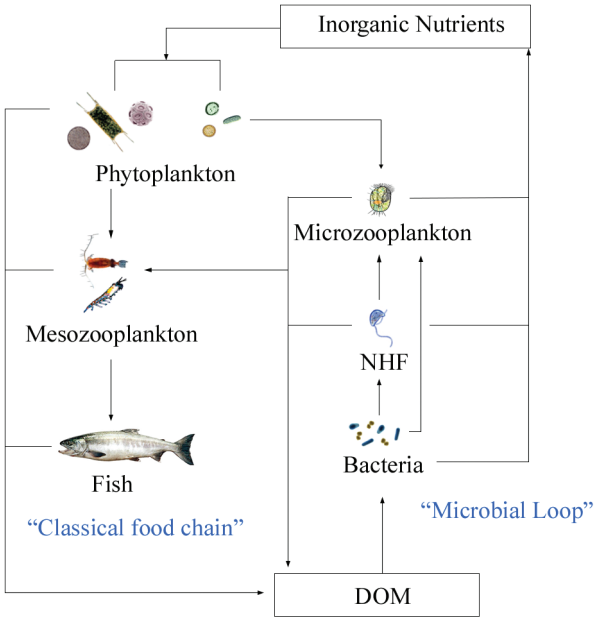

Figure 1. Simplified diagram of the flow of nutrients and organic matter through the traditional grazing food chain and microbial loop. DOM stands for dissolved organic matter, and comes from excretion, death, sloppy feeding and fecal pellets.

Grazing by phagotrophic protists, particularly bacterivorous nanoflagellates, and viral lysis are the main loss factors regulating bacterial populations in aquatic environments (Hahn and Hofle 2001; Pernthaler 2005). However, grazing and viral lysis have differential effects on prokaryotic communities. Protists prey on a wide range of prokaryotic species in a size-selective manner (Pernthaler 2005; Glucksman et al. 2010), while viruses typically have a narrow host range (see section 1.3) and thus regulate prokaryotic species (or even strain) diversity (Thingstad 2000; Weinbauer 2004). Studies comparing microzooplankton grazing and viral lysis reveal both contribute similarly to bacterial mortality, but their relative importance can vary with season or environmental conditions (Fuhrman and Noble 1995; Weinbauer and Peduzzi 1995; Pernthaler 2005; Tsai et al. 2012). The underlying factors regulating the interplay between viruses and protist in the control of marine prokaryotes are still poorly understood, especially with respect to the role of physical processes such as water column stratification.

1.3 Marine viruses

Viruses are the most abundant biological entities in the oceans (Bergh et al. 1989; Fuhrman and Suttle 1993; Suttle 2007). Currently, it is estimated that viruses range from ~3 x10^6 viruses ml^{-1} in the deep sea to ~10^8 ml^{-1} in productive coastal waters (Suttle 2005). Viruses are biological particles comprised of ribonucleic acid (RNA) or deoxyribonucleic acid (DNA) genome protected by a protein coat (i.e., capsid) (Hurst 2000). They are considered as obligate parasites due to their reliance upon a host to provide the energy and metabolic machinery necessary for replication. Viruses typically have a narrow host specificity, with the majority of viruses infecting only one host species. However, within a host species strain-specificity can vary widely (Brussaard 2004; Holmfeldt et al. 2007).

Due to their small size (~100 nm; 10-200 fg; Breitbart 2012), transport is governed by the random wandering of Brownian motion and therefore they obey the laws of diffusion in their approach to larger particles such as hosts (Murray and Jackson 1992). Contact rates are directly dependent on viruses and host abundance; but also can be effected by host size, motion and morphology (Murray and Jackson 1992). Once contact between a viable host and infective virus is accomplished, viral replication can proceed through different life strategies; lytic, lysogenic, chronic and pseudolysogeny. In the lytic cycle, viral replication proceeds immediately after infection and terminates with the lysis of the host and release of viral progeny and host cell content into the surrounding water (Figure 2A). During lysogenic infection, the genetic material of temperate phages (prophage) is stably incorporated into the host genome, and the host continues to live and reproduce normally, transmitting the prophage vertically to daughter cells during each subsequent cell division, until an event triggers the virus to enter the lytic pathway (Figure 2B). Lysogeny appears to be mostly restricted to prokaryotic hosts (Van Etten et al. 2002; Paul 2008), where it is theorized to represent a survival strategy under conditions of low host productivity and abundance (Williamson et al. 2002; Weinbauer et al. 2003; Payet and Suttle 2013). However, the importance of the different life strategies and mechanisms regulating selection over large ocean scales remain largely unknown. While lytic and lysogenic life styles have received the most attention, viral replication has also been shown to occur through chronic infection where viruses are released through budding or extrusion without killing their host (Mackinder et al. 2009; Thomas et al. 2011) or through pseudolysogeny which differs from true lysogeny in that the viral genome does not integrate into the host genome (Williamson et al. 2001).

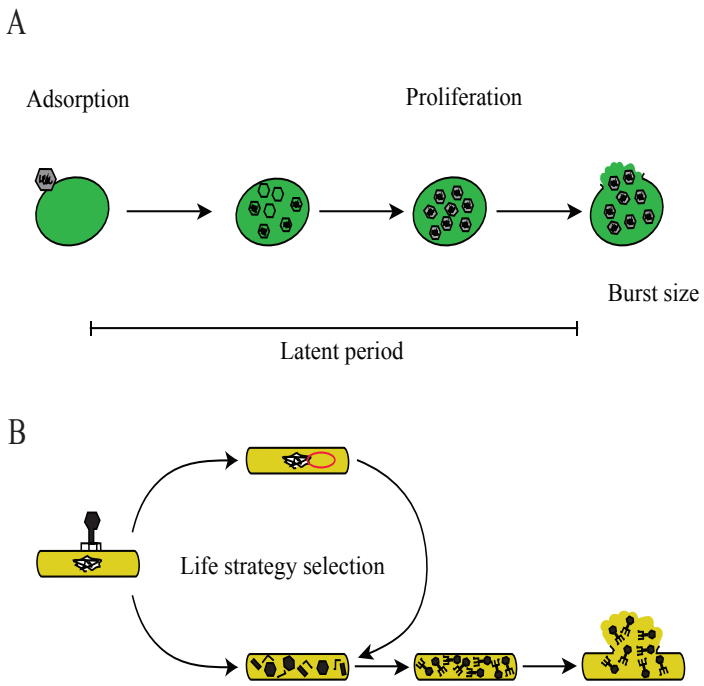

Figure 2. Simplified schematic of how viral replications occurs through the (A) lytic viral replication in autotrophic eukaryotes and (B) through both lytic and lysogenic infection in prokaryotic hosts.

The lysis of microbes diverts energy and biomass away from the classical food web towards microbial-mediated recycling and the dissolved organic matter pool. In this manner, the 'viral shunt' reduces the transfer of carbon and nutrients to higher trophic levels, while enhancing the recycling of potential growth-limiting nutrients (Fuhrman 1999; Wilhelm and Suttle 1999) (Figure 3). Theoretical models have been used to estimated that between 6 and 26% of the photosynthetically fixed carbon (PFC) is shunted to the DOM pool by the activity of viruses (Wilhelm and Suttle 1999). However, our ability to confirm estimates and thus understand the true magnitude of viruses in the marine biogeochemical cycles has been restricted by a lack of quantitative estimates of viral lysis in marine phytoplankton populations (Weitz and Wilhelm 2012), as well as by information regarding how viral lysis rates compare to grazing. In addition, little is known about the existence of large-scale patterns in virus-phytoplankton biogeography (Breitbart 2012) and the factors regulating viral activity and distribution of phytoplankton viruses on global ocean scales.

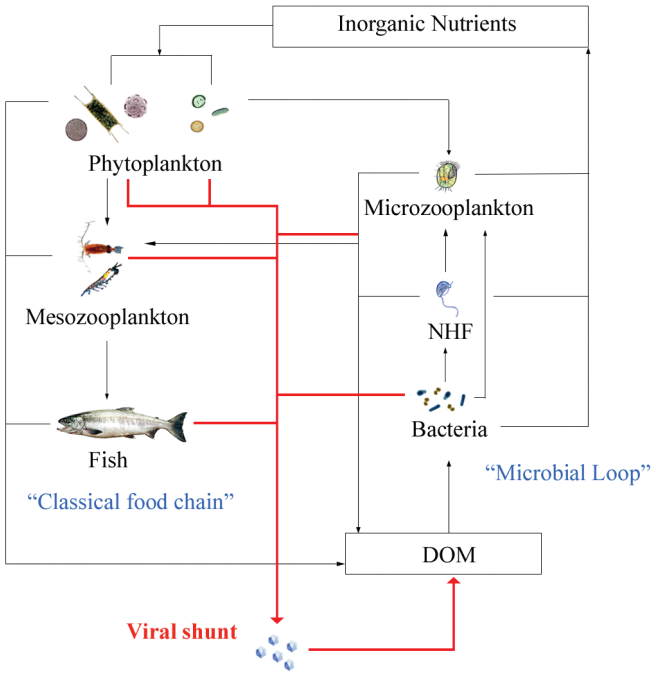

Figure 3. Simplified diagram illustrating the role of viruses in the marine food web. The 'viral shunt' (highlighted by red arrows) moves organic matter and energy away from the higher trophic levels towards the DOM (and after bacterial remineralization to the inorganic nutrient pool). Thus viral lysis is separated from the traditional flow of DOM (largely excretion).

1.4. Global warming and vertical stratification

Global climate has been changing over the last few decades due to anthropogenic-induced increases in atmospheric concentrations of key greenhouse gases such as CO_2 and CH_4 (Meehl et al. 2007). The oceans play an essential role in regulating global climate through the storage and transportation of heat (Levitus et al. 2000; Barnett et al. 2005; Hallegraeff 2010; Hoegh-Guldberg and Bruno 2010) and uptake and sequestration of CO_2 (Hallegraeff 2010), providing an important buffer against climate change. More than 90% of the increase in the global heat content which has occurred over the last 60 years has gone into warming the oceans (Barnett et al. 2005; Hallegraeff 2010; Hoegh-Guldberg and Bruno 2010). As global warming continues, the surface waters of the ocean are envisaged to further rise by 2-6°C over the next 100 years (Timmermann et al. 1999; Meehl et al. 2007). Ocean-climate models predict that this surface warming, in combination with changes in

fresh water input at high latitudes due to rises in precipitation and sea ice melt, will lead to increases vertical stratification processes (Sarmiento et al. 1998; Levitus et al. 2000; Sarmiento 2004; Toggweiler and Russell 2008). The oceans also provide one of the largest natural reservoirs of carbon and the flux and storage of CO_2 into the world's oceans is largely influenced by marine microorganisms living in the upper surface waters. Understanding the ecological and physiological mechanisms controlling changes in microbial community structure across gradients of vertical stability is therefore vital to predicting the response of ocean systems to global climate change. The North Atlantic Ocean provides a meridional gradient in vertical density stratification (Talley et al. 2011) and is an important sink for anthropogenic CO_2 (storing 23% of the global oceanic anthropogenic CO_2) (Sabine et al. 2004) and therefore provides a ideal model area to study the effects of vertical stratification on microbial community dynamics.

Stratification suppresses turbulence and reduces mixing depth, thereby exerting a fundamental control on phytoplankton resource availability, i.e., relaxing of potential light limitation and restricting the nutrient flux from depth (Huisman et al. 1999; Mahadevan et al. 2012). In temperate and high latitude regions, the annual establishment of seasonal stratification often triggers the highly productive phytoplankton spring bloom (Sverdrup 1953; Huisman et al. 1999). However, strong and prolonged stratification can lead to reductions in phytoplankton biomass and productivity in the surface layers as nutrients become depleted due to utilization, a process referred to as ocean oligotrophication. Changes in global climate and resulting alterations in stratification are believed to have led to the 15% increase in the size of the nutrient-poor oligotrophic regions of the Pacific and Atlantic Oceans which has occurred between 1998-2006 (Polovina et al. 2008). In addition, changes in vertical stratification have been linked to alterations in phytoplankton phenology, size, nutritional value, abundance, spatial distribution and community structure (Richardson and Schoeman 2004; Mitra and Flynn 2005; Behrenfeld et al. 2006; Finkel et al. 2010; Hilligsøe et al. 2011; Doney et al. 2012). Consequently, resulting changes in phytoplankton community composition are expected to affect the structure and functioning of marine food webs, as well as the potential for the ocean to act as a long term sink for carbon dioxide (Beaugrand 2009; Hoegh-Guldberg and Bruno 2010). Similarly, the physiological processes of heterotrophic prokaryotes are directly affected by temperature and by expected changes in the quality of DOM due to nutrient limitation (Ducklow et al. 2010; Sarmento et al. 2010).

While it is becoming clear that global warming is directly affecting the production of primary and heterotrophic prokaryotic components of marine microbial food webs, these alterations are also expected to affect mortality processes (i.e., grazing rates, viral lysis rates, and sinking of phytoplankton). However, the effect of global warming on the mortality of microbes remains poorly understood. Alterations in prey populations will affect zooplankton grazing, whereby current evidence suggests that the absolute and relative importance of microzooplankton activities in plankton communities will increase in the future ocean due to increased dominance of small-sized algal prey (Sarmento et al. 2010; Caron and Hutchins 2012). However, few studies have directly compared microzooplankton grazing to viral induced mortality in marine phytoplankton communities. The potential for stratification to regulate viral induced mortality of phytoplankton remains virtually unknown. As viruses rely upon their host to provide the machinery, energy and resources required for viral replication and assembly, factors regulating the physiology, production and removal of hosts are also important in governing viral dynamics (Moebus 1996; Wilson et al. 1996; Baudoux and Brussaard 2008; Maat et al. 2014). Therefore, future changes in stratification have the potential to affect the composition and distribution of viral assemblages associated with microbial communities. There is evidence that changes in inorganic nutrient availability can affect life strategy choice and production of viruses infecting prokaryotes (Wilhelm et al. 2002; Williamson et al. 2002; Bongiorni et al. 2005), however the effect of changes in the strength of vertical stratification is still largely unstudied.

Outline of thesis

The overall aim of this thesis is to investigate how changes in vertical stratification affect autotrophic and heterotrophic microbial communities along a meridional gradient in the Atlantic Ocean. The Northeast Atlantic Ocean is a key area in global ocean circulation and a important sink for atmospheric CO_2. In addition, stratification varies in the North Atlantic from strong permanent stratification in the (sub)tropics to weak seasonal stratification in the North and thus provides an ideal model system to investigate the role of vertical stratification in structuring microbial communities. In order to mechanistically understand the ecological relevance of stratification in structuring microbial populations this thesis specifically aims to (1) provide a comprehensive overview of what is currently

known regarding how environmental factors can regulated virus-host interactions in the marine environment, (2) determine the physicochemical mechanisms structuring phytoplankton communities over a large scale gradient in stratification, (3) determine the relative contribution of viral lysis and grazing to the mortality of phytoplankton and heterotrophic prokaryotes along a north-south gradient regulated by strong stratification and (4) place these finding in the context of implications for the flow of carbon through the marine food web in the present and future North Atlantic Ocean.

Chapter 2 summarizes what is currently known about environmental factors that either directly (i.e., destruction or inactivation of free virus particles) or indirectly (i.e., affecting viral production via host) affect viruses-host interactions. At any spatio-temporal point in the ocean, viral abundance reflects the balance between rates of removal and production through host lysis. Once viral progeny are released from their hosts, they are present in the environment as free virus particles and are directly exposed to environmental factors which may reduce infectivity, degrade or remove virus particles, and adversely affect adsorption to host, thereby reducing the chance of a successful host encounter and infection. Moreover, as obligate parasites, viruses are reliant upon their host to provide not only the cellular machinery but also the necessary energy and resources required for viral replication and assembly. Consequently the factors regulating the physiology of the host, as well as its production and removal are also important in governing virus dynamics.

Chapter 3 presents data obtained from two research cruises conducted in the Northeast Atlantic across a N-S latitudinal gradient during two different seasons, i.e., spring during the onset of stratification and summer when stratification was maximum. The data provide a high-resolution mesoscale description of the phytoplankton community composition in relation to vertical mixing conditions and other key physiological parameters. Phytoplankton were assessed by a combination of flow cytometry and pigment fingerprinting (HPLC-CHEMTAX). Multivariate analysis identified water column stratification (based on depth-integrated Brunt-Väisälä frequency) as one of the key drivers for the distribution and separation of different phytoplankton taxa and size classes. The implications of the findings for the classification of phytoplankton functional types in biogeochemical and ecological ocean models are discussed.

Chapter 4 presents the biogeographical distribution of marine viruses and their contribution to phytoplankton group-specific mortality along a large-

scale gradient in the Northeast Atlantic Ocean (same gradient as in the summer Chapter 3). Virus composition changed with latitude, and was closely associated with the biogeographical distribution of different phytoplankton groups. Average virus-mediated lysis rates were higher for eukaryotic phytoplankton than for the prokaryotic cyanobacteria *Prochlorococcus* and *Synechococcus*. Phytoplankton viral lysis rates were of similar magnitude as microzooplankton grazing rates. Overall, the total phytoplankton mortality rate (viral lysis plus microzooplankton grazing) was comparable to phytoplankton gross growth rate, signifying high turnover rates of marine phytoplankton populations. Moreover, the data show a striking reduction in viral lysis rates of phytoplankton at higher latitudes in the North Atlantic. The importance of these results to future alterations in food web dynamics and biological carbon export in the Northeast Atlantic Ocean are further discussed.

Chapter 5 presents a simple and efficient method optimization for improving virus counts and optimal resolution of viruses populations when measured at low abundances. Flow cytometric enumeration has advanced our ability to analyze aquatic viruses samples and therefore our understanding of the ecological role that viruses play in the ocean (Brussaard et al. 2010). However, low virus abundances such as found in extreme oligotrophic waters, the deep ocean, or resulting from experimental design, require low dilutions in a buffer solution to obtain the optimal even rate (i.e., 200-800 events s^{-1}). This chapter shows that low dilution factors for viruses samples can lead to substantial underestimations in total virus abundances if not corrected by adjusting the buffering capacity of the diluent.

Chapter 6 presents virus induced mortality of prokaryotes relative to grazing and the proportion of lytic and lysogenic viral infection is assessed along a large-scale gradient in the surface waters of the Northeast Atlantic Ocean during summer (same gradient as in Chapter 4). The method applied in the study relies on the ability to quantify the reoccurrence of viruses after reducing *in situ* virus abundance to prevent new infection (Weinbauer et al. 2010). Consequently, to attain optimal virus counts using this approach, the method modification for FCM enumeration at low abundance was applied (Chapter 5). The results demonstrate that viruses were the dominant mortality factor regulating prokaryotic losses, with lytic infection being the favored life strategy in the upper surface layer.

Chapter 7 presents the flux of photosynthetic carbon (C) through the different components of the microbial food web in order to consider how latitudinal changes affected the overall role of the viral shunt. The simultaneous measurements of growth and loss rate rates for phytoplankton (Chapter 4) as well as heterotrophic

bacteria (Chapter 6) provides an ideal dataset to further substantiate the role of the viral shunt in marine systems. The results demonstrate a more prominent role of viral lysis than previously estimated for marine environments (i.e., 6-26%; Wilhelm and Suttle 1999). Our data show higher values for both phytoplankton and heterotrophic prokaryotes, with the strongest increase in flux of PFC from phytoplankton. Moreover, on average the flux of photosynthetically fixed carbon through the viral shunt was 2-fold higher in the southern oligotrophic region (80%) compared to the north (31%), as a consequence of relatively higher viral lysis of both phytoplankton and bacteria. These results have important implications for future shifts in the regional climate of the ocean surface layer of the North Atlantic. In **Chapter 8** the results presented in this thesis are discussed in the context of what is currently known and how these results can be used to increase our predictability of how the oceans will respond to climate change.

References

Agawin NSR, Duarte CM, Agusti S (2000) Nutrient and temperature control of the contribution of picoplankton to phytoplankton biomass and production. Limnology and Oceanography 45:1891-1891

Azam F, Fenchel T, Field JG, Gray JS, Meyerreil LA, Thingstad F (1983) The ecological role of water-column microbes in the sea. Marine Ecology Progress Series 10:257-263

Barnett TP, Pierce DW, AchutaRao KM, Gleckler PJ, Santer BD, Gregory JM, Washington WM (2005) Penetration of human-induced warming into the world's oceans. Science 309:284-287

Baudoux AC, Brussaard CPD (2008) Influence of irradiance on virus-algal host interactions. Journal of Phycology 44:902-908

Beaugrand G (2009) Decadal changes in climate and ecosystems in the North Atlantic Ocean and adjacent seas. Deep-Sea Research, Part II 56:656-673

Behrenfeld MJ, O 'Malley RT, Siegel DA, McClain CR, Sarmiento JL, Feldman GC, Milligan AJ, Falkowski PG, Letelier RM, Boss ES (2006) Climate-driven trends in contemporary ocean productivity. Nature 444:752-755

Bergh O, Borsheim KY, Bratbak G, Heldal M (1989) High abundance of viruses found in aquatic environments. Nature 340:467-468

Bongiorni L, Magagnini M, Armeni M, Noble R, Danovaro R (2005) Viral production, decay rates, and life strategies along a trophic gradient in the North Adriatic Sea. Applied and Environmental Microbiology 71:6644-6650

Breitbart M (2012) Marine viruses: truth or dare. Annual Review of Marine Science 4:425-448

Bricaud A, Claustre H, Ras J, Oubelkheir K (2004) Natural variability of phytoplankton adsorption in oceanic waters: influence of the size structure of algal populations. Journal of Geophysical Research 109:C11010. doi: 10.1029/2004JC002419

Brussaard CPD (2004) Viral control of phytoplankton populations - a review. Journal Eukaryotic Microbiology 51:125-138

Brussaard CPD, Payet JP, Winter C, Weinbauer M (2010) Quantification of aquatic viruses by flow cytometry. In: Wilhelm SW, Weinbauer MG, Suttle CA (eds) Manual of Aquatic Viral Ecology. ASLO

Caron DA, Hutchins DA (2012) The effects of changing climate on microzooplankton grazing and community structure: drivers, predictions and knowledge gaps. Journal of Plankton Research 32: 235-252

Chen BZ, Liu HB (2010) Relationships between phytoplankton growth and cell size in surface oceans: interactive effects of temperature, nutrients, and grazing. Limnology and Oceanography 55:965-972

Cuevas LA, Egge JK, Thingstad TF, Topper B (2011) Organic carbon and mineral nutrient limitation of oxygen consumption, bacterial growth and efficiency in the Norwegian Sea. Polar Biology 34:871-882

Cuvelier ML, Allen AE, Monier A, McCrow JP, Messie M, Tringe SG, Woyke T, Welsh RM, Ishoey T, Lee JH, Binder BJ, DuPont CL, Latasa M, Guigand C, Buck KR, Hilton J, Thiagarajan M, Caler E, Read B, Lasken RS, Chavez FP, Worden AZ (2010) Targeted metagenomics and ecology of globally important uncultured eukaryotic phytoplankton. Proceedings of the National Academy of Sciences of the United States of America 107:14679-14684

del Giorgio PA, Cole JJ (1998) Bacterial growth efficiency in natural aquatic systems. Annual Review of Ecology and Systematics 29:503-541

Delong EF (1992) Archaea in coastal marine environments. Proceedings of the National Academy of Sciences of the United States of America 89:5685-5689

Doney SC, Ruckelshaus M, Duffy JE, Barry JP, Chan F, English CA, Galindo HM, Grebmeier JM, Hollowed AB, Knowlton N, Polovina J, Rabalais NN, Sydeman WJ (2012) Climate change impacts on marine ecosystems. Annual Review of Marine Science 4:11-37

Ducklow HW, Moran XAG, Murray AE (2010) Bacteria in the greenhouse: marine microbes and climate change. In: Mitchell R, Gu J (eds) Environmental Microbiology. Wiley-Blackwell

Ducklow HW, Steinberg DK, Buesseler KO (2001) Upper ocean carbon export and the biological pump. Oceanography 14:50-58

Falkowski PG (2002) The ocean's invisible forest - Marine phytoplankton play a critical role in regulating the earth's climate. Could they also be used to combat global warming? Scientific American 287:54-61

Falkowski PG, Oliver MJ (2007) Mix and match: how climate selects phytoplankton. Nature Reviews Microbiolology 5:813-819

Field CB, Behrenfeld MJ, Randerson JT, Falkowski P (1998) Primary production of the biosphere: integrating terrestrial and oceanic components. Science 281:237-240

Finkel ZV, Beardall J, Flynn KJ, Quigg A, Rees TAV, Raven JA (2010) Phytoplankton in a changing world: cell size and elemental stoichiometry. Journal of Plankton Research 32:119-137

Fuhrman JA (1999) Marine viruses and their biogeochemical and ecological effects. Nature 399:541-548

Fuhrman JA, Noble RT (1995) Viruses and protists cause similar bacterial mortality in coastal seawater. Limnology and Oceanography 40:1236-1242

Fuhrman JA, Suttle CA (1993) Viruses in marine planktonic systems. Oceanography 6:51-63

Gasol JM, Pinhassi J, Alonso-Saez L, Ducklow H, Herndl GJ, Koblizek M, Labrenz M, Luo Y, Moran XAG, Reinthaler T, Simon M (2008) Towards a better understanding of microbial carbon flux in the sea. Aquatic Microbial Ecology 53:21-38

Gibb SW, Barlow RG, Cummings DG, Rees NW, Trees CC, Holligan P, Suggett D (2000) Surface phytoplankton pigment distributions in the Atlantic Ocean: an assessment of basin scale variability between 50 degrees N and 50 degrees S. Progress in Oceanography 45:339-368

Glücksman E, Bell T, Griffiths RI, Bass D (2010) Closely related protist strains have different grazing impacts on natural bacterial communities. Environmental Microbiolology 12:3105-3113

Hahn MW, Hofle MG (2001) Grazing of protozoa and its effect on populations of aquatic bacteria. FEMS Microbiology Ecology 35:113-121

Hallegraeff GM (2010) Ocean climate change, phytoplankton community responses, and harmful algal blooms: a formidable predictive challenge. Journal of Phycology 46:220-235

Henson SA, Sanders R, Madsen E, Morris PJ, Le Moigne F, Quartly GD (2011) A reduced estimate of the strength of the ocean's biological carbon pump. Geophysical Research Letters 38: L04606. doi: 10.1029/2011GL046735

Hilligsøe KM, Richardson K, Bendtsen J, Sorensen LL, Nielsen TG, Lyngsgaard MM (2011) Linking phytoplankton community size composition with temperature, plankton food web structure and sea-air CO_2 flux. Deep-Sea Research, Part I 58:826-838

Hoegh-Guldberg O, Bruno JF (2010) The impact of climate change on the world's marine ecosystems. Science 328:1523-1528

Holmfeldt K, Middelboe M, Nybroe O, Riemann L (2007) Large variabilities in host strain susceptibility and phage host range govern interactions between lytic marine phages and their Flavobacterium hosts. Applied and Environmental Microbiology 73:6730-6739

Huisman J, van Oostveen P, Weissing FJ (1999) Critical depth and critical turbulence: two different mechanisms for the development of phytoplankton blooms. Limnology and Oceanography 44:1781-1787

Hurst CJ (ed) (2000) Viral Ecology. Academic Press, San Diego

Jiao N, Herndl GJ, Hansell DA, Benner R, Kattner G, Wilhelm SW, Kirchman DL, Weinbauer MG, Luo TW, Chen F, Azam F (2010) Microbial production of recalcitrant dissolved organic matter: long-term carbon storage in the global ocean. Nature Reviews Microbiology 8:593-599

Kiørboe T (1993) Turbulence, phytoplankton cell-size, and the structure of pelagic food webs. Advances in Marine Biology 29:1-72

Legendre L, Rassoulzadegan F (1996) Food-web mediated export of biogenic carbon in oceans: hydrodynamic control. Marine Ecology Progress Series 145:179-193

Legendre L, Rivkin RB (2002) Fluxes of carbon in the upper ocean: regulation by food-web control nodes. Marine Ecology Progress Series 242:95-109

Levitus S, Antonov JI, Boyer TP, Stephens C (2000) Warming of the world ocean. Science 287:2225-2229

Maat DS, Crawfurd KJ, Timmermans KR, Brussaard CPD (2014) Elevated partial CO_2 pressure and phosphate limitation favor *Micromonas pusilla* through stimulated growth and reduced viral impact. Applied and Environmental Microbiology 80:3119-3127

Mackinder LCM, Worthy CA, Biggi G, Hall M, Ryan KP, Varsani A, Harper GM, Wilson WH, Brownlee C, Schroeder DC (2009) A unicellular algal virus, *Emiliania huxleyi* virus 86, exploits an animal-like infection strategy. Journal of General Virology 90:2306-2316

Mahadevan A, D'Asaro E, Lee C, Perry MJ (2012) Eddy-driven stratification initiates North Atlantic spring phytoplankton blooms. Science 337:54-58

Malinsky-Rushansky NZ, Legrand C (1996) Excretion of dissolved organic carbon by phytoplankton of different sizes and subsequent bacterial uptake. Marine Ecology Progress Series 132:249-255

Meehl GA, Stocker TF, Collins WD, Friedlingstein P, Gaye AT, Gregory JM, Kitoh A, Knutti R, Murphy JM, Noda A, Raper SCB, Watterson IG, Weaver AJ, Zhao Z-C (2007) Global climate projections. In: Solomon S, Qin D, Manning M, Chen Z, Marquis M, Averyt KB, Tignor M, Miller HL (eds) Climate change 2007: The physical science basis Contribution of working group I to the fourth assessment report of the Intergovernmental Panel on Climate Change. Cambridge University Press, Cambridge, United Kingdom and New York, NY, USA

Mei ZP, Finkel ZV, Irwin AJ (2009) Light and nutrient availability affect the size-scaling of growth in phytoplankton. Journal of Theoretical Biology 259:582-588

Mitra A, Flynn KJ (2005) Predator-prey interactions: is 'ecological stoichiometry' sufficient when good food goes bad? Journal of Plankton Research 27:393-399

Moebus K (1996) Marine bacteriophage reproduction under nutrient-limited growth of host bacteria. I. Investigations with six phage-host systems. Marine Ecology Progress Series 144:1-12

Murray AG, Jackson GA (1992) Viral dynamics: a model of the effects of size, shape, motion and abundance of single-celled planktonic organisms and other particles. Marine Ecology Progress Series 89:103-116

Nagata T, Fukuda H, Fukuda R, Koike I (2000) Bacterioplankton distribution and production in deep Pacific waters: large-scale geographic variations and possible coupling with sinking particle fluxes. Limnology and Oceanography 45:426-435

Not F, Siano R, Kooistra WHCF, Simon N, Vaulot D, Probert I (2012) Diversity and ecology of eukaryotic marine phytoplankton. In: Gwenaël P (ed) Advances in Botanical Research, vol 64. Academic Press

Paul JH (2008) Prophages in marine bacteria: dangerous molecular time bombs or the key to survival in the seas? The ISME Journal 2:579-589

Payet JP, Suttle CA (2013) To kill or not to kill: the balance between lytic and lysogenic viral infection is driven by trophic status. Limnology and Oceanography 58:465-474

Pernthaler A, Preston CM, Pernthaler J, DeLong EF, Amann R (2002) Comparison of fluorescently labeled oligonucleotide and polynucleotide probes for the detection of pelagic marine bacteria and archaea. Applied and Environmental Microbiology 68:661-667

Pernthaler J (2005) Predation on prokaryotes in the water column and its ecological implications. Nature Reviews Microbiology 3:537-546

Pernthaler J, Amann R (2005) Fate of heterotrophic microbes in pelagic habitats: focus on populations. Microbiology and Molecular Biology Reviews 69:440-461

Polovina JJ, Howell EA, Abecassis M (2008) Ocean's least productive waters are expanding. Geophysical Research Letters 35:L03618. doi: 10.1029/2007GL031745

Reche I, Pace ML, Cole JJ (1998) Interactions of photobleaching and inorganic nutrients in determining bacterial growth on colored dissolved organic carbon. Microbial Ecology 36:270-280

Richardson AJ, Schoeman DS (2004) Climate impact on plankton ecosystems in the Northeast Atlantic. Science 305:1609-1612

Sabine CL, Feely RA, Gruber N, Key RM, Lee K, Bullister JL, Wanninkhof R, Wong CS, Wallace DWR, Tilbrook B, Millero FJ, Peng TH, Kozyr A, Ono T, Rios AF (2004) The oceanic sink for anthropogenic CO_2. Science 305:367-371

Sarmento H, Montoya JM, Vazquez-Dominguez E, Vaque D, Gasol JM (2010) Warming effects on marine microbial food web processes: how far can we go when it comes to predictions? Philosophical Transactions of the Royal Society B 365:2137-2149

Sarmiento JL (2004) Response of ocean ecosystems to climate warming. Global Biogeochemical Cycles 18:GB3003. doi: 10.1029/2003GB002134

Sarmiento JL, Hughes TMC, Stouffer RJ, Manabe S (1998) Simulated response of the ocean carbon cycle to anthropogenic climate warming. Nature 393:245-249

Suttle CA (2005) Viruses in the sea. Nature 437:356-361

Suttle CA (2007) Marine viruses - major players in the global ecosystem. Nature Reviews 5:801-812

Sverdrup EU (1953) On conditions for the vernal blooming of phytoplankton. Conseil Permanent International pour l'Exploration de la Mer 18:287-295

Talley L, Pickard G, Emery W, Swift J (2011) Typical distribution of water characteristics. Descriptive Physical Oceanography. Elsevier Ltd., London

Thingstad TF (2000) Elements of a theory for the mechanisms controlling abundance, diversity, and biogeochemical role of lytic bacterial viruses in aquatic systems. Limnology and Oceanography 45:1320-1328

Thomas R, Grimsley N, Escande ML, Subirana L, Derelle E, Moreau H (2011) Acquisition and maintenance of resistance to viruses in eukaryotic phytoplankton populations. Environmental Microbiology 13:1412-1420

Timmermann A, Oberhuber J, Bacher A, Esch M, Latif M, Roeckner E (1999) Increased El Niño frequency in a climate model forced by future greenhouse warming. Nature 398:694-697

Toggweiler JR, Russell J (2008) Ocean circulation in a warming climate. Nature 451:286-288

Tsai AY, Gong GC, Hung J (2012) Seasonal variations of viral- and nanoflagellate-mediated mortality of heterotrophic bacteria in the coastal ecosystem of subtropical Western Pacific Biogeosciences Discussions 9:17235-17261

Van Etten JL, Graves MV, Müller DG, Boland W, Delaroque N (2002) Phycodnaviridae - large DNA algal viruses. Archives of Virology 147:1479-1516

Weinbauer MG (2004) Ecology of prokaryotic viruses. FEMS Microbiology Reviews 28:127-181

Weinbauer MG, Brettar I, Hofle MG (2003) Lysogeny and virus-induced mortality of bacterioplankton in surface, deep, and anoxic marine waters. Limnology and Oceanography 48:1457-1465

Weinbauer MG, Peduzzi P (1995) Significance of viruses versus heterotrophic nanoflagellates for controlling bacterial abundance in the Northern Adriatic Sea. Journal of Plankton Research 17:1851-1856

Weinbauer MG, Rowe JM, Wilhelm SW (2010) Determining rates of virus production in aquatic systems by the virus reduction approach. In: Wilhelm SW, Weinbauer MG, Suttle CA (eds) Manual of Aquatic Viral Ecology. ASLO

Weitz JS, Wilhelm SW (2012) Ocean viruses and their effects on microbial communities and biogeochemical cycles. F1000 Biology Reports 4: 17

Wilhelm SW, Brigden SM, Suttle CA (2002) A Dilution technique for the direct measurement of viral production: a comparison in stratified and tidally mixed coastal waters. Microbial Ecology 43:168-173

Wilhelm SW, Suttle CA (1999) Viruses and nutrient cycles in the sea - Viruses play critical roles in the structure and function of aquatic food webs. Bioscience 49:781-788

Williamson SJ, Houchin LA, McDaniel L, Paul JH (2002) Seasonal variation in lysogeny as depicted by prophage induction in Tampa Bay, Florida. Applied and Environmental Microbiology 68:4307-4314

Williamson SJ, McLaughlin MR, Paul JH (2001) Interaction of the ΦHSIC virus with its host: lysogeny or pseudolysogeny? Applied and Environmental Microbiology 67:1682-1688

Wilson WH, Carr NG, Mann NH (1996) The effect of phosphate status on the kinetics of cyanophage infection in the oceanic cyanobacterium *Synechococcus* sp WH7803. Journal of Phycology 32:506-516

Chapter 2

Factors affecting virus dynamics and microbial host-virus interactions in marine environments

Kristina D. A. Mojica[1*], and Corina P. D. Brussaard[1,2]

[1]Department of Biological Oceanography, Royal Netherlands Institute for Sea Research (NIOZ), P.O. Box 59, 1790 AB Den Burg, Texel, The Netherlands
[2]Department of Aquatic Microbiology, Institute for Biodiversity and Ecosystem Dynamics (IBED), University of Amsterdam, P.O. Box 94248, 1090 GE Amsterdam, The Netherlands

FEMS Microbiology Ecology (2015) 89: 495-515.

Abstract

Marine microorganisms constitute the largest percentage of living biomass and serve as the major driving force behind nutrient and energy cycles. While viruses only comprise a small percentage of this biomass (i.e., 5%), they dominate in numerical abundance and genetic diversity. Through host infection and mortality, viruses affect microbial population dynamics, community composition, genetic evolution and biogeochemical cycling. However, the field of marine viral ecology is currently limited by a lack of data regarding how different environmental factors regulate virus dynamics and host-virus interactions. The goal of the present mini-review is to contribute to the evolution of marine viral ecology, through the assimilation of available data regarding the manner and degree to which environmental factors affect viral decay and infectivity as well as influence latent period and production. Considering the ecological importance of viruses in the marine ecosystem and the increasing pressure from anthropogenic activity and global climate change on marine systems, a synthesis of existing information provides a timely framework for future research initiatives in viral ecology.

Introduction

Since the discovery of high viral abundance in marine environments, the ecological importance of viruses to aquatic systems has become increasingly evident. Most of these viruses infect the numerically dominant microorganisms, which constitute over 90% of the ocean's biomass and serve as the major driving force behind nutrient and energy cycles (Cotner and Biddanda 2002; Suttle 2007; Sorensen 2009). Aside from driving host population dynamics and horizontal gene transfer, viruses influence microbial community structure and function through the conversion of biomass to dissolved and particulate organic matter via host cell lysis (Suttle 2007). Viral activity thus effectively regulates biodiversity and food web efficiency. The extent and efficiency to which viruses are able to drive microbial processes can be regulated by both abiotic and biotic aspects of the environment in which they occur.

At any spatio-temporal point in the ocean, viral abundance reflects the balance between rates of removal and production through host lysis. When viral progeny are released from their hosts, they are present in the environment as free virus particles and are directly exposed to environmental factors which may reduce infectivity, degrade or remove virus particles, and adversely affect adsorption to host, thereby reducing the chance of a successful host encounter and infection (Fig. 1A). Moreover, as obligate parasites, viruses are reliant upon their host to provide not only the cellular machinery but also the necessary energy and resources required for viral replication and assembly. Consequently, the factors regulating the physiology of the host, as well as its production and removal are also important in governing virus dynamics (Fig. 1B).

In the face of continued anthropogenic activity (marine utilization, eutrophication, urbanization, tourism, and global climate change), it will become increasingly important to unravel how environmental factors regulate virus dynamics and virus-host interactions and thus influence the role that viruses have in the marine environment. Reviews on aquatic viruses have thus far only limitedly conversed the influence of 'the environment' in viral ecology. It is therefore an opportune time to synthesize the current available knowledge on factors affecting host-virus interactions in the marine pelagic environment and identify any remaining gaps. The present mini-review focuses on microbe-viruses, both in culture and in the field (with emphasis on the pelagic).

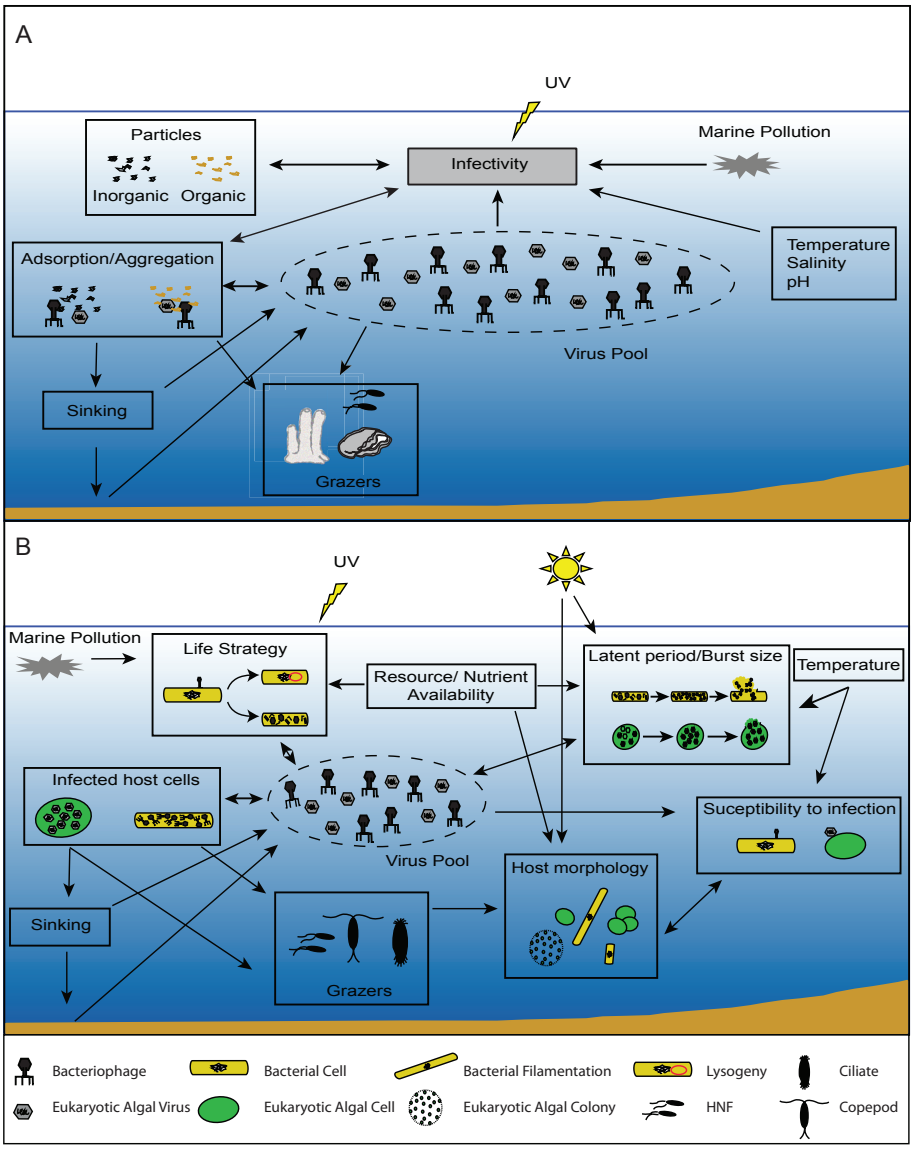

Figure 1. Schematic overview of environmental factors and processes in the marine environment that have been found thus far to affect virus dynamics and virus host interactions. (a). A synopsis of environmental factors that can lead to the removal or inactivation of virus particles reducing the chance of a successful host encounter and infection. (b) Overview of aspects that may influence the viral pool by altering host dynamics and deceasing susceptibility to infection or by modifying characteristics of viral proliferation. Heterotrophic nanoflagellates are abbreviated as NHF.

Temperature

Due to the dependency of viruses on a host for replication, the actual distribution of viruses can be expected to be constrained either by their own sensitivity to an environmental factor or by that of their hosts. Viruses may be more resistant to thermal stress than their host systems, indicating that the temperature distribution of the virus-host system is set by the host. Based on the available data from culture studies, the inactivation temperatures of most marine viruses fall outside of those at which host growth can be maintained (Table 1). Interestingly, the inactivation temperature of the psychrophilic filamentous phage SW1 infecting *Shewanella piezotolerans* showed the largest divergence from the host's optimum growth temperature. To our knowledge, this is the only marine filamentous phage tested thus far and it would be interesting to uncover if this is a general feature of this virus morphotype (Table S1). Apart from the filamentous phage, phages BVW1 and GVE1 of the hydrothermal field bacteria *Bacillus* and *Geobacillus*, respectively, were inactivated at temperatures comparable to that of their thermophilic host's optimum. The fact that non-hydrothermal field viruses have lower absolute inactivation temperatures suggests an ongoing adaption to the lower optimum growth temperature of their host's. One may then speculate that marine viruses have retained (from evolutionary origin) the genetic blueprint that is neutral in the current environment and may be useful for adaptation to (future) environmental increases in temperature.

Even though marine viruses are typically more stable to temperature than their host, it does not necessarily mean that virus-host interactions within the host's growth temperature range will lead to successful viral proliferation. For example, *Pseudomonas putrefaciens* (P19X) can grow well up to 27°C but phage-27 was unable to form plaques above 20°C (Delisle and Levin 1972a) Furthermore, the lower temperature stability of a marine sediment phage (0-23°C for phage versus 0-33°C for the host *Aeromonas* sp.) was due to an apparent inability of irreversible adsorption to host cells, as phage titers only demonstrated limited reduction when exposed to 30°C for 24h in the presence of their host bacterium (Wiebe and Liston 1968). However, whether the inactivation was a consequence of thermal alterations to phage structure or host receptors remains unknown.

Table 1. Temperature (°C) range and optimum for host growth and the range tested and values for inactivation, successful host lysis and maximum plaque forming unit (PFU) of associated viruses. When optimum temperature of the host was not reported, the culture temperature of host employed was assumed to be optimum. Parenthesis indicate that range provided is not strain-specific but obtained from the literature.

Host	Range	Optimum	Virus	Genome Type	Tested	Inactivation	Host lysis	Max PFU	References
Phaeocystis globosa Pg-I	8 to 20	15	Group I PgV	dsDNA	20 to 75	35	15		(Baudoux & Brussaard, 2005), Brussaard unpubl data (host growth)
P. globosa Pg-I	8 to 20	15	Group II PgV	dsDNA	20 to 75	25	15		(Baudoux & Brussaard, 2005)
M. pusilla LAC38	4 to 22	15	MpRNAV-01B	dsRNA	20 to 95	40	4 to 15		(Brussaard et al., 2004), Brussaard unpubl data (host lysis)
M. pusilla LAC38	4 to 22	15	MpV-03T, 06T, 08-12T, 14T, R3-4, B4-5	dsDNA	4 to 45	40	4 to 15		(Martinez-Martinez & Brussaard)
M. pusilla CCMP1545	8 to 24	20	MpV-02T, 04-05T, 07T, 13T, R1-R2, SP1	dsDNA	4 to 45	40	4 to 15		(Martinez-Martinez & Brussaard)
Chaetoceros debilis Ch48	(9 to 30)*	15	CdebDNAV18	ssDNA	4 to 20	>20	15		(Tomaru et al., 2008), (Tomaru et al., 2011a)
C. lorenzianus IT-Dia51	(9 to 27)*	15	ClorDNAV	ssDNA	4 to 20	>20	15		(Tomaru et al., 2011b)
C. setoensis IT07-C11	(7 to 28)*	15	CsetDNAV	ssDNA	4 to 20	>20	15		(Tomaru et al., 2013)
C. socialis	(7 to 28)*	15	CsfrRNAV	ssRNA	4 to 20	>20	15		(Tomaru et al., 2009b)
C. tenuissimus 2-10	(9 to 30)*	15	CtenRNAV01	ssRNA	4 to 20	>20	15		(Shirai et al., 2008) (Tomaru et al., 2011a)
Heterosigma akashiwo H93616	(5 to 30)	20	HaV01	dsDNA	4 to 20	>20	15 to 30		(Tomaru et al., 2005), (Nagasaki & Yamaguchi, 1998), (Graneli & Turner, 2007) (host growth
H. akashiwo NM96	(5 to 30)	20	HaV01	dsDNA	4 to 20	>20	15 to 25		(Nagasaki & Yamaguchi, 1998)
H. akashiwo H93616	(5 to 30)	20	HaV08	dsDNA	4 to 20	>20	20 to 30		(Nagasaki & Yamaguchi, 1998)
H. akashiwo NM96	(5 to 30)	20	HaV08	dsDNA	4 to 20	>20	20 to 25		(Nagasaki & Yamaguchi, 1998)
H. akashiwo H93616	(5 to 30)	20	HaV53	dsDNA	4 to 20	>20	20		(Tomaru et al., 2005)
H. akashiwo H93616	(5 to 30)	20	HaRNAV	ssRNA	4 to 20	>20	20		Tomaru et al., 2005)
Heterocapsa circularisquama HU9433-P	(15 to 30)	20	HcV03	dsDNA	4 to 20	>20	20		(Tomaru et al., 2005), (Yamaguchi et al., 1997) (host growth)
H. circularisquama HU9433-P	(15 to 30)	20	HcV05	dsDNA	4 to 20	>20	20		(Tomaru et al., 2005)
H. circularisquama HU9433-P	(15 to 30)	20	HcV08	dsDNA	4 to 20	>20	20		(Tomaru et al., 2005)
H. circularisquama HU9433-P	(15 to 30)	20	HcV10	dsDNA	4 to 20	>20	20		(Tomaru et al., 2005)
H. circularisquama HU9433-P	(15 to 30)	20	HcRNAV34	ssRNA	4 to 20	>20	20		(Tomaru et al., 2005)

Table 1. Continued.

Host	Range	Optimum	Virus	Genome Type	Tested	Inactivation	Host lysis	Max PFU	References
H. circularisquama HCLG-1	(15 to 30)	20	HcRNAV109	ssRNA	4 to 20	>20	20		(Tomaru et al., 2005
Pseudomonas putrefaciens P19X	2 to 27	2	Phage 27	dsDNA	-5 to 26, 55	55	-5 to 13	-5 to 2	(Delisle & Levin, 1972a), (Delisle & Levin, 1972b)
P. putrefaciens P10	2 to 27	2	Phage 27	dsDNA			2 to 20	2	(Delisle & Levin, 1972a)
P. putrefaciens P13	2 to 27	20	Phage 23	dsDNA	2 to 26, 55	55	2 to 26	20 to 26	(Delisle & Levin, 1972a)
P. putrefaciens P2	2 to 27	2	Phage 25F	dsDNA	2 to 26, 55	55	2 to 26	=	(Delisle & Levin, 1972a)
Pseudoalteromonas marina KCTC 12242†	(2 to 25)	25	φRIO-1	dsDNA	20 to 50	40	10 to 25	20 to 25	(Hardies et al., 2013)
Vibrio sp. ATCC19648	6 to 30	18	unknown	dsDNA	6 to 30, 50	50	6 to 25	=	(Johnson, 1968)
Vibrio (Beneckea) natriegens ATTC 14048	(4 to 40)	27	nt-1	dsDNA	5 to 60	50	27		(Zachary, 1976), (Farmer III & Janda, 2005) (host growth)
V. natriegens ATTC 14048	(4 to 40)	27	nt-6	dsDNA	5 to 60	37	27		(Zachary, 1976)
V. fischeri MJ-1	(5 to 30)	15	rp-1	dsDNA	23 to >45	45	25		(Levisohn et al., 1987), (Waters & Lloyd, 1985) (host growth)
Pseudomonas sp.	25 to 37	25 to 28	06N-58P	ssRNA	5, 45 to 50	45	25		(Hidaka & Ichida, 1976)
Bacillus sp. w13	45 to 85	68	BVW1	dsDNA	60 to 80	70	> 60	60	(Liu et al., 2006)
Geobacillus sp. E26323	45 to 85	65	GVE1	dsDNA	60 to 80	70	> 60	60	(Liu et al., 2006)
Colwellia psychrerythraea 34H	-18 to 18	10 to 18	Phage 9A	dsDNA	-12 to 55	25	-6 to 4		(Wells & Deming, 2006b), (Wells & Deming, 2006a), (Bowman et al., 1998)
C. demingiae ACAM 459^{T}	-10 to 18	10 to 18	Phage 9A	dsDNA			-6 to 8		(Bowman et al., 1998), (Wells & Deming, 2006b)
21C (*C. psychrerythraea)*[b]	0 to 15	4	21c	dsDNA			0 to 5		(Borriss et al., 2003)
Aeromonas sp.	0 to 33	12	unknown	dsDNA	45 to 60	45	0 to 23	5 to 12	(Wiebe & Liston, 1968)
1A *(Shewanella frigidimarina* LMG 19867)[b]	0 to 21	4	1a	dsDNA			0 to 14		(Borriss et al., 2003)
S. piezotolerans WP2	0 to 28	15 to 20	SW1	ssDNA	4-25, 60, 70,	70	4 to 15	4	(Wang et al., 2004), (Wang et al., 2007)

* Values are the reported natural temperature range where strains are found
† highest identities based on 16S analysis
'=, equal efficiency

Temperature affects the structural conformation of proteins and the elasticity of biomolecules such as proteins and membrane lipids, therefore variability in the response of different viruses to modifications in temperature will most likely arise from molecular or structural differences that regulate the sensitivity of viral lipid membranes or capsid proteins to thermal deformation or thermal fracture (Selinger et al. 1991; Evilevitch et al. 2008). Group I PgVs infecting *Phaeocystis globosa* were inactivated above 35°C while infectivity of Group II PgVs could only be maintained below 25°C (Baudoux and Brussaard 2005). These viruses differ in their phylogenetic origin, genome size, and in the size and composition of capsid proteins, most likely underlying the observed variation (Table S1) (Baudoux and Brussaard 2005; Santini et al. 2013). In contrast, the larger dsDNA viruses infecting *Heterocapsa circularisquama* were more sensitive to losses to infectivity at the different temperatures tested compared to the smaller ssRNA virus infecting the same species (Tomaru et al. 2004; Nagasaki et al. 2005; Tomaru et al. 2005). Although very different virus types, it would be interesting to test if the smaller size of the putative major capsid protein of the HcV03 (591 nt) as compared to HcRNAV109 (678 nt) may explain the discrepancy in the expected viral stability (Table S1) (Hickey and Singer 2004; Tomaru et al. 2009a). Although the underlying mechanisms remain unknown, variation in temperature sensitivity provides a driving force for virus and host population dynamics, and can be expected to affect the outcome of adaptation to changing environments (Bolnick et al. 2011). It is important to note that in general unfiltered or 0.2 μm pore-size filtered water which is commonly used for investigating the stability of viruses may include components such as extracellular enzymes that can contribute to the inactivation of viruses in a temperature dependent manner.

Temperature can also regulate infection dynamics and can vary amongst viruses infecting the same host as demonstrated for viruses infecting *Heterosigma akashiwo*. The dsDNA virus HaV01 only infects *H. akashiwo* strain H93616 between 15-30°C, while the comparable virus strain HaV08 is infective between 20-30°C (Nagasaki and Yamaguchi 1998). In addition, phenotypic variability can also be dependent on the host stain being infected. *H. akashiwo* strain H93616 was infected by HaV01 and HaV08 up to 30°C, whereas strain NM96 (with same growth optimum temperature) was not sensitive to infection above 25°C (Nagasaki and Yamaguchi 1998). Similar results have also been found in a bacterium-phage system, wherein Phage 27 could successfully form plaques between 2-20°C on host *P. putrefaciens* P10, but was restricted to 2-13°C on host P19X (Delisle and Levin 1972a). However,

in this case, it was not due to an inability of the virus to adsorb to host cells, as temperature (0 and 26°C) had no effect on the absorption of Phage 27 to P19X. Such virus-host co-occurring variability in temperature sensitivity, within the optimum range host growth, will enhance the temporal intraspecies diversity index.

Temperature is a major regulatory factor for microbial growth (through the regulation of enzyme kinetics, molecular diffusion, and membrane transport) and therefore can be expected to affect viral life strategy and viral production (White et al. 1991; Wiebe et al. 1992). Indeed, seasonal variations in temperature (from 15 to 30°C) correlated to prophage (φHSIC) induction in a eutrophic estuarine environment were found to be a consequence of the 2-fold higher growth rate of the host (*Listonella pelagia)* at 28°C compared to 18°C (Cochran and Paul 1998; Williamson et al. 2002; Williamson and Paul 2006). Temperature-induced difference in growth rate is also the most probable cause for the delay in the onset of viral lysis of infected *H. akashiwo*, i.e., 2 to 3-fold delay in lysis under suboptimal temperature conditions of host (Nagasaki and Yamaguchi 1998). Unfortunately, the authors did not sample for virus abundance so no conclusions can be made on alterations to adsorption, latent period or burst size. Nevertheless, this study illustrates the importance of studying different host strain and virus strain models in order to accurately extrapolate to natural virus-host dynamics (e.g. red-tide bloom dynamics in the case of *H. akaswhiwo*). In contrast, production of a filamentous phage (SW1) in the deep-sea bacterium *S. piezotolerans* WP3 only occurred at temperatures below the optimum of the host, producing 2 to 9-fold more plaques at 4°C compared to 10°C and 15°C (Wang et al. 2007). Moreover, SW1 was shown to have a negative effect on the swarming ability of the host at low temperatures, which may provide energy for SW1 proliferation under suboptimal growth conditions of the host and therefore may play a role in adjusting the fitness of the host cells to the cold deep-sea environments (Jian et al. 2013).

Salinity

Osmotic shock assays demonstrate that viral capsids have differing permeabilities to water and salt ions, which can lead to inactivation or virus particle destruction when exposed to rapid changes in ionic strength (Cordova et al. 2003). There is also evidence which suggests that phage morphology may play a role in resistance. Tailed viruses appear to be the most resistant to changes in ionic strength. In

addition, membrane viruses are more sensitive compared to non-lipid containing, and of the membrane containing viruses, enveloped viruses are more sensitive than those with internal membranes (Kukkaro and Bamford 2009). Similar to temperature, the realized niche of viruses can be constrained either by their own sensitivity to variations in ionic strength or by that of their hosts. Bacteriophages and archaeoviruses isolated from a wide range of ionic strength environments, have been found to be more resistant to variations in ionic strength than their host (Table 2). Moreover, marine bacteriophages appear to have specific ionic requirements to maintain structural stability and remain infective indicating an adaptation to the marine environment. Both sodium and magnesium ions were necessary for retention of viability for bacteriophages NCMB384 and 385 infecting the marine *Cytophaga* sp. NCMB397 (Chen et al. 1966). Keynan and colleagues (1974) found sodium ion concentration was the most important for the stability of h*ν*-1 phage of the marine luminous bacterium *Beneckea harveyi* (maximum stability in seawater, followed by 3% NaCl; Keynan et al. 1974). Stability, infectivity, plating efficiency and uniformity of plaque formation, but not adsorption to host, were improved by divalent ions such as Mg^{2+} and Ca^{2+}, indicating that the requirement was related to infection of phage DNA. Thus salt stress may affect the survival and successful infection of bacteriophages, potentially through decreases in capsid pressure and consequent reductions to DNA injection efficiency or release of phage DNA though cracks in the capsid, which has been shown for the coliphage λ. Wherein the injection of DNA into host is driven by energy stored in the DNA due to its confinement, therefore any changes in ion concentrations can interact with the DNA and change the state of stress and hence the ejection force (Cordova et al. 2003; Evilevitch et al. 2008).

There is high variability in the effect of salt concentration on the adsorption of virus to host, even up to four orders of magnitude, suggesting different mechanisms for host binding (Zachary 1976; Torsvik and Dundas 1980; Kukkaro and Bamford 2009; Wigginton et al. 2012). Marine bacteriophages appear to have maximum host cell binding at salt concentrations similar to seawater, suggesting that viruses adapt to the ionic strength of their native environment. However, this could also be due to the host, as cationic imbalance, particularly deficiencies of various cations are believed to affect the permeability and other properties of cells surface structures in certain marine bacteria, which would impede attachment or penetration mechanisms of the phage (Brown 1964). Slowest binding kinetics were found amongst viruses isolated from Archaea-dominated high salt environments

(Kukkaro and Bamford 2009). The slower adsorption kinetics of archaeoviruses compared to bacteriophages might be explained by dissimilarity of surface structures of bacteria and archaeal hosts (i.e., as Archaea have lower membrane permeability; Valentine 2007). Halophages may have evolved to exert minimal selective pressure on their sensitive hosts (Santos et al. 2012). Prokaryotic hosts are more sensitive to changes in ionic strength and the physiological state of cells decreases at high-salt concentrations (Kukkaro and Bamford 2009; Bettarel et al. 2011). Therefore slow absorption, in combination with slow decay rate, might be selected for as a mechanism to avoid decimating host population under higher ionic stress or could in turn be tied to the low generation times of hosts, as fast adsorption and infection dynamics could decimate host populations (Bettarel et al. 2011). Indeed, over a wide range of salinities (10 - 360) along the coast of Senegal the frequency of infected prokaryotes in was negatively correlated with salinity, whereas a high percentage lysogenic prokaryotes at the higher salinities (> 150) was found to correlate to the abundance of archaeal cells (Bettarel et al. 2011).

Although salinity has been found to trigger the marine temperate phage φHSIC to switch to a lysogenic existence when incubated at brackish salinity, it is likely that this was due to a reduction of host growth rate (Williamson and Paul 2006). However, there is also some indication that salinity can alter viral proliferation independent of host growth. A study employing a estuarine salt marsh bacterium *B. natriengens* reported phage-specific effects on production with alterations in salinity (Zachary 1976). Phage nt-1 showed longer latent periods and highly reduced burst sizes (plaque forming units) at salinities below 18, while nt-6 revealed highest phage production rates at brackish salinities (which was below the host's growth optimum). The differences between these phages exemplify the potential importance of salinity on virus-host interactions and suggest a mechanism for alterations in viral population dynamics under changing salinity, both particularly meaningful for estuarine viral ecology

Table 2. Salinity (expressed as M NaCl) ranges for host growth and the range tested and values for successful infectivity and adsorption of associated viruses. Parenthesis indicate that value was assumed based on range tested for absorbance of virus to host.

Host	Range	Virus	Ions required	Tested	Infective	Max adsorption	References
Salmonella enterica	0 to 0.75	PRD1		0 to 4.50	< 4.25	0	(Kukkaro & Bamford, 2009)
S. enterica	0 to 1.00	P22		0 to 4.50	0 to 4.50	0	(Kukkaro & Bamford, 2009)
Pseudomonas syringae	0 to 0.25	φ6		0 to 4.50	< 2.75	0.25	(Kukkaro & Bamford, 2009)
Pseudolateromonas sp.	0 to 1.75	PM2		0 to 4.50	< 3.25	0.75	(Kukkaro & Bamford, 2009)
Halorubrum sp.	2.00 to 4.50	HRTV-1		0 to 4.50	0 to 4.50	> 4.00	(Kukkaro & Bamford, 2009)
H. hispanica	2.25 to 4.50	HHTV-1		0 to 4.50	0 to 4.50	4	(Kukkaro & Bamford, 2009)
H. hispanica	2.25 to 4.50	HHPV-1		0 to 4.50	> 1.75	3.5	(Kukkaro & Bamford, 2009)
H. hispanica	2.00 to 4.50	SH1	$MgCl_2$ & NaCl*	0 to 4.50	0	> 4.00	(Kukkaro & Bamford, 2009) (Porter et al., 2005)
H. californiae	2.25 to 4.50	HCTV-1		0 to 4.50	0 to 4.50	3	(Kukkaro & Bamford, 2009)
Salicola sp.	1.00 to 3.50	SCTP-1		0 to 4.50	0 to 4.50	3.5	(Kukkaro & Bamford, 2009)
Salicola sp.	1.00 to 4.50	SCTP-2		0 to 4.50‡	0 to 4.50	3	(Kukkaro & Bamford, 2009)
Vibrio (Beneckea) natriegens	0.06 to 0.40	nt-1	Na^+, K^+ †	0 to 0.16	0 to 0.16	> 0.16	(Zachary, 1976)
V. natriegens		nt-6	ns †	0 to 0.16	≥ 0.06	=	(Zachary, 1976)
V. harveyi	0.10 to 0.60	hν-1	Na^+, Ca^{2+}, Mg^{2+}*	0 to 0.60	> 0.085		(Keynan et al., 1974)
V. fischeri MJ-1	(0 to 1.03)	rp-1		0 to 1.37	0 to 1.37	0.34 to 0.68	(Levisohn et al., 1987)
Aeromonas sp.	0.085 to 0.50	unknown	Mg^{2+}, Ca^{2+} ‡				(Wiebe & Liston, 1968)
Cytophaga sp.		NCMB 384	Mg^{2+}, Na^+ *				(Chen et al., 1966)
Cytophaga sp.		NCMB 385	Mg^{2+}, Na^+ *				(Chen et al., 1966)
Colwellia psychrerythraea 34 H	0.29 to 0.96	Phage 9A		0.29 to 0.74	0.29 to 0.74		(Wells & Deming, 2006b)
C. demingiae ACAM 459^T	0.29 to 0.96	Phage 9A		0.40 to 0.50	0.40 to 0.50		(Wells & Deming, 2006b)

* required for stability
† required for adsorption
‡ required for lysis of host
=, equal efficiency
^{T} highest identities based on 16S analysis

UV

Biologically harmful ultraviolet radiation (UV, 100-400 nm) can penetrate to depths exceeding 60 m in clear oceanic waters (Booth et al. 1997; Whitehead et al. 2000) and has been found to be a principal factor contributing to the decline of viral infectivity in bacteriophages, cyanophages and viruses infecting eukaryotic hosts, with average losses of 0.2 h^{-1} and rates up to 0.8 h^{-1} in phage isolates (Table 3). Solar radiation can directly affect free viruses by degrading proteins, altering structure, and decreasing infectivity (Suttle and Chen 1992; Wommack et al. 1996; Wilhelm et al. 1998a; Weinbauer et al. 1999). However, viral particles appear more vulnerable to inactivation than to destruction (Wommack et al. 1996; Jacquet and Bratbak 2003). While a strong link between UVA and loss of infectivity of marine viruses has not been found, UVB shows a clear correlation (Table 3) (Weinbauer et al. 1997; Wilhelm et al. 1998a; Jacquet and Bratbak 2003). The shorter wavelength (290 - 320 nm) can result in the modification of viral proteins and the formation of photoproducts such as cyclobutane pyrimidine dimers (CPD) (Kellogg and Paul 2002; Hotze et al. 2009; Wigginton et al. 2010). As common lethal photoproducts of UV are thymine dimers, DNA viruses (containing thymine) are generally more sensitive to damage by UV than RNA viruses (not containing thymine). Furthermore, double stranded DNA or RNA viruses are more resistant to UV than single stranded viruses (Lytle and Sagripanti 2005). However, these differences have yet to be demonstrated for marine viruses. Interestingly, Kellogg and Paul (2002) found a significant negative correlation between the G+C content of marine phage DNA and the degree of DNA damage induced by solar radiation. Viruses with AT-rich genomes and thus higher potential dimer (T-T) sites, had a higher potential for UV damage (Kellogg and Paul 2002). In addition, AT-rich DNA also enhances the generation of oxygen species, which cause oxidative damage (Wei et al. 1998). Repair mechanisms can reduce the lethal effect of UV, especially for viruses possessing double stranded DNA (Lytle and Sagripanti 2005). The dsDNA virus PBCV of Chlorella contains a DNA repair gene giving it access to 2 DNA repair mechanisms, i.e., photoreactivation using host encoded gene products and a virus-encoded enzyme that initiates dark repair (Furuta et al. 1997). The combined activities of these repair systems should enhance survival and maintenance of viral activity, particularly in the relatively UV-rich surface waters.

Table 3. Average decay rates (h-1) reported for losses in infectivity of virus isolates in the dark, under full sunlight, and in the absence of UVB.

		Infectivity			Sample information		
Host	**Viral isolate**	**Dark**	**Sunlight**	**no UVB**	**Location**	**Time of year**	**Reference**
LMG1	LMG1-P4		0.68[1], 0.27[2]	0.181	Gulf of Mexico	May[1], various[2]	(Suttle & Chen, 1992)[1,†], (Suttle & Chan, 1994)[2]
PWH3a	PWH3a-P1	0.00[*]	0.35[1], 0.24[2], 0.80[3]	0.081	Gulf of Mexico	May[1], various[2], June[3]	(Suttle & Chen, 1992)[1,†], (Suttle & Chan, 1994)[2], (Wilhelm et al., 1998a)[3]
Photobacterium leiognathi (LB1VL)	LB1VL-P1b	0.00[*]	0.52[1], 0.28[2]	0.151	Gulf of Mexico	May[1], various[2]	(Suttle & Chen, 1992)[1,†], (Suttle & Chan, 1994)[2]
CB 38	CB 38Φ	0.05[*]	0.11[*]		York river estuary	October	(Wommack et al., 1996)[‡]
CB 7	CB 7Φ	0.04[*]	0.06[*]		York river estuary	October	(Wommack et al., 1996)[‡]
H2	H2/1	0.02[*]	0.07		Santa Monica Bay	March-July	(Noble & Fuhrman, 1997)[†,§]
H11	H11/1	0.02[*]	0.07		Santa Monica Bay	March-July	(Noble & Fuhrman, 1997)[†,§]
H40	H40/1	0.01[*]	0.09	0.06	Santa Monica Bay	March-July	(Noble & Fuhrman, 1997)[†,§]
H85	H85/1	0.03[*]	0.07	0.04	Santa Monica Bay	March-July	(Noble & Fuhrman, 1997)[†,§]
PR1	PR1/1	0.02[*]	0.05		Santa Monica Bay	March-July	(Noble & Fuhrman, 1997)[†,§]
PR2	PR2/1	0.02[*]	0.04		Santa Monica Bay	March-July	(Noble & Fuhrman, 1997)[†,§]
PR3	PR3/1	0.02[*]	0.05		Santa Monica Bay	March-July	(Noble & Fuhrman, 1997)[†,§]
PR4	PR4/1	0.02[*]	0.04		Santa Monica Bay	March-July	(Noble & Fuhrman, 1997)[†,§]
Synechococcus sp.	S-PWM1		0.19		Gulf of Mexico	various	(Suttle & Chan, 1994)[†]
Synechococcus sp.	Natural Community *Syn DC2 phages*		0.19		Gulf of Mexico	1 year	(Garza & Suttle, 1998)
Synechococcus sp.	Syn DC2 isolates (S-PWM1 and S-PWM3)		0.39		Gulf of Mexico	1 year	(Garza & Suttle, 1998)[b]
Micromonas pusilla	MpV SP1	0.00	0.3		Gulf of Mexico	March-April	(Cottrell & Suttle, 1995)

[*] 0.2 µm filter seawater or artificial seawater

[†] estimated from figures in referred paper.

[‡] light transmission: UVC (200-290nm) 3-23%, UVB (290-320nm) 23-26%; UVA (320-400nm) 26-32%, PAR (400-700 nm) 32-55%

[§] light transmission: UVB (290-320nm) 67%; UVA (320-400nm)

Numerical superscipts link data in table to the appropriate reference

While some large dsDNA algal viruses may encode for their own DNA repair enzymes most viruses rely on repair mechanisms of their hosts, which are achievable only after DNA has been inserted into the host cell (Furuta et al. 1997; Weinbauer et al. 1997; Shaffer et al. 1999; Orgata et al. 2011; Santini et al. 2013). In the summer, Garza and Suttle (1998) found 2-fold lower decay rates of natural cyanophage communities as compared to isolates, whereas in the winter they were equal, suggesting (seasonal) selection for viruses that encoding host-mediated repair mechanisms. Alternatively, this may be explained by the rapid inactivation and removal of more sensitive cyanophages. Either way, it is important to note that UV-impact studies employing viral isolates may not represent the natural community response, and that viruses in surface waters may be more infective than previously thought based on the literature decay values.

CPDs in marine viruses have been found to increase over a latitudinal gradient (i.e., 41°S to 4°N), from 250 in the south to 2000 Mb^{-1} DNA near the equator, consistent with longer solar days and decreased solar angle. In addition, in the Gulf of Mexico, higher rates (i.e., 0.35 h^{-1}) for the loss of infectivity were recorded in natural cyanophage communities and cyanophage isolates (S-PWM1 and S-PWM3) during the summer and early fall when solar insolation was the highest, compared to undetectable levels in winter and spring (Garza and Suttle 1998; Wilhelm et al. 2003). Variations in level of DNA damage in waters with similar transparency and optical properties but different mixing depths have been found (Wilhelm et al. 1998b). When the mixing depth was reduced by half, photoreactivation was prevented and resulted in increased levels of CPD beyond what could be repaired overnight, leading to accumulation of damage over time (Wilhelm et al. 1998b). Similarly, Wilhelm and coworkers found high residual CDP levels in the surface water viral community of the pacific coastal waters of South America at high latitudes, at the time experiencing an equatorial upwelling event (Wilhelm et al. 2003). Viruses were, therefore, constricted to the surface waters leading to higher residence times and DNA damage levels exceeding normal daily levels. There is substantial evidence that marine viruses may adapt to local conditions of solar radiation; making them less susceptible to the degradation. Phages isolated from the coastal waters of Santa Monica Bay (USA) were 50 - 75% less susceptible to decay under local solar radiation than non-native phages of the North Sea (Noble and Fuhrman 1997). In addition, phages isolated from tropical waters have higher G+C content and higher survival rates over a range of UV radiation compared to phages isolated from temperature regions (Kellogg and Paul 2002). Similarly,

the proportion of lysogens induced by sunlight was found to be lower at oceanic than at coastal stations, which may be due to higher resistance to induction in the more transparent oligotrophic open ocean, or to induction of most UV-inducible lysogens. Natural solar radiation may thus alter the viral life cycle by inducing lysogenic phage production, but it does not appear to be an important source of phage production (max. 3.5%; Wilcox and Fuhrman 1994; Jiang and Paul 1998; Weinbauer and Suttle 1999; Weinbauer and Suttle 1996).

Due to the difference in susceptibility and abilities of viruses to repair the damaging effects of UV, it is not surprising that a considerable amount of variability exists in the sensitivity of viral particles to UV radiation, which has important implications for host population dynamics and species diversity (Suttle and Chen 1992; Wommack et al. 1996; Noble and Fuhrman 1997; Kellogg and Paul 2002; Jacquet and Bratbak 2003; Lytle and Sagripanti 2005). Five large dsDNA algal viruses, showed varying sensitivities to UVB from no effect for PoV infecting *Pyramimonas orientalis* to complete inactivation for PpV infecting *Phaeocystis pouchetii* (Jacquet and Bratbak 2003). Interestingly, the same study showed that some of these algal viruses, i.e., of *P. pouchetii* and *M. pusilla*, had a protective effect on surviving host cells when exposed to UVB subsequent to infection (Jacquet and Bratbak 2003). Although the mechanisms of UVB stress and resistance to viral infection remain largely unclear it demonstrates the complexity of how environmental factors interact with host-virus systems.

Photosynthetic Active Radiation (PAR)

Light is the essential energy source for photosynthetic organisms and most often drives synchronization of phytoplankton cell division and thus DNA synthesis and mitosis. Production of the virus infecting *P. orientalis* was found to depend on the host cell cycle, with 3 to 8-fold increase in progeny viruses when infection occurred at the end of cell division cycle (around the onset of the light period; Thyrhaug et al. 2002). During a mesocosm study of *E. huxleyi* blooms, EhV abundance increased during the first part of the day (light period) suggesting that viral production was also synchronized to host cell cycle (Jacquet et al. 2002). A diel cycle-dependent cyanophage infection has been hypothesized, with maximal phage production and reinfection occurring at night, to explain the sharp decline in *Synechococcus* abundance at the onset of darkness (Suttle 2000). However, support

for this hypothesis from field observations vary (Bettarel et al. 2002; Clokie et al. 2006). Light-dependent viral infection and proliferation which triggers infection by dawn and lysis by dusk or dark, would reduce exposure of the viruses to light (UV) and allow viral replication to align with its host's reproduction cycle (Clokie and Mann 2006). Diel patterns have even been described in virally infected bacterioplankton (Winter et al. 2004), i.e., viral lysis of bacteria with high viral progeny occurring around noon or early afternoon when bacterial activity was most likely responding to photosynthetic extracellular release (in combination with increased bioavailability of dissolved organic carbon by UV radiation). In addition, the newly released phages may accumulate less DNA damage (by UV) in the afternoon (Winter et al. 2004). This concept would also explain the diel variability described for a natural microbial community of NW Mediterranean Sea (Bettarel et al. 2002). One mechanism by which viruses could synchronize infection with host cell cycle is to have light dependent absorption. The effect of light on the adsorption of 9 cyanophages to *Synechococcus* sp. (WH7803) were found to be either light-independent (S-PWM1, S-BM3, S-MM4, S-MM1, S-MM5) or light-dependent (S-BnM1, S-BP3, S-PWM3, S-PM2) (Jia et al. 2010). However, the adsorption rate and dependence on light was host strain-specific. Light-dependent adsorption may be due to light-induced charge neutralization at the cell surface or by light-induced alterations to the ionic composition of the host cell surfaces, which could vary according to the host (Cseke and Farkas 1979).

In contrast, the production of PpV infecting *P. pouchetii* was cell cycle-independent which was in agreement with earlier work showing that the duration of the lytic cycle of PpV was of similar duration in darkness as in light and therefore not dependent on photophosphorylation (Bratbak et al. 1998). Similarly, the latent period of algal viruses infecting Chlorella (PBCV-1, first algal virus characterized, although not marine) and *H. akashiwo* (1 ssRNA and 2 uncharacterized DNA viruses) were unaffected by darkness (Van Etten et al. 1983; Juneau et al. 2003; Lawrence and Suttle 2004). However, the viral burst size strongly decreased (50% for PBCV and 90% for PpV), implying that light independent processes such as exploitation of host energy via chlororespiration, ATP reserves and/or production via respiration could provide the energy needed for viral replication and host cell lysis (Juneau et al. 2003). The degree to which darkness affects viral production can also depend upon the previous light conditions experienced by the host (Baudoux and Brussaard 2008). Viral production in *P. globosa* pre-adapted to a low irradiance level (25 μmol quanta m^{-2} s^{-1}) was inhibited under darkness but resumed once

light was reinitiated. Conversely, mid and high light (100 and 250 µmol quanta m^{-2} s^{-1}) pre-adapted host cells did not show additional viral production when reintroduced to the light. The burst sizes of the low and high light-adapted *P. globosa* cells were only half of the mid light cultures indicating PgV proliferation is sensitive to shortage of energy (low light) as well as high irradiance inhibition that likely induces reactive oxygen species formation. Conversely, light level did not affect the virus growth cycle of MpV infecting *Micromonas pusilla* (Baudoux and Brussaard 2008). Yet, prolonged darkness (48 - 65h) did delay host cell lysis and consequent release of virus progeny (Brown et al. 2007; Baudoux and Brussaard 2008). It is presumed that energy and potentially reductants derived from stored metabolic intermediates were sufficient to permit viral multiplication to proceed, but at the expense of the host DNA replication (Brown et al. 2007). Late stages of infection and lysis, however, may be too energy expensive to be overcome in the dark and thus required host photosynthetic energy. We speculate that such response to viral infection under darkness is related to cell size, with the small sized picophytoplankton having insufficient reserves to complete the virus growth cycle under darkness. Darkness is an extreme condition of light limitation, in nature phytoplankton cells are exposed periodically to dark at night and prolonged darkness occurs only once cells sink out of the euphotic zone. However, within the euphotic zone, light conditions are far from static and algae can experience changes in light of several orders of magnitude throughout the day depending on mixing conditions and cloud cover.

These studies show that viral production of phytoplankton species may occur at low light levels and even below the photic zone, although the extent is species-specific and dependent on the growth conditions prior to viral infection. Typically, the dependence of viral replication on light is characterized by a gradual shut down of host photosynthesis, with a portion of photosynthetic capacity being maintained until the end of the lytic cycle (Waters and Chan 1982; Suttle and Chan 1993; Juneau et al. 2003; Brown et al. 2007; Baudoux and Brussaard 2008). In some hosts this dependence was investigated in more detail and key photosynthetic complexes such as the chloroplasts, and ratios of several key photosynthetic proteins (rubisco, PSI, PSII and ATP synthase) were maintained during the course of infection (Juneau et al. 2003; Brown et al. 2007). The importance of light in marine virus-host systems is further exemplified by the acquisition of key photosynthetic functional genes by cyanophages infecting *Prochlorococcus* and *Synechococcus* during the course of evolution (Sullivan et al. 2006). These photosynthetic genes are expressed during

viral replication and aid in maintaining host photosynthesis and ensuring the provision of energy for viral replication until the onset of lysis (Lindell et al. 2005). To our knowledge, no studies on the potential impact of the color (wavelength) of the photosynthetically active radiation (PAR, 400 - 700nm) have been reported.

Nutrients

Lysogeny often prevails in systems with a lower trophic status, independent of geographical location (Williamson et al. 2002; Weinbauer et al. 2003; Payet and Suttle 2013). In the deep-sea, microbes, experiencing a low nutrient flux and rapidly changing conditions, have high numbers of lysogenic hosts (Weinbauer et al. 2003; Williamson et al. 2008; Anderson et al. 2011). Hence, lysogeny seems to represent a survival strategy under conditions of low host productivity and abundance, and exemplifies the crucial role that host physiology plays in determining viral life strategy. Seasonal studies and nutrient addition experiments demonstrate that viral production can be enhanced through alterations in bacterial host metabolism either by increasing host growth rate or by prophage induction (Williamson et al. 2002; Motegi and Nagata 2007; Payet and Suttle 2013). Likewise, P-limitation of cyanobacterium *Synechococcus* sp. induces lysogens, while P-addition stimulated the production of temperate cyanophage from natural P-depleted *Synechococcus* spp. (Wilson et al. 1996; Wilson et al. 1998). Viral-induced lysis of host resulting from lytic infection, may then act as a switch for lytic infection of prophages of the community in uninfected host which can utilize the cellular compounds released from lysed cells. These findings illustrate the highly dynamic and responsive nature of viral life strategies to environmental factors. As the impact on host population dynamics, food web functioning and biogeochemical cycling are very different for lysogenic or lytic viral infection, there is need for more detailed studies on this topic.

In addition to altering virus life strategies, environmental conditions that affect host physiology can also regulate the characteristics of a lytic viral infection. The latent period of marine bacteriophages typically corresponds closely with host generation time (Proctor et al. 1993; Middelboe 2000). Similarly, viral production is often found to have a negative relationship to host growth phase, i.e., lowest for host cells in stationary phase in comparison to exponentially growing cultures (Moebus 1996; Middelboe 2000). Interestingly, no distinct trend has been found between

burst size (mostly determined by whole cell TEM analysis) and bacterial production across different systems (Parada et al. 2006), which may be due to high bacterial host diversity under these natural conditions or selection for lysogeny under non-favorable conditions. However, in some algal host-virus model systems, burst size has been found to be linked to host growth phase (Van Etten et al. 1983; Bratbak et al. 1998). Experiments with Chlorella virus PBCV-1 revealed that this was not due to differences in adsorption but rather enhanced viral replication in actively growing cells (Van Etten et al. 1983). Shirai and coauthors (2008) found that while host growth phase had no effect on the burst size of the ssRNA virus CtenRNAV01 infecting the diatom *Chaeotoceros tenuissimus*, viral lysis occurred earlier in the stationary-phase culture. Interestingly, Nagasaki and Yamaguchi (1998) showed that the harmful algal bloom-forming *H. akashiwo* was sensitive to infection by both dsDNA viruses HaV01 and HaV08 when growing exponentially, but became resistant to HaV01 when in stationary phase. While, the underlying mechanism is unknown, the results indicate that the functional status of the host cell is an important determinant of virus-host interactions. Despite the potential importance of host growth as a driving factor of virus-host dynamics and subsequent organic matter cycling, there is surprisingly little attention focused on this area of research. A large proportion of the seas and oceans are oligotrophic and phytoplankton growth is often limited by inorganic nutrient (P, N, Si, Fe) availability, increasing the potential importance of host growth as a regulatory factor of virus-host interactions. Only two studies have investigated the consequence of N-depletion in host cells on viral production and demonstrate either no effect or reduced virus yield (Bratbak et al. 1993; Bratbak et al. 1998). Alternatively, the few studies which have focused on the effect of P-depletion on algal host-virus interactions consistently show reductions in the production of viruses, i.e., on average 70% for EhV infecting *E. huxleyi*, 30% for PpV infecting *P. pouchetii* after correction for growth phase differences and 80% for MpV infecting *M. pusilla* (Bratbak et al. 1993; Bratbak et al. 1998; Jacquet et al. 2002; Maat et al. in press). Furthermore, the length of the latent period of *M. pusilla* virus MpV-08T was positively correlated to the degree of P-limitation (Maat et al. in press). Although in theory viral production can be depressed in P-limited cultures due to insufficient intracellular P for the production of nucleic acid-rich (and thus P-rich) viruses, it may also be caused by reduced energy availability (Clasen and Elser 2007; Maat et al. in press).

Wikner and colleagues (1993) have shown that bacterial host nucleic acids serve as a major source of nucleotides for marine bacteriophages, and suggests a mechanism

by which marine phages limit their sensitivity to P-limitation which may be common in some open ocean areas (Paytan and McLaughlin 2007). Interestingly, *Prochlorococcus* cyanophage genomes may contain the putative ribonucleotide reductase (RNR) domain, which could function as extra nucleotide-scavenging genes in P-limited environments (Sullivan et al. 2005). The highest fraction of cyanophage genomes containing host-like P-assimilation genes originate from low-P source waters (Sullivan et al. 2010; Anderson et al. 2011; Kelly et al. 2013). Moreover, host-derived *pho*-regulon genes, which regulate phosphate uptake and metabolism under low-phosphate conditions, are found specifically in marine phages (40% of marine vs 4% of non-marine phage genomes (Goldsmith et al. 2011). Recently, Zeng and Chisholm (2012) showed enhanced transcription of the *Prochlorococcus* cyanophage-encoded alkaline phosphatase gene (phoA) and the high-affinity phosphate-binding protein gene (pstS), both of which have host orthologs, in phages infecting P-starved hosts. Such adaptations suggests that manipulation of host-PO_4 uptake may be an important adaptation strategy for viral proliferation in many marine ecosystems (Monier et al. 2011). Moreover, phage-genes are controlled by the host's PhoR/PhoB system, illustrating nicely the regulation of lytic phage genes by nutrient limitation of host.

Inorganic particles

Turbidity not only affects light penetration in sea but may also passively adsorb viruses. In natural waters, viruses possess a net negative surface charge due primarily to the ionization of carboxyl groups present on the external surfaces of viral capsid proteins (Wait and Sobsey 1983). Low molecular weight peptides and amino acids have a natural binding affinity for clay minerals, with the amount being absorbed and bound dependent on the type of clay and the type of cation saturating the clay (Dashman and Stotzky 1984). The addition of functional groups, such as amino or carboxyl groups, enhances absorption suggesting that these molecules play an important role in the absorption kinetics (Dashman and Stotzky 1984). Many studies have demonstrated the capacity of viruses to adsorb and bind to sediment and clay particles in the marine system (Kapuscinski and Mitchell 1980; Kimura et al. 2008). These reveal that association with particles can enhance survival and persistence of viruses by providing protection against UV radiation (most likely due to shading) and chemical pollutants relative to free

viruses in seawater (Vettori et al. 2000; Templeton et al. 2005; Kimura et al. 2008). In addition, the ability of marine viruses to irreversibly or reversibly bind to clay particles depends on virus and clay type and can be affected by environmental factors such as temperature, mixing, changes in ionic strength, organic matter type, size and concentration that either enhance adsorption or induce desorption of viruses from some particles (Kapuscinski and Mitchell 1980; Lipson and Stotzky 1984). However, these studies only focused on the effect of particles on enteric phages. Hewson and Furhman (2003) reported that between 20 - 90% of natural marine viruses can be absorbed by mineralogically uncharacterized suspended sediments, dependent on sediment concentration, size and source. The marine (cold-active) heterotrophic bacteriophage-9A failed to be inactivated by incubation with different ecologically relevant clay types, however, this could have been due to the high concentration of organics in the medium used, as organic matter can inhibit phage adsorption to clays, presumably by outcompeting phage for binding sites (Lipson and Stotzky 1984; Wells and Deming 2006a). Alternatively, a marine bacteriophage under simple media conditions has been shown to serve as nuclei for iron adsorption and precipitation, presumably via the same binding mechanism as clays, i.e., carboxyl and amino functional group reactive sites enabling iron atoms to penetrate and bind to the protein capsid (Daughney et al. 2004). Anthropogenic pollution has also led to the introduction of non-native particles such as black carbon to the marine environment, which has also been shown to adsorb viruses (Cattaneo et al. 2010). Due to the lack of scrutiny applied to the study the effects of clay and sediment on native marine viruses, as well as other native and non-native particles, additional research is needed to understand the ecological role, either as protective or removal agents, that the association of marine viruses with these particles has in seas and oceans.

Organic particles

In the marine environment, phytoplankton and bacteria generate large amounts of extracellular polysaccharides (EPS). In addition, intracellular substances released during viral lysis, or sloppy feeding also contribute to the organic matter pool. One important type of EPS is transparent exoploymer particles (TEP). TEP particles originate from colloidal DOM precursors, which may also bind to viruses and lead to inactivation, and might explain the discrepancy of inactivation rates in the <0.2

μm fraction of seawater (Mitchell and Jannasch 1969; Suttle and Chen 1992; Noble and Fuhrman 1997; Passow 2002; Finiguerra et al. 2011). TEP form a chemically and heterogeneous group of particles and their chemical composition and physical properties are dependent on the species releasing them and the prevailing environmental conditions. TEP aggregation is non-selective implying that all categories of particles present in the water become incorporated into aggregates (including viruses). In addition, TEP is primarily composed of negatively charged polysaccharides which would have a high affinity to viruses.

TEP is abundant in all marine waters (1 - 8000 ml^{-1} for the TEP > 5 μm and 3000 - 40000 ml^{-1} for the >2 μm fraction) and is often in the same size range as phytoplankton, dramatically increasing the potential collusion frequency of particles. Suttle and Chen (1992) estimated that viruses can adsorb to microaggregates at a rate of 0.41 d^{-1} (averaged over the upper 10 m of the water column), which rivaled the loss due to solar radiation (0.38 d^{-1}), indicating that ocean wide virus association with TEP could be a significant mechanism leading to the inactivation or removal of viruses from the pelagic system. Weinbauer and coworkers (2009) reviewed that viral abundance on suspended matter ranges between 10^5 to 10^{11} viruses cm^{-3} of aggregate, although it remains largely unclear how many viruses are truly attached and how many occur in the pore water of the TEP matrix and aggregates. In *P. globosa* mesocosms, TEP production resulting from colony disintegration and viral lysis adsorbed large quantities of the viral progeny (10 - 80%, also depending on whether N or P was limiting algal growth; Brussaard et al. 2005b). This could provide a mechanism by which viruses can be rapidly removed from the pelagic system after the collapse of a bloom. Conversely, reversible virus association may prolong survival and infectivity (Weinbauer et al. 2009). In addition, TEP colonized by microorganisms may continue to produce viral progeny, as viral production measurements of TEP have been shown to rival those of surrounding seawater (Proctor and Fuhrman 1991; Wommack and Colwell 2000; Weinbauer et al. 2009). Viral-induced cell lysis of the prokaryotic hosts releases organic matter that can further stimulate aggregation. While bacterial exo-enzymes (such as aminopeptidase) and dissolved extracellular proteases and nucleases (through cell lysis) within TEP may degrade viral capsid proteins and inactivate the viruses attached to aggregates (Simon et al. 2002; Bongiorni et al. 2007) in a similar manner to that found in seawater (although not always; Finiguerra et al. 2011) and sediment (Cliver and Herrmann 1972; Noble and Fuhrman 1997; Corinaldesi et al. 2010) and contribute to the disintegration of TEP aggregates. The magnitude to which

viruses are associated with different type, quality, size, and age of aggregates thus represents the sum of passive adsorption and the active production by the microbial community living on the aggregates (Weinbauer et al. 2009).

Grazing

Removal of viruses by heterotrophic nanoflagellate (HNF) grazing seem to play only a minor role in the removal of viruses (0.1% of virus community h^{-1}; Suttle and Chen 1992). Gonzalez and co-authors (1993) demonstrated that fluorescently labeled viruses were ingested and digested by cultured and natural HNFs at clearance rates of about 4% of those for bacterial prey, with rates depending on abundance and species of grazer and virus grazed. In contrast, Hadas et al. (2006) showed a removal of viruses by a coral reef sponge at an average efficiency of 23%, which may affect the virus-to-host ratios in the surrounding waters (depending on the removal rate of bacteria by the sponge) (Hadas et al. 2006). Enteric viruses have been found to accumulate in filter-feeding shell-fish (oysters, clams and mussels), revealing the potential of these organisms to dilute ambient virus concentrations (Rao et al. 1986; Enriquez et al. 1992; Faust et al. 2009). In addition to the direct removal of virus particles, organic particles present in seawater can also be grazed (Passow 2002). As these particles may have adsorbed viruses, the rate of viral removal by grazing might actually be underestimated.

Virus-specific selective grazing has the potential (when in high enough rates) to influence the specific virus-host dynamics and affect biodiversity. This effect can be further influenced by selective grazing on the virally infected host. Grazing of infected host cells will also alter the contact rate between virus and uninfected host cell by reducing the number of progeny viruses released from infected hosts (Ruardij et al. 2005). Preferential grazing of infected cells has been observed for *E. huxleyi* (Evans and Wilson 2008), but was unconfirmed using lower, more ecologically relevant algal abundances (Martínez-Martínez and Brussaard unpubl. data). Preferential grazing has also been hypothesized as a response to the inhibited release of star-like structures from infected *P. globosa* cells (Sheik et al. 2012). These rigid chitinous filaments are thought to provide a protective benefit against grazers (Zingone et al. 1999; Dutz and Koski 2006). In addition to increasing the susceptibility to grazers, this process directly reduces the availability of newly released PgVs by the release of hydrated flocculants, i.e., the intracellular precursors of the star-like structures

which exist in a fluid state within vesicles in the cell (Chretinennot-Dinet et al. 1997), which passively adsorb a high percentage of the viral progeny (~68%; Sheik et al. 2012). Through the use of nanoSIMS technology and single cell investigations, it has been revealed that viral infection of *P. globosa* results in a leakage or excretion of ^{13}C-labeled compounds prior to lysis which elicited an immediate response by the microbial community (Sheik et al. 2012). Leakage of intracellular material prior to lysis would provide a chemical trail which could be followed by chemotaxic grazers, thereby supporting a mechanism by which preferential grazing of infected cells could occur.

Grazing may also result in the release of viral antagonists. Upon grazing of *E. huxleyi* cells by *Oxyrrhis marina*, dimethyl sulfide (DMS) and acrylic acid was released which diminished the viral titers of EhV (Evans et al. 2006; Evans et al. 2007). While viral lysis of *E. huxleyi* also led to the production of DMS and acrylic acid the rate was reduced, which has been postulated to serve as a counter strategy of the virus to protect the infectivity of progeny viruses (Evans et al. 2006). The same mechanism might explain the earlier results by Thyrhaug and colleagues (2003) who demonstrated that the viral lysate of *E. huxleyi* contained inhibitory compounds that delayed cell lysis. The finding that the DMS concentrations differ between *E. huxleyi* strains (because of diverse intracellular dimethylsulfoniopropionate (DMSP) concentrations and DMSP lyase activities; Steinke et al. 1998), clearly illustrates how quickly multiple ecologically relevant factors complicate natural virus-host dynamics and promote co-existence of host and virus. Moreover, uninfected *E. huxleyi* cells subjected to viral glycosphingolipids, normally produced by infected *E. huxleyi* to induce the release of EhV progeny, promptly executed programmed cell death (Vardi et al. 2009). It has been suggested that during blooms of *E. huxleyi*, production of viral glycosphingolipids may act as a strategy to limit viral propagation through clonal host populations.

Host morphology

Grazing on heterotrophic prokaryotes can also lead to alterations in bacterial phenotypes (Pernthaler 2005). Filamentation, and the formation of microcolonies or biofilms reduces the likelihood that a specific prokaryotic host cell encounters a phage due to partial shading (Abedon 2012). On the other hand, if successfully infected, progeny viruses might have easy access to host in such an arrangement,

decreasing encounter time (Abedon 2012). However, the extent to which these processes influence viral encounter rate and host survival in the marine environment remain unknown, as detailed studies using marine phage-bacteria model systems are largely missing. Such information is essential as many marine bacteria are found in filaments or attached to particles (Tang et al. 2012).

It has been argued that not all host cell morphotypes of *E huxleyi* are equally sensitive to viral infection, and that exposure of *E. huxleyi* diploid cells to EhV would promote transition to the more infection resistant haploid phase, thereby ensuring that that genes of dominant diploid clones are passed on to the next generation in a virus-free environment (Frada et al. 2008). However, during a natural bloom of *E. huxleyi* both the diploid coccolith-bearing C-cells and the haploid scale-bearing S-cells were found to be virally infected (Brussaard et al. 1996). Another prymnesiophyte, *Phaeocystis,* also has a polymorphic life cycle phase which consists of solitary cells and cells embedded in a colony matrix. In this case, the haploid flagellated single cells are readily infected whereas the colonial stage protects against viral infection (Brussaard et al. 2005a; Jacobsen et al. 2007; Rousseau et al. 2007). Model evidence shows that the probability of a virus coming in contact with an individual colonial cell decreased with the size of the colony (Murray and Jackson 1992; Ruardij et al. 2005). *P. globosa* colony formation requires sufficient light for excess carbon fixation necessary to form the colonial matrix. Under reduced light conditions (20 µmol quanta m^{-2} s^{-1}) only exponential growth of the flagellated single cell morphotype was maintained and consequently viruses were able to control host abundance at low abundance and prevent bloom formation (Brussaard et al. 2005a; Brussaard et al. 2007).

Outlook

The present mini-review summarizes our current understanding of how environmental factors can influence virus dynamics and regulate virus-microbe host interactions. Marine viruses affect microbial host population abundance, community structure, and biogeochemical cycling in the ocean. Identifying environmental factors which regulate these processes is therefore essential to our understanding of global geochemical cycling and ecosystem functioning. This review illustrates a variety of factors in the marine environment which can influence viruses at all stages of their life cycle (Fig. 2). Moreover, it highlights the

fact that we are currently restricted by the availability of information regarding the effect that different environmental factors have on marine viruses and by the scarcity of reported rates. Factors which have been studied in more detail, e.g. UV radiation, provide useful insights into how viruses have multiple strategies by which they can adapt to their environment emphasizing the need for more detailed studies. We therefore encourage further research aimed at unraveling the role that the environment plays in regulating virus dynamics and virus-host interactions and recommend using both prokaryotic (both bacterial and archaeal) and eukaryotic virus model systems from a variety of locations and depths. We would also like to stress the importance of reporting the physicochemical and biological characteristics during field studies which is crucial for optimal interpretation. Moreover, standardization of approaches is warranted in order to allow comparison between different studies.

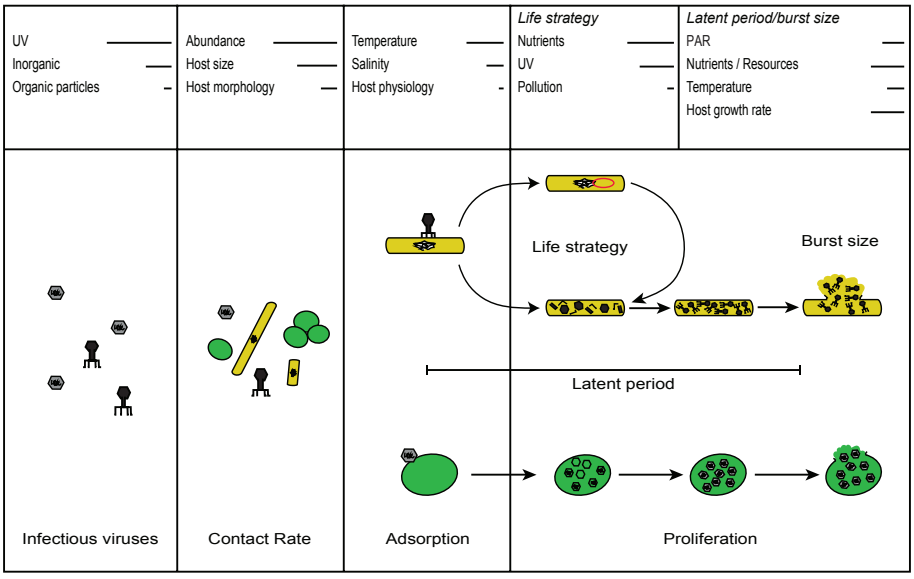

Figure 2. Conceptual diagram illustrating the influence of environmental factors on the different stages of virus life cycle. Horizontal bars indicate the amount of information known about the effect of the specific environmental variable on life cycle stage.

In order to fully understand the ecological relevance of environmental factors to viral ecology, the mechanisms behind losses of infectivity and absorption under natural conditions need to be elucidated. It may therefore be beneficial to consider extreme environments, where adaptations may be more apparent due to their

necessity for survival under such conditions, i.e., the stability of viral proteins in and around deep sea hydrothermal vents, resistance to extreme pH values near black smokes, and adaptation of viral G+C content to UV in the surface versus the deep ocean. In addition, some aspects which have not been addressed here, due to the scarcity of data, may have devastating consequences for marine ecosystems and should be considered in future endeavors. For example, lysogens have been found to be very sensitive to anthropogenic pollution. Pesticides, PCBs, trichloroethylene, PAHs, fuel oil and sunscreen, have all been reported to cause substantial prophage induction, even at low concentrations (Cochran et al. 1998; Paul et al. 1999; Danovaro et al. 2003). In addition, organic UV filters originating from sunscreen triggered lytic infection in prophages of symbiotic zooxanthellae resulting in the release of large amounts of coral mucous and complete bleaching within few days of exposure (Danovaro et al. 2008). There is also very little known about the stability of marine viruses to changes in pH, particularly for eukaryotic viruses. Although the few studies including pH sensitivity demonstrate that virus inactivation only occurred at relatively low pH values <7, pH could be an important environmental factor in some marine systems, as pH can vary both on local and seasonal scales (Hidaka and Ichida 1976; Borsheim 1993; Brussaard et al. 2004; Hofmann et al. 2011; Traving et al. 2013).

Finally, it is important to recognize that changing environmental conditions are most often multifactorial, thus shifting of one factor that influences viral infectivity, production or decay may change the sensitivity of the viruses to other factors. Therefore, it would be valuable to investigate interactions between different environmental stimuli. Especially considering that changing environmental conditions are themselves often comprised of multiple factors, i.e., alterations in sea surface temperature may be accompanied by changes in salinity, as well as UV exposure and nutrient limitation due to alterations in stratification. The lack of mechanistic understanding strongly restrains insight and predictive capacity of how, for example, global warming induced climate change (affecting multiple environmental variables) will influence viral production, activity and decay. Realizing the important ecological role viruses have for biodiversity and element fluxes, we would advocate for additional focus on this particular topic.

In summary, at this moment in time it is difficult to identify general patterns on how environmental factors regulate virus dynamics and virus-host interactions. In order to provide a broader overview which would permit viral ecologists to identify ecological functional patterns, virus-host systems need to be investigated in more

detail, across different types of environment and/or factors. While the current review is far from exhaustive, it provides a useful framework for identifying gaps in our understanding of (1) model host/virus systems (Table S1) and (2) field based testing which will likely lead to exciting new discoveries in marine viral ecology.

References

Abedon ST (2012) Spatial vulnerability: bacterial arrangements, microcolonies, and biofilms as responses to low rather than high phage densities. Viruses 4:663-687

Anderson RE, Brazelton WJ, Baross JA (2011) Is the genetic landscape of the deep subsurface biosphere affected by viruses? Frontiers in Microbiology 2:19. doi: 10.3389/fmicb.2011.00219

Baudoux A, Brussaard CPD (2005) Characterization on different viruses infecting the marine harmful algal bloom species *Phaeocystis globosa*. Virology 341:80-90

Baudoux AC, Brussaard CPD (2008) Influence of irradiance on virus-algal host interactions. Journal of Phycology 44:902-908

Bettarel Y, Bouvier T, Bouvier C, Carre C, Desnues A, Domaizon I, Jacquet S, Robin A, Sime-Ngando T (2011) Ecological traits of planktonic viruses and prokaryotes along a full-salinity gradient. FEMS Microbiology Ecology 76:360-372

Bettarel Y, Dolan JR, Hornak K, Lemee R, Masin M, Pedrotti μ, Rochelle-Newall E, Simek K, Sime-Ngando T (2002) Strong, weak, and missing links in a microbial community of the NW Mediterranean Sea. FEMS Microbiology Ecology 42:451-462

Bolnick DI, Amarasekare P, Araujo MS, Burger R, Levine JM, Novak M, Rudolf VHW, Schreiber SJ, Urban MC, Vasseur DA (2011) Why intraspecific trait variation matters in community ecology. Trends in Ecology and Evolution 26:183-192

Bongiorni L, Armeni M, Corinaldesi C, Dell'Anno A, Pusceddu A, Danovaro R (2007) Viruses, prokaryotes and biochemical composition of organic matter in different types of mucilage aggregates. Aquatic Microbial Ecology 49:15-23

Booth CR, Morrow JH, Coohill TP, Cullen JJ, Frederick JE, Hader DP, Holm Hansen O, Jeffrey WH, Mitchell DL, Neale PJ, Sobolev I, vanderLeun J, Worrest RC (1997) Impacts of solar UVR on aquatic microorganisms. Photochemistry and Photobiology 65:252-253

Borriss M, Helmke E, Hanschke R, Schweder T (2003) Isolation and characterization of marine psychrophilic phage-host systems from Artic sea ice. Extremophiles 7:377-384

Borsheim KY (1993) Native marine bacteriophages. FEMS Microbiology Ecology 102:141-159

Bowman JP, Gosink JJ, McCammon SA, Lewis TE, Nichols DS, Nichols PD, Skerratt JH, Staley JT, McMeekin TA (1998) *Colwellia demingiae* sp. nov., *Colwellia hornerae* sp. nov., *Colwellia rossensis* sp. nov. and *Colwellia psychrotropica* sp. nov.: psychrophilic Antarctic species with the ability to synthesize docosahexaenoic acid (22 : 6ω3). International Journal of Systematic Bacteriology48:1171-1180

Bratbak G, Egge JK, Heldal M (1993) Viral mortality of the marine alga *Emiliania huxleyi* (Haptophyceae) and termination of algal blooms. Marine Ecology Progress Series 93:39-48

Bratbak G, Jacobsen A, Heldal M, Nagasaki K, Thingstad F (1998) Virus production in *Phaeocystis pouchetii* and its relation to host cell growth and nutrition. Aquatic Microbial Ecology 16:1-9

Brown AD (1964) Aspects of bacterial response to ionic environment. Bacteriology Reviews 28:296-329

Brown CM, Campbell DA, Lawrence JE (2007) Resource dynamics during infection of *Micromonas pusilla* by virus MpV-Sp1. Environmental Microbiology 9:2720-2727

Brussaard CPD, Bratbak G, Baudoux AC, Ruardij P (2007) *Phaeocystis* and its interaction with viruses. Biogeochemistry 83:201-215

Brussaard CPD, Kempers RS, Kop AJ, Riegman R, Heldal M (1996) Virus-like particles in a summer bloom of *Emiliania huxleyi* in the North Sea. Aquatic Microbial Ecology 10:105-113

Brussaard CPD, Kuipers B, Veldhuis MJW (2005a) A mesocosm study of *Phaeocystis globosa* population dynamics. I. Regulatory role of viruses in bloom control. Harmful Algae 4:859-874

Brussaard CPD, Mari X, Van Bleijswijk JDL, Veldhuis MJW (2005b) A mesocosm study of *Phaeocystis globosa* (Prymnesiophyceae) population dynamics II. Significance for the microbial community. Harmful Algae 4:875-893

Brussaard CPD, Noordeloos AAM, Sandaa RA, Heldal M, Bratbak G (2004) Discovery of a dsRNA virus infecting the marine photosynthetic protist *Micromonas pusilla*. Virology 319:280-291

Cattaneo R, Rouviere C, Rassoulzadegan F, Weinbauer MG (2010) Association of marine viral and bacterial communities with reference black carbon particles under experimental conditions: an analysis with scanning electron, epifluorescence and confocal laser scanning microscopy. FEMS Microbiology Ecology 74:382-396

Chen PK, Citarella RV, Salazar O, Colwell RR (1966) Properties of two marine bacteriophages. Journal of Bacteriology 91:1136-1139

Chrétiennot-Dinet M-J, Giraud-Guille M-M, Vaulot D, Puteaux J-L, Saito Y, Chanzy H (1997) The chitinous nature of filaments ejected by *Phaeocystis* (Prymnesiophyceae). Journal of Phycology 33:666-672

Clasen JL, Elser JJ (2007) The effect of host *Chlorella* NC64A carbon : phosphorus ratio on the production of *Paramecium bursaria Chlorella Virus*-1. Freshwater Biology 52:112-122

Cliver DO, Herrmann JE (1972) Proteolytic and microbial inactivation of Enteroviruses. Water Research 6:797-805

Clokie MRJ, Mann NH (2006) Marine cyanophages and light. Environmental Microbiology 8:2074-2082

Clokie MRJ, Millard AD, Mehta JY, Mann NH (2006) Virus isolation studies suggest short-term variations in abundance in natural cyanophage populations of the Indian Ocean. Journal of the Marine Biological Association of the United Kingdom 86:499-505

Cochran PK, Kellogg CA, Paul JH (1998) Prophage induction of indigenous marine lysogenic bacteria by environmental pollutants. Marine Ecology Progress Series 164:125-133

Cochran PK, Paul JH (1998) Seasonal abundance of lysogenic bacteria in a subtropical estuary. Applied and Environmental Microbiology 64:2308-2312

Cordova A, Deserno M, Gelbart WM, Ben-Shaul A (2003) Osmotic shock and the strength of viral capsids. Biophysical Journal 85:70-74

Corinaldesi C, Dell'Anno A, Magagnini M, Danovaro R (2010) Viral decay and viral production rates in continental-shelf and deep-sea sediments of the Mediterranean Sea. FEMS Microbiology Ecology 72:208-218

Cotner JB, Biddanda BA (2002) Small players, large role: microbial influence on biogeochemical processes in pelagic aquatic ecosystems. Ecosystems 5:105-121

Cottrell MT, Suttle CA (1995) Dynamics of a lytic virus infecting the photosynthetic marine picoflagellate *Micromonas pusilla*. Limnology and Oceanography 40:730-739

Cseke C, Farkas GL (1979) Effect of light on the attachment of cyanophage AS-1 to *Anacystis nidulans*. Journal of Bacteriology 137:667-669

Danovaro R, Armeni M, Corinaldesi C, Mei ML (2003) Viruses and marine pollution. Marine Pollution Bulletin 46:301-304

Danovaro R, Bongiorni L, Corinaldesi C, Giovannelli D, Damiani E, Astolfi P, Greci L, Pusceddu A (2008) Sunscreens cause coral bleaching by promoting viral infections. Environmental Health Perspective 116:441-447

Dashman T, Stotzky G (1984) Adsorption and binding of peptides on homoionic montmorillonite and kaolinite. Soil Biology and Biochemistry 16:51-55

Daughney CJ, Chatellier X, Chan A, Kenward P, Fortin D, Suttle CA, Fowle DA (2004) Adsorption and precipitation of iron from seawater on a marine bacteriophage (PWH3A-P1). Marine Chemistry 91:101-115

Delisle AL, Levin RE (1972a) Characteristics of three phages infectious for psychrophilic fishery isolates of *Pseudomonas putrefaciens*. Antonie van Leeuwenhoek 38:1-8

Delisle AL, Levin RE (1972b) Effect of temperature on an obligately psychrophilic phage-host system of *Pseudomonas putrefaciens*. Antonie van Leeuwenhoek 38:9-15

Dutz J, Koski M (2006) Trophic significance of solitary cells of the prymnesiophyte *Phaeocystis globosa* depends on cell type. Limnology and Oceanography 51:1230-1238

Enriquez R, Frösner GG, Hochstein-Mintzel V, Riedemann S, Reinhardt G (1992) Accumulation and persistence of hepatitis A virus in mussels. Journal of Medical Virology 37:174-179

Evans C, Kadner SV, Darroch LJ, Wilson WH, Liss PS, Malin G (2007) The relative significance of viral lysis and microzooplankton grazing as pathways of dimethylsulfoniopropionate (DMSP) cleavage: an *Emiliania huxleyi* culture study. Limnology and Oceanography 52:1036-1045

Evans C, Malin G, Wilson WH, Liss PS (2006) Infectious titers of *Emiliania huxleyi* virus 86 are reduced by exposure to millimolar dimethyl sulfide and acrylic acid. Limnology and Oceanography 51:2468-2471

Evans C, Wilson WH (2008) Preferential grazing of *Oxyrrhis marina* on virus-infected *Emiliania huxleyi*. Limnology and Oceanography 53:2035-2040

Evilevitch A, Fang LT, Yoffe AM, Castelnovo M, Rau DC, Parsegian VA, Gelbart WM, Knobler CM (2008) Effects of salt concentrations and bending energy on the extent of ejection of phage genomes. Biophysical Journal 94:1110-1120

Farmer III JJ, Janda JM (2005) Vibrionaceae. In: Brenner DJ, Krieg NR, Staley JR (eds) Bergey's Manual of Systematic Baceriology: The Proteobacteria, vol 2. Springer-Verlag, New York

Faust C, Stallknecht D, Swayne D (2009) Filter-feeding bivalves can remove avian influenza viruses from water and reduce infectivity. Proceedings from the Royal Society B: Biological Sciences 276:3727-3735

Finiguerra MB, Escribano DF, Taylor GT (2011) Light-independent mechanisms of virion inactivation in coastal marine systems. Hydrobiologia 665:51-66

Frada M, Probert I, Allen MJ, Wilson WH, de Vargas C (2008) The "Cheshire Cat" escape strategy of the coccolithophore *Emiliania huxleyi* in response to viral infection. Proceedings of the National Academy of Sciences of the United States of America 105:15944-15949

Furuta M, Schrader JO, Schrader HS, Kokjohn TA, Nyaga S, McCullough AK, Lloyd RS, Burbank DE, Landstein D, Lane L, VanEtten JL (1997) Chlorella virus PBCV-1 encodes a homolog of the bacteriophage T4 UV damage repair gene denV. Applied and Environmental Microbiology 63:1551-1556

Garza DR, Suttle CA (1998) The effect of cyanophages on the mortality of *Synechococcus* spp. and selection for UV resistant viral communities. Microbial Ecology 36:281-292

Goldsmith DB, Crosti G, Dwivedi B, McDaniel LD, Varsani A, Suttle CA, Weinbauer MG, Sandaa RA, Breitbart M (2011) Development of phoH as a novel signature gene for assessing marine phage diversity. Applied and Environmental Microbiology 77:7730-7739

Graneli E, Turner JT (eds) (2007) Ecology of Harmful Algae. Springer, Berlin

Hadas E, Marie D, Shpigel M, Ilan M (2006) Virus predation by sponges is a new nutrient-flow pathway in coral reef food webs. Limnology and Oceanography 51:1548-1550

Hardies SC, Hwang YJ, Hwang CY, Jang GI, Cho BC (2013) Morphology, physiological characteristics, and complete sequence of marine bacteriophage ϕRIO-1 infecting *Pseudoalteromonas marina*. Journal of Virology 87:9189-9198

Hickey DA, Singer GAC (2004) Genomic and proteomic adaptations to growth at high temperature. Genome Biology 5

Hidaka T, Ichida K (1976) Properties of a marine RNA-containing bacteriophage. Memoirs of the Faculty of Fisheries, Kagoshima University 25:77-89

Hofmann GE, Smith JE, Johnson KS, Send U, Levin LA (2011) High-frequency dynamics of ocean pH: a multi-ecosystem comparison. PLOS One 6:e28983. doi: 10.1371/journal.pone.0028983

Hotze EM, Badireddy AR, Chellam S, Wiesner MR (2009) Mechanisms of bacteriophage inactivation via singlet oxygen generation in UV illuminated fullerol suspensions. Environmental Science and Technology 43:6639-6645

Jacobsen A, Larsen A, Martinez-Martinez J, Verity PG, Frischer ME (2007) Susceptibility of colonies and colonial cells of *Phaeocystis pouchetii* (Haptophyta) to viral infection. Aquatic Microbial Ecology 48:105-112

Jacquet S, Bratbak G (2003) Effects of ultraviolet radiation on marine virus-phytoplankton interactions. FEMS Microbiology Ecology 44:279-289

Jacquet S, Heldal M, Iglesias-Rodriguez D, Larsen A, Wilson W, Bratbak G (2002) Flow cytometric analysis of an *Emiliana huxleyi* bloom terminated by viral infection. Aquatic Microbial Ecology 27:111-124

Jia Y, Shan JY, Millard A, Clokie MRJ, Mann NH (2010) Light-dependent adsorption of photosynthetic cyanophages to *Synechococcus* sp WH7803. FEMS Microbiology Letters 310:120-126

Jian H, Xiao X, Wang F (2013) Role of filamentous phage SW1 in regulating the lateral flagella of *Shewanella piezotolerans* strain WP3 at low temperatures. Applied and Environmental Microbiology 79:7101-7109

Jiang SC, Paul JH (1998) Significance of lysogeny in the marine environment: studies with isolates and a model of lysogenic phage production. Microbial Ecology 35:235-243

Johnson RM (1968) Characteristics of a marine vibrio-bacteriophage system. Journal of the Arizona Academy of Science 5:28-33

Juneau P, Lawrence JE, Suttle CA, Harrison PJ (2003) Effects of viral infection on photosynthetic processes in the bloom-forming alga *Heterosigma akashiwo*. Aquatic Microbial Ecology 31:9-17

Kapuscinski RB, Mitchell R (1980) Processes controlling virus inactivation in coastal waters. Water Research 14:363-371

Kellogg CA, Paul JH (2002) Degree of ultraviolet radiation damage and repair capabilities are related to G+C content in marine vibriophages. Aquatic Microbial Ecology 27:13-20

Kelly L, Ding H, Huang KH, Osburne MS, Chisholm SW (2013) Genetic diversity in cultured and wild marine cyanomyoviruses reveals phosphorus stress as a strong selective agent. The ISME Journal 7:1827-1841

Keynan A, Nealson K, Sideropo.H, Hastings JW (1974) Marine transducing bacteriophage attacking a luminous bacterium. Journal of Virology 14:333-340

Kimura M, Jia Z, Nakayama N, Asakawa S (2008) Ecology of viruses in soils: past, present and future perspectives. Soil Science and Plant Nutrition 54:1-32

Kukkaro P, Bamford DH (2009) Virus-host interactions in environments with a wide range of ionic strengths. Environmental Microbiology Reports 1:71-77

Lawrence JE, Suttle CA (2004) Effect of viral infection on sinking rates of *Heterosigma akashiwo* and its implications for bloom termination. Aquatic Microbial Ecology 37:1-7

Levisohn R, Moreland J, Nealson KH (1987) Isolation and characterization of a generalized transducing phage for the marine luminous bacterium *Vibrio fischeri* MJ-1. Journal of General Microbiology 133:1577-1582

Lindell D, Jaffe JD, Johnson ZI, Church GM, Chisholm SW (2005) Photosynthesis genes in marine viruses yield proteins during host infection. Nature 438:86-89

Lipson SM, Stotzky G (1984) Effects of proteins on reovirus adsorption to clay minerals. Applied and Environmental Microbiology 48:525-530

Liu B, Wu SJ, Song Q, Zhang XB, Xie LH (2006) Two novel bacteriophages of thermophilic bacteria isolated from deep-sea hydrothermal fields. Current Microbiology 53:163-166

Lytle CD, Sagripanti JL (2005) Predicted inactivation of viruses of relevance to biodefense by solar radiation. Journal of Virology 79:14244-14252

Maat DS, Crawfurd KJ, Timmermans KR, Brussaard CPD (2014) Elevated partial CO_2 pressure and phosphate limitation favor *Micromonas pusilla* through stimulated growth and reduced viral impact. Applied and Environmental Microbiology 80:3119-3127

Martinez-Martinez J, Brussaard CPD unpublished data.

Middelboe M (2000) Bacterial growth rate and marine virus-host dynamics. Microbial Ecology 40:114-124

Mitchell R, Jannasch HW (1969) Processes controlling virus inactivation in seawater. Environmental Science and Technology 3:941-943

Moebus K (1996) Marine bacteriophage reproduction under nutrient-limited growth of host bacteria. I. Investigations with six phage-host systems. Marine Ecology Progress Series 144:1-12

Monier A, Welsh RM, Gentemann C, Weinstock G, Eisen JA, Worden AZ (2011) Phosphate transporters in marine phytoplankton and their viruses: cross-domain commonalities in viral-host gene exchanges. Environmental Microbiology 14:162-176

Motegi C, Nagata T (2007) Enhancement of viral production by addition of nitrogen or nitrogen plus carbon in subtropical surface waters of the South Pacific. Aquatic Microbial Ecology 48:27-34

Murray AG, Jackson GA (1992) Viral dynamics: a model of the effects of size, shape, motion and abundance of single-celled planktonic organisms and other particles. Marine Ecology Progress Series 89:103-116

Nagasaki K, Shirai Y, Tomaru Y, Nishida K, Pietrokovski S (2005) Algal viruses with distinct intraspecies host specificities include identical intein elements. Applied and Environmental Microbiology 71:3599-3607

Nagasaki K, Yamaguchi M (1998) Effect of temperature on the algicidal activity and the stability of HaV (*Heterosigma akashiwo* virus). Aquatic Microbial Ecology 15:211-216

Noble RT, Fuhrman JA (1997) Virus decay and its causes in coastal waters. Applied and Environmental Microbiology 63:77-83

Orgata H, Ray J, Toyoda K, Sandaa R-A, Nagasaki K, Bratbak G, Claverie J-M (2011) Two new subfamilies of DNA mismatch repair proteins (MutS) specifically abundant in the marine environment. The ISME Journal 5:1143-1151

Parada V, Herndl GJ, Weinbauer MG (2006) Viral burst size of heterotrophic prokaryotes in aquatic systems. Journal of the Marine Biological Association of the United Kingdom 86:613-621

Passow U (2002) Transparent exopolymer particles (TEP) in aquatic environments. Progress in Oceanography55:287-333

Paul JH, Cochran PK, Jiang SC (1999) Lysogeny and transduction in the marine environment. In: Bell CR, Brylinsky M, Johnson-Green P (eds) Microbial Biosystems: New Frontiers. Atlantic Canada Society for Microbial Ecology, Halifax, Canada

Payet JP, Suttle CA (2013) To kill or not to kill: the balance between lytic and lysogenic viral infection is driven by trophic status. Limnology and Oceanography 58:465-474

Paytan A, McLaughlin K (2007) The oceanic phosphorus cycle. Chemical Reviews 107:563-576

Pernthaler J (2005) Predation on prokaryotes in the water column and its ecological implications. Nature Reviews Microbiology 3:537-546

Porter K, Kukkaro P, Bamford JKH, Bath C, Kivela HM, Dyall-Smith ML, Bamford DH (2005) SHI: A novel, spherical halovirus isolated from an Australian hypersaline lake. Virology 335:22-33

Proctor LM, Fuhrman JA (1991) Roles of viral infection in organic particle flux. Marine Ecology Progress Series 69:133-142

Proctor LM, Okubo A, Fuhrman JA (1993) Calibrating estimates of phage-induced mortality in marine bacteria: ultrastructural studies of marine bacteriophage development from one-step growth experiments. Microbial Ecology 25:161-182

Rao VC, Metcalf TG, Melnick JL (1986) Human viruses in sediments, sludges, and soils. Bulletin of the World Health Organization 64:1-13

Rousseau V, Chrétiennot-Dinet MJ, Jacobsen A, Verity P, Whipple S (2007) The life cycle of *Phaeocystis*: state of knowledge and presumptive role in ecology. Biogeochemistry 83:29-47

Ruardij P, Veldhuis MJW, Brussaard CPD (2005) Modeling the bloom dynamics of the polymorphic phytoplankter *Phaeocystis globosa*: impact of grazers and viruses. Harmful Algae 4:941-963

Santini S, Jeudy S, Bartoli J, Poirot O, Lescot M, Abergel C, Barbe V, Wommack KE, Noordeloos AAM, Brussaard CPD, Claverie J-M (2013) Genome of *Phaeocystis globosa* virus PgV-16T highlights the common ancestry of the largest known DNA viruses infecting eukaryotes. Proceedings from the National Academy of Sciences of the United States of America 110:10800-10805

Santos F, Yarza P, Parro V, Meseguer I, Rosselló-Móra R, Antón J (2012) Culture-independent approaches for studying viruses from hypersaline environments. Applied and Environmental Microbiology 78:1635-1643

Selinger RLB, Wang Z, Gelbart WM, Ben-Shaul A (1991) Statistical-thermodynamic approach to fracture. Physical Review A 43:4396-4400

Shaffer JJ, Jacobsen LM, Schrader JO, Lee KW, Martin EL, Kokjohn TA (1999) Characterization of *Pseudomonas aeruginosa* bacteriophage UNL-1, a bacterial virus with a novel UV-A-inducible DNA damage reactivation phenotype. Applied and Environmental Microbiology 65:2606-2613

Sheik AR, Brussaard CPD, Lavik G, Foster RA, Musat N, Adam B, Kuypers MMM (2012) Viral infection of *Phaeocystis globosa* impedes release of chitinous star-like structures: quantification using single cell approaches. Environmental Microbiology 15:1441-1451

Shirai Y, Tomaru Y, Takao Y, Suzuki H, Nagumo T, Nagasaki K (2008) Isolation and characterization of a single-stranded RNA virus infecting the marine planktonic diatom *Chaetoceros tenuissimus* Meunier. Applied and Environmental Microbiology 74:4022-4027

Simon M, Grossart HP, Schweitzer B, Ploug H (2002) Microbial ecology of organic aggregates in aquatic ecosystems. Aquatic Microbial Ecology 28:175-211

Sorensen G (2009) The role of the virus-phytoplankton system in marine biogeochemical cycling: possible impacts of climate change. The Plymouth Student Scientist 2:289-302

Steinke M, Wolfe GV, Kirst GO (1998) Partial characterisation of dimethylsulfoniopropionate (DMSP) lyase isozymes in 6 strains of *Emiliania huxleyi*. Marine Ecology Progress Series 175:215-225

Sullivan MB, Coleman ML, Weigele P, Rohwer F, Chisholm SW (2005) Three *Prochlorococcus* cyanophage genomes: signature features and ecological interpretations. PLOS Biology 3:790-806

Sullivan MB, Huang KH, Ignacio-Espinoza JC, Berlin AM, Kelly L, Weigele PR, DeFrancesco AS, Kern SE, Thompson LR, Young S, Yandava C, Fu R, Krastins B, Chase M, Sarracino D, Osburne MS, Henn MR, Chisholm SW (2010) Genomic analysis of oceanic cyanobacterial myoviruses compared with T4-like myoviruses from diverse hosts and environments. Environmental Microbiology 12:3035-3056

Sullivan MB, Lindell D, Lee JA, Thompson LR, Bielawski JP, Chisholm SW (2006) Prevalence and evolution of core photosystem II genes in marine cyanobacterial viruses and their hosts. PLOS Biology 4:1344-1357

Suttle CA (2000) Viral infection of cyanobacteria and eukaryotic algae. In: Hurst CJ (ed) Viral Ecology. Academic Press, San Diego

Suttle CA (2007) Marine viruses - major players in the global ecosystem. Nature Reviews 5:801-812

Suttle CA, Chan AM (1993) Marine cyanophages infecting oceanic and coastal strains of *Synechococcus*: abundance, morphology, cross-infectivity and growth characteristics. Marine Ecology Progress Series 92:99-109

Suttle CA, Chan AM (1994) Dynamics and distribution of cyanophages and their effect on marine *Synechococcus* Spp. Applied and Environmental Microbiology 60:3167-3174

Suttle CA, Chen F (1992) Mechanisms and rates of decay of marine viruses in seawater. Applied and Environmental Microbiology 58:3721-3729

Tang X, Chao J, Chen D, Shao K, Gao G (2012) Organic-aggregate-attached bacteria in aquatic ecosystems: abundance, diversity, community dynamics and function. In: Marcelli PM (ed) Oceanography. InTech Open Access Publisher

Templeton MR, Andrews RC, Hofmann R (2005) Inactivation of particle-associated viral surrogates by ultraviolet light. Water Research 39:3487-3500

Thyrhaug R, Larsen A, Brussaard CPD, Bratbak G (2002) Cell cycle dependent virus production in marine phytoplankton. Journal of Phycology 38:338-343

Tomaru Y, Fujii N, Oda S, Toyoda K, Nagasaki K (2011a) Dynamics of diatom viruses on the western coast of Japan. Aquatic Microbial Ecology 63:223-230

Tomaru Y, Katanozaka N, Nishida K, Shirai Y, Tarutani K, Yamaguchi M, Nagasaki K (2004) Isolation and characterization of two distinct types of HcRNAV, a single-stranded RNA virus infecting the bivalve-killing microalga *Heterocapsa circularisquama*. Aquatic Microbial Ecology 34:207-218

Tomaru Y, Mizumoto H, Takao Y, Nagasaki K (2009a) Co-occurrence of DNA- and RNA-viruses infecting the bloom-forming dinoflagellate *Heterocapsa circularisquama*, on the Japan coast. Plankton and Benthos Research 4:129-134

Tomaru Y, Shirai Y, Suzuki H, Nagumo T, Nagasaki K (2008) Isolation and characterization of a new single-stranded DNA virus infecting the cosmopolitan marine diatom *Chaetoceros debilis*. Aquatic Microbial Ecology 50:103-112

Tomaru Y, Takao Y, Suzuki H, Nagumo T, Koike K, Nagasaki K (2011b) Isolation and characterization of a single-stranded DNA virus infecting *Chaetoceros lorenzianus* Grunow. Applied and Environmental Microbiology 77:5285-5293

Tomaru Y, Takao Y, Suzuki H, Nagumo T, Nagasaki K (2009b) Isolation and characerization of a single-stranded RNA virus infecting the bloom-forming diatom *Chaetoceros socialis*. Applied and Environmental Microbiology 75:2375-2381

Tomaru Y, Tanabe H, Yamanaka S, Nagasaki K (2005) Effects of temperature and light on stability of microalgal viruses, HaV, HcV, and HcRNAV. Plankton Biology and Ecology 52:1-6

Tomaru Y, Toyoda K, Suzuki H, Nagumo T, Kimura K, Takao Y (2013) New single-stranded DNA virus with a unique genomic structure that infects marine diatom *Chaetoceros setoensis*. Scientific Reports 3. doi: 10.1038/srep03337

Torsvik T, Dundas ID (1980) Persisting phage infection in *Halobacterium salinarium* str. 1. Journal of General Virology 47:29-36

Traving SJ, Clokie MRJ, Middelboe M (2013) Increased acidification has profound effect on the interactions between the cyanobacterium *Synechococcus* sp. WH7803 and its viruses. FEMS Microbiology Ecology

Valentine DL (2007) Adaptations to energy stress dictate the ecology and evolution of the Archaea. Nature Reviews Microbiology 5:316-323

Van Etten JL, Burbank DE, Xia Y, Meints RH (1983) Growth cycle of a virus, PBCV-1, that infects *Chlorella*-like algae. Virology 126:117-125

Vardi A, Van Mooy BAS, Fredricks HF, Popendorf KJ, Ossolinski JE, Haramaty L, Bidle KD (2009) Viral glycosphingolipids induce lytic infection and cell death in marine phytoplankton. Science 326:861-865

Vettori C, Gallori E, Stotzky G (2000) Clay minerals protect bacteriophage PBS1 of *Bacillus subtilis* against inactivation and loss of transducing ability by UV radiation. Canadian Journal of Microbiology 46:770-773

Wait DA, Sobsey MD (1983) Method for recovery of enteric viruses from estuarine sediments with chaotrophic agents. Applied and Environmental Microbiology 46:379-385

Wang F, Wang FP, Li Q, Xiao X (2007) A novel filamentous phage from the deep-sea bacterium *Shewanella piezotolerans* WP3 is induced at low temperature. Journal of Bacteriology 189:7151-7153

Wang FP, Wang P, Chen MX, Xiao X (2004) Isolation of extremophiles with the detection and retrieval of Shewanella strains in deep-sea sediments from the west Pacific. Extremophiles 8:165-168

Waters P, Lloyd D (1985) Salt, pH and temperature dependencies of growth and bioluminescence of three species of luminous bacteria analysed on gradient plates. Journal of General Microbiology 131:2865-2869

Waters RE, Chan AT (1982) *Micromonas pusilla* Virus: the virus growth cycle and associated physiological events within the host cells; host range mutation. Journal of General Virology 63:199-206

Wei HC, Ca QY, Rahn R, Zhang XS, Wang Y, Lebwohl M (1998) DNA structural integrity and base composition affect ultraviolet light-induced oxidative DNA damage. Biochemistry 37:6485-6490

Weinbauer MG, Bettarel Y, Cattaneo R, Luef B, Maier C, Motegi C, Peduzzi P, Mari X (2009) Viral ecology of organic and inorganic particles in aquatic systems: avenues for further research. Aquatic Microbial Ecology 57:321-341

Weinbauer MG, Brettar I, Hofle MG (2003) Lysogeny and virus-induced mortality of bacterioplankton in surface, deep, and anoxic marine waters. Limnology and Oceanography 48:1457-1465

Weinbauer MG, Suttle CA (1996) Potential significance of lysogeny to bacteriophage production and bacterial mortality in coastal waters of the Gulf of Mexico. Applied and Environmental Microbiology 62:4374-4380

Weinbauer MG, Suttle CA (1999) Lysogeny and prophage induction in coastal and offshore bacterial communities. Aquatic Microbial Ecology 18:217-225

Weinbauer MG, Wilhelm SW, Suttle CA, Garza DR (1997) Photoreactivation compensates for UV damage and restores infectivity to natural marine virus communities. Applied and Environmental Microbiology 63:2200-2205

Weinbauer MG, Wilhelm SW, Suttle CA, Pledger RJ, Mitchell DL (1999) Sunlight-induced DNA damage and resistance in natural viral communities. Aquatic Microbial Ecology 17:111-120

Wells LE, Deming JW (2006a) Characterization of a cold-active bacteriophage on two psychrophilic marine hosts. Aquatic Microbial Ecology 45:15-29

Wells LE, Deming JW (2006b) Effects of temperature, salinity and clay particles on inactivation and decay of cold-active marine Bacteriophage 9A. Aquatic Microbial Ecology 45:31-39

White PA, Kalff J, Rasmussen JB, Gasol JM (1991) The effect of temperature and algal biomass on bacterial production and specific growth-rate in fresh water and marine habitats. Microbial Ecology 21:99-118

Whitehead RF, de Mora SJ, Demers S (2000) Enhanced UV radiation - a new problem for the marine environment. In: de Mora S, Demers S, Vernet M (eds) The Effects of UV Radiation in the Marine Environment. Cambridge University Press, Cambridge, UK

Wiebe WJ, Liston J (1968) Isolation and characterization of a marine bacteriophage. Marine Biology 1:244-249

Wiebe WJ, Sheldon WM, Pomeroy LR (1992) Bacterial growth in the cold: evidence for an enhanced substrate requirement. Applied and Environmental Microbiology 58:359-364

Wigginton KR, Menin L, Montoya JP, Kohn T (2010) Oxidation of virus proteins during UV254 and singlet oxygen mediated inactivation. Environmental Science and Technology 44:5437-5443

Wigginton KR, Pecson BM, Sigstam T, Bosshard F (2012) Virus inactivation mechanisms: impact of disinfection on virus function and structural integrity. Environmental Science and Technology 46:12069-12078

Wikner J, Vallino JJ, Steward GF, Smith DC, Azam F (1993) Nucleic acids from the host bacterium as a major source of nucleotides for three marine bacteriophages. FEMS Microbiology Ecology 12:237-248

Wilcox RM, Fuhrman JA (1994) Bacterial viruses in coastal seawater: lytic rather than lysogenic production. Marine Ecology Progress Series 114:35-45

Wilhelm SW, Jeffrey WH, Dean AL, Meador J, Pakulski JD, Mitchell DL (2003) UV radiation induced DNA damage in marine viruses along a latitudinal gradient in the southeastern Pacific Ocean. Aquatic Microbial Ecology 31:1-8

Wilhelm SW, Weinbauer MG, Suttle CA, Jeffrey WH (1998a) The role of sunlight in the removal and repair of viruses in the sea. Limnology and Oceanography 43:586-592

Wilhelm SW, Weinbauer MG, Suttle CA, Pledger RJ, Mitchell DL (1998b) Measurements of DNA damage and photoreactivation imply that most viruses in marine surface waters are infective. Aquatic Microbial Ecology 14:215-222

Williamson SJ, Cary SC, Williamson KE, Helton RR, Bench SR, Winget D, Wommack KE (2008) Lysogenic virus-host interactions predominate at deep-sea diffuse-flow hydrothermal vents. The ISME Journal 2:1112-1121

Williamson SJ, Houchin LA, McDaniel L, Paul JH (2002) Seasonal variation in lysogeny as depicted by prophage induction in Tampa Bay, Florida. Applied and Environmental Microbiology 68:4307-4314

Williamson SJ, Paul JH (2006) Environmental factors that influence the transition from lysogenic to lytic existence in the phi HSIC/*Listonella pelagia* marine phage-host system. Microbial Ecology 52:217-225

Wilson WH, Carr NG, Mann NH (1996) The effect of phosphate status on the kinetics of cyanophage infection in the oceanic cyanobacterium *Synechococcus* sp WH7803. Journal of Phycology 32:506-516

Wilson WH, Turner S, Mann NH (1998) Population dynamics of phytoplankton and viruses in a phosphate-limited mesocosm and their effect on DMSP and DMS production. Estuarine, Coastal and Shelf Science 46:49-59

Winter C, Herndl GJ, Weinbauer MG (2004) Diel cycles in viral infection of bacterioplankton in the North Sea. Aquatic Microbial Ecology 35:207-216

Wommack KE, Colwell RR (2000) Virioplankton: viruses in aquatic ecosystems. Microbiology and Molecular Biology Reviews 64:69-114

Wommack KE, Hill RT, Muller TA, Colwell RR (1996) Effects of sunlight on bacteriophage viability and structure. Applied and Environmental Microbiology 62:1336-1341

Yamaguchi M, Itakura S, Nagasaki K, Matsuyama Y, Uchida T, Imai I (1997) Effects of temperature and salinity on the growth of the red tide flagellates *Heterocapsa circularisquama* (Dinophyceae) and *Chattonella verruculosa* (Raphidophyceae). Journal of Plankton Research 19:1167-1174

Zachary A (1976) Physiology and ecology of bacteriophages of the marine bacteruim *Beneckea natriegens*: salinity. Applied and Environmental Microbiology 31:415-422

Zingone A, Chretinnot-Dinet M-J, Lange M, Medlin L (1999) Morphological and genetic characterization of *Phaeocystis cordata* and *P. Jahnii* (Prymesiophyceae), two new species from the Mediterranean Sea. Journal of Phycology 35:1322-1337

Supporting Information

Table S1. Overview of marine viruses discussed in the review sections of temperature, salinity, and UV (Table 1-3).

Host	Virus	Family	genome type	genome size (kb)	Shape	Capsid size (nm)	Tail (W x L)	Size of major polypeptides (kDa	Latent period (h)	Particle accumulation site and pattern	Burst size (cell^{-1})	Strain specificity	Source
Eukaryote Algal Viruses													
Phaeocystis globosa (Pg-I)	Group I: PgV-06, -07T, -09T, -12T, -13T, -T14	*Phycodnaviridae*	dsDNA	466 ± 4	icosahedral l	153 ± 8		257, 161, 111, 52	10	cytoplasm	248 ± 120	4/12	water, North Sea [1]
P. globosa (Pg-I)	Group IIA:PgV-03T, -05T	*Phycodnaviridae*	dsDNA	177 ± 3	icosahedral	106 ± 7		119, 99, 75, 44	12	cytoplasm	344 ± 100	5/12	water, North Sea[1]
P. globosa (Pg-I)	Group IIB:PgV-04T, -10T, -11T	*Phycodnaviridae*	dsDNA	177 ± 3	icosahedral	106 ± 7		119, 99, 75, 44	16	cytoplasm	382 ± 26	5/12	water, North Sea[1]
P. globosa (Pg-I)	Group IIC:PgV-01T	*Phycodnaviridae*	dsDNA	177 ± 3	icosahedral	106 ± 7		119, 99, 75, 44	16	cytoplasm	378	12/12	water, North Sea[1]
Micromonas pusilla (LAC 38)	MpRNAV-01B	*Reoviridae*	Segmented, dsRNA	25.5	icosahedral	65-80		120, 95, 67, 53, 32	36	cytoplasm	460-520	1/6	coastal, water, Norway[2]
M. pusilla (LAC 38)	MpV-03T, 06T, 08-12T, 14T, R3-4, B4-5[3]	*Phycodnaviridae*	dsDNA		icosahedral								water, North Sea
M. pusilla (CCMP 1545)	MpV-02T, 04-05T, 07T, 13T, R1-R2, SP1[3]	*Phycodnaviridae*	dsDNA		icosahedral								water, North Sea
M. pusilla (27)	SP1	*Phycodnaviridae*	dsDNA										coastal water, Scripps pier [4]
Chaetoceros debilis (Ch48)	CdebDNAV18		ssDNA	unknown	icosahedral	30 ± 2		41, 37.5	12-24	cytoplasm, random	55 [a]	3/4	water and sediment, Japan[5]

Table S1. Continued.

Host	Virus	Family	genome type	genome size (kb)	Shape	Capsid size (nm)	Tail (W x L)	Size of major polypeptides (kDa	Latent period (h)	Particle accumulation site and pattern	Burst size (cell^{-1})	Strain specificity	Source
C. lorenzianus (IT-Dia51)	ClorDNAV	*Bacilladnavirus*	ssDNA, circular and dsDNA linear	5.9, 0.9	icosahedral	32 ± 2			<48	nucleus, random	22,000 [a]		coastal, water, Hiroshima Bay[6]
C. socialis	CsfrRNAV	*Bacilladnavirus*	ssRNA	9.5	icosahedral	22		32, 28, 25	< 48	cytoplasm, random	66 [a]		coastal, water, Hiroshima Bay [8]
C. tenuissimus	CtenRNAV01		ssRNA, circular?	9.4	icosahedral	31 ±2		33.5, 31.5, 30.0	<24	cytoplasm, crystalline arrays	12,000 [a]		water, Ariake Sound
Heterosigma. akashiwo (93616)	HaV01		dsDNA	294 [9]	icosahedral [10]	202 ± 6 [10]			30-33 [11]		770 [11]	13/18 [12]	coastal, water, Nomi Bay[10]
H. akashiwo (H93616)	HaV08		dsDNA										
H. akashiwo (H93616)	HaV53		dsDNA										
H. akashiwo (H93616)	HaRNAV		ssRNA	9100 nt [13]	icosahedral [13]	25 [13]		33.9, 29.0, 26.1, 24.6, 24.0 [13]	29 [14]	cytoplasm, crystalline arrays [13]	21,000 [14]		river plume, Strait of Georgia [13]
Heterocapsa circularisquama (HU9433-P)	HcV03		dsDNA		icosahedral	197 ± 8			48-72	cytoplasm, viroplasm	~1300	18/18	coastal, water, Japan [15]
H. circularisquama (HU9433-P)	HcV05		dsDNA										coastal, water, Japan [16]
H. circularisquama (HU9433-P)	HcV08		dsDNA									12/14	coastal, water, Japan [16]

Table S1. Continued.

Host	Virus	Family	genome type	genome size (kb)	Shape	Capsid size (nm)	Tail (W x L)	Size of major polypeptides (kDa	Latent period (h)	Particle accumulation site and pattern	Burst size (cell^{-1})	Strain specificity	Source
H. circularisquama (HU9433-P)	HcV10		dsDNA										coastal, water, Japan [16]
H. circularisquama (HU9433-P)	HcRNAV34		ssRNA	4.4 [17]	icosahedral	30 ± 2		38 [17]	24-48	cytoplasm, crystalline arrays or random	21000 [a]	2/4 [b]	coastal, water, Japan [17]
H. circularisquama (HCLG-1)	HcRNAV109		ssRNA	4.4 [17]	icosahedral	30 ± 2		38 [17]	24-48	cytoplasm, crystalline arrays or random	3400 [a]	2/4 [b]	coastal, water, Japan [17]
Bacteriophages													
Pseudomonas putrefaciens P19X	Phage 27		dsDNA		icosahedral	77	14 x 176						coastal, water [18]
P. putrefaciens P13	Phage 23		dsDNA		icosahedral	76	?						fish [18]
P. putrefaciens P2	Phage 25F		dsDNA		icosahedral	55	14 x 176						coastal, water [18]
Pseudoalteromonas marina	φRIO-1	*Podoviridae*	dsDNA		icosahedral	51	12 x 15		1		118	1/2	water, East Sea [19]
Vibrio sp.	unknown		dsDNA		hexagonal	60	?						Deep, water, mud, Indian Ocean [20]
Vibrio (Beneckea) harveyi	h*v*-1		dsDNA	43.9	icosahedral	70	12 x 220		0.75		100		squid/mud, Atlantic [21]
V. natriegens	nt-1	*Myoviridae* [22]	dsDNA		prolate	120	? X 110						estuary water, Chesapeake Bay [23]
V. natriegens	nt-6		dsDNA		icosahedral	60	? X 40						estuary water, Chesapeake Bay [23]

Table S1. Continued.

Host	Virus	Family	genome type	genome size (kb)	Shape	Capsid size (nm)	Tail (W x L)	Size of major polypeptides (kDa	Latent period (h)	Particle accumulation site and pattern	Burst size (cell^{-1})	Strain specificity	Source
V. fischeri MJ-1	rp-1		dsDNA		icosahedral	83	16 x 83		0.3833		100	21/27	coastal water, Mexico [24]
PWH3a	PWH3a-P1		dsDNA			50	? x ?						coastal water, Gulf of Mexico [25]
Pseudomonas sp.	06N-58P		ssRNA		icosahedral	60			0.5833		170		seawater, 5 miles offshore, Japan [26]
Bacillus sp. w13	BVW1		dsDNA	18	icosahedral	70	15 x 300	32, 45, 50, 57, 60, 70				1/5	deep, water and sediment, hydrothermal fields, Pacific Ocean [27]
Geobacillus sp. E26323	GVE1	*Siphoviridae*	dsDNA	41	icosahedral	130	30 x 180	34, 37, 43, 60, 66, 100				1/4	deep, water and sediment, hydrothermal fields, Pacific Ocean [27]
Colwellia psychrerythraea 34 H	Phage 9A	*Siphoviridae* [c 28]	dsDNA	104 [28]	icosahedrall	90	? X 200		4-5		55	2/8	water, nepheloid layer, Arctic [29]
21C (C. *psychrerythraea)* [d]	21c	*Siphoviridae*	dsDNA	40-50	icosahedral	46-48	9-11 x 151-188						sea ice, Artic [30]
Aeromonas sp.	unknown				icosahedral	53	15 x 160						sediment, Pacific Ocean [31]

Table S1. Continued.

Host	Virus	Family	genome type	genome size (kb)	Shape	Capsid size (nm)	Tail (W x L)	Size of major polypeptides (kDa	Latent period (h)	Particle accumulation site and pattern	Burst size (cell^{-1})	Strain specificity	Source
Listonella pelagia	φHSIC	*Siphoviridae*	dsDNA	36	icosahedral	47±3.7	? x 146±3.7		1.5		47		coastal water, Hawaii [32]
Shewanella piezotolerans	SW1		ssDNA	7,718 nt [33]	filamen-tous[33]								prophage, host was isolated from deep, sediment, Pacific [34]
1A (*S. frigidimarina* LMG 19867)[d]	1a	*Myoviridae*	dsDNA	70	icosahedral	94-103	11-15 x 94-103						sea ice, Artic [30]
Salmonella enterica	PRD1	*Tectiviridae* [22]	dsDNA	15 [22]	icosahedral	66 [22]							sewage
S. enterica	P22		dsDNA		icosahedral								
Pseudomonas syringae	φ6		dsRNA										
Pseudolateromonas sp.	PM2	*Corticoviridae* [35]	circular, dsDNA [35]	10.1 [35]	icosahedral	60 [36]			1 [36]	Cytoplasm [36]	50-600 [36]		coastal, water, Pacific [35]
Salicola sp.	SCTP-1				Icosahedral	55	? x 95						water, solar salterns, Italy [37]
Salicola sp.	SCTP-2				Icosahedral	125	? x 145						water, solar salterns, Italy [37]
Cytophaga sp.	NCMB 384		dsDNA						2.5		28		coastal, water, North Sea [38]
Cytophaga sp.	NCMB 385		dsDNA			78	? x 97		3.0		20		coastal, water, North Sea [38]
Photobacterium leiognathi	LB1VL-P1b		dsDNA										

Table S1. Continued.

Host	Virus	Family	genome type	genome size (kb)	Shape	Capsid size (nm)	Tail (W x L)	Size of major polypeptides (kDa	Latent period (h)	Particle accumulation site and pattern	Burst size (cell^{-1})	Strain specificity	Source
Unknown bacteria	LMG1-P4		dsDNA			83	? x 104						water, hypersaline lagoon, Gulf of Mexico [25]
Unknown CB 38	CB 38Φ												
Unknown CB 7	CB 7Φ												
Unknown H2	H2/1		dsDNA		Icosahedral	64	? x 71						water, North Sea [39]
Unknown H11	H11/1		dsDNA		Icosahedral	62	? x 75						water, North Sea [39]
Unknown H40	H40/1		dsDNA		Icosahedral	62	? x 117						water, North Sea [39]
Unknown H85	H85/1		dsDNA		Icosahedral	57	? x 120						water, North Sea [39]
Unknown PR1	PR1/1		dsDNA		Icosahedral	41							Coastal waters, Santa Monica Bay [39]
Unknown PR2	PR2/1		dsDNA		Icosahedral	86	? x 142						Coastal waters, Santa Monica Bay [39]
Unknown PR3	PR3/1		dsDNA		Icosahedral	42	? x ?						Coastal waters, Santa Monica Bay [39]

Table S1. Continued.

Host	Virus	Family	genome type	genome size (kb)	Shape	Capsid size (nm)	Tail (W x L)	Size of major polypeptides (kDa	Latent period (h)	Particle accumulation site and pattern	Burst size (cell^{-1})	Strain specificity	Source
Unknown PR4	PR4/1		dsDNA		Icosahedral	52	? x ?						Coastal waters, Santa Monica Bay [39]
Archaeal Viruses													
Halorubrum sp.	HRTV-1				Icosahedral	55	? x 85						water, solar salterns, Italy [37]
Haloarcula hispanica	HHTV-1				Icosahedral	55	? x 110						water, solar salterns, Italy [37]
H. hispanica	HHPV-1		dsDNA		pleomorphic								water, solar salterns, Italy [37]
H. hispanica	SH1		dsDNA	30.9±1.0 [40]	Icosahedral	70 [40]			5-6 [40]		200 [40]		water, hypersaline lake, Australia
H. californiae	HCTV-1				Icosahedral	70	? x 80						water, solar salterns, Italy [37]
Cyanophages													
Synechococcus sp. DC2	S-PWM1	*Myoviridae*	dsDNA	65	Icosahedral							1/8	coastal water, Gulf of Mexico [41]
Synechococcus sp. DC2	S-PWM3	*Myoviridae*	dsDNA		Icosahedral							4/8	coastal water, Gulf of Mexico [41]

[a] infectious units, [b]viruses infectious against different hosts, [c]"*unclassified*", [d] highest identities based on 16S analysis

References

1 Baudoux A, Brussaard CPD (2005) Characterization on different viruses infecting the marine harmful algal bloom species *Phaeocystis globosa*. Virology 341: 80-90

2 Brussaard CPD, Noordeloos AAM, Sandaa RA, Heldal M, Bratbak G (2004) Discovery of a dsRNA virus infecting the marine photosynthetic protist *Micromonas pusilla*. Virology 319: 280-291. doi: DOI 10.1016/j.virol.2003.10.033

3 Martinez-Martinez J, Brussaard CPD (unpublished data)

4 Cottrell MT, Suttle CA (1995) Dynamics of a lytic virus infecting the photosynthetic marine picoflagellate *Micromonas Pusilla*. Limnology and Oceanography 40: 730-739

5 Tomaru Y, Shirai Y, Suzuki H, Nagumo T, Nagasaki K (2008) Isolation and characterization of a new single-stranded DNA virus infecting the cosmopolitan marine diatom *Chaetoceros debilis*. Aquatic Microbial Ecology 50: 103-112. doi: 10.3354/ame01170

6 Tomaru Y, Takao Y, Suzuki H, Nagumo T, Koike K, Nagasaki K (2011) Isolation and characterization of a single-stranded DNA virus infecting *Chaetoceros lorenzianus* Grunow. Applied and Environmental Microbiology 77:5285-5293

7 Tomaru Y, Toyoda K, Suzuki H, Nagumo T, Kimura K, Takao Y (2013) New single-stranded DNA virus with a unique genomic structure that infects marine diatom *Chaetoceros setoensis*. Scientific Reports 3. doi: 10.1038/srep03337

8 Tomaru Y, Takao Y, Suzuki H, Nagumo T, Nagasaki K (2009) Isolation and characerization of a single-stranded RNA virus infecting the bloom-forming diatom *Chaetoceros socialis*. Applied and Environmental Microbiology 75: 2375-2381

9 Nagasaki K, Shirai Y, Tomaru Y, Nishida K, Pietrokovski S (2005) Algal viruses with distinct intraspecies host specificities include identical intein elements. Applied and Environmental Microbiology 71: 3599-3607

10 Nagasaki K, Yamaguchi M (1997) Isolation of a virus infectious to the harmful bloom causing microalga *Heterosigma akashiwo* (Raphidophyceae). Aquatic Microbial Ecology 13: 135-140

11 Nagasaki K, Tarutani K, Yamaguchi M (1999) Growth characteristics of *Heterosigma akashiwo* virus and its possible use as a microbiological agent for red tide control. Applied and Environmental Microbiology 65: 898-902

12 Nagasaki K, Yamaguchi M (1998) Intra-species host specificity of HaV (*Heterosigma akashiwo* virus) clones. Aquatic Microbial Ecology 14: 109-112

13 Tai V, Lawrence JE, Lang AS, Chan AM, Culley AI, Suttle CA (2003) Characterization of HaRNAV, a single-stranded RNA Virus causing lysis of *Hetersigma akashiwo* (Raphidophyceae). Journal of Phycology 39: 343-352

14 Lawrence JE, Brussaard CPD, Suttle CA (2006) Virus-specific responses of *Heterosigma akashiwo* to infection. Applied and Environmental Microbiology 72: 7829-7834

15 Tarutani K, Nagasaki K, Itakura S, Yamaguchi M (2001) Isolation of a virus infecting the novel shellfish-killing dinoflagellate *Heterocapsa circularisquama*. Aquatic Microbial Ecology 23: 103-111

16 Nagasaki K, Tomaru Y, Tarutani K, Katanozaka N, Yamanaka S, Tanabe H, Yamaguchi M (2003) Growth characteristics and intraspecies host specificity of a large virus infecting the dinoflagellate *Heterocapsa circulatisquama*. Applied and Environmental Microbiology 69: 2580-2586

17 Tomaru Y, Katanozaka N, Nishida K, Shirai Y, Tarutani K, Yamaguchi M, Nagasaki K (2004) Isolation and characterization of two distinct types of HcRNAV, a single-stranded RNA virus infecting the bivalve-killing microalga *Heterocapsa circularisquama*. Aquatic Microbial Ecology 34:207-218

18 Delisle AL, Levin RE (1972) Characteristics of three phages infectious for psychrophilic fishery isolates of *Pseudomonas putrefaciens*. Antonie van Leeuwenhoek 38: 1-8

19 Hardies SC, Hwang YJ, Hwang CY, Jang GI, Cho BC (2013) Morphology, physiological characteristics, and complete sequence of marine bacteriophage ϕRIO-1 infecting *Pseudoalteromonas marina*. Journal of Virology 87:9189-9198

20 Johnson, RM (1968) Characteristics of a marine vibrio-bacteriophage system. Journal of the Arizona Academy of Science 5: 28-33

21 Keynan A, Nealson K, Sideropo H, Hastings JW (1974) Marine transducing bacteriophage attacking a luminous bacterium. Journal of Virology 14: 333-340

22 Fauquet CM, Mayo M A, Maniloff J, Desselberger U, Ball LA (2005) Virus Taxonomy, Eighth Report of the International Committee on Taxonomy of Viruses. Elsevier/Academic Press, London

23 Zachary A (1976) Physiology and ecology of bacteriophages of the marine bacteruim *Beneckea natriegens*: salinity. Applied and Environmental Microbiology 31: 415-422

24 Levisohn R, Moreland J, Nealson KH (1987) Isolation and characterization of a generalized transducing phage for the marine luminous bacterium *Vibrio fischeri* MJ-1. Journal of General Microbiology 133: 1577-1582

25 Suttle CA, Chen F (1992) Mechanisms and rates of decay of marine viruses in seawater. Applied and Environmental Microbiology 58: 3721-3729

26 Hidaka T, Ichida K (1976) Properties of a marine RNA-containing bacteriophage. Memoirs of the Faculty of Fisheries, Kagoshima University 25: 77-89

27 Liu B, Wu SJ, Song Q, Zhang XB, Xie LH (2006) Two novel bacteriophages of thermophilic bacteria isolated from deep-sea hydrothermal fields. Current Microbiology 53: 163-166

28 Colangelo-Lillis JR, Deming JW (2013) Genomic analysis of cold-active *Colwelliaphage* 9A and psychrophilic phage-host interactions. Extremophiles 17: 99-114

29 Wells LE, Deming JW (2006) Characterization of a cold-active bacteriophage on two psychrophilic marine hosts. Aquatic Microbial Ecology 45: 15-29

30 Borriss M, Helmke E, Hanschke R, Schweder T (2003) Isolation and characterization of marine psychrophilic phage-host systems from Artic sea ice. Extremophiles 7: 377-384

31 Wiebe WJ, Liston J (1968) Isolation and characterization of a marine bacteriophage. Marine Biology 1: 244-249, doi: Doi 10.1007/Bf00347117

32 Jiang SC, Kellogg CA, Paul JH (1998) Characterization of marine temperate phage-host systems isolated from Mamala Bay, Oahu, Hawaii. Applied and Environmental Microbiology 64: 535-542

33 Wang F, Wang FP, Li Q, Xiao X (2007) A novel filamentous phage from the deep-sea bacterium *Shewanella piezotolerans* WP3 is induced at low temperature. Journal of Bacteriology 189: 7151-7153

34 Jian H, Xiao X, Wang F (2013) Role of filamentous phage SW1 in regulating the lateral flagella of *Shewanella piezotolerans* strain WP3 at low temperatures. Applied and Environmental Microbiology 79: 7101-7109

35 Abrescia NG, Grimes JM, Kivelä HM, Assenberg R, Sutton GC, Butcher SJ, Bamford JK, Bamford DH, Stuart DI (2008) Insights into virus evolution and membrane biogenesis from the structure of the marine lipid-containing bacteriophage PM2. Molecular Cell 31: 749-761

36 Kivela HM, Mannisto RH, Kalkkinen N, Bamford DH (1999) Purification and protein composition of PM2, the first lipid-containing bacterial virus to be isolated. Virology 262: 364-374

37 Kukkaro P, Bamford DH (2009) Virus-host interactions in environments with a wide range of ionic strengths. Environmental Microbiology Reports 1: 71-77

38 Chen PK, Citarella RV, Salazar O, Colwell RR (1966) Properties of two marine bacteriophages. Journal of Bacteriology 91: 1136-1139

39 Noble RT, Fuhrman JA (1997) Virus decay and its causes in coastal waters. Applied and Environmental Microbiology 63: 77-83

40 Porter K, Kukkaro P, Bamford JKH, Bath C, Kivela HM, Dyall-Smith ML, Bamford DH (2005) SHI: A novel, spherical halovirus isolated from an Australian hypersaline lake. Virology 335: 22-33

41 Suttle CA, Chan AM (1993) Marine cyanophages infecting oceanic and coastal strains of *Synechococcus*: abundance, morphology, cross-infectivity and growth characteristics. Marine Ecology Progress Series 92: 99-109

Chapter 3

Phytoplankton community structure in relation to vertical stratification along a north-south gradient in the Northeast Atlantic Ocean

Kristina D. A. Mojica[1], Willem H. van de Poll[1], Michael Kehoe[2], Jef Huisman[2], Klaas R. Timmermans[1, 3], Anita G. J. Buma[3], Hans J. van der Woerd[4], Lisa Hahn-Woernle[5], Henk A. Dijkstra[5] and Corina P. D. Brussaard[1,2]

[1]Department of Biological Oceanography, NIOZ - Royal Netherlands Institute for Sea Research, NL 1790 AB, Den Burg, Texel, The Netherlands
[2]Department of Aquatic Microbiology, Institute for Biodiversity and Ecosystem Dynamics (IBED), University of Amsterdam, P.O. Box 94248, 1090 GE, Amsterdam, The Netherlands
[3]Department of Ocean Ecosystems, Energy and Sustainability Research Institute Groningen, University of Groningen, Nijenborgh 7, 9747 AG Groningen, The Netherlands
[4]Institute for Environmental Studies (IVM), VU University Amsterdam, De Boelelaan 1087, 1091 HV, Amsterdam, The Netherlands
[5]Institude for Marine and Atmospheric research Utrecht (IMAU), Department of Physics and Astronomy, Utrecht University, Princetonplein 5, 3584 CC Utrecht, The Netherlands

Limnology and Oceanography (2015) doi: 10.1002/lno.10113

Abstract

Climate change is affecting the hydrodynamics of the world's oceans. How these changes will influence the productivity, distribution and abundance of phytoplankton communities is an urgent research question. Here we provide a unique high-resolution mesoscale description of the phytoplankton community composition in relation to vertical mixing conditions and other key physicochemical parameters along a meridional section of the Northeast Atlantic Ocean. Phytoplankton, assessed by a combination of flow cytometry and pigment fingerprinting (HPLC-CHEMTAX), and physicochemical data were collected from the top 250 m water column during the spring of 2011 and summer of 2009. Multivariate analysis identified water column stratification (based on 100 m depth-integrated Brunt-Väisälä frequency N^2) as one of the key drivers for the distribution and separation of different phytoplankton taxa and size classes. Our results demonstrate that increased stratification (i) broadened the geographic range of *Prochlorococcus* as oligotrophic areas expanded northward, (ii) increased the contribution of picoeukaryotic phytoplankton to total autotrophic organic carbon (< 20 μm), and (iii) decreased the abundances of diatoms and cryptophytes. We discuss the implications of our findings for the classification of phytoplankton functional types in biogeochemical and ecological ocean models. As phytoplankton taxonomic composition and size affects productivity, biogeochemical cycling, ocean carbon storage and marine food web dynamics, the results provide essential information for models aimed at predicting future states of the ocean.

Introduction

The oceans play an essential role in regulating global climate through the storage and transportation of heat and the uptake and sequestration of carbon dioxide (Levitus et al. 2000; Hoegh-Guldberg and Bruno 2010). As global warming continues, the surface waters of the ocean are envisaged to rise by 2-6°C over the next 100 years (Meehl et al. 2007; Collins et al. 2013). Ocean-climate models predict that surface warming, in combination with changes in freshwater input at high latitudes (due to rises in precipitation, land run off and sea ice melt) will lead to increases in vertical stratification (Sarmiento et al. 1998; Sarmiento 2004). Vertical stratification affects the production of the world's oceans as it determines the general availability of light and nutrients to phytoplankton in the ocean (Behrenfeld et al. 2006; Huisman et al. 2006; Hoegh-Guldberg and Bruno 2010). Stratification suppresses turbulence and reduces the mixed layer depth, thereby relaxing light limitation but at the same time restricting the flow of nutrients from depth (Mahadevan et al. 2012). In temperate and high latitude regions, the annual establishment of seasonal stratification often triggers the highly productive phytoplankton spring bloom (Sverdrup 1953; Huisman et al. 1999; Siegel et al. 2002). However, strong and prolonged stratification often leads to ocean oligotrophication as phytoplankton become nutrient limited by depletion of the nutrients in the surface layer. As a consequence of increases in sea surface temperature (SST) and resultant increases in vertical stratification, oligotrophic areas (i.e., defined as areas below 0.07 mg Chl m^{-3}) of the North Atlantic subtropical gyre are estimated to be expanding at a rate of up to 4.3% yr^{-1} (Polovina et al. 2008).

Projected alterations to stratification and vertical mixing have the potential to affect phytoplankton species composition (Huisman et al. 2004), phenology (Edwards and Richardson 2004), productivity (Gregg et al. 2003; Behrenfeld et al. 2006; Polovina et al. 2008), size structure (Li 2002; Daufresne et al. 2009; Hilligsøe et al. 2011), nutritional value (Mitra and Flynn 2005; van de Waal et al. 2010), abundance (Richardson and Schoeman 2004) and spatial distribution (Doney et al. 2012; van de Poll et al. 2013). Consequently, affecting the functioning and biogeochemistry of pelagic and benthic ecosystems, and altering their capacity for carbon sequestration (Beaugrand 2009; Hoegh-Guldberg and Bruno 2010). Understanding the ecological and physiological mechanisms controlling changes in phytoplankton community structure across gradients of vertical stability is therefore vital to assessing the response of marine systems to global climate change.

The North Atlantic Ocean is key to global climate and ocean circulation, due to North Atlantic deep water formation, accounting for 20% of the net ocean uptake of CO_2 (Deser and Blackmon 1993; Dawson and Spannagle 2008). The Northeast Atlantic Ocean provides a meridional gradient in stratification, with permanent stratification in the subtropics and seasonal stratification in the temperate zones (Talley et al. 2011; Jurado et al. 2012a). To assess potential alterations in phytoplankton community structure of the North Atlantic due to future changes in vertical stratification, a firm baseline is required that accurately describes the status quo. Yet, even for the relatively well-investigated North Atlantic, comprehensive descriptions of phytoplankton community structure in relation to vertical stratification patterns at the ocean basin scale are scarce (Partensky et al. 1996; Tarran et al. 2006; Bouman et al. 2011). Here we investigate how phytoplankton abundance, size and community composition are related to vertical stratification along a latitudinal gradient in the Northeast Atlantic Ocean during spring and summer. Comparison between two seasons with different vertical density distributions offers an unique opportunity to study how phytoplankton dynamics change as stratification develops. The results presented here provide an important baseline to study the effect of future climate change on marine ecosystems in the North Atlantic.

Methods

Study area and sampling procedure

During two research cruises, STRATIPHYT I taking place in the summer (July-August) of 2009 and STRATIPHYT II in spring (April-May) of 2011, samples were collected over a transect traversing a North-South stratification gradient in the Northeast Atlantic Ocean (Fig. 1) on board of the R/V Pelagia. During each cruise, thirty-two stations (separated by approximately 100 km) were sampled over the course of a month in the area located between 29°N and 63°N, which spans from the Canary Islands to Iceland. Water samples were collected in the top 250 m from at least 10 separate depths using 24 plastic samplers (General Oceanics type Go-Flow, 10 liter) during STRATIPHYT I and Teflon samplers (NIOZ design Pristine Bottles, 27 liters) during STRATIPHYT II. Samplers were mounted on an ultra-clean (trace-metal free) system consisting of a fully titanium sampler frame equipped with CTD (Seabird 9+; standard conductivity, temperature and pressure sensors) and auxiliary sensors for chlorophyll autofluorescence (Chelsea

Aquatracka Mk III), light transmission (Wet-Labs C-star) and photosynthetic active radiation (PAR; Satlantic). Data from the chlorophyll autofluorescence sensor were calibrated against HPLC data according to van de Poll et al. (2013) in order to determine total Chlorophyll *a* (Chl *a*) for the present study. Samples were taken inside a 6 m Clean Container from each depth for inorganic nutrients (5 ml), flow cytometry (10 ml), and phytoplankton pigments (10 L).

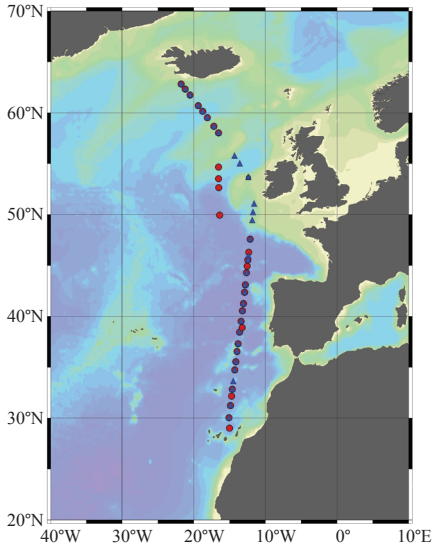

Figure 1. Ocean Data View (ODV) (Schlitzer, 2002) bathymetric map of the Northeast Atlantic Ocean depicting station locations for the summer 2009 (blue triangles) and spring 2011 (red circles) STRATIPHYT cruises.

Physicochemical data

Temperature eddy diffusivity (K_T) data, referred to here as the vertical mixing coefficient, were derived from temperature and conductivity microstructure profiles measured using the commercial microstructure profiler SCAMP (Self Contained Autonomous Microprofiler) (Stevens et al. 1999). A detailed description of SCAMP methodology and data for both STRATIPHYT cruises have been described by Jurado et al. (2012 a,b). The SCAMP was deployed at fewer stations (i.e., 17 and 14 in spring and summer, respectively) and to lower depths (up to 100 m) than the remainder of the data (23 stations and up to 250 m depth) in the present study. In order to correct for this deficiency, data were interpolated using the spatial kriging function 'krig' executed in R using the 'fields' package (Furrer et al. 2012).

Interpolated K_T values were bounded below by the minimum value measured for each of the two cruise datasets; the upper values were left unbounded. This resulted in estimated K_T values which preserved the qualitative pattern and range of values previously reported (Jurado et al. 2012a; Jurado et al. 2012b), i.e., continuous stratification during the summer STRATIPHYT I cruise and two distinct zones of mixing during the spring STRATIPHYT II cruise; stratification in the south and deep strong mixing in the north. SCAMP data were also used to quantify the strength of background stratification according to the square of the Brunt-Väisälä frequency: $N^2 = (g/\rho)(\partial\rho/\partial z)$ where z is depth measured positively downward (m), ρ is the density of water (kg m^{-3}) and g is the gravitational acceleration (9.8 m s^{-2}) (Houry et al. 1987; Jurado et al. 2012a; Jurado et al. 2012b). The Brunt-Väisälä frequency represents the angular velocity (i.e., the rate) at which a small perturbation of the stratification will re-equilibrate. Hence, it is a simple measure of the stability of the vertical stratification. N^2 values were depth averaged over the top 100 m of the water column and classified based on the following criteria: $N^2 < 2x10^{-5}$ rad^2 s^{-2} for non-stratified, $2x10^{-5} < N^2 < 5x10^{-5}$ rad^2 s^{-2} for weakly stratified and $N^2 > 5x10^{-5}$ rad^2 s^{-2} for strongly stratified. In addition, the depth of the mixed layer (Z_m), was determined as the depth at which the temperature difference with respect to the surface was 0.5°C (Levitus et al. 2000; Jurado et al. 2012b). As shown by Brainerd and Gregg (1995), this definition of the mixed layer provides an estimate of the depth through which surface waters have been mixed in recent days. On the few occasions where SCAMP data were not available Z_m was determined from CTD data. Station mean temperature profiles obtained from SCAMP and CTD measurements were compared and were found to have a good correlation.

Discrete water samples for dissolved inorganic phosphate (PO_4^{3-}), ammonium (NH_4^+), nitrate (NO_3^-), and nitrite (NO_2^-) were gently filtered through 0.2 µm pore size polysulfone Acrodisk filters (32 mm, Pall Inc.), after which samples were stored at -20°C until analysis. Dissolved inorganic nutrients were analyzed onboard using a Bran+Luebbe Quaatro AutoAnalyzer for dissolved orthophosphate (Murphy and Riley 1962), inorganic nitrogen (nitrate + nitrite: NO_x) (Grasshoff 1983) and ammonium (Koroleff 1969; Helder and De Vries 1979). Detection limits ranged between the two cruises from 0.06-0.10 µM for NO_x, 0.010-0.028 µM for PO_4^{3-} and 0.05-0.09 µM for NH_4^+.

Phytoplankton data

Phytoplankton consisting of photoautotrophic prokaryotic cyanobacteria and eukaryotic algae < 20 µm were enumerated on fresh samples using a Becton-Dickinson FACSCalibur flow cytometer (FCM) equipped with an air-cooled Argon laser with an excitation wavelength of 488 nm (15 mW). Samples were measured for 10 minutes using a high flow rate with the discriminator set on red chlorophyll autofluorescence. Phytoplankton populations were distinguished using bivariate scatter plots of autofluorescent properties (orange autofluorescence from phycoerythrin for the cyanobacteria *Synechococcus* spp. and red autofluorescence from Chl *a* for photoautotrophs) against side scatter. The obtained list-mode files were analyzed using the freeware CYTOWIN (Vaulot 1989).

Regularly throughout the cruise transect, size-fractionation was performed to provide average cell size for the different phytoplankton subpopulations. Specifically, a whole water sample (10 ml) was size-fractionated by sequential gravity filtration through 8, 5, 3, 2, 1, 0.8, and 0.4 μm pore-size polycarbonate filters. Each fraction was then analyzed using FCM as described above. The equivalent spherical diameter for each population was determined as the size displayed by the median (50%) number of cells retained for that cluster. In total 9 different phytoplankton populations were distinguished, consisting of 6 eukaryotic and 3 cyanobacterial populations, i.e., *Synechococcus* spp. (average size range between the two cruises of 0.9-1.0 µm), *Prochlorococcus* high light population (HL; 0.6 µm) and *Prochlorococcus* low light population (LL; 0.7-0.8 µm). The photosynthetic eukaryotic populations consisted of 2 pico-sized groups, i.e., Pico I (1.0-1.4 µm) and Pico II (1.5-2.0 µm), and 4 nano-sized groups, i.e., Nano I (3-4 µm), Nano II (6-8 µm), Nano III (8-9 µm) and Nano IV (9 µm). In order to estimate the contribution of the different phytoplankton groups to carbon biomass, carbon-conversion factors were applied to FCM cell counts. Specifically, cell counts were transformed assuming spherical diameters equivalent to the average cell size determined from size fractionation and applying conversion factors of 237 fg C μm^{-3} (Worden et al. 2004) and 196.5 fg C μm^{-3} for pico- and nano-sized plankton (Garrison et al. 2000), respectively.

Phytoplankton taxonomic composition was determined by pigment analysis of 10 L GF/F filtered samples (47 mm, Whatman; flash frozen and stored at -80°C until analysis) using HPLC as described by Hooker et al. (2009). In short, filters were freeze-dried (48 h) and pigments extracted using 5 ml 90% acetone (v/v, 48 h, 4°C, darkness) and separated using a HPLC (Waters 2695 separation module, 996 photodiode array detector) equipped with a Zorbax Eclipse XDB-C_8 3.5 µm column

(Agilent Technologies, Inc.). Peak identification was based on retention time and diode array spectroscopy. Pigments standards (DHI LAB products) were used for quantification of chlorophyll a_1, chlorophyll a_2, chlorophyll *b*, chlorophyll c_2, chlorophyll c_3, peridinin, 19-butanoyloxyfucoxanthin, 19-hexanoyloxyfucoxanthin, fucoxanthin, neoxanthin, prasinoxanthin, alloxanthin, and zeaxanthin. The sum of chlorophyll *a* and divinyl chlorophyll *a* was used as indicator for algal biomass as these pigments are universal in algae and *Prochlorococcus*. Specific marker pigments were used to reveal the presence of taxonomically distinct pigment signatures using CHEMTAX (version 195; Mackey et al. 1996) software, thereby estimating the concentration of each taxonomic group relative to chlorophyll *a*. CHEMTAX was run separately for oligotrophic and non-oligotrophic stations and for spring and summer samples. Oligotrophic areas defined by nutrient (i.e., $NO_3^- \leq 0.13$ µM and $PO_4^{3-} \leq 0.03$ µM; van de Poll et al. 2013) or by Chl *a* concentrations (< 0.07 mg Chl m^{-3}), delineating regions south of 40°N and 45°N as oligotrophic for the spring and summer, respectively. CHEMTAX was run with 500 iterations, with all elements varied (100% for chlorophyll *a* and divinyl chlorophyll *a* and 500% for the other pigments). Initial pigment ratios in the iterations were based on van de Poll et al. (2013), where high-light initial pigment ratios were implemented for surface samples (0-50 m) of oligotrophic stations and low-light initial pigment ratios for subsurface samples (> 50 m) of oligotrophic and all non-oligotrophic samples. In order to compare to taxonomic composition data provided by CHEMTAX, the percent contribution of different FCM distinguished groups to total carbon biomass (< 20 µm) was also determined. Likewise, Chl *a* and CHEMTAX taxonomic composition were used to determine the group-specific Chl *a* concentrations.

In order to provide additional taxonomic information, seawater samples were also fixed for occasional microscopic analysis. Specifically, 150 ml of seawater was fixed in Lugol's iodine solution (1% final concentration) supplemented with formaldehyde and stored at 4 °C until analysis. Samples were processed according to the Utermöhl method (Edler and Elbrächter 2010). Briefly, 10-50 ml of fixed sample was aliquoted into a settling chamber and after a 48 h settling time, phytoplankton species composition was determined along one or two meridians at 40x and 200x magnification using an Olympus IMT-2 inverted microscope.

Statistical Analysis

Measured quantities included in the multivariate analysis were: the vertical mixing coefficient, N^2, temperature, salinity, density, PO_4^{3-}, NH_4^+, NO_2^- and NO_3^-. The ratio

of nitrogen to phosphorus (N:P) was also included and calculated as the ratio of total dissolved inorganic nitrogen (i.e., NO_2^- + NO_3^- + NH_4^+) to PO_4^{3-}. In addition, several variables were included as factors (i.e., single value per station/sample) in order to better discriminate how environmental conditions relate to phytoplankton abundance and taxonomic composition. These included depth layer, euphotic depth, stratification level, mixed layer depth, the ratio of mixed layer depth to the euphotic depth and nutrient flux of NO_3^-, NO_2^- and PO_4^{3-} into both the mixed layer and euphotic zone. The depth of each sample was classified as either within the mixed layer (Z_m) or below mixed layer depth (BZ_m). Euphotic depth (Z_{eu}), calculated based on the light attenuation coefficient (K_d), was defined as the depth at which irradiance was 0.1% of the surface value (Moore and Chisholm 1999) in order to account for the dominance and vertical distribution (down to 200 m) of *Prochlorococcus*. The ratio of the mixed layer depth to the euphotic depth (Z_m/Z_{eu}) was used as an index of light availability in the mixed layer. Thus, if mixed layer depth exceeds the euphotic depth (i.e., $Z_m/Z_{eu} > 1.0$), phytoplankton cells are more likely to be exposed to light limited conditions. Finally, the nutrient flux at a depth z* was defined as $\varphi(z^*)=-K_T(z)(\partial N/\partial z)|_{z^*}$ and calculated based on measured vertical profiles of the vertical mixing coefficient (K_T) and individual nutrients (N) of PO_4^{3-}, NO_2^- and NO_3^-. The nutrient fluxes were determined at the depths Z_{eu} and Z_m, and coded according to the depth and nutrient being considered, e.g. $Z_{eu}PO_4$ represents the PO_4^{3-} flux into the euphotic zone.

A multivariate statistical analysis was performed using the R statistical software (R Development Core Team 2012) supplemented by vegan (Oksanen et al. 2013). Data exploration was carried out following the protocol described in Zuur et al. (2010). Because CHEMTAX pigment data and FCM abundance data occasionally did not coincide, each dataset was analyzed separately in order to maximize the size of the data matrices. In addition, depth profiles of N^2 were restricted to depths less than 100 m due to the limitations of the SCAMP. Consequently, N^2 was incorporated into the analysis as the factor stratification level according to Fig. 2. FCM phytoplankton carbon (C) data, N:P, NH_4^+, and all nutrient fluxes were log (x+1) transformed and vertical mixing coefficient and Z_m/Z_{eu} were log transformed in order to reduce the effect of outliers. In order to identify and remove collinearity, variance inflation factors (VIF) were calculated using the R function corvif written by Zuur et al. (2009). Sequentially, explanatory variables with the largest VIF were removed until all variables resulting in VIF < 10. Two exceptions were the removal of NO_3^- instead of PO_4^{3-} (Pearson correlation: $r = 0.99$, $p < 0.001$) and the

removal of $Z_{eu}NO_2$ instead of $Z_{eu}PO_4$ (Pearson correlation: r = 0.96; $p < 0.001$). Any residual collinearity was identified and removed based on correlation pair plots and boxplots of variables across factor levels. At this stage, the vertical mixing coefficient was excluded due to collinearity with stratification level and depth layer. The final selection resulted in 12 explanatory variables: Salinity, PO_4^{3-}, NH_4^+, NO_2^-, Z_{eu}, Z_m/Z_{eu}, N:P, $Z_{eu}PO_4$, Z_mPO_4, Z_mNO_2, stratification level and depth level. Initial scatter plots of response variables and covariates did not show a strong non-linear pattern and therefore redundancy analysis (RDA) (Legendre and Legendre 1998) was chosen over canonical correspondence analysis (CCA) to model the response of phytoplankton carbon data (i.e., FCM phytoplankton size fractionated C) and taxonomic community composition as a function of selected explanatory variables. In all cases, RDA was performed on a correlation matrix (i.e., all phytoplankton groups equally important) and used species conditional scaling in order to better determine the relationship between phytoplankton variables and environmental covariates. Subsequent to RDA, a forward selection procedure was applied to select only those explanatory variables that contributed significantly to the RDA model, while removing non-significant terms. Significance was assessed by a permutation test, using the multivariate pseudo-F-value as the test statistic (Zuur et al. 2009). A total of 9999 permutations were used to estimate *p*-values associated with the pseudo-F statistic. Variance partitioning was applied to the final RDA model to estimate how much of the variation in the data was explained by stratification and how much by other factors.

More specifically, multivariate analysis of phytoplankton C biomass (from FCM counts) was performed on 8 different phytoplankton groups in a total of 315 samples from various depths within the upper 200 m of 23 stations along the cruise track (i.e., 166 and 149 samples in summer and spring, respectively). Forward selection and permutation tests revealed that 9 of the 12 explanatory variables significantly ($\alpha < 0.05$) contributed to the model (Table 1). Consequently, NO_2^-, $Z_m/Z_{eu,}$ and Z_mNO_2 (pseudo-F = 1.7, 1.6 and 1.7; $p = 0.13$, 0.16 and 0.13, respectively) were removed. When phytoplankton C biomass data were expressed as group-specific percentage of total C forward selection and step-wise permutation tests showed that all 12 of the explanatory variables now significantly ($\alpha < 0.05$) contributed to the model (Table 1).

Analysis of the CHEMTAX pigment data was based on 8 different taxonomic groups and total Chl *a* from 188 samples obtained from various depths within the upper 200 m water column of 23 stations (i.e., 93 and 95 samples in summer and

spring, respectively). Forward selection and step-wise permutation tests revealed that 10 of the 12 selected variables significantly contributed to the RDA model (Table 1). Subsequently, Z_mPO_4 and Z_mNO_2 (pseudo-F = 2.4, and 1.8; p = 0.06 and 0.13, respectively) were removed. When expressed as group-specific percentage of total Chl *a*, 8 variables significantly contributed to the RDA model (Table 1). Initial analysis resulted in the removal of $Z_{eu}PO_4$ and Z_mNO_2 (pseudo-F = 2.1 and 1.6; p = 0.06 and 0.13, respectively) and subsequent analysis resulted in the further removal of N:P and Z_mPO_4 (pseudo-F = 2.2 and 1.7; p = 0.05 and 0.13, respectively). When interpreting RDA correlation triplots, line lengths of the arrows representing the covariates signify their correlation with the axis (RDA1 horizontal axis and RDA2 vertical axis). For response variables, line lengths represent how well they are represented within the RDA model. The correlation between response and explanatory variables, as well as between response variables or explanatory variables themselves, is reflected in the angles between lines. Wherein, a small angle between two lines represents a high positive correlation, a 90° angle represents no correlation and 180° a strong negative correlation.

Data matrices are accessible via ftp://dmgftp.nioz.nl/zko_public/dataset/00082.

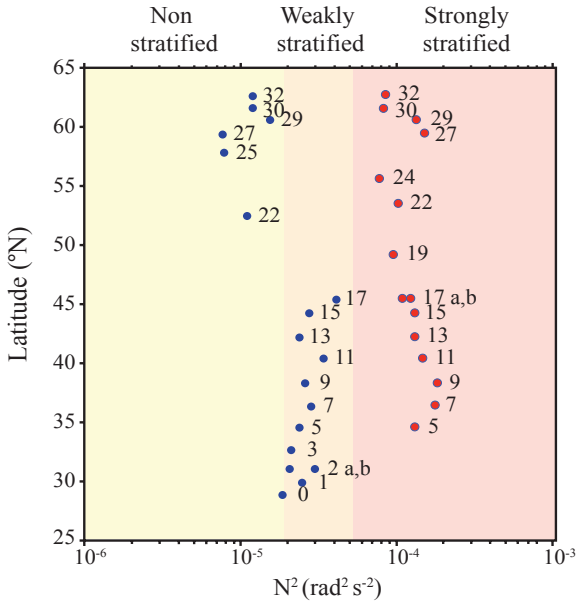

Figure 2. Brunt-Väisälä frequency (N^2) values averaged over the upper 100 m depth for the summer 2009 (red) and spring 2011 (blue) STRATIPHYT cruises and used to classification the level of stratification based on the following criteria: $N^2 < 2x10^{-5}$ rad^2 s^{-2} non-stratified, $2x10^{-5} < N^2 < 5x10^{-5}$ rad^2 s^{-2} weakly stratified and $N^2 > 5x10^{-5}$ rad^2 s^{-2} strongly stratified.

Table 1. Significance of the explanatory variables in the RDA correlation triplot of phytoplankton community composition in relation to environmental variables, as presented in Fig. 11A-D. Significance (P-value) was assessed by a permutation test, using the multivariate pseudo-F (F) as test statistic and on the Akaike Information Criterion (AIC) in case of ties (Legendre and Legendre, 1998).

A. Phytoplankton carbon			
Variable	AIC	F	P
PO_4^{3-}[a]	613.4	47.6	0.0001
Salinity[b]	551.5	70.2	0.0001
Strat. Level	511.7	23.2	0.0001
Depth Layer	500.4	13.3	0.0001
N:P	492.9	9.4	0.0001
Z_{eu}	486.7	8.1	0.0001
$Z_{eu}PO_4$	482.7	5.9	0.0002
NH_4^+	478.0	6.6	0.0002
Z_mPO_4	475.5	4.4	0.0023
B. Percentual distribution of phytoplankton carbon			
Salinity[b]	610.4	48.7	0.0001
Strat Level	582.5	16.6	0.0001
Z_{eu}	568.0	16.7	0.0001
Depth Level	544.6	15.4	0.0001
NO_2^-	549.7	6.8	0.0001
Z_mNO_2	544.8	6.8	0.0001
Z_m/Z_{eu}	541.9	4.8	0.0001
NH_4^+	539.1	4.7	0.0001
PO_4^{3-}[a]	537.4	3.6	0.0020
N:P	534.3	5.0	0.0001
$Z_{eu}PO_4$	533.9	2.2	0.0396
Z_mPO_4	533.6	2.3	0.0384
C. Chl *a* concentration			
Z_m/Z_{eu}	393.5	23.7	0.0001
Z_{eu}	377.0	19.2	0.0001
PO_4^{3-}[a]	359.0	21.1	0.0001
Salinity[b]	337.0	24.7	0.0001
Strat Level	318.6	11.4	0.0001
Depth Layer	307.8	12.7	0.0001
NH_4^+	305.3	4.3	0.0078
N:P	302.6	4.5	0.0055
$Z_{eu}PO_4$	301.1	3.3	0.0237
NO_2^-	300.0	2.9	0.0380
D. Percentual distribution of Chl *a* concentration			
Salinity[b]	356.3	41.2	0.0001
Strat Level	311.0	27.6	0.0001
Depth Layer	287.6	26.5	0.0001
Z_{eu}	269.8	20.1	0.0001
NH_4^+	266.2	5.5	0.0002
NO_2^-	263.7	4.4	0.0009
PO_4^{3-}[a]	260.0	5.5	0.0002
Z_m/Z_{eu}	256.8	4.9	0.0002

[a] $PO_4^{3-} = NO_3^-$; Pearson: $r = 0.99$, $p < 0.001$

[b] Salinity ≈ Temperature; Pearson: r=0.87, $p < 0.001$

Results

Physicochemical data

During the spring, the southern half of the cruise transect (29-46°N; stations 0-17) was classified as weakly stratified with $2x10^{-5} < N^2 < 5x10^{-5}$ rad^2 s^{-2} (Fig. 2) and Z_m depths ranged from 22 to 67 m. While the northern part (53-62°N; stations 22-32) of the transect had $Z_m > 100$ m and was considered as non-stratified ($N^2 < 2x10^{-5}$ rad^2 s^{-2}) (Fig. 2). Conversely, all stations sampled during the summer cruise were strongly stratified with $N^2 > 5x10^{-5}$ rad^2 s^{-2} (Fig. 2) and had relatively consistent and shallow mixed layer depths which ranged from 18 to 46 m. Water temperature displayed a latitudinal gradient in the spring with surface temperatures ranging from 18.6°C in the south to 8.9°C in the north (Fig. 3A). Temperatures were higher during the summer and displayed strong gradients with both latitude and depth (Fig. 3E). Temperatures were highest in the surface waters ranging from 22.8°C between 30-33°N to 13.0°C between 60-63°N. A prominent thermocline (i.e., rapid decrease in temperature from surface mixed layer to cold deep water) persisted over the latitudinal range of the cruise. Salinity demonstrated similar latitudinal trends as temperature for both seasons; however, vertical depth gradients were only apparent in the south during the summer (Fig. 3B, F). Resultant from the vertical and latitudinal gradients in temperature and salinity, seawater density exhibited strong gradients with depth and geographical location (Fig. 3C, G). During the spring, extrapolated vertical mixing coefficients (K_T) were low (10^{-3} m^2 s^{-1}) in the surface waters of southern stations indicating weak vertical mixing, while at the northern stations strong vertical mixing extended down to 100 m, indicating a well-mixed water column as a result of strong wind prior to our arrival (Jurado et al. 2012a). Vertical mixing was on average one order of magnitude lower in the summer and showed a sharp decline (from 10^{-5} to 10^{-1} m^2 s^{-1}) towards the bottom of the mixed layer (Fig. 3D). Around 33°N, vertical mixing in the mixed layer stabilized around 10^{-3} m^2 s^{-1} (i.e., $\log_{10}(K_T) \approx -3$) until 59°N, where values in the upper 20 m declined by an order of magnitude to 10^{-4} m^2 s^{-1}.

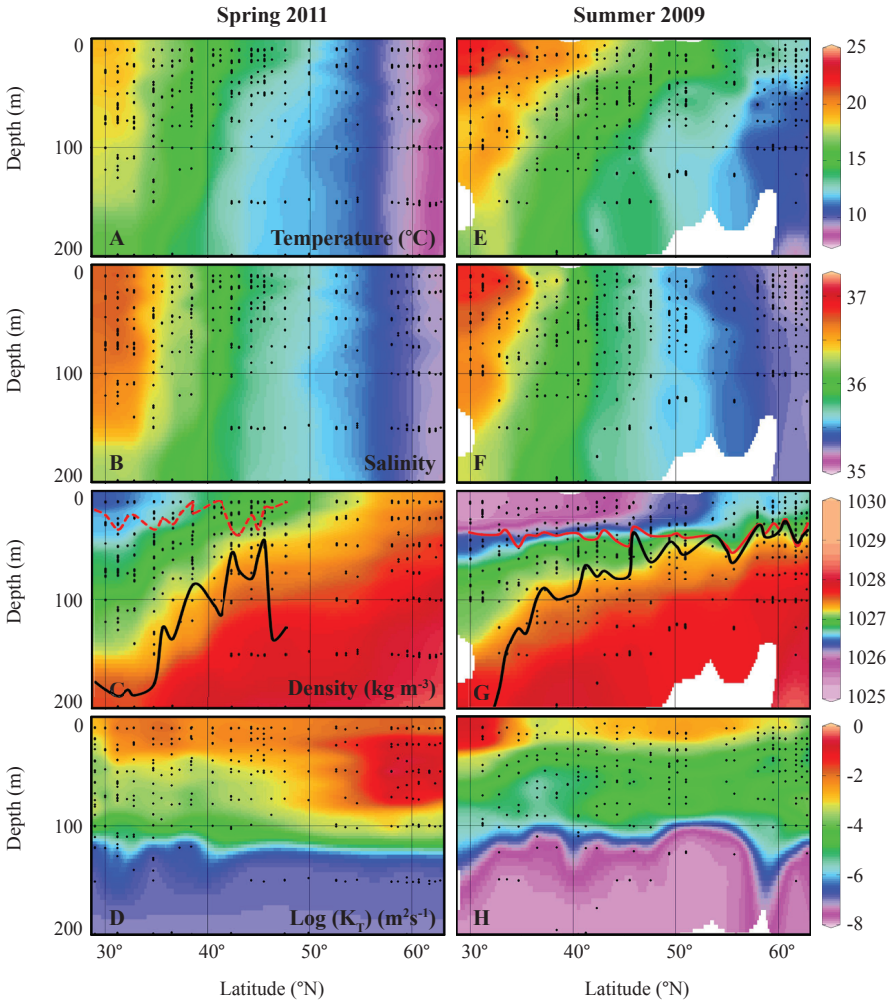

Figure 3. Physical characteristics of water column sampled over the spring (A-D) and summer (E-H) STRATIPHYT cruises. Black dots indicate measurement points. Lines in figure panels C & G represent the pycnocline depth (red) and nutricline depth (black). The pycnocline depth was defined as the depth with the greatest $\Delta\rho/\Delta z$. The dotted line indicates a weak pycnocline in spring. Nutricline depth was defined by a 5 µM change in NO_3^- relative to surface values. In the northern region during the spring, the pycnocline and nutricline were not detected within the depths sampled, and consequently the lines end at the station where they were last detected.

Nitrate (NO_3^-) and phosphate (PO_4^{3-}) were highly depleted (below detection limit) in the mixed layer up to 40°N in the spring and 45°N in summer. A steep nutricline for NO_3^- and PO_4^{3-} was observed in the stratified regions during both seasons (Fig. 4A, E and B, F, respectively). In the north (58-63°N) spring surface concentrations averaged 11.5 µM NO_3^- and 0.8 µM PO_4^{3-}, whereas lower average concentrations were observed during summer, i.e., 1.2 and 0.14 µM for NO_3^- and PO_4^{3-}, respectively. In

the spring, nitrite (NO_2^-) concentration was maximal at the base of the nutricline (around 0.4 µM), which also corresponded closely with Z_{eu}. In the summer, NO_3^- concentrations were typically below the detection limit south of 49°N, with the highest concentration (0.8 µM) around 60 m just north of 50°. Ammonium concentrations in spring were typically below detection limit except between 41-55°N, and in summer north of 49°N. Overall N:P ratio in the Z_m in the spring averaged 8.8±6.5 south and 15.4±1.2 north of 45°N and averaged 10.6±9.4 in summer.

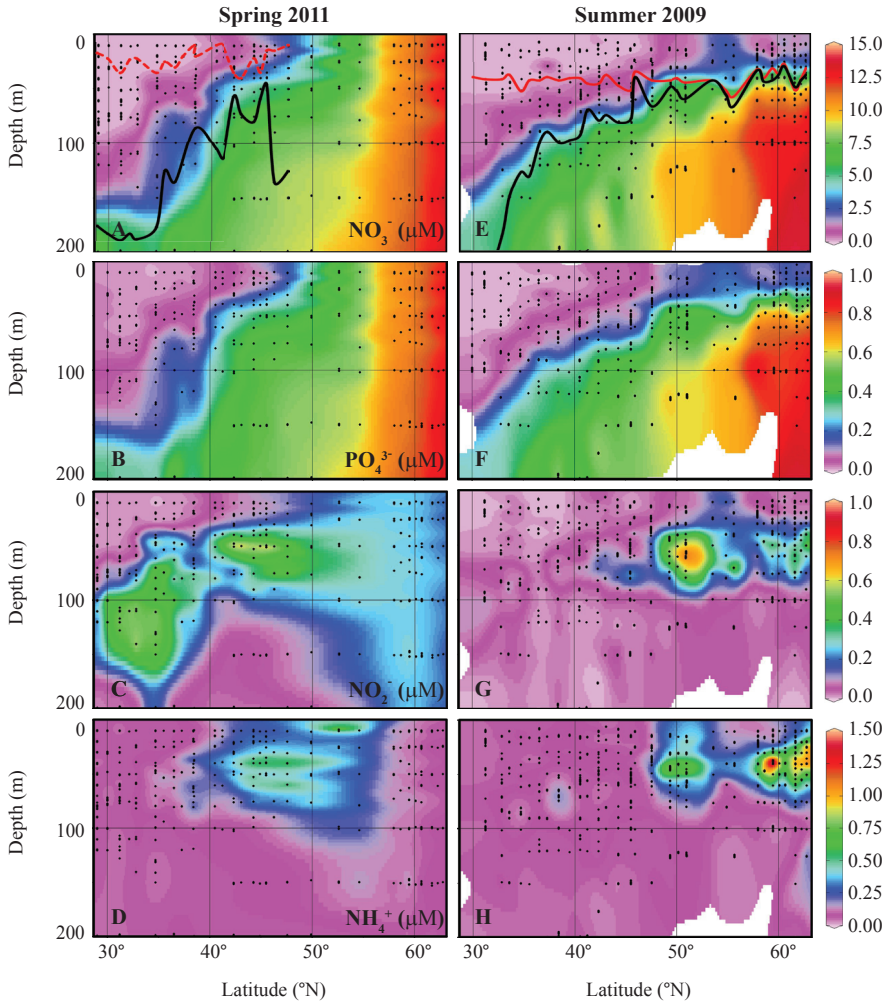

Figure 4. Nutrient profiles of water column sampled over the spring (A-D) and summer (E-H) STRATIPHYT cruises. Black dots indicate measurement points. Lines in figure panels A & E represent the pycnocline depth (red) and nutricline depth (black). The pycnocline depth was defined as the depth with the greatest $\Delta\rho/\Delta z$. The dotted line indicates a weak pycnocline in spring. Nutricline depth was defined by a 5 µM change in NO_3^- relative to surface values. In the northern region during the spring, the pycnocline and nutricline were not detected within the depths sampled, and consequently the lines end at the station where they were last detected.

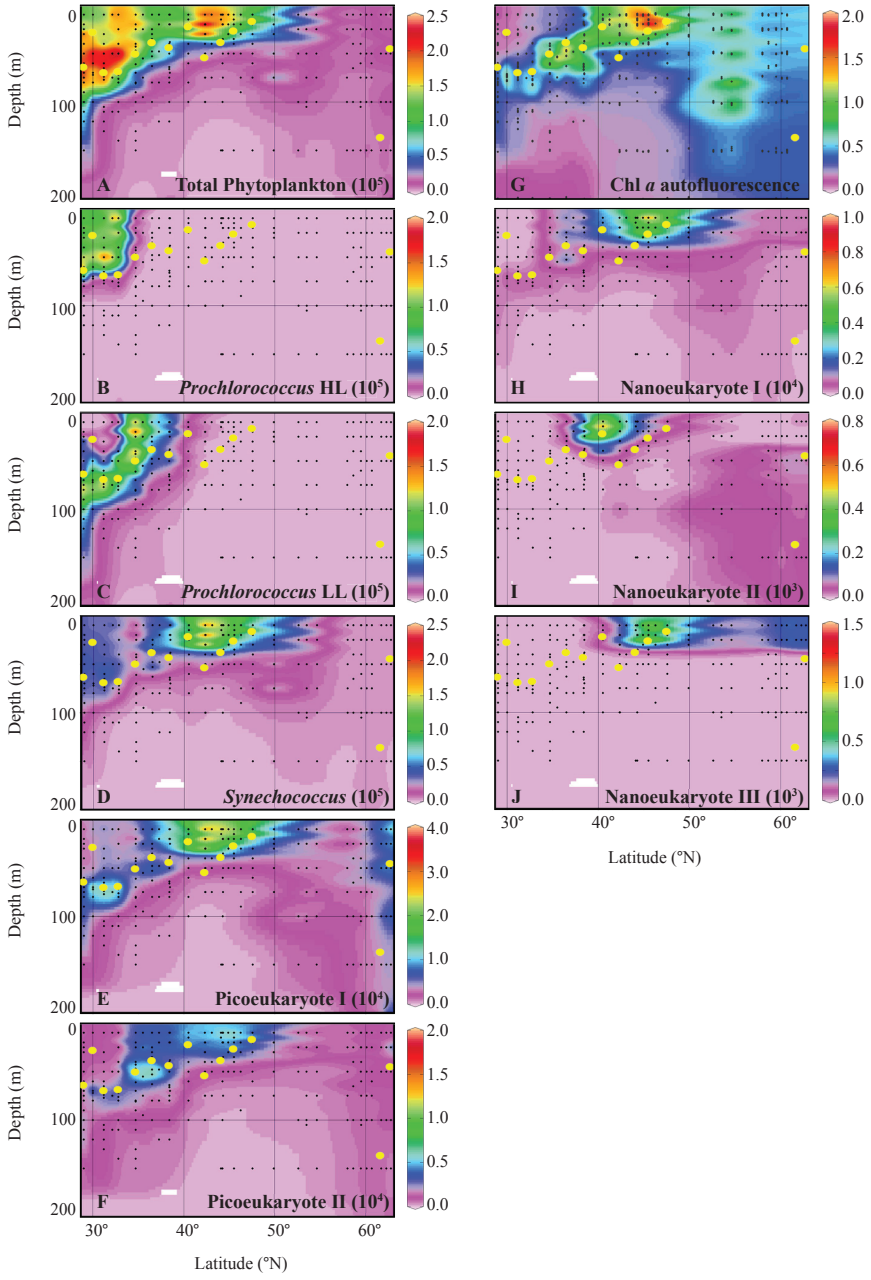

Figure 5. ODV plots of the abundance (ml^{-1}) of total phytoplankton < 20 µm (A), photosynthetic picoprokaryotes (B-D), picoeukaryotes (E and F), HPLC calibrated Chl a autofluorescence (mg m^{-3}) and nanoeukaryote abundance determined by flow cytometry during the spring STRATIPHYT cruise. Black dots indicate measurement points. Yellow dots illustrate Z_m; the absence of yellow points between 50-60°N is due to Z_m deeper than maximal sampling depth. During the spring, Nano IV was not detected.

Phytoplankton data

Spring

In the spring, pico-sized photoautotrophs dominated the total phytoplankton enumerated by FCM (on average 97%) (Fig. 5). Total phytoplankton abundance was highest in the south and declined towards the north, corresponding to strong vertical mixing and deep mixing depths (Fig. 3). South of 35°N, *Prochlorococcus* populations were the numerically dominant phytoplankton groups (Fig. 5B,C). North of 35°N, phytoplankton became confined to the surface mixed layer and the abundance of eukaryotic phytoplankton increased. Nano I-IV maxima occurred between 35-50°N, which corresponded with a peak in Chl *a* (Fig. 5G). The Chl *a* depth profile showed clearly the deep mixing of phytoplankton north of 50°N (Z_m = 225-311 m). At the northernmost stations, calm weather conditions prior to measurements allowed the water column to become more stabilized, reducing mixing depths to < 200 m, and permitting abundances of Pico I and II, and Nano III to once again increase in the surface layer.

Oligotrophic areas as defined by nutrient concentrations (i.e., NO_3^- ≤ 0.13 µM and PO_4^{3-} ≤ 0.03 µM; van de Poll et al. 2013) or Chl *a* concentrations (< 0.07 mg Chl m^{-3}) extended to 40°N. Phytoplankton pigment analysis showed that the deep chlorophyll maximum (DCM) of the most oligotrophic region (28-35°N) was largely comprised of *Prochlorococcus*, prasinophytes, pelagophytes and *Synechococcus* (25, 20, 16 and 10%, respectively; Fig. 6). The surface (0-40 m) peak in Chl *a* between 40-50°N (Fig. 6G) was largely made up by haptophytes (53%; Fig. 6D), diatoms (13%; Fig. 6H) and prasinophytes (12%; Fig. 6C). North of 50°N, haptophytes and diatoms dominated until 58°N where cryptophytes became one of the major groups with an average 22% of total (as compared to 19% for haptophytes and diatoms, Fig. 6). Microscopic analysis showed that diatoms of northern stations consisted mainly of large *Bacteriastrum* sp. (> $1.0x10^3$ cells l^{-1}), with pennates (i.e., *Nitzschia longissima*) and small *Chaetoceros* spp. in lower numbers. Haptophytes consisted of cf. *Emiliania huxleyi* as well as *Phaeocystis*-like cells. The diatom composition at southern stations consisted of the small *Pseudonitzschia* cf. *delicatissima*, and short *Leptocylindrus mediterraneus* chains.

Depth-integrated (0-250 m) cellular C from FCM phytoplankton counts (< 20 µm diameter) ranged between 1.2 and 1.7 g C m^{-2} at the southern oligotrophic stations (Fig. 7A). Pico-sized phytoplankton (pico-prokaryotes and –eukaryotes) comprised the largest percentage (57 - 92%) of the algal C biomass of this region (Fig. 7B). Of the cyanobacteria, both *Synechococcus* and *Prochlorococcus* LL had

an equal contribution to algal biomass of (on average) 24% with a much lower contribution from *Prochlorococcus* HL of 8.5%. Depth-integrated algal C was maximum around 46°N at 7.4 g C m^{-2} and ranged between 1.01 - 2.57 g C m^{-2} in the non-stratified regions of the north (> 50°N; Fig. 7A). Nanoeukaryotes (Nano I-IV) were responsible for the greatest proportion of total algal biomass in the northern half of the transect, comprising between 74 and 92% (Fig. 7B). S-N differences in the contribution of Pico I and II to group-specific C were not present and Pico II made up the largest percentage (on average 69%) over the entire latitudinal range. Nano I comprised all of the nanoeukaryotic phytoplankton C until 42°N, while in non-stratified stations (> 50°N) groups II and III were responsible for the majority of cellular C (53 - 82%).

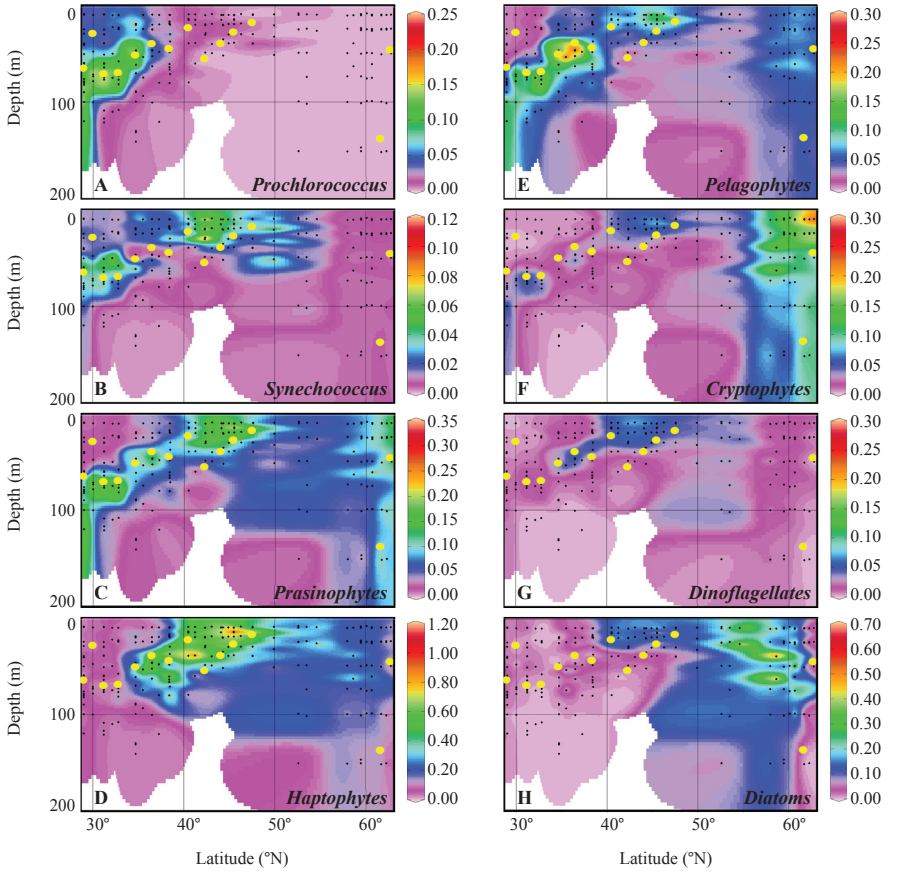

Figure 6. ODV plots of relative Chl a concentrations (mg Chl a m^{-3}) of taxonomic groups determined by HPLC pigment analysis using CHEMTAX identification following the spring STRATIPHYT cruise. Black dots indicate measurement points. Yellow dots indicate Z_m.

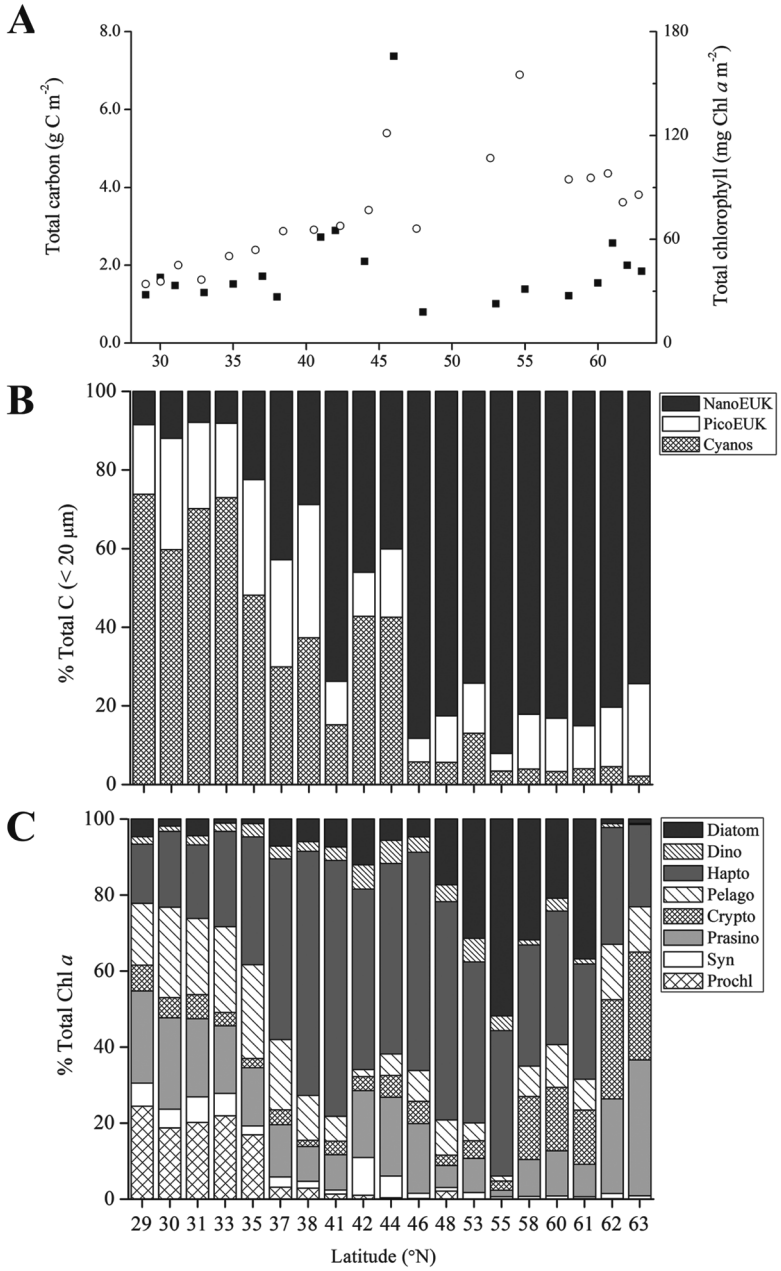

Figure 7. Depth-integrated total phytoplankton carbon (< 20 µm) determined from flow cytometry (closed squares) and depth-integrated total Chl a determined from HPLC calibrated Chl a autofluorescence (open circles) (A), the percent composition of depth-integrated (0 - 250 m) total carbon (< 20 µm) (B), and taxonomic composition of depth-integrated (0 - 250 m) total Chl a determined by HPLC pigment analysis using CHEMTAX identification (C) during the spring.

Depth-integrated Chl *a* concentration varied between 36 - 66 mg Chl *a* m^{-2} in southern oligotrophic region (< 40°N) (Fig. 7A). The taxonomic composition of depth integrated Chl *a* in this region was primarily comprised of haptophytes (37%), pelagophytes (18%), prasinophytes (17%) and *Prochlorococcus* (14%) (Fig. 7C). North of 40°, depth-integrated Chl *a* ranged between 62-155 mg m^{-2}, with an average concentration of 94 mg m^{-2}. Haptophytes (40%), diatoms (19% up to 50% at station 55) and cryptophytes (12%) were important contributors to total Chl *a* of mesotrophic regions. Similar to depth integrated carbon, Chl *a* demonstrated a peak in concentrations at 46°N reaching concentrations of 121 mg m^{-2} (Fig. 7A). The relaxation of the vertical mixing in the northern most stations reduced the contribution of diatoms again to 13%.

Summer

Similar to spring, pico-sized phytoplankton dominated, i.e., 95% of the total phytoplankton enumerated by FCM (Fig. 8). In contrast to spring, however, phytoplankton abundances were lower in the surface layer (0 - 25 m). South of 45°N, total abundance was maximal ($1.6\pm0.4x10^5$ cells ml^{-1}) below the Z_m and tapered off towards the depth of the nutricline, which is characteristic for a deep-chlorophyll maximum (DCM). The prokaryote *Prochlorococcus* was the most abundant member of the phytoplankton community in the southern most region (31 - 33°N), with the HL population dominating the upper 0 - 55 m surface waters (92%; Fig. 8B) and the LL population being more abundant at the DCM (93%; Fig. 8C). The DCM shallowed with latitude, giving over to a surface maximum north of 45°N. This also marked the upper boundary of oligotrophic areas, which occurred 5° north compared to the spring. When the base of the Z_m was situated above the nutricline, picoeukaryotic photoautotrophs became maximal in the surface waters and *Prochlorococcus* disappeared. The cyanobacteria *Synechococcus* spp. showed highest abundances in the north ($7.0\pm0.4x10^5$ ml^{-1}; Fig 8D) numerically dominating the photosynthetic community < 20 µm (making up 74% of the total counts). The abundance of the picoeukaryotic phytoplankton increased north of 38°N with Pico II being more dominant in the northern half of the transect (Fig. 8E, F). Chl *a* and cell size increased towards the north (Fig. 8G - K). Although nanoeukaryotic phytoplankton abundance was relatively low, their larger cell size contributed substantially to Chl *a* autofluorescence (Fig. 8G). The abundance of the different nanoeukaryotic phytoplankton groups was inversely related to cell size, whereby the largest sized Nano III and IV were the least abundant and found only in the surface waters of the most northern stations (Fig. 8K).

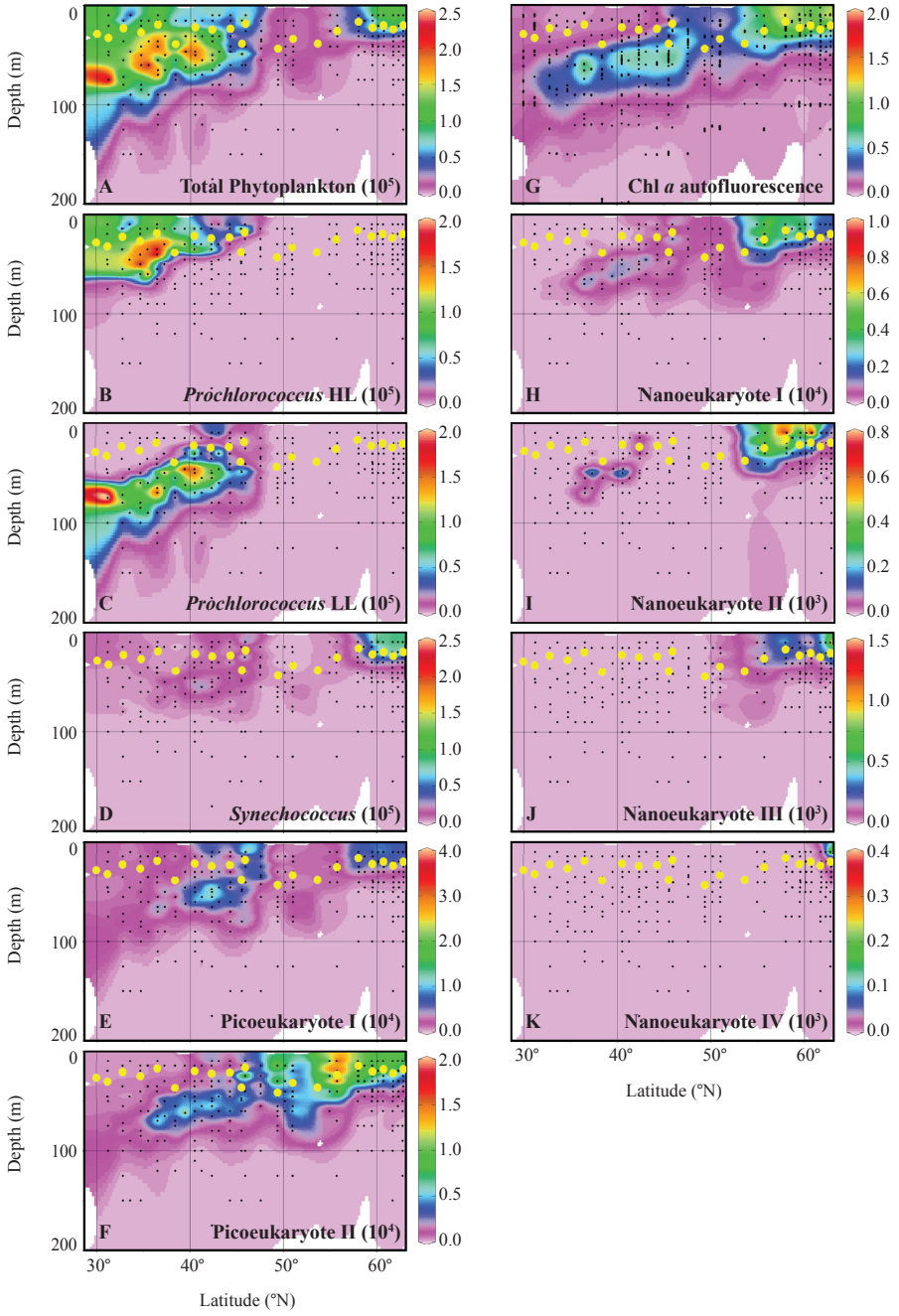

Figure 8. ODV plots of the abundance (ml^{-1}) of total phytoplankton < 20 µm (A), photosynthetic picoprokaryotes (B - D), picoeukaryotes (E and F), HPLC calibrated Chl a autofluorescence (mg m^{-3}) and nanoeukaryote abundance determined by flow cytometry during the summer STRATIPHYT cruise. Black dots indicate measurement points. Yellow dots illustrate Z_m.

Phytoplankton pigment analysis (Fig. 9) indicated that northern surface populations were largely made up by haptophytes (around 48%), followed by prasinophytes (16%), pelagophytes (12%), and dinoflagellates (12%). *Synechococcus*, cryptophytes and diatoms also had pigment concentration maxima in these regions (> 60°N), but contributed very little to the total community composition (≤ 5%) (Fig. 9). In the strongly stratified southern stations (30 - 45°N), haptophytes remained a principal component of the algal community based on Chl *a* (average 24%; Fig. 9D) with *Prochlorococcus*, prasinophytes, pelagophytes and *Synechococcus* contributing 23, 17, 12 and 12%, respectively (Fig. 9A - D). Microscopic analysis revealed that diatoms of the northern stations consisted of pennates with *Nitzschia longissima* and *Pseudonitzschia* cf. *delicatissima* as main representatives. The haptophyte *Phaeocystis* increased towards the north reaching maximum cell numbers at 58°N of around $2x10^3$ cells ml^{-1}. In contrast to spring, *Phaeocystis* was primarily found in colonial form with colony bladders often colonized by other phytoplankton species as well as heterotrophs (i.e., dinoflagellates, ciliates).

Integrated over depth (0 - 250 m), cellular C from FCM counts were 2 to 4-fold lower in the summer compared to spring and ranged between 0.33 and 2.53 g C m^{-2} (Fig. 10), with the lowest values (max. 0.81 g C m^{-2}) in the oligotrophic south (< 45°N). Pico-sized phytoplankton dominated (70 - 97%) the south, with cyanobacteria contributing an average of 19, 29 and 8% for *Prochlorococcus* HL, *Prochlorococcus* LL and *Synechococcus*, respectively. As latitude increased nanoeukaryotes (Nano I - IV) became responsible for the greatest proportion of total carbon biomass (with *Synechococcus* and picoeukaryotic phytoplankton sharing the residual 15 - 40%). Depth-integrated Chl *a* biomass was also 2-fold lower in summer compared to spring, varying between 17 - 27 mg Chl *a* m^{-2} in oligotrophic regions (Fig. 10A), with *Prochlorococcus*, haptophytes and prasinophytes as the principal contributors (24, 24, and 18%, respectively). Moving north, the importance of haptophytes increased (Fig. 10C). Similar to that of total organic C, the highest values for total Chl *a* were found north of 55°N with maximum values of around 43 mg Chl *a* m^{-2} (Fig. 10A).

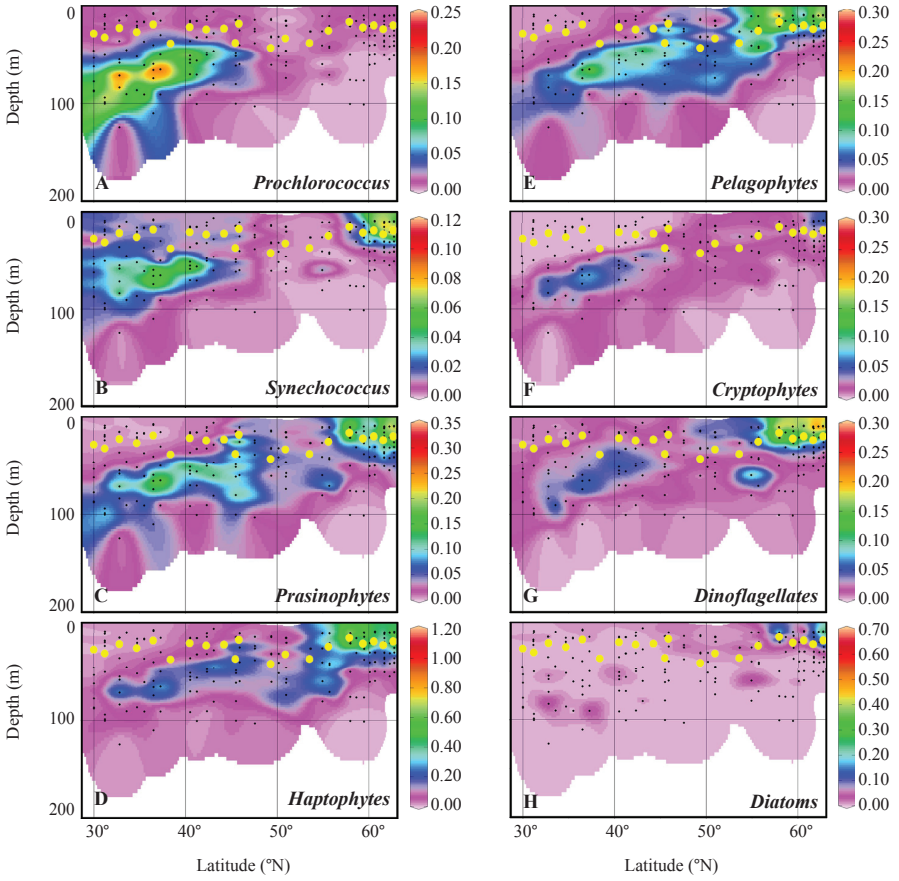

Figure 9. ODV plots of taxonomic group specific Chl a concentrations (mg Chl a m^{-3}:based on CHEMTAX) for the STRATIPHYT summer cruise. Black dots indicate measurement points. Yellow dots indicate Z_m.

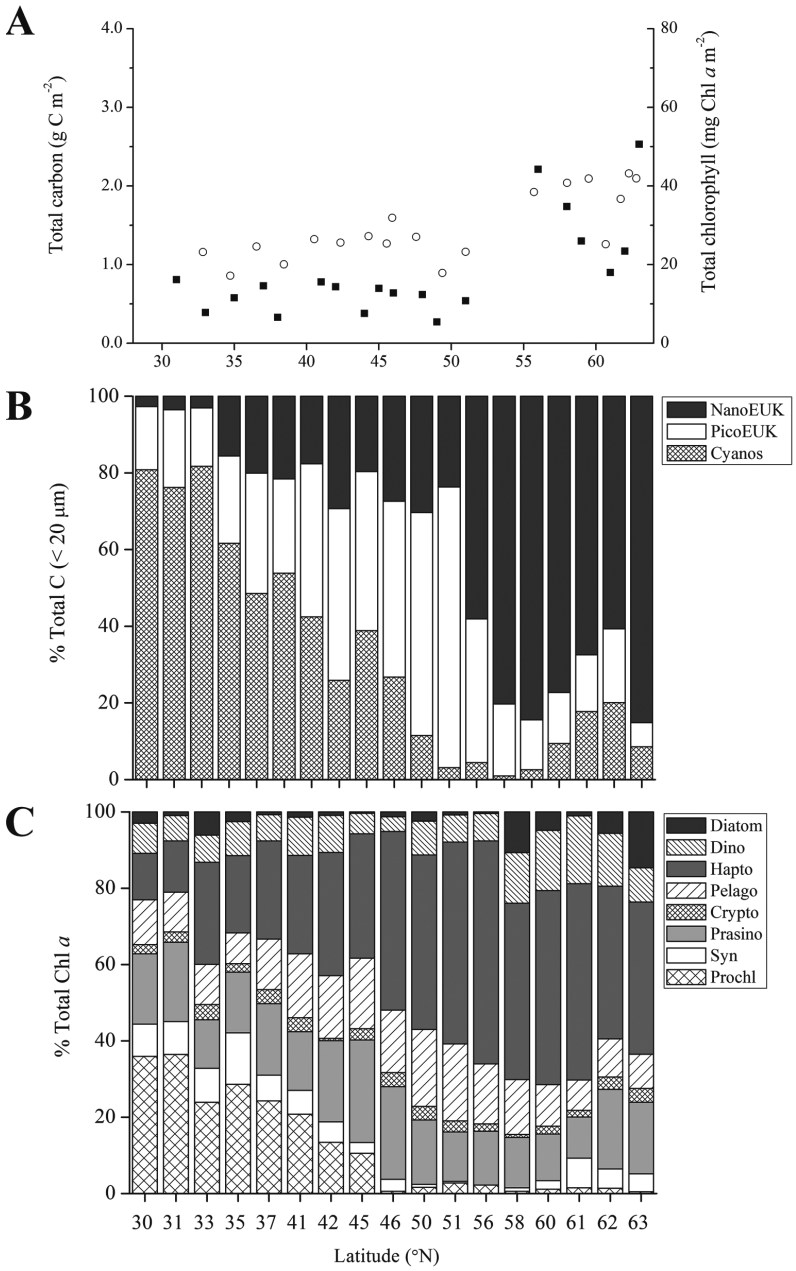

Figure 10. (A) Depth-integrated total phytoplankton carbon (cell size < 20 µm) determined by flow cytometry (closed squares) and depth-integrated total Chl a determined by HPLC calibrated Chl a autofluorescence. (B) Community composition based on total phytoplankton carbon determined by flow cytometry. (C) Community composition based on total Chl a determined by HPLC pigment analysis using CHEMTAX identification during summer.

Statistical Analysis

Redundancy analysis (RDA) was used to investigate relationships between the phytoplankton community composition (red lines) and the environmental variables (blue lines in Fig. 11). Lines in the RDA triplots pointing in the same direction are positively correlated, while lines pointing in opposite directions are negatively correlated. In addition, the triplots show how stratification and depth level (symbols) are associated with the community composition and environmental variables. We note that the RDA does not show NO_3^- and temperature as environmental variables, because PO_4^{3-} was collinear with NO_3^- (Pearson correlation: $r = 0.99$, $p < 0.001$) and salinity was collinear with temperature ($r = 0.87$, $p < 0.001$). In Fig. 11A, the phytoplankton community composition is quantified in terms of carbon based on FCM analysis. The eigenvalues (obtained from model output) revealed that the first two axes of this RDA triplot explained 27% and 12% of the variation in the dataset. The main environmental variables contributing to the formation of the first axis were PO_4^{3-} and depth level, while the second axis was mainly influenced by salinity (temperature) and PO_4^{3-} (NO_3^-). *Prochlorococcus* C was associated with relatively high salinity/temperature environments with deep Z_{eu} and low nutrient concentrations, all characteristic of stratified subtropical waters (Fig. 9A). Moreover, the HL and LL *Prochlorococcus* populations were differentiated by the stronger association of the HL population to higher salinity/temperature and lower association with the Z_m (Fig. 11A). *Synechococcus* and Pico I and II were associated with the Z_m of relatively high temperature, low nutrient waters. Conversely, nanoeukaryotic phytoplankton C was correlated to the Z_m of relatively lower temperature, higher nutrient and shallow Z_{eu} waters.

When the phytoplankton was quantified as percentage distribution of total C, multivariate analysis showed that the first two axes of the RDA explain approximately 16% and 10% of the variation in the data, respectively (Fig. 11B). The most influential variables to the formation of the first axis were again PO_4^{3-} and salinity, while the second axis was mainly influenced by depth layer, Z_m/Z_{eu}, NO_2^- and stratification level. *Prochlorococcus*, *Synechococcus* and picoeukaryotic phytoplankton had high contributions to total C at high salinity/temperature, low nutrient environments and were differentiated by higher contributions of *Prochlorococcus* HL, and *Synechococcus* in the Z_m. Nano I - IV on the other hand showed higher contributions to total C in relatively lower temperature, higher nutrient environments. A higher proportion of Nano I cellular C was associated with BZ_m environments with higher N:P ratios, while Nano II and III were associated with Z_m environments with high Z_m/Z_{eu}.

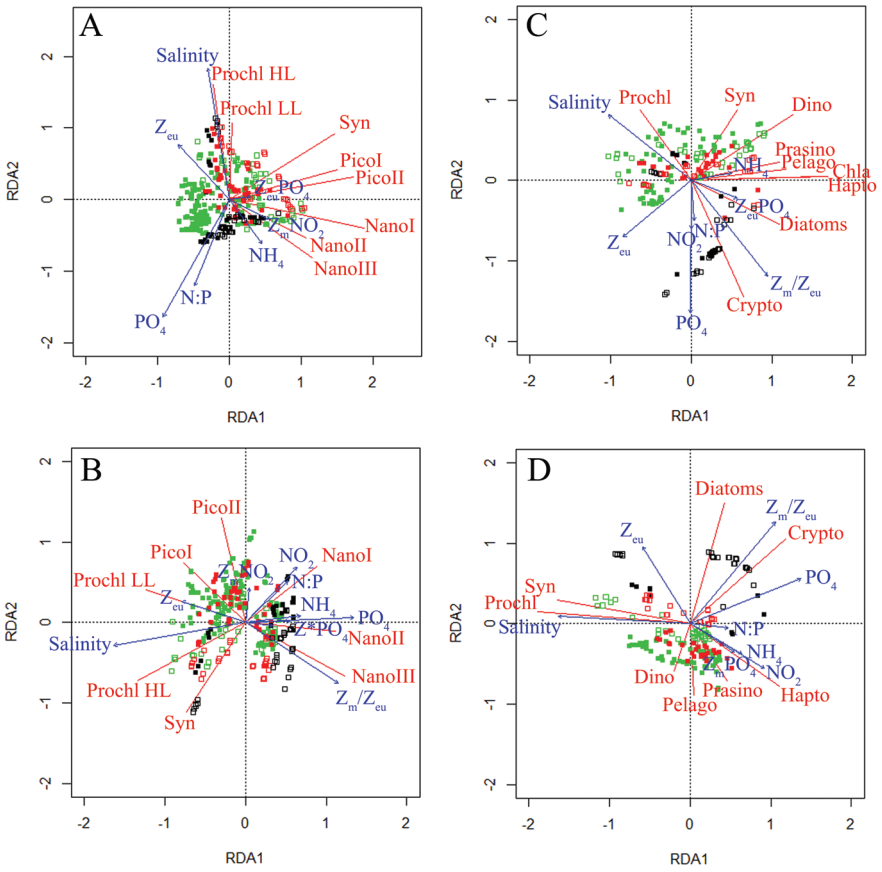

Figure 11. Redundancy Analysis (RDA) correlation triplots of phytoplankton community composition (in red) in relation to environmental variables (in blue). The community composition is quantified in terms of (A) phytoplankton carbon (cell size < 20 µm) and (B)[1] percentual distribution of phytoplankton carbon, both calculated from the FCM counts, (C) Chlorophyll a concentration and (D) percentual distribution of the Chlorophyll a concentration, both calculated from the pigment analysis using CHEMTAX. Data represented in figures are compiled from both the summer and spring STRATIPHYT cruises. Symbols illustrate from what stratification and depth level the samples originated from; according to depth layer (open = mixed layer and closed = below mixed layer) and colored according to stratification level (green = strongly stratified, red =weakly stratified, and black = non-stratified stations). Environmental variables: Z_{eu} = euphotic zone depth, N:P = ratio of DIN to PO_4^{3-}, Z_m/Z_{eu} = ratio of mixed layer depth to euphotic zone depth, $Z_mPO_4 = PO_4^{3-}$ flux into the mixed layer, $Z_{eu}PO_4 = PO_4^{3-}$ flux into the euphotic zone, $Z_mNO_2 = NO_2^-$ flux into the mixed layer, and [1] $Z^*PO_4 = Z_{eu}PO_4$ & Z_mPO_4, which are labeled together to improve readability as arrows overlay one another. PO_4^{3-} is collinear with NO_3^- (Pearson correlation: r = 0.99, p < 0.001) and salinity is collinear with temperature (r = 0.9, p < 0.001). Biological variables: Prochl HL = Prochlorococcus high-light, Prochl LL = Prochlorococcus low-light), Syn = Synechococcus, Pico = picoeukaryotes, Nano = nanoeukaryotes, Dino = dinoflagellates, Hapto = haptophytes, Prasino = prasinophytes, Crypto = cryptophytes, and Pelago = pelagophytes.

When the community composition was based on pigment analysis and expressed in terms of Chl *a*, the first two axes of the RDA explained 29% and 13% of the variation (Fig. 11C). The first axis was mainly influenced by Z_m/Z_{eu} and inversely by salinity. The second axis was mainly formed by PO_4^{3-} and stratification. *Prochlorococcus*-specific Chl *a* was associated with strongly stratified waters with high temperature/salinity, low nutrients and low Z_m/Z_{eu}. Conversely, cryptophytes and diatoms were related to relatively colder, non-stratified waters with high availability of nutrients and high Z_m/Z_{eu}. Total Chl *a* and the remaining taxonomic groups were moderately coupled to warmer stratified waters with shallow $Z_{eu.}$

When the community composition was based on the percentage distribution of the Chl *a* concentration, the first two axes of the RDA explained 24% and 15% of the variation in the data (Fig. 11D). The first axis was mainly influenced by salinity (negative correlation) and PO_4^{3-}, and the second axis by depth layer and Z_m/Z_{eu}. Diatoms and cryptophytes were related to non-stratified waters with relaxed nutrient limiting conditions and a higher Z_m/Z_{eu} ratio. Conversely, an increased contribution of dinoflagellates were associated with BZ_m of stations with stronger stratification and fewer nutrients. Consistent with phytoplankton C analysis, the contribution of *Prochlorococcus* was associated with high temperature/salinity and low nutrient environments. However, one notable difference was the high correlation of *Synechococcus* with *Prochlorococcus*, which is absent from FCM measurements. Finally, prasinophytes, haptophytes and pelagophytes were related to BZ_m of stations characterized by lower temperatures/salinities, higher nutrients and shallower Z_{eu}.

Overall, environmental data explained 47, 37, 52 and 56% of the total variation in phytoplankton group-specific C, %C, Chl *a* and %Chl *a*, respectively (Table 2). As ecological data are general quite noisy and consequently can never be expected to yield a high value of R^2 (Legendre and Legendre 1998), these values provide confidence that the major patterns within the data have been captured by the RDA model. Variance partitioning demonstrated that stratification level alone explained 4 - 8% of the variation (Table 2). Therefore, inclusion of Brunt-Väisälä frequency (N^2) as an index of stratification increased the variation explained by the environmental data. Running the models without considering nutrient flux into the surface waters demonstrated nearly equivalent R^2, demonstrating equal coverage by both models. However, in the case of size composition data, inclusion of nutrient flux reduced the explained variation partitioned to stratification level (from 7.4 to 4.1%).

Table 2. Variance decomposition of the RDA models in Fig. 11A - D, based on phytoplankton carbon (< 20 µm), percentual distribution of phytoplankton carbon (%Carbon), Chlorophyll *a* concentration and percentual distribution of the Chlorophyll *a* concentration (%Chl *a*). RDA models were partitioned to show the percentage of variance explained by all the variables, all the variables except stratification level, stratification level alone, shared variance (collinearity present in the model which could not be removed) and residual variance (remaining variance not explained by the model).

		Variance (%)			
Component	Source	A. Carbon	B. %Carbon	C. Chl *a*	D. %Chl *a*
	All variables	47.09	37.26	51.50	55.71
A	All variables – stratification level	41.52	28.36	42.31	40.02
B	stratification level	6.91	4.07	6.98	7.84
C	Shared	-1.35	4.83	2.21	7.85
D	Residual	52.91	62.74	48.50	44.29

Discussion

Comparing CHEMTAX and FCM

FCM provides detailed information about abundance and size structure of the phytoplankton community. In contrast, pigment analysis with CHEMTAX provides information regarding taxonomic composition including larger-sized algae that are typically missed by FCM, but lacks information regarding cell abundances and is unable to differentiate size differences within taxonomic groups (Uitz et al. 2006; Uitz et al. 2008). These differences between CHEMTAX and FCM analysis became apparent when comparing depth-integrated Chl *a* (obtained from pigment analysis) and total phytoplankton C (obtained by FCM) across the two seasons. While the results of both methods were tightly coupled during the summer (when small-sized phytoplankton dominated), they deviated from each other in the spring where there was a higher contribution of larger-sized phytoplankton taxa north of 40°N. Using a fixed carbon : chlorophyll ratio of 50 (Brown et al. 1999), carbon determined from pigments and FCM counts were in good agreement during the summer and within oligotrophic regions during the spring. However, Chl *a* carbon concentrations were up to 5-fold higher during the spring in the well-mixed high latitude regions, which coincided with a higher presence of larger diatoms species as seen from both CHEMTAX and microscopy observations. In spite of methodological differences between FCM and pigment analysis, combining the two methods permitted us to examine how changes in vertical stratification affected both the size structure and taxonomic composition of

phytoplankton communities, and provided additional information regarding the potential taxonomic groups comprising different phytoplankton size classes. Based on our results, we recommend that future studies combine FCM and CHEMTAX analysis, and use size-fractionation for both FCM and HPLC samples. This would provide useful information regarding the size composition of taxa as well as of numerically abundant groups, and may improve taxonomic identification of FCM groups.

Although phytoplankton pigment analysis confirmed the general spatial distributions of the prokaryotic phytoplankton, there were some notable discrepancies compared to FCM. Pigments specific for *Prochlorococcus* were low for near-surface samples despite their high numerical abundance determined by FCM. This indicates either a low cellular concentration of this pigment in the HL population or could indicate a reduced retention of small cells during filtration. The smaller average cell diameter of *Prochlorococcus* HL in this study (i.e., 0.6 μm) compared to the LL population (i.e., 0.7 - 0.8 μm) does support the latter. Photoacclimation related changes are most strongly observed in photoprotective pigments (e.g., diadinoxanthin, diatoxanthin and violaxanthin, antheraxanthin and zeaxanthin) and subsequently these pigments show steep vertical gradients within the water column. As a result, photoprotective pigments are to be avoided when using CHEMTAX analysis when alternative pigments are available. In addition, photoacclimation can alter cellular pigment concentrations. Pigments specific for *Prochlorococcus* (e.g. divinyl chlorophyll *a*) have been shown to be reduced by 37 - 50% in high-light acclimated cells of *Prochlorococcus* HL ecotype eMED45 (Partensky et al. 1993). In addition, a twelve fold difference in cellular divinyl chlorophyll *a* concentrations has been reported for field populations of *Prochlorococcus* (Partensky et al. 1999b). This suggests that the variability in carbon to chlorophyll *a* ratios of this species may be a main cause for the discrepancy between flow cytometry derived carbon data and pigment based data from CHEMTAX found for oligotrophic stations. Pigment and FCM based detection of *Synechococcus* also revealed inconsistencies. Detection of *Synechococcus* based on zeaxanthin indicated a higher signature in the DCM regions compared to detection based on phycoerythrin fluorescence as determined by FCM. Phycoerythrin has higher specificity than zeaxanthin and is most likely a better indicator for this genus, however, it is not soluble in acetone, excluding its utility in CHEMTAX due to the pigment extraction method. The use of two separate pigments for the identification of this taxa does not appear to permit a direct comparison between these two methods.

Phytoplankton distributions in relation to vertical stratification

Pico-sized phytoplankton, and particularly cyanobacteria, dominated the total phytoplankton abundance and biomass (< 20 μm) of the stratified southern region, consistent with evidence for the importance of this size class for the production in warm, low nutrient waters (Partensky et al. 1996; Maranon et al. 2000; Perez et al. 2006; Uitz et al. 2006). *Prochlorococcus* was the main photosynthetic prokaryotic group, with the northern edge of its distributions closely matching oligotrophic boundaries (varying from 42 to 48°N between spring and summer). The contribution to total biomass (i.e., 32 and 48% in the spring and summer, respectively) and geographic distribution of *Prochlorococcus* are both in the upper range of those reported in the literature (i.e., 21 - 43% and typically found 40°S - 45°N; Johnson et al. 2006; Whitton and Potts 2012). The northern edge of the distribution of *Prochlorococcus* coincided closely with a reduction in temperature, supporting evidence that temperature acts as a critical factor regulating the distribution of this genus (Johnson et al. 2006; Zinser et al. 2007; Flombaum et al. 2013). The ubiquity and numerical dominance of *Prochlorococcus* within stratified oligotrophic waters of the world's oceans is thought to be a consequence of both genetic streamlining (and subsequent reduction in cell size), and diversity in genomic evolution within the genus facilitating a range of niche partitioning (Partensky and Garczarek 2010). Coherent with this hypothesis, FCM distinguished two distinct populations of *Prochlorococcus* (Johnson et al. 2006; Zinser et al. 2007) that dominated at different depths and latitudes. *Prochlorococcus* HL dominated over *Synechococcus* 2-fold under conditions of strong stratification, which was reversed under weak stratification. The prevalence of *Prochlorococcus* LL changed very little between the two seasons, which is consistent with a study revealing a shift from cyanobacteria with a small genome (i.e., *Prochlorococcus* HLII) to those with a larger genome (i.e., *Prochlorococcus* LL and *Synechococcus*) with increased vertical mixing in the upper 10 m water column (Bouman et al. 2011). The dominance of *Synechococcus* over *Prochlorococcus* following deep winter mixing is often attributed to the inability of *Prochlorococcus* to utilize the increased nitrate concentrations (Whitton and Potts 2012). Our results suggest that future alterations in stratification will also play a role in governing phylogeography within the unicellular cyanobacterial populations.

The geographical distribution of *Synechococcus* extended further northwards than that of *Prochlorococcus*, illustrating the broader temperature range of *Synechococcus* (Moore et al. 1995; Partensky et al. 1999a; Peloquin et al. 2013). Recently, it was suggested that the ability of *Synechococcus* spp. to regulate photochemistry over a

range of temperatures through temperature dependent association of phycobilisome (PBS) to the different photosystems may explain the larger geographic range of this group relative to *Prochlorococcus* spp., which lack PBS (Mackey et al. 2013). However, we also provide evidence that nutrients are important in regulating the abundance of *Synechococcus*. *Synechococcus* demonstrated lowest abundances in oligotrophic regions and abundances were maximal where the nutricline was the shallowest. In addition, the contribution of *Synechococcus* to total C was higher in the spring (up to 43% compared to 25% in the summer). The success of this genus under high nutrient concentrations is in line with maximal abundances observed in the highly productive upwelling regions where concentrations can be up to a magnitude higher than in oceanic regions (Morel 1997; Whitton and Potts 2012). The predominance of pico-sized cells in the oligotrophic regions is often attributed to a competitive advantage over larger phytoplankton in low nutrient environments afforded by the lower nutrient requirements, small diffusion boundary layers and large surface area per unit volume of small cell size (Raven 1986; Chisholm 1992; Finkel et al. 2010). This is consistent with our finding of nutrients as an important agent for phytoplankton size structure. Aside from picoprokaryotic autotrophs, eukaryotic haptophytes (ranging 23 - 36% between summer and spring), prasinophytes (17 - 19%) and pelagophytes (13 - 18%) substantially contributed to depth integrated Chl *a* concentration within the oligotrophic regions. This concurs with evidence from literature that these groups are important components of picoeukaryotic phytoplankton communities, and can represent up to 35% of total picoeukaryotic cells (Guillou et al. 2004; Liu et al. 2009; Jardillier et al. 2010). As even tiny haptophytes may produce organic plate scales this genus may play a significant role in the biological pump of stratified areas (Liu et al. 2009).

Vertical stratification affects the phytoplankton dynamics by regulating the availability of light and nutrients to phytoplankton in the ocean (Behrenfeld et al. 2006; Huisman et al. 2006; Hoegh-Guldberg and Bruno 2010). Our results demonstrate that incorporating an index for stratification, such as Brunt-Väisälä frequency (N^2), can improve the explained variation in phytoplankton data, both in terms of cell size and taxonomic composition. The underlying reason is probably that this stratification index captures the impact of stratification on various physicochemical processes, such as the flux of nutrients into the euphotic zone. Our finding that the inclusion of nutrient flux into the surface waters reduces the variation explained by stratification level, without improving the overall coverage of the model, tends to support this hypothesis.

In general, phytoplankton biomass and primary production (van de Poll et al. 2013) were highest where the nutricline was the shallowest, suggesting a strong coupling between the nutricline, the rate of nutrient supply to the euphotic zone and the photosynthetic performance of phytoplankton in the North Atlantic Ocean (Behrenfeld et al. 2006). The depth of the nutricline was closely tied to the shift in dominance of key phytoplankton genera and size classes. Besides the switch in the dominant cyanobacterial group from *Prochlorococcus* in waters with a deep nutricline to *Synechococcus* in waters with a shallow nutricline, a switch from picoeukaryotic to nanoeukaryotic phytoplankton as the principal contributors to C biomass < 20 µm was also apparent during both seasons. Nutricline depth is thought to reflect nutrient supply into the upper mixed layer and when implemented as a proxy for water column stability has successfully explained basin-scale changes in the relative contribution of diatoms and coccolithophores to total phytoplankton biomass (Cermeño et al. 2008). We found that the maximum group-specific Chl *a* concentrations for prasinophytes, haptophytes, phototrophic dinoflagellates and some extent pelagophytes (summer) coincided with the shallowing of the nutricline. The association of phototrophic dinoflagellates and pelagophytes with higher nutrient concentrations is not surprising considering their relatively large cell size (Irigoien et al. 2004; Edwards et al. 2012). Dinoflagellates, however, were most prevalent during the summer in the north, which agrees with their tendency to favor warmer waters, with shallower Z_m, higher mean irradiance and reduced vertical mixing (Irwin et al. 2012). Although the current study estimated phytoplankton contribution based on taxon-specific pigments, the mixotrophic capacity of some phytoplankton species cannot be excluded. Haptophytes, prasinophytes, cryptophytes and dinoflagellates have all been shown to contain mixotrophic representatives (McKie-Krisberg and Sanders 2014; Unrein et al. 2014). Such nutritional flexibility would provide a competitive advantage under low light and low (inorganic) nutrient regimes.

During the spring the water column north of 53°N remained non-stratified, which resulted in the vertical uniformity of temperature, salinity, density and nutrients in the upper 200 m. This is consistent with observations of high latitude regions of the Atlantic remaining well mixed in the upper 200 m between December to April (van Aken 2000). Deep mixing and high turbulence in the north (> 50°N) during the spring dispersed cells to depths greater than 200 m, reducing phytoplankton abundance and phytoplankton pigment concentrations. However, when integrated over the sampled water column, these northern stations demonstrated the highest Chl *a* concentrations per m^2 indicating high phytoplankton C biomass in these regions,

despite being dispersed over hundreds of meters. Chlorophyll *a* concentrations specific for diatoms and cryptophytes were greatest in these homogeneously mixed waters. The association of these taxa with higher macronutrient concentrations is consistent with their lower half-saturation constants for nutrient uptake and nutrient-limited growth (Litchman et al. 2006; Irwin et al. 2012).

Modeling the phytoplankton composition of future oceans

The current study provides a high-resolution mesoscale description of physical, chemical and biological (phytoplankton community composition and size) characteristics in the upper 200 m water column along a stratification gradient in the Northeast Atlantic Ocean during two periods of stratification. The multivariate approach identified ocean stratification as one of the key drivers for the distribution and separation of different phytoplankton taxa and size classes. Here we elaborate on key features of our results pertinent to biogeochemical and ecological modeling studies of the present and future oceans.

Models can improve our understanding and prediction of climate-induced changes in plankton community composition, primary production and associated biogeochemical cycles. During recent years, interesting model approaches have been developed in which a broad spectrum of phytoplankton "species" with different growth parameters and different responses to light and nutrients become self-organized into distinct biogeographical communities across the global ocean (e.g. Follows et al. 2007). The predictions of these models critically depend on questions as to which traits best differentiate phytoplankton functional groups and which environmental variables regulate primary production and community structure (Behrenfeld et al. 2006; Irwin et al. 2012). In this sense, predictions of how the ocean ecosystem will respond to climate change are still limited by a lack of information regarding which taxonomic groups are essential and what environmental controls determine the distribution and succession of these taxonomic groups (Falkowski et al. 2000; Litchman et al. 2006; Finkel et al. 2010).

The classification of phytoplankton functional types (PFT) is dependent on the scientific question to be addressed by the model (Claustre 1994; Falkowski et al. 1998; Le Quéré et al. 2005). For biogeochemical models based on functional taxa, PFT should, for example (i) play a specific biogeochemical role, (ii) be defined by distinct set of physiological, environmental or nutritional requirements which regulate biomass and productivity, and (iii) be of quantitative importance in some regions of the ocean (Le Quéré et al. 2005). Based on this definition, we

can classify our phytoplankton groups into several PFTs. Picocyanobacteria and picoeukaryotic phytoplankton were highest in abundance and showed largest contributions to phytoplankton biomass in stratified waters ($N^2 > 2x10^{-5}$ rad^2 s^{-2}). The picocyanobacteria PFT could be distinguished by a higher association with warm temperatures and high water clarity (deep Z_{eu}), and conversely, the picoeukaryote PFT by a higher association with nutrient flux into the surface layers ($Z_m NO_2$ and $Z_{eu}PO_4$). Furthermore, our results indicate that in addition to temperature and light (as recently reported by Flombaum et al. 2013) incorporation of the N:P ratio and vertical turbulence structure of the water column will be useful to distinguish between the niches of the different picocyanobacterial populations (*Prochlorococcus* HL, *Prochlorococcus* LL and *Synechococcus*). Another main PFT, the diatoms, were distinguished by their association with the surface layers of non-stratified waters ($N^2 < 2x10^{-5}$ rad^2 s^{-2}), colder water temperatures, higher nutrient concentrations and higher potential for light limitation. There is some evidence for successional shifts in dominance between diatoms and cryptophytes (Moline et al. 2004; Mendes et al. 2013) and several studies have reported selective grazing by different zooplankton species on either diatoms or cryptophytes (Cotonnec et al. 2001; Haberman et al. 2003; Liu et al. 2010), which may advocate for an additional PFT for cryptophytes. If warranted, our analysis suggests that this cryptophyte PFT can be distinguished from diatoms by the closer association of cryptophytes with high Z_m/Z_{eu} and conversely of diatoms with high $Z_{eu}PO_4$.

Some models combine autotrophic dinoflagellates, prasinophytes, pelagophytes and haptophytes together into one or more 'mixed phytoplankton' PFT due to their lack of a distinguishable biochemical role or absence of bloom formation (Le Quéré et al. 2005). In our data, these taxa were distinguished from other phytoplankton by their high contribution to total Chl *a* in the DCM of the stratified waters. However, dinoflagellates were associated to waters with a shallow Z_{eu}, whereas the haptophytes and prasinophytes showed a higher association with NH_4^+ and NO_2^-. This is consistent with observations that haptophytes contain several species (e.g., *Phaeocystis* spp., *Emiliania huxleyi*) that have relatively high NH_4^+ uptake rates (Tungaraza et al. 2003) and can develop dense blooms in N-rich parts of the global ocean (Schoemann et al. 2005; Lacroix et al. 2007). In addition, haptophytes have the ability to produce organic or calcium carbonate plates (Not et al. 2012) and may thereby directly contribute to the biological pump (with obvious contributions by calcifying coccolithophores). Mixotrophy, although not exclusive to this taxa (McKie-Krisberg and Sanders 2014; Unrein et al. 2014), toxicity and

bioluminescence can be distinct traits of relevance to dinoflagellates. Hence, dinoflagellates, prasinophytes and haptophytes play different ecological roles (Not et al. 2012) and our data show that they can be discriminated as separate PFTs.
Taxonomic groups often contain different size classes, which may provide more information than PFT discrimination based on taxonomic affiliation alone. Cell size is an important feature to consider from an ecological point of view, as it affects numerous functional characteristics of phytoplankton (Litchman et al. 2007). Important advances have therefore been made by models that predict phytoplankton community composition from the size structure of the constituent species (Armstrong 1994; Baird and Suthers 2007; Ward et al. 2012). This matches our data, where we find clear differences in the biogeographical distributions of picocyanobacteria (0.6 - 1 µm), picoeukaryotic phytoplankton (1 - 2 µm), small nanoeukaryotic phytoplankton (Nano I; 6 - 8 µm) and larger nanoeukaryotes (Nano II & III; 8 - 9 µm). However, our results also show that phytoplankton groups of similar size (such as the different picocyanobacterial groups) may still respond very differently to the environmental conditions. Hence, size structure alone is not sufficient to describe community structure, and other physiological traits (e.g., pigment composition, nutrient preferences, motility) need to be considered as well.
Our results indicate that in addition to the classic environmental factors temperature, nutrients and light, incorporation of the vertical turbulence structure of the water column is likely to improve existing models. In our statistical analysis, vertical mixing was described by two parameters, the Brunt-Väisälä frequency N^2 and mixing depth Z_m, which improved differentiation between the different PFT. In mathematical models vertical mixing is usually described by partial differential equations for the transport of heat, solutes and phytoplankton cells. Indeed, models and field experiments have shown that changes in vertical turbulent mixing can have dramatic impacts on the species composition of phytoplankton communities (Huisman et al. 2004; Jäger et al. 2008; Ryabov et al. 2010). However, numerical simulation of vertical mixing processes at a sufficiently high resolution to capture the vertical redistribution of phytoplankton species is computationally quite demanding (Huisman and Sommeijer 2002; Pham Thi et al. 2005), and computational power is one of the main limiting factors for their application in ecosystem models of the global ocean. Yet, vertical mixing processes provide a vital link between changes in the global climate, thermal stratification of the water column, nutrient fluxes and the growth, spatial distribution and species composition of phytoplankton communities (Follows and Dutkiewicz 2001; Jöhnk et al. 2008; Dutkiewicz et al.

2013). Hence, our results stress the need for an improved description of the vertical turbulence structure in global ocean models if we want to capture this vital link.

Conclusions

While we are confident that the major trends within our data were captured by the RDA models, not all of the variation in the distribution of phytoplankton over the Northeast Atlantic could be explained. The remaining variation could be an indication for the importance of loss factors to structuring phytoplankton communities. Loss factors including viral lysis and grazing can be substantial enough to counterbalance growth of natural phytoplankton communities (K. D. A. Mojica unpubl.)(Behrenfeld and Boss 2014). As the fate of photosynthetically fixed carbon is essential for ecosystem efficiency and the functioning of the biological pump, more information is needed to understand how climate-induced changes in stratification will alter these loss processes.

Our results support the prediction that future increases in temperature will expand the geographic range of *Prochlorococcus* as oligotrophic areas continue to expand northward (Polovina et al. 2008; Flombaum et al. 2013). Furthermore, the data indicate that the increased contribution of *Prochlorococcus* to C biomass will occur at the expense of *Synechococcus* spp., leading to alterations in phylogeography within the unicellular cyanobacterial populations. Besides alterations to picocyanobacteria populations, future increases in (summer) stratification will likely increase the contribution of haptophytes, prasinophytes and pelagophytes in the northern region of the North Atlantic relative to cryptophytes and diatoms.

Acknowledgements

The STRATIPHYT project was supported by the division for Earth and Life Sciences Foundation (ALW), with financial aid from the Netherlands Organization for Scientific Research (NWO). We thank the captains and shipboard crews of R/V Pelagia and scientific crews during the cruises. We acknowledge the support of NIOZ-Marine Research Facilities (MRF) on-shore and on-board. Furthermore, we thank Harry Witte (Department Biological Oceanography, NIOZ, Texel) for his assistance with the initial statistical analysis.

References

Armstrong RA (1994) Grazing limitation and nutrient limitation in marine ecosystems: steady state solutions of an ecosystem model with multiple food chains. Limnology and Oceanography 39: 597-608

Baird ME, Suthers IM (2007) A size-resolved pelagic ecosystem model. Ecological Modelling 203: 185-203

Beaugrand G (2009) Decadal changes in climate and ecosystems in the North Atlantic Ocean and adjacent seas. Deep-Sea Research, Part II 56: 656-673

Behrenfeld MJ, Boss ES (2014) Resurrecting the ecological underpinnings of ocean plankton blooms. Annual Review of Marine Science 6: 167-194

Behrenfeld MJ, O'Malley RT, Siegel DA, McClain CR, Sarmiento JL, Feldman GC, Milligan AJ, Falkowski PG, Letelier RM, Boss ES (2006) Climate-driven trends in contemporary ocean productivity. Nature 444: 752-755

Bouman HA, Ulloa O, Barlow R, Li WKW, Platt T, Zwirglmaier K, Scanlan DJ, Sathyendranath S (2011) Water-column stratification governs the community structure of subtropical marine picophytoplankton. Environmental Microbiology Reports 3: 473-482

Brainerd KE, Gregg MC (1995) Surface mixed and mixing layer depths. Deep-Sea Research, Part I 42: 1521-1543

Brown SL, Landry MR, Barber RT, Campbell L, Garrison DL, Gowing MM (1999) Picophytoplankton dynamics and production in the Arabian Sea during the 1995 Southwest Monsoon. Deep-Sea Research, Part II 46: 1745-1768

Cermeño P, Dutkiewicz S, Harris RP, Follows M, Scholfield O, Falkowski PG (2008) The role of nutricline depth in regulating the ocean carbon cycle. Proceedings of the National Academy of Sciences of the United States of America 105: 20344-20349

Chisholm SW (1992) Phytoplankton size. In: Falkowski PG, Woodhead AD (eds) Primary Productivity and Biogeochemical Cycles. Plenum Press

Claustre H (1994) The trophic status of various oceanic provinces as revealed by phytoplankton pigment signatures. Limnology and Oceanography 39: 1206-1210

Collins M, Knutti R, Arblaster J, Dufresne J-L, Fichefet T, Friedlingstein P, Gao X, Gutowski WJ, Johns T, Krinner G, Shongwe M, Tebaldi C, Weaver AJ, Wehner M (2013) Long-term climate change: projections, commitments and irreversibility. In: Stocker TF, Qin D, Plattner G-K, Tignor M, Allen SK, Boschung J, Nauels A, Xia Y, Bex V, Midgley PM et (eds) Climate change 2013: The physical science basis. Contribution of working group I to the fifth assessment report of the Intergovernmenal Panel on Climate Change. Cambridge University Press

Cotonnec G, Brunet C, Sautour B, Thoumelin G (2001) Nutritive value and selection of food particles by copepods during a spring bloom of *Phaeocystis* sp. in the English Channel, as determined by pigment and fatty acid analyses. Journal of Plankton Research 23: 693-703

Daufresne M, Lengfellner K, Sommer U (2009) Global warming benefits the small in aquatic ecosystems. Proceedings of the National Academy of Sciences of the United States of America 106: 12788-12793

Dawson B, Spannagle M (2008) The Complete Guide to Climate Change. Taylor & Francis.

Deser C, Blackmon ML (1993) Surface climate variations over the North Atlantic ocean during winter: 1900-1989.Journal of Climate 6: 1743-1753

Doney, SC, Ruckelshaus M, Duffy JE, Barry JP, Chan F, English CA, Galindo HM, Grebmeier JM, Hollowed AB, Knowlton N, Polovina J, Rabalais NN, Sydeman WJ (2012) Climate change impacts on marine ecosystems. Annual Review of Marine Science 4: 11-37

Dutkiewicz S, Scott JR, Follows MJ (2013) Winners and losers: ecological and biogeochemical changes in a warming ocean. Global Biogeochemical Cycles 27: 463-477

Edler L, Elbrächter M (2010) The Utermöhl method for quantitative phytoplankton analysis. In: Karlson B, Cusack C, Bresnan E (eds) Microscopic and Molecular Methods for Quantitative Phytoplankton Analysis. Intergovernmental Oceanographic Commission of © UNESCO

Edwards KF, Thomas MK, Klausmeier CA, Litchman E (2012) Allometric scaling and taxonomic variation in nutrient utilization traits and maximum growth rate of phytoplankton. Limnology and Oceanography 57: 554-566

Edwards M, Richardson AJ (2004) Impact of climate change on marine pelagic phenology and trophic mismatch. Nature 430: 881-884

Falkowski P, Scholes RJ, Boyle E, Canadell J, Canfield D, Elser J, Gruber N, Hibbard K, Hogberg P, Linder S, Mackenzie FT, Moore III B, Pedersen T, Rosenthal Y, Seitzinger S, Smetacek V, Steffen W, (2000) The global carbon cycle: a test of our knowledge of Earth as a system. Science 290: 291-296

Falkowski PG, Barber RT, Smetacek V (1998) Biogeochemical controls and feedbacks on ocean primary production. Science 281: 200-206

Finkel ZV, Beardall J, Flynn KJ, Quigg A, Rees TAV, Raven JA (2010) Phytoplankton in a changing world: cell size and elemental stoichiometry. Journal of Plankton Research 32: 119-137

Flombaum P, Gallegos JL, Gordillo RA, Rincon J, Zabala LL, Jiao N, Karl DM, Li WKW, Lomas MW, Veneziano D, Vera CS, Vrugt JA, Martiny AC (2013) Present and future global distributions of the marine cyanobacteria *Prochlorococcus* and *Synechococcus*. Proceedings of the National Academy of Sciences of the United States of America 110: 9824-9829

Follows MJ, Dutkiewicz S, Grant S, Chisholm SW (2007) Emergent biogeography of microbial communities in a model ocean. Science 315: 1843-1846

Follows MJ, Dutkiewicz SW (2001) Meteorological modulation of the North Atlantic spring bloom. Deep-Sea Research, Part II 49: 321-344

Furrer R, Nychka D, Sain S (2012) fields: Tools for spatial data. http://CRAN.R-project.org/package=fields

Garrison DL, Gowing MM, Hughes MP, Campbell L, Caron DA, Dennett MR, Shalapyonok A, Olson RJ, Landry MR, Brown SL, Liu HB, Azam F, Steward GF, Ducklow HW, Smith DC (2000) Microbial food web structure in the Arabian Sea: a US JGOFS study. Deep-Sea Research, Part II 47: 1387-1422

Grasshoff K (1983) Determination of nitrate. In: Grasshoff K, Erhardt M, Kremeling K (eds) Methods of Seawater Analysis. Verlag Chemie

Gregg WW, Conkright ME, Ginoux P, O'Reilly JE, Casey NW (2003) Ocean primary production and climate: global decadal changes. Geophysical Research Letters 30: 1809. doi: 10.1029/2003GL016889

Guillou L, Eikrem W, Chrétiennot-Dinet MJ, Le Gall F, Massana R, Romari K, Pedros-Alio C, Vaulot D (2004) Diversity of picoplanktonic prasinophytes assessed by direct nuclear SSU rDNA sequencing of environmental samples and novel isolates retrieved from oceanic and coastal marine ecosystems. Protist 155: 193-214

Haberman KL, Ross RM, Quetin LB (2003) Diet of the Antarctic krill (*Euphausia superba* Dana): II. Selective grazing in mixed phytoplankton assemblages. Journal of Experimental Marine Biology and Ecology 283: 97-113

Helder W, De Vries RTP (1979) An automatic phenol-hypochlorite method for the determination of ammonia in sea and brackish water. Netherlands Journal of Sea Research 13: 154-160

Hilligsøe KM, Richardson K, Bendtsen J, Sorensen LL, Nielsen TG, Lyngsgaard MM (2011) Linking phytoplankton community size composition with temperature, plankton food web structure and sea-air CO_2 flux. Deep-Sea Research, Part I 58: 826-838

Hoegh-Guldberg,O, Bruno JF (2010) The impact of climate change on the world's marine ecosystems. Science 328: 1523-1528

Hooker SB, Van Heukelem L, Thomas CS, Claustre H, Ras J, Schluter L, Clementson L, vanderLinde D, Eker-Develi E, Berthon J-F, Barlow R, Sessions H, Ismail H, Perl J (2009) The third SeaWiFS HPLC analysis round-robin experiment (SeaHARRE-3). NASA Technical Memorandum 2009-215849. Greenbelt: NASA Goddard Space Flight Center

Houry S, Dombrowsky E, De May P, Minster J-F (1987) Brunt-Väisälä frequency and rossby radii in the South Atlantic. Journal of Physical Oceanography17: 1619-1626

Huisman J, Sharples J, Stroom JM, Visser PM, Kardinaal WEA, Verspagen JMH, Sommeijer B (2004) Changes in turbulent mixing shift competition for light between phytoplankton species. Ecology 85: 2960-2970

Huisman J, Sommeijer B (2002) Population dynamics of sinking phytoplankton in light-limited environments: simulation techniques and critical parameters. Journal of Sea Research 48: 83-96

Huisman J, Thi NNP, Karl DM, Sommeijer B (2006) Reduced mixing generates oscillations and chaos in the oceanic deep chlorophyll maximum. Nature 439: 322-325

Huisman J, Van Oostveen P, Weissing FJ (1999) Critical depth and critical turbulence: two different mechanisms for the development of phytoplankton blooms. Limnology and Oceanography 44: 1781-1787

Irigoien X, Huisman J, Harris RP (2004) Global biodiversity patterns of marine phytoplankton and zooplankton. Nature 429: 863-867

Irwin AJ, Nelles AM, Finkel ZV (2012) Phytoplankton niches estimated from field data. Limnology and Oceanography 57: 787-797

Jäger CG, Diehl S, Schmidt GM (2008) Influence of water-column depth and mixing on phytoplankton biomass, community composition, and nutrients. Limnology and Oceanography 53: 2361-2373

Jardillier L, Zubkov MV, Pearman J, Scanlan DJ (2010) Significant CO_2 fixation by small prymnesiophytes in the subtropical and tropical northeast Atlantic Ocean. The ISME Journal 4: 1180-1192

Jöhnk KD, Huisman J, Sharples J, Sommeijer B, Visser PM, Stroom JM (2008) Summer heatwaves promote blooms of harmful cyanobacteria. Global Change Biology 14: 495-512

Johnson ZI, Zinser ER, Coe A, McNulty NP, Woodward EMS, Chisholm SW (2006) Niche partitioning among *Prochlorococcus* ecotypes along ocean-scale environmental gradients. Science 311: 1737-1740

Jurado E, Dijkstra HA, Van Der Woerd HJ (2012a) Microstructure observations during the spring 2011 STRATIPHYT-II cruise in the northeast Atlantic. Ocean Science 8: 945-957

Jurado E, Van Der Woerd HJ, Dijkstra HA (2012b) Microstructure measurements along a quasi-meridional transect in the northeastern Atlantic Ocean. Journal of Geophysical Research 117: C04016. doi: 10.1029/2011JC007137

Koroleff F (1969) Direct determination of ammonia in natural waters as indophenol blue. Coun. Meet. int. Coun. Explor. Sea **C.M.-ICES/C:** 9

Lacroix G, Ruddich K, Gypens N, Lancelot C (2007) Modelling the relative impact of rivers (Scheldt/Rhine/Seine) and Western Channel waters on the nutrient and diatoms/*Phaeocystis* distributions in Belgian waters (Southern North Sea). Continental Shelf Research 27: 1422-1446

Le Quéré C, Harrison SP, Prentice IC, Buitenhuis ET, Aumont O, Bopp L, Claustre H, Da Cunha LC, Geider R, Giraud X, Klaas C, Kohfeld KE, Legendre L, Manizza M, Platt T, Rivkin RB, Sathyendranath S, Uitz J, Watson AJ, Wolf-Gladrow D (2005) Ecosystem dynamics based on plankton functional types for global ocean biogeochemistry models. Global Change Biology 11: 2016-2040

Legendre P, Legendre L (1998) Numerical ecology, 2nd English ed. Elsevier Science BV

Levitus S, Antonov JI, Boyer TP, Stephens C (2000) Warming of the world ocean. Science 287: 2225-2229

Li WKW (2002) Macroecological patterns of phytoplankton in the northwestern North Atlantic Ocean. Nature 419: 154-157

Litchman E, Klauseier CA, Miller JR, Schofield OM, Falkowski PG (2006) Multi-nutrient, multi-group model of present and future oceanic phytoplankton communities. Biogeosciences 3: 585-606

Litchman E, Klausmeier CA, Schofield OM, Falkowski PG (2007) The role of functional traits and trade-offs in structuring phytoplankton communities: scaling from cellular to ecosystem level. Ecology Letters10: 1170-1181

Liu H, Probert I, Uitz J, Claustre H, Aris-Brosou S, Frada M, Not F, De Vargas C (2009) Extreme diversity in noncalcifying haptophytes explains a major pigment paradox in open oceans. Proceedings of the National Academy of Sciences of the United States of America 106: 12803-12808

Liu HB, Chen MR, Suzuki K, Wong CK, Chen BZ (2010) Mesozooplankton selective feeding in subtropical coastal waters as revealed by HPLC pigment analysis. Marine Ecology Progress Series **407:** 111-123.

Mackey, K. R. M., A. Paytan, K. Caldeira, A. R. Grossman, D. Moran, M. Mcilvin, and M. A. Saito. 2013. Effect of temperature on photosynthesis and growth in marine *Synechococcus* spp. Plant Physiol. 163: 815-829

Mackey MD, Mackey DJ, Higgins HW, Wright SW (1996) CHEMTAX - A program for estimating class abundances from chemical markers: application to HPLC measurements of phytoplankton. Marine Ecology Progress Series 144: 265-283

Mahadevan A, D'Asaro E, Lee C, Perry MJ (2012) Eddy-driven stratification initiates North Atlantic spring phytoplankton blooms. Science 337: 54-58

Maranon E, Holligan PM, Varela M, Mourino B, Bale AJ (2000) Basin-scale variability of phytoplankton biomass, production and growth in the Atlantic Ocean. Deep-Sea Research, Part I 47: 825-857

McKie-Krisberg ZM, Sanders RW (2014) Phagotrophy by the picoeukaryotic green algal *Micromonas*: implications for Arctic Oceans. The ISME Journal 8: 1953-1961

Meehl GA, Stocker TF, Collins WD, Friedlingstein P, Gaye AT, Gregory JM, Kitoh A, Knutti R, Murphy JM, Noda A, Raper SCB, Watterson IG, Weaver AJ, Zhao Z-C (2007) Global climate projections. In: Solomon S, Qin D, Manning M, Chen Z, Marquis M, Averyt KB, Tignor M, Miller HL (eds) Climate change 2007: The physical science basis. Contribution of working group I to the fourth assessment report of the Intergovernmental Panel on Climate Change. Cambridge University Press

Mendes CRB, Tavano VM, Leal MC, De Souza MS, Brotas V, Garcia CAE (2013) Shifts in the dominance between diatoms and cryptophytes during three late summers in the Bransfield Strait (Antarctic Peninsula). Polar Biology 36: 537-547

Mitra A, Flynn KJ (2005) Predator-prey interactions: is 'ecological stoichiometry' sufficient when good food goes bad? Journal of Plankton Research 27: 393-399

Moline MA, Claustre H, Frazer TK, Schofield O, Vernet M (2004) Alteration of the food web along the Antarctic Peninsula in response to a regional warming trend. Global Change Biology 10: 1973-1980

Moore LR, Chisholm SW (1999) Photophysiology of the marine cyanobacterium *Prochlorococcus*: Ecotypic differences among cultured isolates. Limnology and Oceanography 44: 628-638

Moore LR, Goericke R, Chisholm SW (1995) Comparative physiology of *Synechococcus* and *Prochlorococcus* - influence of light and temperature on growth, pigments, fluorescence and absorptive properties. Marine Ecology Progress Series 116: 259-275

Morel A (1997) Consequences of a *Synechococcus* bloom upon the optical properties of oceanic (case 1) waters. Limnology and Oceanography 48: 1746-1754

Murphy J, Riley JP (1962) A modified single solution method for the determination of phosphate in natural waters. Analytica Chimica Acta 27: 31-36

Not F, Siano R, Kooistra WHCF, Simon N, Vaulot D, Probert I (2012) Diversity and ecology of eukaryotic marine phytoplankton. In: Gwenaël P (ed) Advances in Botanical Research. Academic Press

Oksanen J, Blanchet FG, Kindt R, Legendre P, Minchin PR, O'Hara RB, Simpson GL, Solymos, P, Stevens MHH, Wagner H (2013) vegan: Community ecology package. http://CRAN.R-project.org/package=vegan

Partensky F, Blanchot J, Lantoine F, Neveux J, Marie D (1996) Vertical structure of picophytoplankton at different trophic sites of the tropical northeastern Atlantic Ocean. Deep-Sea Research, Part I 43: 1191-1213

Partensky F, Blanchot J, Valout D (1999a) Differential distribution and ecology of *Prochlorococcus* and *Synechococcus* in oceanic waters: a review. Bulletin de l'Institut océanographique (Monaco) 19: 457-475

Partensky F, Garczarek L (2010) *Prochlorococcus*: advantages and limits of minimalism. Annual Review of Marine Science 2: 305-331

Partensky F, Hess WR, Vaulot D (1999b) *Prochlorococcus*, a marine photosynthetic prokaryote of global significance. Microbiology and Molecular Biology Reviews 63: 106-127

Partensky, F., N. Hoepffner, W. K. W. Li, O. Ulloa, and D. Vaulot. 1993. Photoacclimation of *Prochlorococcus* sp. (Prochlorophyta) strains isolated from the North Atlantic and the Mediteranean Sea. Plant Physiology 101: 285-296

Peloquin J, Swan C, Gruber N, Vogt M, Claustre H, Ras J, Uitz J, Barlow R, Behrenfeld M, Bidigare R, Dierssen H, Ditullio G, Fernandez E, Gallienne C, Gibb S, Goericke R, Harding L, Head E, Holligan PM, Hooker SB, Karl D, Landry M, Letelier R, Llewellyn CA, Lomas N, Lucas M, Mannino A, Marty J-C, Mitchell BG, Muller-Karger F, Nelson N, O'Brien C, Prezelin B, Repeta D, Smith Jr WO, Smythe-Wright D, Stumpf R, Sybramaniam A, Suzuki K, Trees C, Vernet M, Wasmund N, Wright S (2013) The MAREDAT global database of high performance liquid chromatography marine pigment measurements. Earth System Science Data 5: 109-123

Perez V, Fernandez E, Maranon E, Moran XAG, Zubkovc MV (2006) Vertical distribution of phytoplankton biomass, production and growth in the Atlantic subtropical gyres. Deep-Sea Research, Part I 53: 1616-1634

Pham Thi NN, Huisman J, Sommeijer BP (2005) Simulation of three-dimensional phytoplankton dynamics: competition in light-limited environments. Journal of Computational and Applied Mathematics 174: 57-77

Polovina JJ, Howell EA, Abecassis M (2008) Ocean's least productive waters are expanding. Geophysical Research Letters 35: L03618. doi: 10.1029/2007GL031745

R Development Core Team (2012) R: A language and environment for statistical computing. http://www.R-project.org

Raven JA (1986) Physiological consequences of extremely small size for autotrophic organisms in the sea. In: Platt T, Li WKW (eds) Photosynthetic Picoplankton. Canadian Bulletin of Fisheries and Aquatic Sciences

Richardson AJ, Schoeman DS (2004) Climate impact on plankton ecosystems in the Northeast Atlantic. Science 305: 1609-1612

Ryabov AB, Rudolf L, Blasius B (2010) Vertical distribution and composition of phytoplankton under the influence of an upper mixed layer. Journal of Theoretical Biology 263: 120-133

Sarmiento JL (2004) Response of ocean ecosystems to climate warming. Global Biogeochemical Cycles 18: GB3003. doi: 10.1029/2003GB002134

Sarmiento JL, Hughes TMC, Stouffer RJ, Manabe S (1998) Simulated response of the ocean carbon cycle to anthropogenic climate warming. Nature 393: 245-249

Schoemann V, Becquevort S, Stefels J, Rousseau V, Lancelot C (2005) *Phaeocystis* blooms in the global ocean and their control mechanisms: a review. Journal of Sea Research 53: 43-66

Siegel DA, Doney SC, Yoder JA (2002) The North Atlantic spring phytoplankton bloom and Sverdrup's critical depth hypothesis. Science 296: 730-733

Stevens C, Smith M, Ross A (1999) SCAMP: measuring turbulence in estuaries, lakes, and coastal waters. NIWA - Water Atmosphere 7: 20-21

Sverdrup, E. U. 1953. On conditions for the vernal blooming of phytoplankton. Journal du Conseil / Conseil Permanent International pour l'Exploration de la Mer 18: 287-295

Talley L, Pickard G, Emery W, Swift J (2011) Typical distribution of water characteristics. Descriptive Physical Oceanography. Elsevier Ltd

Tarran GA, Heywood JL, Zubkov MV (2006) Latitudinal changes in the standing stocks of nano- and picoeukaryotic phytoplankton in the Atlantic Ocean. Deep-Sea Research, Part II 53: 1516-1529

Tungaraza C, Rousseau V, Brion V, Lancelot C, Gichuki J, Baeyens W, Goeyens L (2003) Contrasting nitrogen uptake by diatom and *Phaeocystis*-dominated phytoplankton assemblages in the North Sea. Journal of Experimental Marine Biology and Ecology 292: 19-41.

Uitz J, Claustre H, Morel A, Hooker SB (2006) Vertical distribution of phytoplankton communities in open ocean: An assessment based on surface chlorophyll. Journal of Geophysical Research 111: C08005. doi: 10.1029/2005JC003207

Uitz J, Huot Y, Bruyant F, Babin M, Claustre H (2008) Relating phytoplankton photophysiological properties to community structure on large scales. Limnology and Oceanography 53: 614-630

Unrein F, Gasol JM, Not F, Forn I, Massana R (2014) Mixotrophic haptophytes are key bacterial grazers in oligotrophic coastal waters. The ISME Journal 8: 164-176

van Aken HM (2000) The hydrography of the mid-latitude Northeast Atlantic Ocean II: The intermediate water masses. Deep-Sea Research, Part I 47: 789-824

van de Poll WH, Kulk G, Timmermans KR, Brussaard CPD, van der Woerd HJ, Kehoe MJ. Mojica KDA, Visser RJW, Rozeman PD, Buma AGJ (2013) Phytoplankton chlorophyll *a* biomass, composition, and productivity along a temperature and stratification gradient in the northeast Atlantic Ocean. Biogeosciences 10: 4227-4240

van de Waal DB, Verschoor AM, Verspagen JMH, Van Donk E, Huisman J (2010) Climate-driven changes in the ecological stoichiometry of aquatic ecosystems. Frontiers in Ecology and the Environment 8: 145-152

Vaulot D (1989) CYTOPC: Processing software for flow cytometric data. Signal and Noise 2: 8

Ward BA, Dutkiewicz S, Jahn O, Follows MJ (2012) A size-structured food-web model for the global ocean. Limnology and Oceanography 57: 1877-1891

Whitton BA, Potts M (eds) (2012) Ecology of cyanobacteria II: Their diversity in space and time. Springer Netherlands

Worden AZ, Nolan JK, Palenik B (2004) Assessing the dynamics and ecology of marine picophytoplankton: The importance of the eukaryotic component. Limnology and Oceanography 49: 168-179

Zinser ER, Johnson ZI, Coe A, Karaca E, Veneziano D, Chisholm SW (2007) Influence of light and temperature on *Prochlorococcus* ecotype distributions in the Atlantic Ocean. Limnology and Oceanography 52: 2205-2220

Zuur A, Ieno EN, Walker N, Saveliev AA, Smith GM (2009) Mixed Effects Models and Extensions in Ecology with R. Springer

Zuur AF, Ieno EN, Elphick CS (2010) A protocol for data exploration to avoid common statistical problems. Methods in Ecology and Evolution 1: 3-14

Chapter 4

Latitudinal variation in virus-induced mortality of phytoplankton across the North Atlantic Ocean

Kristina D. A. Mojica[1], Jef Huisman[2], Steven W. Wilhelm[3], and Corina P. D. Brussaard[1,2]

[1]Department of Biological Oceanography, Royal Netherlands Institute for Sea Research (NIOZ), P.O. Box 59, 1790 AB Den Burg, Texel, The Netherlands.
[2]Department of Aquatic Microbiology, Institute for Biodiversity and Ecosystem Dynamics (IBED), University of Amsterdam, P.O. Box 94248, 1090 GE Amsterdam, The Netherlands.
[3]Department of Microbiology, University of Tennessee, Knoxville, Tennessee 37996, USA.

The ISME Journal (2015) *in press*

Abstract

Viral lysis of phytoplankton constrains marine primary production, food web dynamics, and biogeochemical cycles in the ocean. Yet, little is known about the biogeographical distribution of viral lysis rates across the global ocean. To address this, we investigated phytoplankton group-specific viral lysis rates along a latitudinal gradient within the North Atlantic Ocean. The data show large-scale distribution patterns of different virus groups across the North Atlantic that are associated with the biogeographical distributions of their potential microbial hosts. Average virus-mediated lysis rates of the picocyanobacteria *Prochlorococcus* and *Synechococcus* were lower than those of the picoeukaryotic and nanoeukaryotic phytoplankton (i.e., 0.14 d^{-1} compared to 0.19 and 0.23 d^{-1}, respectively). Total phytoplankton mortality (virus plus grazer-mediated) was comparable to the gross growth rate, demonstrating high turnover rates of phytoplankton populations. Virus-induced mortality was an important loss process at low and mid latitudes whereas phytoplankton mortality was dominated by microzooplankton grazing at higher latitudes (> 56°N). This shift from a viral-lysis-dominated to a grazing-dominated phytoplankton community was associated with a decrease in temperature and salinity, and the decrease in viral lysis rates was also associated with increased vertical mixing at higher latitudes. Ocean-climate models predict that surface warming will lead to an expansion of the stratified and oligotrophic regions of the world's oceans. Our findings suggest that these future shifts in the regional climate of the ocean surface layer are likely to increase the contribution of viral lysis to phytoplankton mortality in the higher-latitude waters of the North Atlantic, which may potentially reduce transfer of matter and energy up the food chain and thus affect the capacity of the northern North Atlantic to act as a long-term sink for CO_2.

Introduction

Viruses are important mortality agents for marine phytoplankton (Evans et al. 2003; Brussaard 2004a; Tomaru et al. 2004; Baudoux et al. 2006). Through the lysis of their autotrophic hosts viruses regulate primary production (Suttle et al. 1990) and play key roles in species competition and succession of phytoplankton populations (Gobler et al. 1997; Mühling et al. 2005; Haaber and Middelboe 2009). Moreover, lysis of microbes diverts energy and biomass away from the classical grazer-mediated food web towards microbial-mediated recycling and the dissolved organic matter pool. This 'viral shunt' reduces the transfer of carbon and nutrients to higher trophic levels, while enhancing the recycling of potential growth-limiting nutrients (Fuhrman 1999; Wilhelm and Suttle 1999). In this manner, viruses have major effects on nutrient cycles and energy flow in the ocean (Brussaard and Martinez 2008; Weitz and Wilhelm 2012). As microbial photoautotrophs are responsible for roughly half of the global annual carbon dioxide fixation and sustain the higher trophic levels in marine ecosystems (Field et al. 1998), their viruses also have the potential to influence these global scale processes.

Marine virus dynamics and virus-host interactions are affected by both abiotic and biotic factors (Mojica and Brussaard 2014), which can vary on both spatial and temporal scales. However, despite biogeographical distributions of bacteria and phytoplankton being extensively studied (Irigoien et al. 2004; Martiny et al. 2006; Fuhrman et al. 2008), the possible existence of biogeographical patterns in marine viral populations (and how these may vary) has received less attention (Breitbart and Rohwer 2005; Angly et al. 2006; Matteson et al. 2013). For example, thermal stratification is an important factor regulating phytoplankton dynamics and ocean-climate models predict that global warming will lead to an expansion of the stratified regions of the world's oceans (Sarmiento et al. 1998; Toggweiler and Russell 2008). Projected alterations to stratification and vertical mixing have the potential to affect the species composition (Huisman et al. 2004; Mojica et al. 2015), phenology (Edwards and Richardson 2004), productivity (Gregg et al. 2003; Behrenfeld et al. 2006; Polovina et al. 2008), size structure (Daufresne et al. 2009; Hilligsøe et al. 2011), nutritional value (Mitra and Flynn 2005; van de Waal et al. 2010), abundance (Richardson and Schoeman 2004) and biogeographical distribution (Doney et al. 2012; Flombaum et al. 2013; van de Poll et al. 2013) of marine phytoplankton. As obligate parasites, viruses rely upon their host to provide the machinary, energy and resources required for viral replication and assembly.

Consequently, factors regulating the physiology, production and removal of the host are also important in governing viral dynamics (Van Etten et al. 1983; Moebus 1996; Baudoux and Brussaard 2008; Maat et al. 2014). Therefore, future changes in stratification also have the potential to affect the composition and distribution of viral assemblages associated with phytoplankton communities, and the sensitivity of marine phytoplankton populations to grazing and viral infection.

The North Atlantic Ocean offers a large-scale latitudinal gradient, with permanent stratification in the subtropics and seasonal stratification in the temperate zones (Longhurst 2007; Jurado et al. 2012). The spring phytoplankton bloom is triggered by reduced vertical mixing and the onset of seasonal stratification due to warming of the surface waters (Sverdrup 1953; Huisman et al. 1999; Taylor and Ferrari 2011), and represents one of the most important biological events in the North Atlantic (Siegel et al. 2002). The bloom begins in December–January at a latitude of ~35° N, just north of the permanently stratified waters of the North Atlantic Subtropical Gyre and subsequently spreads across the North Atlantic throughout spring and summer, expanding northwards to Arctic waters in June (Siegel et al. 2002). The spring bloom takes up large amounts of CO_2, and owing to deep water formation at high latitudes the North Atlantic plays a key role in oceanic CO_2 sequestration (Deser and Blackmon 1993). Yet, little is known about biogeographical patterns in viral abundances and viral lysis rates of phytoplankton across the North Atlantic, and how these may affect the transfer of the photosynthetically acquired carbon and energy to higher trophic levels. This is primarily due to a severe lack of quantitative estimates of phytoplankton losses due to viral lysis (Weitz and Wilhelm 2012), and how these relate to changes in environmental variables.

In this study, we therefore investigate large-scale distribution patterns of (i) marine viral groups and their potential hosts, and (ii) viral lysis and grazing rates of marine phytoplankton over a latitudinal gradient across the North Atlantic Ocean. Specifically, we assess the following hypotheses: (H1) The abundances and composition of the microbial host populations (i.e., bacteria and phytoplankton) vary with latitude (H1a), and are strongly affected by changes in water column stratification (H1b). (H2) The biogeographical distributions of the different viruses depend on the biogeographical distributions of their microbial host populations. (H3) Viral lysis rates of marine phytoplankton vary with latitude, affecting the relative importance of the viral shunt versus the classic grazing-mediated food web.

Materials and methods

Sampling and physicochemical variables

In July-August of 2009, 32 stations were sampled in the Northeast Atlantic Ocean during the shipboard expedition of STRATIPHYT (Changes in vertical stratification and its impacts on phytoplankton communities) (Figure 1). Water samples were collected from at least 10 separate depths in the top 250 m water column using GO-Flo, 10 liter samplers mounted on an ultra-clean (trace-metal free) system equipped with CTD (Seabird 9+) with standard sensors and auxiliary sensors for chlorophyll autofluorescence (Chelsea Aquatracka Mk III). Data from the chlorophyll autofluorescence sensor were calibrated against HPLC data according to van de Poll et al. (2013) in order to determine total Chlorophyll *a* (Chl *a*). Samples were taken inside a 6 m clean lab for analysis of inorganic nutrients (5 ml) and flow cytometry (10 ml). Samples for dissolved inorganic nutrients (5 ml) were analyzed onboard using a Bran+Luebbe Quaatro AutoAnalyzer for dissolved orthophosphate (Murphy and Riley 1962), nitrate and nitrite (NO_x) (Grasshoff, 1983) and ammonium (Koroleff 1969; Helder and de Vries 1979). Detection limits were 0.028 µmol L^{-1} for PO_4^{3-}, 0.10 µmol L^{-1} for NO_x, and 0.09 µmol $L^{-1}$for NH_4^+. Water samples for the modified dilution assay, to determine viral lysis and microzooplankton grazing rates on phytoplankton, were taken from the depth with maximal phytoplankton Chl *a* autofluorescence, i.e., the deep chlorophyll maximum (DCM) or mixed layer (ML). All materials used for sampling water for dilution experiments were prewashed in acid (0.1 M HCl, overnight), rinsed with Milli-Q water (3 times) and rinsed with *in situ* water before use.

Density of seawater was expressed as sigma-t (σ_T) values, defined as $\sigma_T = \rho(S,T) - 1000$, where $\rho(S,T)$ is the density of seawater at temperature T and salinity S measured in kg m^{-3} at standard atmospheric pressure. Temperature eddy diffusivity (K_T) data, referred to here as the vertical mixing coefficient, were derived from temperature and conductivity microstructure profiles measured using a SCAMP (Self Contained Autonomous Microprofiler) (Stevens et al. 1999; Jurado et al. 2012). The SCAMP was deployed at fewer stations (i.e., 14) and to lower depths (up to 100 m) than the remainder of the data in the present study. In order to correct for this deficiency, data were interpolated using the spatial kriging function 'krig' executed in R using the 'fields' package (Furrer et al. 2012). Interpolated K_T values were bounded below by the minimum value measured; the upper values were left unbounded. This resulted in estimated K_T values which preserved the

qualitative pattern and range of values previously reported (Jurado et al. 2012). In addition, the depth of the mixed layer (Z_m) was determined as the depth at which the temperature difference with respect to the surface was 0.5°C (Levitus et al. 2000; Jurado et al. 2012). As shown by Brainerd and Gregg (1995), this definition of the mixed layer provides an estimate of the depth through which surface waters have been mixed in recent days. On the few occasions where SCAMP data were not available, Z_m was determined from CTD data. Temperature profiles obtained from SCAMP and CTD measurements were compared and showed good agreement. To quantify the strength of stratification, CTD data was processed with SBE Seabird software to calculate the Brunt-Väisälä frequency (N^2, in $rad^2\ s^{-2}$) using the Fofonoff adiabatic leveling method (Bray and Fofonoff 1981). The Brunt-Väisälä frequency represents the angular velocity (i.e., the rate) at which a small perturbation of the stratification will re-equilibrate. Hence, it is a simple measure of the stability of the vertical stratification.

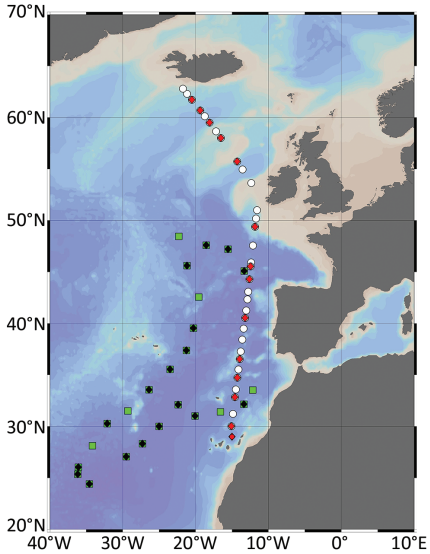

Figure 1. Bathymetric map of the stations sampled during the cruises STRATIPHYT (white circles and red diamonds) and MEDEA (green squares and black diamonds). Modified dilution assays to determine viral lysis and microzooplankton grazing rates were performed at stations indicated by the red and black diamonds. Cruise track was prepared using Ocean Data View (ODV version 4.6.5, Schlitzer, 2002).

In October-November 2011, an opportunity was presented to join the MEDEA (Microbial Ecology of the Deep Atlantic) cruise, to conduct additional modified dilution experiments in the oligotrophic area of the Northeast Atlantic Ocean

(Figure 1). During MEDEA, physicochemical parameters were measured from 3-5 depths per station within the upper 120 m water column using the same methods as for STRATIPHYT. However, no SCAMP measurements were conducted during MEDEA, and ammonium concentrations were not determined. Samples for modified dilution assays were taken mostly from the DCM depth (Table S1).

Microbial abundances

Viruses, bacteria, cyanobacteria and eukaryotic phytoplankton < 20 µm were enumerated using a Becton-Dickinson FACSCalibur flow cytometer (FCM) equipped with an air-cooled Argon laser with an excitation wavelength of 488 nm (15 mW). Approximately 1 ml of fresh seawater was used for enumeration of phytoplankton using methods described by Marie et al. (2005). Phytoplankton were differentiated based on their auto-fluorescence properties using bivariate scatter plots of either orange (i.e., phycoerythrin, present in *Synechococcus* spp.) or red fluorescence (i.e., chlorophyll *a*, present in all phytoplankton) against side scatter. Average cell size for phytoplankton subpopulations were determined by size-fractionation of whole water by sequential gravity filtration through 8, 5, 3, 2, 1, 0.8, and 0.4 μm pore-size polycarbonate filters, by assuming spherical diameter (Ø) of size displayed by the median (50%) number of cells retained for that cluster. In total, eight distinct phytoplankton groups were detected and sized by sequential size-fractioned gravity filtration, i.e., 2 picoeukaryotic groups (average Ø of 1.4 and 1.5 µm, respectively), 3 nanoeukaryotic groups (3, 6 and 8 µm Ø, respectively), and 3 picocyanobacteria groups (*Synechococcus* spp. of 0.9 µm Ø, and ecotypes *Prochlorococcus* high-light (HL) of 0.6 µm Ø in surface waters and *Prochlorococcus* low-light (LL) of 0.7 µm Ø in the DCM).

Bacteria and viruses were enumerated according to Marie et al. (1999) and Brussaard et al. (2010), respectively, with modifications according to Mojica et al. (2014). Briefly, samples were fixed with 25% glutaraldehyde (EM-grade, Sigma-Aldrich, Netherlands) to a final concentration of 0.5% for 15-30 min at 4 ^{0}C, flash frozen and stored at -80 ^{0}C until analysis. Thawed samples were diluted in TE buffer (pH 8.2, 10 mM Tris-HCL, 1 mM EDTA; Mojica *et al*., 2014), stained with the nucleic acid-specific green fluorescence dye SYBR Green I (final concentration of 1 x 10^{-4} and 5 x 10^{-5} of the commercial stock concentration; Life Technologies, Netherlands) and incubated in the dark at either room temperature for 15 min or at 80 ^{0}C for 10 min, for bacteria and viruses, respectively. Cooled samples (5 min, room temperature) were then analyzed on the flow cytometer with the

discriminator set on green fluorescence. Five distinct virus groups, labeled V1-V5, were identified based on their green fluorescence and side scatter characteristics (Figure 2). Low fluorescing viral groups, V1 and V2, are considered to be primarily dominated by phages infecting heterotrophic bacteria, although some evidence suggests that eukaryotic algal viruses can also display similar low fluorescence signatures (Brussaard and Martinez 2008; Brussaard et al. 2010). The other virus groups generally contain more algal viruses, with both pro- and eukaryotic algal viruses contributing to the V3 group, while the higher side scatter groups, V4 and V5, commonly represent large dsDNA algal viruses (Jacquet et al. 2002; Brussaard 2004b; Baudoux et al. 2006).

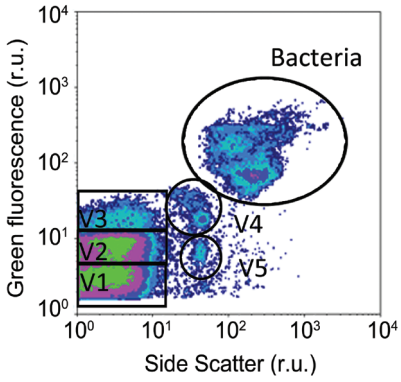

Figure 2. A typical dot plot of viruses counted with flow cytometry in a sample of the STRATIPHYT cruise. Viruses (and bacteria)were discriminated by green fluorescence versus side scatter; V1-V5 indicate the 5 virus groups distinguished by flow cytometry.

Redundancy analysis

We applied multivariate statistical analysis to data obtained from STRATIPHYT to test hypotheses (H1) and (H2) put forth in the Introduction. The analysis was performed using R statistical software (R Development Core Team, 2012) supplemented by the vegan package (Oksanen et al. 2013).

First, we performed a data exploration following the protocol described in Zuur et al. (2010). Most phytoplankton groups distinguished by flow cytometry had limited biogeographical distributions within our study area and consequently suffered from zero inflation (e.g., zeroes in > 20% of the data points for almost every phytoplankton group). To avoid issues arising from zero inflation and provide good quality explanatory data, phytoplankton groups were clustered into

different categories: total picocyanobacteria (*Synechococcus*, *Prochlorococcus* HL-ecotype and *Prochlorococcus* LL-ecotype), total picoeukaryotes (picoeukaryotes I+II), total nanoeukaryotes (nanoeukaryotes I+II+III), and total phytoplankton. For hypothesis (H1), the response variables were the abundances of the bacteria and different phytoplankton groups and total Chl *a*, while the explanatory variables were latitude, vertical mixing coefficient (K_T, temperature eddy diffusivity), a stratification index (N^2, Brunt Väisälä frequency), and temperature. For hypothesis (H2), the response variables were the virus groups V1-V5 and total viral abundance, while the explanatory variables were the bacteria, different phytoplankton groups, total Chl *a* and the environmental variables latitude, K_T, N^2, and temperature. Virus, bacteria, phytoplankton and chlorophyll data were log(x+1) transformed and the vertical mixing coefficient and temperature were log transformed to improve the homogeneity of variance.

Next, to obtain the most parsimonious model, data were examined for collinearity of the explanatory variables by calculating variance inflation factors (VIF) using the R function corvif (Zuur *et al.*, 2009). In a stepwise fashion, all explanatory variables with VIF > 8 were removed from the model. For hypothesis (H1), VIF analysis resulted in the selection of 4 explanatory variables: latitude, K_T, N^2 and temperature. For hypothesis (H2), VIF analysis resulted in the selection of 8 explanatory variables: picocyanobacteria (Cyano), picoeukaryotic phytoplankton (PicoEUK), nanoeukaryotic phytoplankton (NanoEUK), bacteria, Chl *a*, latitude, N^2 , K_T and temperature.

Initial scatterplots of the response and explanatory variables revealed strong linear relationships and therefore redundancy analysis (RDA) (Zuur et al. 2009) was chosen over canonical correspondence analysis (CCA). RDA is a combination of multiple regression analysis and principal component analysis for multivariate data. Forward selection was applied to select only those explanatory variables that contributed significantly to the RDA model, while removing non-significant terms. Significance was assessed by a permutation test, using the multivariate pseudo-F as test statistic (Zuur et al. 2009). A total of 9,999 permutations were used to estimate *p*-values associated with the pseudo-F statistic.

RDA was based on all sampling points for which we had a complete dataset of explanatory and response variables. For hypothesis (H1), this amounted to 80 samples (ranging from 0-225 m depth, with 4-11 depths sampled per station) from 15 stations of the STRATIPHYT cruise. For hypothesis (H2), the explanatory variable N^2 was not significant (see *Results*). Hence, RDA could be performed on

96 samples, as the removal of N^2 permitted the inclusion of sampling points from STRATIPHYT stations that lacked N^2 data.

Modified dilution experiments

To investigate hypothesis (H3) we determined viral lysis and microzooplankton grazing rates of the different phytoplankton groups using the modified dilution assay according to Kimmance and Brussaard (2010). For both the STRATIPHYT and MEDEA cruises, experiments were conducted onboard, using water samples obtained from those depths where Chl *a* autofluorescence was maximal (i.e., DCM or ML). Natural seawater, gently passed through a 200 µm mesh to remove mesozooplankton (while retaining microzooplankton), was combined with 0.45 µm diluent or 30 kDa ultrafiltrate in proportions of 100, 70, 40 and 20% to gradually decrease the mortality impact with increasing dilution (Figure S1a). The 0.45 µm filtrate, prepared with the goal of removing the microzooplankton grazers, was achieved by gravity filtration of natural seawater through a 0.45 µm Sartopore capsule filter with a 0.8 µm prefilter (Sartopore 2 300, Sartorius stedim biotech). The 30 kDa ultrafiltrate, prepared to remove grazers and viruses, was generated by tangential flow filtration using a polyethersulfone membrane (Vivaflow 200, Vivascience). All experiments were performed in triplicate in 1 L clear polycarbonate bottles. After preparation of the two parallel dilution series (12 bottles each), a 3 ml subsample was taken and phytoplankton was enumerated by FCM as specified previously. The bottles were then incubated for 24 hours in an on-deck flow-through seawater incubator at *in situ* temperature and light (using neutral density screen) conditions. After the 24-hour incubation period, a second FCM phytoplankton count was executed and the resulting growth rate for each phytoplankton group determined. Dual measurements of viral lysis and grazing rates were obtained for all phytoplankton groups, except for *Prochlorococcus* HL which was largely absent from the sampled depths.

The microzooplankton grazing rate was estimated from the regression coefficient of the apparent growth rate versus fraction of natural seawater for the 0.45 µm series, while the combined rate of viral-induced lysis and microzooplankton grazing was estimated from a similar regression for the 30 kDa series (Figure S1b and c) (Baudoux et al. 2006; Kimmance and Brussaard 2010). A significant difference between the two regression coefficients (as tested by ANCOVA) indicates a significant viral lysis rate. Phytoplankton gross growth rate (μ_{gross}, in the absence of grazing and viral lysis) was derived from the y intercept of the 30 kDa series regression.

The viral lysis and grazing rates were analyzed with a two-way analysis of variance with type II sum of squares to assess differences between the two sources of mortality (viral lysis versus grazing) and among the phytoplankton groups (*Synechococcus*, *Prochlorococcus* LL, total picoeukaryotes and total nanoeukaryotes). Homogeneity of variance was confirmed by Levene's test, and post-hoc comparison of the means was based on Tukey's HSD test using SPSS version 22.0. Potential relationships between biological parameters obtained from the modified dilution assays (e.g., phytoplankton abundance, μ_{gross}, viral lysis and grazing rates) and environmental parameters were examined by Spearman's rank correlation coefficient. Probability values were adjusted with Holm's correction for multiple hypothesis testing using the corr.p function of psych (Revelle 2014) implemented in R (R Development Core Team 2012). The correlation analysis was performed on the complete data set (n = 105) with a significance level (α) of 0.05.

Results

During both the STRATIPHYT and MEDEA cruise, the North Atlantic was characterized by a strong temperature-induced vertical stratification resulting in very low concentrations of dissolved inorganic nitrogen and phosphorus in the upper 50-100 m water column at latitudes south of 45°N (Figure 3a-g; Figure S2). Towards the north stratification weakened, slightly relaxing nutrient limitation in the upper 50 m surface layer.

For both cruises, pico-sized phytoplankton (< 2 µm Ø) accounted for more than 95% of the total phytoplankton < 20 µm enumerated by FCM. South of 45°N, both total phytoplankton abundance (up to 1.6 ± 0.4 x 10^5 cells ml^{-1}) and Chl *a* (Figure 3g; Figure S2e) were maximal between 30 and 100 m depth, characteristic of a deep-chlorophyll maximum (DCM). Cyanobacteria were the most abundant members of the phytoplankton community in this southern region (Figure 4a), and consisted mainly of *Prochlorococcus*-HL and *Prochlorococcus*-LL (Figure S3a and b). The DCM shallowed with latitude, giving over to a surface maximum north of 45°N, marking the northern boundary of the oligotrophic areas (defined by Chl *a* concentrations < 0.07 mg Chl m^{-3}; Polovina et al. 2008). Cyanobacterial abundance decreased with the loss of the DCM and disappearance of *Prochlorococcus* spp. north of 45°N (Figure 4a, Figure S3a and b). However, the cyanobacteria *Synechococcus* spp. showed highest abundances in the most northern stations, beyond 56°N, where

they numerically dominated the photosynthetic community < 20 µm (Figure S3c). Picoeukaryotic and nanoeukaryotic phytoplankton were relatively abundant in the DCM between 38°N and 45°N, and reached maximal abundances in the surface waters of the stations north of 54°N (Figure 4b and c, Figure S3d-h). Bacterial abundance was maximal in the surface waters of the most northern stations (Figure 4d).

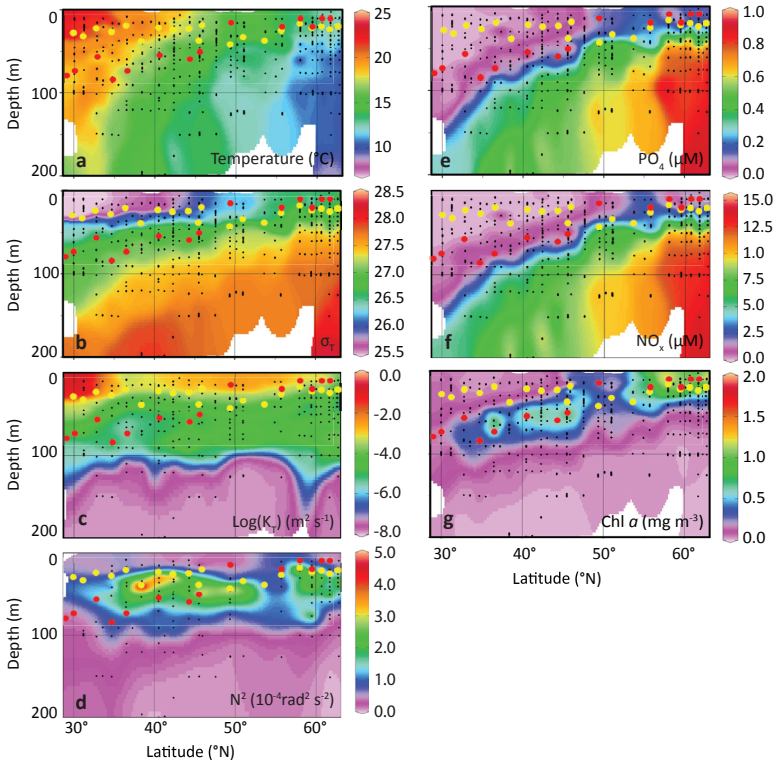

Figure 3. Latitudinal and depth distribution of (a) temperature, (b) sigma-t (σ_T), (c) Temperature eddy diffusivity (K_T), (d) Brunt-Väisälä frequency (N^2), (e) inorganic phosphorus, (f) NO_x (nitrate + nitrite) and (g) Chl a concentrations measured during STRATIPHYT. Black dots indicate sampling points, yellow dots indicate mixed layer depth (Z_m), and red dots the sampling depths for modified dilution assays. Figure panels were prepared using Ocean Data View (ODV version 4.6.5, Schlitzer, 2002).

The 5 virus groups showed distinct biogeographical distributions (Figure 4e-i). Although V1 and V2 viruses were the numerically dominant virus groups in the DCM of the strongly stratified waters below 45°N, they were even more abundant in the top 50 m of the weakly stratified waters at latitudes above 45°N (Figure 4e and f). Conversely, V3 viruses reached their highest abundances between 30-100

m depth in the DCM of stratified waters south of 45°N (Figure 4g). V4 and V5 viruses were present throughout the latitudinal range, but V4 reached its maximum abundance in the subsurface waters located between latitudes 40-45°N (Figure 4h) and V5 had its highest abundance in the upper 50 m surface waters in the weakly stratified waters at the higher latitudes (Figure 4i).

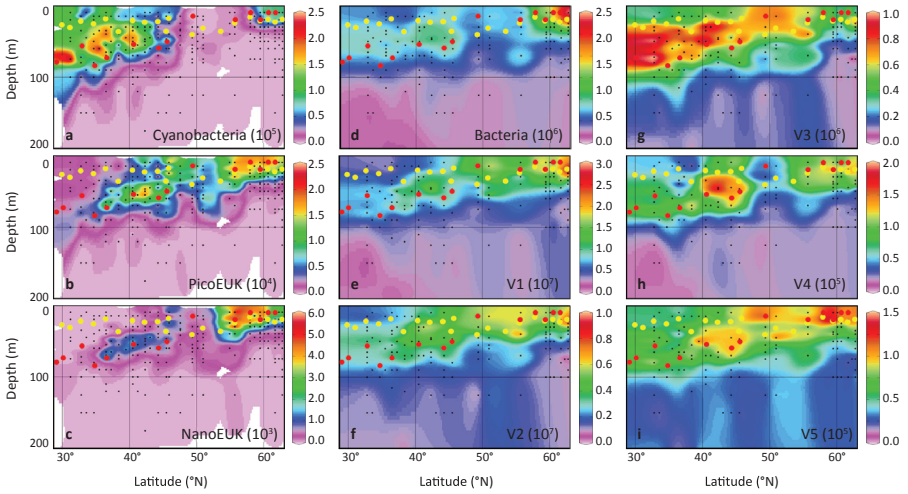

Figure 4. Biogeographical distributions of phytoplankton (a-c), bacteria (d) and virus groups (e-i) across the Northeast Atlantic Ocean based on flow cytometry counts obtained during the STRATIPHYT cruise. Abundances are expressed in (a-c) cells ml^{-1}, (d) bacteria ml^{-1} and (e-i) viruses ml^{-1}. Black dots indicate sampling points, yellow dots indicate mixed layer depth (Z_m), and red dots the sampling depths for modified dilution assays. Graphs were prepared with Ocean Data View (ODV version 4.6.5, Schlitzer, 2002).

The hypothesis (H1) that abundances and composition of the microbial host populations (e.g., bacteria and phytoplankton) vary with latitude (H1a), and are strongly affected by changes in water column stratification (H1b) is confirmed by the RDA results. Forward selection revealed that latitude and the stratification variables K_T, N^2 and temperature all contributed significantly to the RDA model (Table 1). The results are presented in a RDA triplot (Figure 5a). The first two axes in the RDA triplot explained 27% and 4% of the variation in the data. The concentrations of bacteria, cyanobacteria, picoeukaryotic and nanoeukaryotic phytoplankton were all positively correlated with K_T and N^2. The strong positive correlation between picoeukaryotes and N^2 is particularly noteworthy, indicating that picoeukaryotes reached their highest concentrations at or near the pycnocline. In comparison to the other species groups, cyanobacteria showed a relatively strong

correlation with temperature and nanoeukaryotes a relatively strong correlation with latitude.

Table 1. Significance of the selected explanatory variables in the RDA correlation triplots (see Figure 5a and b).

Explanatory variable	AIC*	Pseudo-F	P
Host populations (H1)			
K_T	103.5	33	0.005
Temperature	95.4	10.4	0.005
Latitude	79.7	18.9	0.005
N^2	71.1	10.6	0.005
Virus populations (H2)			
Bacteria	89.5	135.0	0.005
PicoEUK	71.7	21.4	0.005
NanoEUK	64.8	8.9	0.005
Temperature	58.5	8.3	0.005
Cyano	54.1	6.1	0.005
Latitude	52.9	3.1	0.025

Footnote: AIC = Akaike Information Criterion. The explanatory variables were selected by forward selection based on the pseudo-F statistic, using 9,999 permutations to assess their significance. Total variation explained by the RDA models was 57 and 75%, respectively.

RDA was also applied to investigate hypothesis (H2) that the biogeographical distributions of the viruses depend on the biogeographical distributions of their hosts. Forward selection revealed that latitude, temperature and the four different potential host groups contributed significantly to the RDA model (Table 1), whereas the environmental variables K_T, Chl *a* and N^2 (pseudo-F = 1.1, 0.8, and 0.2; $p = 0.39$, 0.53, and 0.91, respectively) did not. The first two axes of the RDA triplot (Figure 5b) explained 51% and 3% of the variation in the data. In line with expectation, the RDA triplot shows that the biogeographical distribution of V1 viruses was tightly coupled to the distribution of total bacterial abundance (Figure 5b).The distribution of V2 viruses was correlated with total picoeukaryotic phytoplankton abundance, while the distribution of V3 viruses was strongly correlated with total picocyanobacterial abundance. Furthermore, distributions of V4 and V5 viruses were associated with high abundances of nanoeukaryotic phytoplankton and bacteria (Figure 5b).

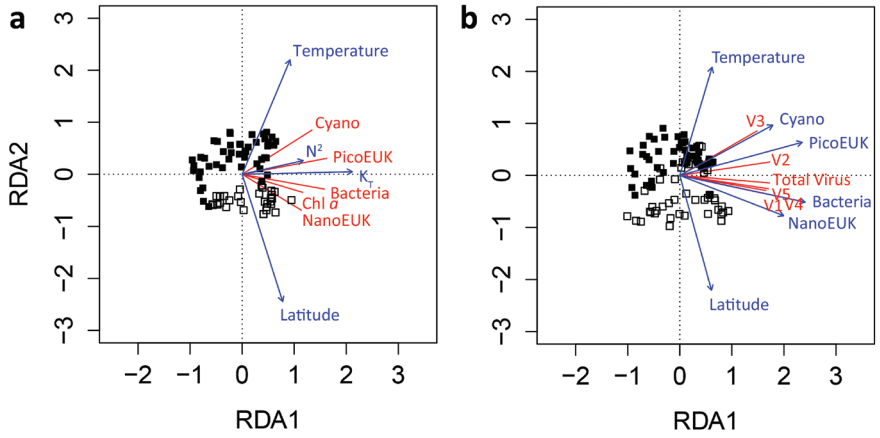

Figure 5. Redundancy Analysis (RDA) correlation triplot describing (**a**) the biogeographical distribution of potential microbial hosts (response variables, in red) in relation to environmental variables relevant to stratification (explanatory variables, in blue) and (**b**) the biogeographical distributions of the viruses (response variables, in red) in relation to latitude and the biogeographical distributions of their hosts (explanatory variables, in blue) using data obtained during the STRATIPHYT cruise. Symbols represent individual sampling points (n = 80 and 96 in panels a and b, respectively), where closed squares represent sampling points at stations with a deep chlorophyll maximum (DCM) and open squares represent sampling points at stations without a DCM. The DCM was defined by the presence of a subsurface peak in the vertical profile of Chl a autofluorescence, which is a common feature of vertically stratified oligotrophic waters. All explanatory variables in the triplot are significant (Table 1). Total variation explained by the RDA models in panels a and b were 57 and 75%, respectively.

To assess hypothesis (H3), we quantified the contributions of viral lysis and grazing to the mortality of the different phytoplankton groups by conducting 34 modified dilution assays across the North Atlantic during the two cruises (Figure 1; see Tables S1 and S2 for details). We first tested whether the modified dilution assays themselves had any undesirable side effects on phytoplankton performance. In general, we found no associated reduction in growth rate for any of the phytoplankton groups in the 20% fraction of the 30Ka series, where potential enhanced nutrient limitation would be greatest due to reduced remineralization (as a result of removal of bacteria and grazers). Furthermore, the photosynthetic capacity remained high for all dilutions (Fv/Fm = 0.6).

Viral lysis rates varied from 0 to 1.05 d^{-1} (Table S2). Two-way analysis of variance of the mortality rates revealed a significant main effect of the phytoplankton groups ($F_{3,188}$ = 4.761; p = 0.003), while the main effect of the mortality source (grazing vs viral lysis) ($F_{1,188}$ = 2.316; p > 0.05) and the interaction term ($F_{3,188}$ = 0.115; p > 0.05) were both non-significant. In other words, viral lysis rates were comparable to microzooplankton grazing rates for all phytoplankton groups measured (Figure

6), demonstrating that virus-mediated lysis contributed to approximately half of the total phytoplankton mortality. However, mortality rates differed between the phytoplankton groups. The mortality rates of nanoeukaryotic and picoeukaryotic phytoplankton were not significantly different, and these two groups demonstrated the highest average viral lysis rates of 0.23 and 0.19 d^{-1} and grazing rates of 0.27 and 0.21 d^{-1}, respectively (Figure 6). *Synechococcus* and *Prochlorococcus* experienced significantly lower mortality rates compared to the nanoeukaryotes, with viral lysis rates of 0.14 d^{-1} and grazing rates of 0.13 d^{-1}.

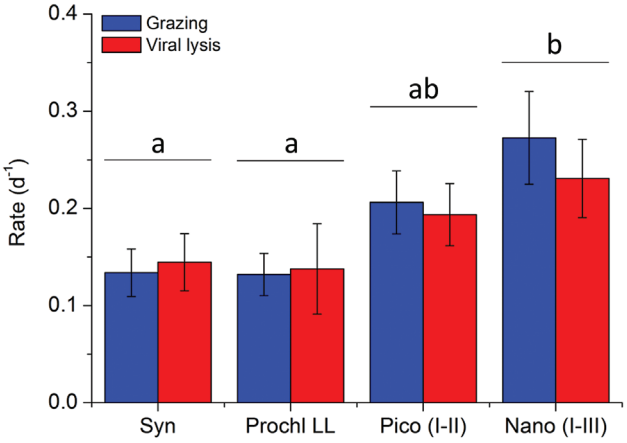

Figure 6. Grazing and viral lysis rates of the different phytoplankton groups. Grazing and viral lysis rates were determined using the modified dilution assay. The phytoplankton groups include Synechococcus (Syn, sample size N = 19), low-light adapted Prochlorococcus (Prochl LL, N = 13), picoeukaryotes (Pico I-II, N = 45), and nanoeukaryotes (Nano I-III, N = 28). High-light adapted Prochlorococcus was largely absent at the depths sampled for the modified dilution assays. Error bars represent standard error. Bars with different letters are significantly different ($p<0.05$), as tested by two-way analysis of variance followed by post hoc comparison of the means using Tukey's HSD.

Total mortality rates of the specific phytoplankton groups ranged from 0.01 to 1.20 d^{-1}, and were in balance with gross growth rates (Figure 7a), emphasizing fast turnover of the photoautotrophic production. Moreover, our data show a remarkable reduction in the ratio of viral lysis rates to microzooplankton grazing rates (V:G) at higher latitudes (> 56°N)(Figure 7b). This switch from a viral lysis-dominated to a grazing-dominated plankton community was consistent across different phytoplankton groups (Figure 7b). The pattern is corroborated by a significant negative correlation of V:G with latitude and a significant positive correlation with temperature and salinity (Table 2). Similarly, viral lysis rates but not the grazing rates showed a significant negative correlation with latitude and K_T and positive

correlation with temperature and salinity, suggesting that the reduction in V:G was due to decreased viral lysis rates at higher latitudes (Table 2).

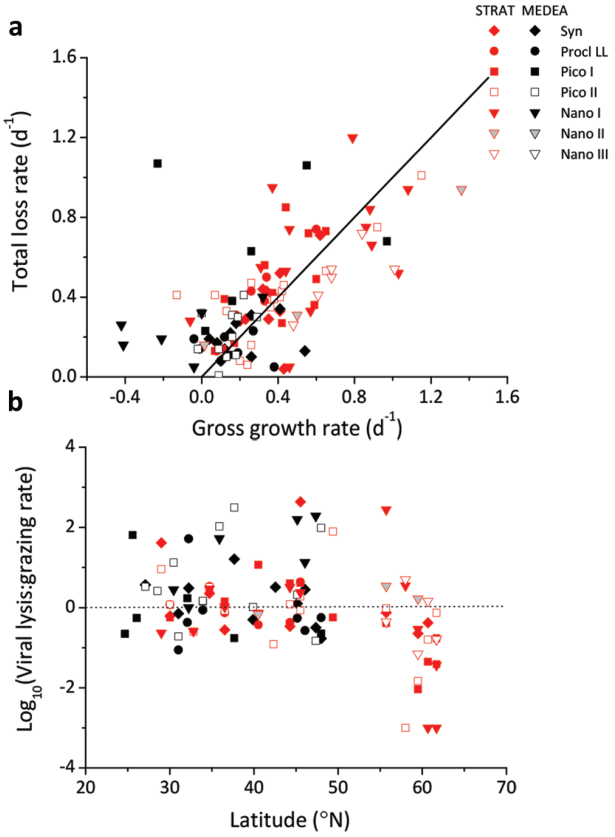

Figure 7. The contribution of viral lysis to phytoplankton mortality. (a) Relationship between the total loss rate (grazing + viral lysis) and gross growth rate of the 7 phytoplankton groups (< 20 µm). The black line indicates a 1:1 relationship. (b) Ratio of viral lysis to microzooplankton grazing rates for each of the 7 phytoplankton groups (< 20 µm) distinguished by flow cytometry, as function of latitude. Rates were obtained by the modified dilution technique during the STRATIPHYT (red symbols) and MEDEA (black symbols) cruises. High-light adapted Prochlorococcus were not included as they were largely absent at the depths sampled for the modified dilution assays. Dotted line indicates a 1:1 relationship of viral lysis to grazing.

Table 2. Spearman rank correlation coefficients (above the diagonal) and associated p-values (below the diagonal, with significant values highlighted in bold) of environmental and biological data obtained from modified dilution assays conducted during the STRATIPHYT and MEDEA cruises (N=105). Abbreviations represent phytoplankton host abundance (P0), gross growth rate (μgross), grazing rate (G), viral lysis rate (V), total mortality rate (TM) and the ratio of viral lysis to grazing rate (V:G).

	Latitude	Temperature	Salinity	sigma-t	K_T	N^2	PO_4	NO_x	P_0	μ_{gross}	G	V	T_M	V:G
Latitude		-0.95	-0.96	-0.67	0.68	n.s.	0.76	0.57	n.s.	n.s.	n.s.	-0.47	n.s.	-0.47
Temperature	**0.00**		0.89	0.56	-0.66	n.s.	-0.79	-0.61	n.s.	n.s.	n.s.	0.39	n.s.	0.41
Salinity	**0.00**	**0.00**		0.72	-0.65	n.s.	-0.77	-0.57	n.s.	n.s.	n.s.	0.45	n.s.	0.47
sigma-t	**0.00**	**0.00**	**0.00**		-0.76	n.s.	-0.65	-0.44	n.s.	n.s.	n.s.	0.48	n.s.	0.36
K_T	**0.00**	**0.00**	**0.00**	**0.00**		n.s.	0.63	0.43	n.s.	n.s.	n.s.	-0.43	n.s.	n.s.
N^2	1.00	1.00	1.00	1.00	0.34		n.s.	n.s.	n.s.	n.s.	n.s.	n.s.	n.s.	n.s.
PO_4	**0.00**	**0.00**	**0.00**	**0.00**	**0.00**	1.00		0.89	n.s.	n.s.	n.s.	n.s.	n.s.	n.s.
NO_x	**0.00**	**0.00**	**0.00**	**0.00**	**0.00**	1.00	**0.00**		n.s.	n.s.	n.s.	n.s.	n.s.	n.s.
P_0	1.00	1.00	1.00	1.00	1.00	1.00	1.00	1.00		-0.51	n.s.	n.s.	-0.38	n.s.
μ_{gross}	1.00	1.00	1.00	1.00	1.00	0.54	1.00	1.00	**0.00**		0.43	n.s.	0.64	n.s.
G	0.94	1.00	0.28	1.00	1.00	1.00	0.70	1.00	1.00	**0.00**		n.s.	0.67	-0.68
V	**0.00**	**0.00**	**0.00**	**0.00**	**0.00**	1.00	0.41	1.00	0.36	0.40	1.00		0.48	0.76
T_M	1.00	1.00	1.00	1.00	1.00	1.00	1.00	1.00	**0.00**	**0.00**	**0.00**	**0.00**		n.s.
V:G	**0.00**	**0.00**	**0.00**	**0.01**	0.11	1.00	0.22	1.00	1.00	1.00	**0.00**	**0.00**	1.00	

n.s. indicates non-significance at $\alpha = 0.05$

Discussion

Our results demonstrate distinct biogeographical distributions of different virus groups and their potential host microbial populations across the North Atlantic Ocean (Figure 4). Metagenomic analyses of marine viral assemblages suggest that most viruses are widely dispersed across different oceanic regions (Angly et al. 2006), providing a seeding community for recruitment once the environmental conditions turn favorable (Breitbart and Rohwer 2005; Suttle 2007; Thingstad et al. 2014). Therefore, the classical tenet of 'all microbes are everywhere, but the environment selects' (Baas Becking 1931; de Wit and Bouvier 2006) is likely to apply to marine viruses. Accordingly, large-scale biogeographical variation in viral composition across the oceans is probably not caused by dispersal limitation but largely due to spatial variation in environmental conditions (Figure 5a). In particular, in agreement with hypothesis (H1) and (H2), our results show that the observed biogeographical distributions of marine viruses across the North Atlantic are strongly associated with the distributions of bacteria and phytoplankton that serve as their main hosts (Figure 5b). The large-scale distributions of these host species are in turn dependent on the latitudinal gradient from warm permanently stratified waters in the subtropical North Atlantic to colder seasonally stratified waters at higher latitudes (Figure 5a).

Yang et al. (2010) described a correlation between V3 viruses and picophytoplankton (including picocyanobacteria and picoeukaryotes) in the Pacific Ocean, with highest V3 virus abundances in tropical and subtropical waters. Our results show that the distribution of V3 viruses is closely related to the distribution of picocyanobacteria (*Prochlorococcus* and *Synechococcus*) (Figure 5b), indicating that the cluster of V3 viruses contains many cyanophages, which is in line with previous observations that cyanophages are particularly widespread in the (sub)tropical oceans (Suttle and Chan 1994; Wilson et al. 1999; Angly et al. 2006). In contrast, the distribution of V2 viruses appears to be linked to picoeukaryotic phytoplankton, and both the V2 viruses and picoeukaryotic phytoplankton are abundant at mid and high latitudes (Figure 4b, f and Figure 5b). Furthermore, our observation that V4 and V5 viruses are correlated to nanoeukaryotic phytoplankton (Figure 5b) corroborates earlier studies documenting similar FCM signatures for viruses infective against haptophytes (Jacquet et al. 2002; Brussaard 2004b; Baudoux et al. 2006).

The fate of primary production has important implications for the ecology and biogeochemical recycling of marine food webs. Estimates of viral lysis rates

of natural phytoplankton populations remain scarce, and consequently the importance of viruses in comparison to other loss factors remains unclear. Rates of viral-mediated mortality for *Synechococcus* (i.e., 0.03 - 0.49 d^{-1}), picoeukaryotic phytoplankton (i.e., 0 - 0.81 d^{-1}) and nanoeukaryotic phytoplankton (i.e., 0 - 1.05 d^{-1}) were comparable to the ranges reported in the literature (Baudoux et al. 2007, 2008; Evans and Brussaard 2012; Tsai et al. 2012). The viral lysis rates of *Prochlorococcus* (i.e., 0.02 - 0.57 d^{-1}) presented here were higher than the maximal 0.06 d^{-1} reported thus far (Baudoux et al. 2007). The typical set-up of the modified dilution assay (i.e., 2 parallel series, 4 dilutions, 3 replicates) lacks the sensitivity required to detect significance of viral lysis rates when rates are very low (Evans et al. 2003; Kimmance et al. 2007; Baudoux et al. 2008). Hence, we note that estimates of viral lysis rates < 0.1 d^{-1} should be interpreted with caution. To improve sensitivity of the method at low viral lysis rates, more replicates should be used.

Among the different phytoplankton groups, *Synechococcus* and *Prochlorococcus* experienced the lowest average viral lysis rates (i.e., 0.14 d^{-1}) (Figure 6). Considering the dominance of cyanophages and their hosts, the low viral mortality may seem surprising (Suttle and Chan 1993; Wang et al. 2011). However, *Synechococcus* and *Prochlorococcus* populations display high genotypic diversity and have the ability to develop resistance against viral infection (Waterbury and Valois 1993; Scanlan and West 2002), which could potentially reduce the impact of viral-induced mortality of these phytoplankton groups.

Virus-mediated lysis was responsible for approximately half of the total phytoplankton mortality in all four phytoplankton groups that we investigated, and comparable in magnitude to the mortality rate exerted by microzooplankton grazing (Figure 6). Total mortality of phytoplankton populations was in balance with gross growth (Figure 7a), indicating fast turnover of the photoautotrophic production within the North Atlantic Ocean. These results emphasize the need for the incorporation of viral lysis into ecosystems models (Franks 2001; Keller and Hood 2011; Keller and Hood 2013). Moreover, our results support hypothesis (H3) that viral lysis rates vary with latitude, and point at a striking reduction in the ratio of viral lysis rates to grazing rates of marine phytoplankton at higher latitudes (Figure 7b). While this observation might be a local or seasonal phenomenon, our findings are consistent with a smaller-scale study in the North Sea (Baudoux et al. 2008), which reported low viral lysis rates of picophytoplankton in offshore waters above 55°N. Furthermore, data from the Southern Ocean point at low viral lysis rates of phytoplankton over a relatively broad geographic range from at least 43°S

to 70°S on the southern hemisphere (Evans and Brussaard 2012). This suggests that low viral lysis rates at higher latitudes are not unique for our data set, but may represent a global pattern.

The underlying causes for the reduction in viral lysis rates with latitude remain unclear. Our results reveal a positive relationship between temperature and viral lysis rates of marine phytoplankton. While temperature has been shown to regulate viral infection of marine phytoplankton (Cottrell and Suttle 1995; Nagasaki and Yamaguchi 1998), evidence that temperature affects viral production rates is thus far largely restricted to bacterial hosts (Matteson et al. 2012; Mojica and Brussaard 2014). Vertical stratification represses turbulence and reduces mixed layer depth, thereby determining the general availability of light and nutrients to phytoplankton in the ocean (Behrenfeld et al. 2006; Huisman et al. 2006). These factors have been shown to be important factors regulating the production of viruses in phytoplankton hosts (Van Etten et al. 1983; Bratbak et al. 1998; Jacquet et al. 2002; Maat et al. 2014). Yet, we did not find a significant association between viral lysis rates and nutrient concentrations, host abundance or growth rate in our data (Table 2). In addition, viral lysis rates declined with latitude despite the latitudinal increase in total virus abundance as well as increases in V1 and V2 viruses (Figure 4; Table S3). An exception is the decline of the V3 viruses with latitude (Figure 4g; Table S3), which was due to the dominance of their picocyanobacterial hosts in the (sub) tropical southern region. Metagenomic analysis has revealed that lysogeny and prophage-like sequences are common in the Arctic Ocean (Angly et al. 2006). If this is a more general feature at higher latitudes, it may reduce the lytic viral lysis rates measured by the dilution assay. However, evidence for lysogeny in photoautotrophs is mostly restricted to prokaryotes (Paul 2008). Consequently, lysogeny would not fully explain the low viral lysis rates at higher latitudes for eukaryotic phytoplankton populations. An alternative explanation might be that latitudinal changes in phytoplankton species composition result in more virus-resistant phytoplankton species at higher latitudes, however we have no evidence to support this. We speculate that removal or inactivation rates of marine viruses by transparent exopolymer particles (TEP) might be higher at the higher latitudes (Brussaard et al. 2005b; Mari et al. 2007). TEP concentrations have been found to be correlated to phytoplankton biomass, photosynthetic activity and bacterial production (Claquin et al. 2008; Ortega-Retuerta et al. 2010), which were highest in the northern latitudes of our study (see also van de Poll et al. 2013). As fluid shear is one of the primary factors controlling aggregation in pelagic systems

(Jackson 1990; Malits and Weinbauer 2009), the increase of K_T with latitude might have promoted higher aggregate formation and increase the potential for viral (temporary) inactivation rates at higher latitudes.

Due to deep water formation, the North Atlantic is key to ocean circulation and global climate, absorbing ~23% of the global anthropogenic CO_2 emission (Sabine et al. 2004). Several studies predict that global warming will result in a stronger temperature stratification in the North Atlantic Ocean (Sarmiento 2004; Polovina et al. 2008), accompanied by changes in phytoplankton community structure as oligotrophic regions of the ocean expand northwards (Flombaum et al. 2013; Mojica et al. 2015). This in turn will result in alterations to virus community structure as virus populations respond to changing host distributions. Currently, grazing dominates phytoplankton mortality at higher latitudes, whereas the contribution of viral lysis is relatively small. However, our results indicate that warming of the surface layers will shift the ecosystem at high latitudes towards a more viral-lysis dominated system. The partitioning of photosynthetic carbon through these different pathways (i.e., grazing versus cell lysis) has important implications for ecosystem function as each pathway differentially affects the structure and functioning of pelagic microbial food webs. Grazing transfers carbon, nutrients and energy to higher trophic levels, thereby increasing the overall efficiency and carrying capacity of the ecosystem. In addition, the production of fecal pellets by mesozooplankton is responsible for much of the carbon transported out of the euphotic zone into the deeper ocean (Ducklow et al. 2001). Viral lysis redirects carbon and energy away from larger organisms towards the microbial loop, and thereby rapidly returns most of the organic carbon fixed by phytoplankton into the surface layer (Fuhrman 1999; Wilhelm and Suttle 1999; Brussaard et al. 2005a; Weitz and Wilhelm 2012). A more prominent role of viral lysis in the northern North Atlantic would thus markedly reduce biological carbon export into the ocean's interior in one of the key areas of global carbon sequestration, reducing the ocean's capacity to function as a long-term sink for anthropogenic carbon dioxide.

Acknowledgments

We thank the captains and crews of the R/V Pelagia for their great help with sampling during the cruises. Furthermore, we thank Jan Finke, Douwe Maat, Richard Doggen and Anna Noordeloos for their on-board assistance, Lisa Hahn-

Woernle for providing the physical data, Klaas Timmermans for providing Fv/Fm measurements and Harry Witte for his useful discussions regarding statistical analysis. This research was part of the STRATIPHYT project (ZKO-grant 839.08.420 for CPDB), supported by the Earth and Life Sciences Foundation (ALW), which is subsidised by the Netherlands Organisation for Scientific Research (NWO). We further acknowledge the OPTIMON project (ZKO) for JH and KDAM, the Turner-Kirk Charitable Trust of the Isaac Newton Institute for JH, and NSF grants OCE-1061352 and OCE- 1030518 for SWW.

References

Angly FE, Felts B, Breitbart M, Salamon P, Edwards RA, Carlson C, Chan AM, Haynes M, Kelley S, Liu H, Mahaffy JM, Mueller JE, Nulton J, Olson R, Parsons R, Rayhawk S, Suttle CA, Rohwer F (2006) The marine viromes of four oceanic regions. PLOS Biology 4: e368. doi: 10.1371/journal.pbio.0040368

Baas Becking LGM (1931) Geobiologie of inleiding tot de milieukunde. W.P. Van Stockum & Zoon, the Netherlands

Baudoux AC, Noordeloos AAM, Veldhuis MJW, Brussaard CPD (2006) Virally induced mortality of *Phaeocystis globosa* during two spring blooms in temperate coastal waters. Aquatic Microbial Ecology 44: 207-217

Baudoux AC, Veldhuis MJW, Witte HJ, Brussaard CPD (2007) Viruses as mortality agents of picophytoplankton in the deep chlorophyll maximum layer during IRONAGES III. Limnology and Oceanography 52: 2519-2529

Baudoux AC, Brussaard CPD (2008) Influence of irradiance on virus-algal host interactions. Journal of Phycology 44: 902-908

Baudoux AC, Veldhuis MJW, Noordeloos AAM, van Noort G, Brussaard CPD (2008) Estimates of virus- vs. grazing induced mortality of picophytoplankton in the North Sea during summer. Aquatic Microbial Ecology 52: 69-82

Behrenfeld MJ, O 'Malley RT, Siegel DA, McClain CR, Sarmiento JL, Feldman GC, Milligan AJ, Falkowski PG, Letelier RM, Boss ES (2006) Climate-driven trends in contemporary ocean productivity. Nature 444: 752-755

Brainerd KE, Gregg MC (1995) Surface mixed and mixing layer depths. Deep-Sea Research, Part I 42: 1521-1543

Bratbak G, Jacobsen A, Heldal M, Nagasaki K, Thingstad F (1998) Virus production in *Phaeocystis pouchetii* and its relation to host cell growth and nutrition. Aquatic Microbial Ecology 16: 1-9

Bray NA, Fofonoff NP (1981) Available potential energy for mode eddies. Journal of Physical Oceanography 11: 30-47

Breitbart M, Rohwer F (2005) Here a virus, there a virus, everywhere the same virus? Trends Microbiology 13: 278-284

Brussaard CPD (2004a) Viral control of phytoplankton populations - a review. Journal of Eukaryotic Microbiology 51: 125-138

Brussaard CPD (2004b) Optimization of procedures for counting viruses by flow cytometry. Applied and Environmental Microbiology 70: 1506-1513

Brussaard CPD, Kuipers B, Veldhuis MJW (2005a) A mesocosm study of *Phaeocystis globosa* population dynamics: I. Regulatory role of viruses in bloom control. Harmful Algae 4: 859-874

Brussaard CPD, Mari X, Van Bleijswijk JDL, Veldhuis MJW (2005b) A mesocosm study of *Phaeocystis globosa* (Prymnesiophyceae) population dynamics: II. Significance for the microbial community. Harmful Algae 4: 875-893

Brussaard CPD, Martinez JM (2008) Algal bloom viruses. Plant Viruses 2: 1-13

Brussaard CPD, Payet JP, Winter C, Weinbauer M (2010) Quantification of aquatic viruses by flow cytometry. In: Wilhelm SW, Weinbauer MG, Suttle CA (eds). Manual of Aquatic Viral Ecology. ASLO

Cottrell MT, Suttle CA (1995) Dynamics of a lytic virus infecting the photosynthetic marine picoflagellate *Micromonas pusilla*. Limnology and Oceanography 40: 730-739

Daufresne M, Lengfellner K, Sommer U (2009) Global warming benefits the small in aquatic ecosystems. Proceedings of the National Academy of Sciences of the United States of America 106: 12788-12793

de Wit R, Bouvier T (2006) 'Everything is everwhere, but, the environment selects'; what did Baas Becking and Beijerinck really say? Environmental Microbiology 8: 755-758

Deser C, Blackmon ML (1993) Surface climate variations over the North Atlantic ocean during winter: 1900-1989. Journal of Climate 6: 1743-1753

Doney SC, Ruckelshaus M, Duffy JE, Barry JP, Chan F, English CA, Galindo HM, Grebmeier JM, Hollowed AB, Knowlton N, Polovina J, Rabalais NN, Sydeman WJ, Talley LD (2012) Climate change impacts on marine ecosystems. Annual Review of Marine Science 4: 11-37

Ducklow HW, Steinberg DK, Buesseler KO (2001) Upper ocean carbon export and the biological pump. Oceanography 14: 50-58

Edwards M, Richardson AJ (2004) Impact of climate change on marine pelagic phenology and trophic mismatch. Nature 430: 881-884

Evans C, Archer SD, Jacquet S, Wilson WH (2003) Direct estimates of the contribution of viral lysis and microzooplankton grazing to the decline of a *Micromonas* spp. population. Aquatic Microbial Ecology 30: 207-219

Evans C, Brussaard CPD (2012) Viral lysis and microzooplankton grazing of phytoplankton throughout the Southern Ocean. Limnology and Oceanography 57: 1826-1837

Field CB, Behrenfeld MJ, Randerson JT, Falkowski P (1998) Primary production of the biosphere: Integrating terrestrial and oceanic components. Science 281: 237-240

Flombaum P, Gallegos JL, Gordillo RA, Rincon J, Zabala LL, Jiao N, Karl DM, Li WKW, Lomas MW, Veneziano D, Vera CS, Vrugt JA, Martiny AC (2013) Present and future global distributions of the marine cyanobacteria *Prochlorococcus* and *Synechococcus*. Proceedings of the National Academy of Sciences of the United States of America 110: 9824-9829

Franks PJS (2001) Phytoplankton blooms in a fluctuating environment: the roles of plankton response time scales and grazing. Journal of Plankton Research 23: 1433-1441

Fuhrman JA (1999) Marine viruses and their biogeochemical and ecological effects. Nature 399: 541-548

Fuhrman JA, Steele JA, Hewson I, Schwalbach MS, Brown MV, Green JL, Brown JH (2008) A latitudinal diversity gradient in planktonic marine bacteria. Proceedings of the National Academy of Sciences of the United States of America 105: 7774-7778

Furrer R, Nychka D, Sain S (2012) fields: Tools for spatial data. R package version 6.7: http://CRAN.R-project.org/package=fields

Gobler CJ, Hutchins DA, Fisher NS, Cosper EM, Sanudo-Wilhelmy SA (1997) Release and bioavailability of C, N, P, Se, and Fe following viral lysis of a marine chrysophyte. Limnology and Oceanography 42: 1492-1504

Grasshoff K (1983) Determination of nitrate. In: Grasshoff K, Erhardt M, Kremeling K (eds) Methods of Seawater Analysis. Verlag Chemie: Weinheim, Germany

Gregg WW, Conkright ME, Ginoux P, O 'Reilly JE, Casey NW (2003) Ocean primary production and climate: global decadal changes. Geophysical Research Letters 30: 1809. doi:10.1029/2003GL016889

Haaber J, Middelboe M (2009) Viral lysis of *Phaeocystis pouchetii*: Implications for algal population dynamics and heterotrophic C, N and P cycling. The ISME Journal 3: 430-441

Helder W, de Vries RTP (1979) An automatic phenol-hypochlorite method for the determination of ammonia in sea and brackish water. Netherlands Journal of Sea Research 13: 154-160

Hilligsøe KM, Richardson K, Bendtsen J, Sorensen LL, Nielsen TG, Lyngsgaard MM (2011) Linking phytoplankton community size composition with temperature, plankton food web structure and sea-air CO_2 flux. Deep-Sea Research, Part I 58: 826-838

Huisman J, van Oostveen P, Weissing FJ (1999) Critical depth and critical turbulence: two different mechanisms for the development of phytoplankton blooms. Limnology and Oceanography 44: 1781-1787

Huisman J, Sharples J, Stroom JM, Visser PM, Kardinaal WEA, Verspagen JMH, Sommeijer B (2004) Changes in turbulent mixing shift competition for light between phytoplankton species. Ecology 85: 2960-2970

Huisman J, Thi NNP, Karl DM, Sommeijer B (2006) Reduced mixing generates oscillations and chaos in the oceanic deep chlorophyll maximum. Nature 439: 322-325

Irigoien X, Huisman J, Harris RP (2004) Global biodiversity patterns of marine phytoplankton and zooplankton. Nature 429: 863-867

Jackson GA (1990) A model of the formation of marine algal flocs by physical coagulation processes. Deep-Sea Research, Part A 37: 1197-1211

Jacquet S, Heldal M, Iglesias-Rodriguez D, Larsen A, Wilson W, Bratbak G (2002) Flow cytometric analysis of an *Emiliana huxleyi* bloom terminated by viral infection. Aquatic Microbial Ecology 27: 111-124

Jurado E, van der Woerd HJ, Dijkstra HA (2012) Microstructure measurements along a quasi-meridional transect in the northeastern Atlantic Ocean. Journal of Geophysical Research 117: C04016. doi: 10.1029/2011JC007137

Keller DP, Hood RR (2011) Modeling the seasonal autochthonous sources of dissolved organic carbon and nitrogen in the upper Chesapeake Bay. Ecological Modelling 222: 1139-1162

Keller DP, Hood RR (2013) Comparative simulations of dissolved organic matter cycling in idealized oceanic, coastal, and estuarine surface waters. Journal of Marine Systems109: 109-128

Kimmance SA, Wilson WH, Archer SD (2007) Modified dilution technique to estimate viral versus grazing mortality of phytoplankton: limitations associated with method sensitivity in natural waters. Aquatic Microbial Ecology 49: 207-222

Kimmance SA, Brussaard CPD (2010) Estimation of viral-induced phytoplankton mortality using the modified dilution method. In: Wilhelm SW, Weinbauer M, Suttle CA (eds) Manual of Aquatic Viral Ecology. ASLO

Koroleff F (1969) Direct determination of ammonia in natural waters as indophenol blue. Coun. Meet. int. Coun. Explor. Sea **C.M.-ICES/C:** 9

Levitus S, Antonov JI, Boyer TP, Stephens C (2000) Warming of the world ocean. Science 287: 2225-2229

Longhurst AR (2007) Ecological Geography of the Sea. Academic Press, London

Maat DS, Crawfurd KJ, Timmermans KR, Brussaard CPD (2014) Elevated partial CO_2 pressure and phosphate limitation favor *Micromonas pusilla* through stimulated growth and reduced viral impact. Applied and Environmental Microbiology 80: 3119-3127

Malits A, Weinbauer MG (2009) Effect of turbulence and viruses on prokaryotic cell size, production and diversity. Aquatic Microbial Ecology 54: 243-254

Mari X, Kerros ME, Weinbauer MG (2007) Virus attachment to transparent exopolymeric particles along trophic gradients in the southwestern lagoon of New Caledonia. Applied and Environmental Microbiology 73: 5245-5252

Marie D, Brussaard CPD, Thyrhaug R, Bratbak G, Vaulot D (1999) Enumeration of marine viruses in culture and natural samples by flow cytometry. Applied and Environmental Microbiology 65: 45-52

Marie D, Simon N, Vaulot D (2005) Phytoplankton cell counting by flow cytometry. In: Andersen RA (ed) Algal culturing techniques. Elsevier Academic Press, Burlington

Martiny JBH, Bohannan BJM, Brown JH, Colwell RK, Fuhrman JA, Green JL, Horner-Devine MC, Kane M, Krumins JA, Kuske CR, Morin PJ, Naeem S, Ovreas L, Reysenbach AL, Smith VH, Staley JT (2006) Microbial biogeography: putting microorganisms on the map. Nature Reviews Microbiology 4: 102-112

Matteson AR, Loar SN, Pickmere S, DeBruyn JM, Ellwood MJ, Boyd PW, Hutchins DA, Wilhelm SW (2012) Production of viruses during a spring phytoplankton bloom in the South Pacific Ocean near of New Zealand. FEMS Microbiology Ecology 79: 709-719

Matteson AR, Rowe JM, Ponsero AJ, Pimentel TM, Boyd PW, Wilhelm SW (2013) High abundances of cyanomyoviruses in marine ecosystems demonstrate ecological relevance. FEMS Microbiology Ecology 84: 223-234

Mitra A, Flynn KJ (2005) Predator-prey interactions: is 'ecological stoichiometry' sufficient when good food goes bad? Journal of Plankton Research 27: 393-399

Moebus K (1996) Marine bacteriophage reproduction under nutrient-limited growth of host bacteria. I. Investigations with six phage-host systems. Marine Ecology Progress Series 144: 1-12

Mojica KDA, Brussaard CPD (2014) Factors affecting virus dynamics and microbial host-virus interactions in marine environments. FEMS Microbiology Ecology 89: 495-515

Mojica KDA, Evans C, Brussaard CPD (2014) Flow cytometric enumeration of marine viral populations at low abundances. Aquatic Microbial Ecology 71: 203-209

Mojica KDA, van de Poll WH, Kehoe M, Huisman J, Timmermans KR, Buma AGJ, van der Woerd HJ, Hahn-Woernle L, Dijkstra HA, Brussaard CPD (2015). Phytoplankton community structure in relation to vertical stratification along a north-south gradient in the Northeast Atlantic Ocean. Limnology and Oceanography (in press). doi: 10.1002/lno.10113

Mühling M, Fuller NJ, Millard A, Somerfield PJ, Marie D, Wilson WH, Scanlan DJ, Post AF, Joint I, Mann NH (2005) Genetic diversity of marine *Synechococcus* and co-occurring cyanophage communities: evidence for viral control of phytoplankton. Environmental Microbiology 7: 499-508

Murphy J, Riley JP (1962) A modified single solution method for the determination of phosphate in natural waters. Analytica Chimica Acta 27: 31-36

Nagasaki K, Yamaguchi M (1998) Effect of temperature on the algicidal activity and the stability of HaV (*Heterosigma akashiwo* virus). Aquatic Microbial Ecology 15: 211-216

Oksanen J, Blanchet FG, Kindt R, Legendre P, Minchin PR, O'Hara RB, Simpson GL, Solymos, P, Stevens MHH, Wagner H (2013) vegan: Community ecology package. http://CRAN.R-project.org/package=vegan

Paul JH (2008) Prophages in marine bacteria: dangerous molecular time bombs or the key to survival in the seas? The ISME Journal 2: 579-589

Polovina JJ, Howell EA, Abecassis M (2008) Ocean's least productive waters are expanding. Geophysical Research Letters 35: L03618. doi: 10.1029/2007GL031745

R Development Core Team (2012) R: A language and environment for statistical computing. R Foundation for Statistical Computing: Vienna, Austria, ISBN 3-900051-07-0, http://www.R-project.org

Revelle W (2014) psych: Procedures for Psychological, Psychometric, and Personality Research. R Package Version 1.4.5. http://CRAN.R-project.org/package=psych

Richardson AJ, Schoeman DS (2004) Climate impact on plankton ecosystems in the Northeast Atlantic. Science 305: 1609-1612

Sabine CL, Feely RA, Gruber N, Key RM, Lee K, Bullister JL, Wanninkhof R, Wong CS,

Wallace DWR, Tilbrook B, Millero FJ, Peng T-H, Kozyr A, Ono T, Rios AF (2004) The oceanic sink for anthropogenic CO_2. Science 305: 367-371

Sarmiento JL, Hughes TMC, Stouffer RJ, Manabe S (1998) Simulated response of the ocean carbon cycle to anthropogenic climate warming. Nature 393: 245-249

Sarmiento JL (2004) Response of ocean ecosystems to climate warming. Global Biogeochemical Cycles 18: GB3003. doi: 10.1029/2003GB002134

Scanlan DJ, West NJ (2002) Molecular ecology of the marine cyanobacterial genera *Prochlorococcus* and *Synechococcus*. FEMS Microbiology Ecology 40: 1-12

Schlitzer R (2002) Interactive analysis and visualization of geoscience data with Ocean Data View. Computers and Geosciences 28: 1211-1218

Siegel DA, Doney SC, Yoder JA (2002) The North Atlantic spring phytoplankton bloom and Sverdrup's critical depth hypothesis. Science 296: 730-733

Stevens C, Smith M, Ross A (1999) SCAMP: measuring turbulence in estuaries, lakes, and coastal waters. NIWA - Water Atmosphere 7: 20-21

Suttle CA, Chan AM, Cottrell MT (1990) Infection of phytoplankton by viruses and reduction of primary productivity. Nature 347: 467-469

Suttle CA, Chan AM (1993) Marine cyanophages infecting oceanic and coastal strains of *Synechococcus*: abundance, morphology, cross-infectivity and growth characteristics. Marine Ecology Progress Series 92: 99-109

Suttle CA, Chan AM (1994) Dynamics and distribution of cyanophages and their effect on marine *Synechococcus* spp. Applied and Environmental Microbiology 60: 3167-3174

Suttle CA (2007) Marine viruses - major players in the global ecosystem. Nature Reviews 5: 801-812

Sverdrup, EU (1953) On conditions for the vernal blooming of phytoplankton. Journal du Conseil / Conseil Permanent International pour l'Exploration de la Mer 18: 287-295

Taylor JR, Ferrari R (2011) Shutdown of turbulent convection as a new criterion for the onset of spring phytoplankton blooms. Limnology and Oceanography 56: 2293-2307

Thingstad TF, Våge S, Storesund JE, Sandaa R-A, Giske J (2014) A theoretical analysis of how strain-specifc viruses can control microbial species diversity. Proceedings of the National Academy of Sciences of the United States of America 111: 7813-7818

Toggweiler JR, Russell J (2008) Ocean circulation in a warming climate. Nature 451: 286-288

Tomaru Y, Tarutani K, Yamaguchi M, Nagasaki K (2004) Quantitative and qualitative impacts of viral infection on a *Heterosigma akashiwo* (Raphidophyceae) bloom in Hiroshima Bay, Japan. Aquatic Microbial Ecology 34: 227-238

Tsai AY, Gong GC, Sanders RW, Chiang KP, Huang JK, Chan YF (2012) Viral lysis and nanoflagellate grazing as factors controlling diel variations of *Synechococcus* spp. summer abundance in coastal waters of Taiwan. Aquatic Microbial Ecology 66: 159-167

van de Poll WH, Kulk G, Timmermans KR, Brussaard CPD, van der Woerd HJ, Kehoe MJ. Mojica KDA, Visser RJW, Rozeman PD, Buma AGJ (2013) Phytoplankton chlorophyll *a* biomass, composition, and productivity along a temperature and stratification gradient in the northeast Atlantic Ocean. Biogeosciences 10: 4227-4240

van de Waal DB, Verschoor AM, Verspagen JMH, Van Donk E, Huisman J (2010) Climate-driven changes in the ecological stoichiometry of aquatic ecosystems. Frontiers in Ecology and the Environment 8: 145-152

Van Etten JL, Burbank DE, Xia Y, Meints RH (1983) Growth cycle of a virus, PBCV-1, that infects Chlorella-like algae. Virology 126: 117-125

Wang K, Wommack KE, Chen F (2011) Abundance and distribution of Synechococcus spp. and cyanophages in the Chesapeake Bay. Applied and Environmental Microbiology 77: 7459-7468

Waterbury JB, Valois FW (1993) Resistance to co-occurring phages enables marine *Synechococcus* communities to coexist with cyanophages abundant in seawater. Applied and Environmental Microbiology 59: 3393-3399

Weitz JS, Wilhelm SW (2012) Ocean viruses and their effects on microbial communities and biogeochemical cycles. F1000 Biology Reports 4

Wilhelm SW, Suttle CA (1999) Viruses and nutrient cycles in the sea - Viruses play critical roles in the structure and function of aquatic food webs. Bioscience 49: 781-788

Wilson WH, Nicholas JF, Joint IR, Mann NH (1999) Analysis of cyanophage diversity and population structure in a south-north transect of the Atlantic Ocean. Bulletin of the Institute of Oceanography and Fisheries 19: 209-216

Yang YH, Motegi C, Yokokawa T, Nagata T (2010) Large-scale distribution patterns of virioplankton in the upper ocean. Aquatic Microbial Ecology 60: 233-246

Zuur A, Ieno EN, Walker N, Saveliev AA, Smith GM (2009) Mixed Effects Models and Extensions in Ecology with R. Springer, New York

Zuur AF, Ieno EN, Elphick CS (2010) A protocol for data exploration to avoid common statistical problems. Methods in Ecology and Evolution 1: 3-14

Supporting information

Table S1. Location and physicochemical characteristics of water sampled in the North Atlantic for modified dilution experiments during the STRATIPHYT and MEDEA cruises. Abbreviations for depth layer are mixed layer (ML) and deep chlorophyll maximum (DCM).

Cruise	Experiment No.	Station	Latitude (^{0}N)	Longitude (^{0}E)	Depth (m)	Depth Layer	Temperature (^{0}C)	Salinity	Sigma-t	PO_4^{3-} (µM)	NO_x (µM)	NO_2^- (µM)	NH_4^+ (µM)
STRATIPHYT	1	0	29.000	-15.000	80	DCM	19.0	36.8	26.8	0.02	0.02	0.01	0.07
STRATIPHYT	2	1	30.018	-15.071	74	DCM	18.2	36.7	26.8	0.03	0.11	0.09	0.06
STRATIPHYT	3	3	32.825	-14.589	57	DCM	18.0	36.5	26.7	0.00	0.15	0.02	0.06
STRATIPHYT	4	5	34.720	-14.258	85	DCM	16.3	36.3	27.0	0.04	0.15	0.06	0.15
STRATIPHYT	5	7	36.526	-13.934	75	DCM	16.1	36.3	27.0	0.02	0.11	0.00	0.08
STRATIPHYT	6	11	40.528	-13.191	55	DCM	15.2	36.0	26.9	0.04	0.03	0.03	0.07
STRATIPHYT	7	13	42.337	-12.884	47	DCM	14.7	35.8	26.9	0.05	0.10	0.01	0.00
STRATIPHYT	8	15	44.283	-12.605	60	DCM	14.4	35.8	27.0	0.17	2.21	0.16	0.07
STRATIPHYT	9	17	45.526	-12.426	50	DCM	14.2	35.7	26.9	0.10	1.15	0.09	0.13
STRATIPHYT	10	19	49.382	-11.829	15	ML	15.8	35.5	26.3	0.12	1.18	0.04	0.36
STRATIPHYT	11	24	55.713	-14.278	20	ML	13.9	35.3	26.6	0.20	2.71	0.13	0.09
STRATIPHYT	12	25	58.002	-16.516	10	ML	13.5	35.3	26.6	0.11	1.18	0.05	0.09
STRATIPHYT	13	27	59.499	-18.067	20	ML	14.0	35.2	26.5	0.18	2.11	0.03	0.19
STRATIPHYT	14	29	60.684	-19.339	10	ML	13.0	35.3	26.6	0.19	2.07	0.09	0.14
STRATIPHYT	15	30	61.712	-20.485	10	ML	13.2	35.2	26.6	0.13	1.02	0.02	0.24
MEDEA	16	2	45.150	-13.700	45	DCM	17.5	35.8	26.0	0.08	0.61	0.13	
MEDEA	17	3	47.360	-15.930	35	DCM	16.5	35.7	26.2	0.06	0.14	0.05	
MEDEA	18	4	48.000	-18.890	35	ML	16.4	35.7	26.2	0.06	0.14	0.04	
MEDEA	19	6	46.080	-21.310	52	ML	15.2	35.8	26.6	0.24	3.34	0.30	
MEDEA	20	7	42.560	19.550	70	DCM	15.8	36.0	26.6				
MEDEA	21	8	39.900	-20.470	77	DCM	16.4	36.2	26.6	0.04	0.47	0.09	
MEDEA	22	9	37.660	-21.400	86	DCM	17.2	36.3	26.5	0.02	0.14	0.03	
MEDEA	23	10	35.900	-23.830	85	DCM	15.9	36.2	26.7	0.12	1.82	0.14	
MEDEA	24	11	33.930	-26.610	90	DCM	19.3	36.7	26.2	0.01	0.07	0.04	

Table S1. Continued.

Cruise	Experiment No.	Station	Latitude (°N)	Longitude (°E)	Depth (m)	Depth Layer	Temperature (°C)	Salinity	Sigma-t	PO_4^{3-} (µM)	NO_x (µM)	NO_2^- (µM)	NH_4^+ (µM)
MEDEA	25	13	30.460	-32.210	100	DCM	19.2	36.7	26.3	0.01	0.02	0.01	
MEDEA	26	15	26.060	-36.120	120	DCM	21.1	37.1	26.1	0.02	0.10	0.06	
MEDEA	27	16	24.670	-34.940	116	DCM	21.6	37.2	26.0	0.01	0.04	0.03	
MEDEA	28	17	25.580	-32.270	121	DCM	20.7	37.1	26.2				
MEDEA	29	18	27.100	-29.820	108	DCM	21.2	37.2	26.1	0.01	0.03	0.01	
MEDEA	30	19	28.540	-27.460	106	DCM	19.7	36.8	26.3	0.02	0.05	0.01	
MEDEA	31	20	30.460	-24.500	103	DCM	19.7	36.8	26.3	0.01	0.03	0.02	
MEDEA	32	21	32.090	-22.420	100	DCM	18.7	36.6	26.3	0.01	0.06	0.01	
MEDEA	33	22	31.030	-20.090	93	DCM	18.5	36.6	26.4	0.02	0.08	0.02	
MEDEA	34	24	32.250	-13.580	84	DCM	19.3	36.5	26.1	0.01	0.03	0.01	

Table S2. Abundance (P0; 103 cells mL-1) and the rates (d-1) of gross growth (μgross), total mortality (TM), grazing (G) and viral lysis (V) of different phytoplankton groups sampled in the North Atlantic modified dilution experiments conducted during the STRATIPHYT and MEDEA cruises.

Experiment No.	*Synechococcus*					*Prochlorococcus* LL					Pico I					Pico II				
	P_0	μ_{gross}	T_M	G	V	P_0	μ_{gross}	T_M	G	V	P_0	μ_{gross}	T_M	G	V	P_0	μ_{gross}	T_M	G	V
1	17.0	0.43*	0.04	0.00	0.04											2.4	0.36*	0.35*	0.03	0.31
2	64.5	0.20*	0.28*	0.17*	0.11	136	0.18*	0.31*	0.14	0.17	30.0	0.12*	0.39*	0.25*	0.14	5.8	0.41*	0.40*	0.18	0.21
3																0.8	0.92*	0.75*	0.60*	0.15
4	1.7	0.62*	0.71*	0.22	0.49*	65	0.60*	0.74*	0.17	0.57*	1.3	0.56*	0.72*	0.21	0.52*	0.8	1.15*	1.01*	0.24	0.77*
5	5.3	0.23*	0.29*	0.23*	0.06	113	0.26*	0.43*	0.25*	0.18	2.2	0.37*	0.42*	0.18	0.25	3.4	0.42*	0.43*	0.23*	0.19
6						112	0.08*	0.13*	0.09*	0.03	5.1	0.07*	0.13*	0.01	0.12*					
7																2.8	0.07*	0.41*	0.37*	0.04
8	5.9	0.35*	0.29*	0.22*	0.07	21	0.33*	0.38*	0.27*	0.11	4.7	0.42*	0.27*	0.05	0.22	4.0	0.43*	0.46	0.21*	0.25
9	10.3	0.32*	0.44*	0.00	0.44*	44	0.34*	0.50*	0.09	0.41*	4.8	0.60*	0.49*	0.10	0.40*	4.7	-0.13	0.41*	0.14	0.26
10											1.9	0.17	0.17	0.11	0.06	7.9	0.20*	0.08	0.00	0.08
11	3.3	0.41*	0.52*	0.30*	0.22*						2.0	0.44*	0.85*	0.60	0.25	16.1	0.26*	0.47*	0.24*	0.23
12																11.5	0.26*	0.16	0.16*	0.00
13	43.9	0.34*	0.43*	0.35*	0.08						6.0	0.33*	0.56*	0.56*	0.01	6.4	0.38*	0.39*	0.38*	0.01
14	72.3	0.41*	0.33*	0.23*	0.10						6.6	0.59*	0.36*	0.35	0.02	4.3	0.65*	0.53*	0.45	0.07
15											7.1	0.11	0.14	0.12	0.02	6.4	0.24*	0.06	0.03	0.02
16	9.4	0.18*	0.27*	0.12*	0.15*	75	0.12*	0.20*	0.13	0.07						2.5	0.00	0.32*	0.10*	0.21*
17	25.2	0.15*	0.22*	0.17*	0.05											3.9	-0.02	0.14*	0.12	0.02
18	25.2	0.10*	0.08	0.07*	0.01	47	0.19*	0.12*	0.08	0.04	2.2	0.14*	0.11	0.09	0.02	4.6	0.13	0.10	0.00	0.10
19	3.8	0.04*	0.19*	0.05	0.14	122	-0.04*	0.19*	0.15	0.04										
20	3.9	0.08*	0.17*	0.04	0.13															
21	0.3	0.26*	0.10	0.07	0.03											1.1	0.09*	0.14*	0.07	0.07
22	0.6	0.12*	0.14	0.01	0.13						0.9	0.02	0.23*	0.20	0.03	1.8	0.16*	0.31*	0.00	0.31*
23																0.9	0.18*	0.11	0.00	0.11
24						91	-0.01	0.14*	0.08*	0.07	0.1	0.26	0.63	0.26	0.37	0.8	0.19	0.30	0.12	0.18

25
Table S2. Continued.

Experiment No.	*Synechococcus*					*Prochlorococcus* LL					Pico I					Pico II				
	P_0	μ_{gross}	T_M	G	V	P_0	μ_{gross}	T_M	G	V	P_0	μ_{gross}	T_M	G	V	P_0	μ_{gross}	T_M	G	V
26											0.2	0.16	0.38	0.24	0.13					
27											0.1	0.97*	0.68	0.56	0.12					
28											0.3	-0.23	1.07*	0.02	1.05*					
29	0.3	0.26*	0.31	0.07	0.25											0.5	0.22*	0.41*	0.10	0.31*
30																0.5	0.16*	0.20*	0.06	0.15
31																0.8	0.09	0.00	0.00	0.00
32						48	0.10*	0.08	0.05	0.02	0.1	0.55*	1.06*	0.39	0.67					
33	0.5	0.41*	0.34*	0.20	0.14	80	0.27*	0.23*	0.21*	0.02						0.6	0.29*	0.30*	0.25	0.05
34	3.7	0.54*	0.13	0.03	0.10	99	0.38*	0.05	0.00	0.05										

Footnotes: *Significant results $\alpha<0.10$; viral lysis rates are only signified as significant when the interaction term between grazing and grazing + viral lysis regressions was significant.

Table S2. Continued.

Experiment No.	Nano I					Nano II					Nano III				
	P_0	μ_{gross}	T_M	G	V	P_0	μ_{gross}	T_M	G	V	P_0	μ_{gross}	T_M	G	V
1	0.2	0.37	0.95*	0.77	0.18										
2															
3	0.1	0.88*	0.84*	0.67*	0.17										
4	0.2	0.79*	1.20*	0.31	0.89*										
5	1.0	0.44*	0.53*	0.26	0.27										
6	0.7	0.57*	0.33*	0.19	0.14	0.3	0.50*	0.31	0.19	0.13					
7															
8	0.5	1.08*	0.94*	0.22	0.71										
9	0.8	0.31*	0.55*	0.16	0.39										
10															
11	2.2	-0.06	0.28*	0.00	0.28	0.2	0.01	0.16	0.04	0.13	0.1	1.01*	0.54	0.38	0.17
12	1.8	1.03*	0.52*	0.12	0.41						0.4	0.68*	0.50	0.08	0.42
13	2.4	0.89*	0.66*	0.51*	0.15	0.1	1.36*	0.94*	0.36	0.59	0.5	0.68*	0.54*	0.50	0.03
14	1.2	0.86*	0.75*	0.75*	0.00						0.1	0.48	0.26	0.11	0.15
15	1.5	0.46*	0.05	0.05	0.00						0.3	0.61*	0.41	0.35	0.06
16	0.5	-0.41	0.16	0.00	0.16										
17	1.1	-0.21*	0.19*	0.00	0.19										
18															
19	1.1	0.00	0.32*	0.02	0.29										
20															
21															
22															
23	0.1	-0.04	0.05	0.00	0.05										
24															
25	0.3	-0.42*	0.26	0.07	0.19										

Table S2. Continued.

Experiment No.	Nano I					Nano II					Nano III				
	P_0	μ_{gross}	T_M	G	V	P_0	μ_{gross}	T_M	G	V	P_0	μ_{gross}	T_M	G	V
26															
27															
28															
29															
30															
31															
32															
33															
34	0.3	0.32*	0.40*	0.20	0.20										

Table S3. Spearman rank correlation coefficients (above the diagonal) and associated p-values (below the diagonal with significant values highlighted in bold) relating virus abundance data to the viral lysis rate obtained from modified dilution assays conducted during the STRATIPHYT cruise (N = 64). Abbreviations represent viral lysis rate (VL), abundances of individual virus populations (V1 - V5), total virus abundance (Total V) and the ratio of viral lysis to grazing rate (V:G).

	Latitude	VL	V1	V2	V3	V4	V5	Total V	V:G
Latitude		-0.60	0.70	0.72	-0.72	n.s.	n.s.	0.75	-0.54
VL	**0.00**		-0.63	-0.44	0.42	n.s.	n.s.	-0.66	0.81
V1	**0.00**	**0.00**		0.80	-0.51	n.s.	0.68	0.99	-0.61
V2	**0.00**	**0.03**	**0.00**		n.s.	n.s.	0.75	0.85	n.s.
V3	**0.00**	**0.05**	**0.00**	0.07		n.s.	n.s.	-0.53	0.43
V4	1.00	1.00	1.00	1.00	1.00		0.47	n.s.	n.s.
V5	0.19	0.11	**0.00**	**0.00**	0.23	**0.01**		0.69	n.s.
Total V	**0.00**	**0.00**	**0.00**	**0.00**	**0.00**	1.00	**0.00**		-0.61
V:G	**0.00**	**0.00**	**0.00**	0.75	**0.05**	1.00	1.00	**0.00**	

n.s. indicates non-significance at $\alpha = 0.05$

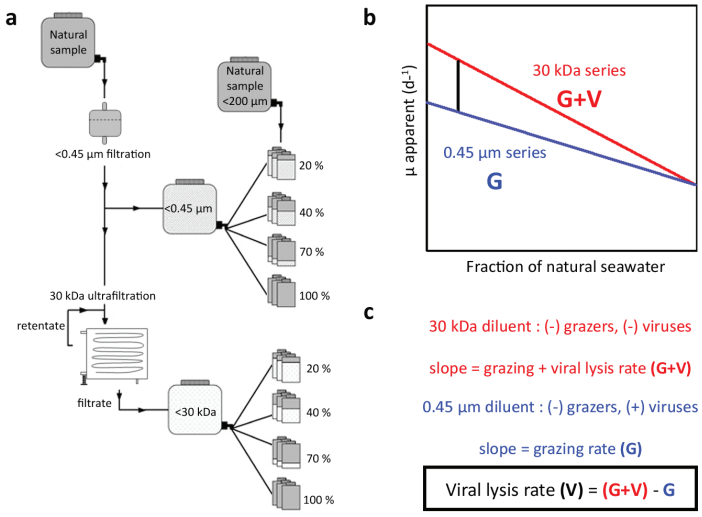

Figure S1. (**a**) Experimental set-up of the modified dilution method for estimating loss rates of natural phytoplankton populations. Filtered samples are mixed with unfiltered samples ("natural water") at different proportions. Filtration < 0.45 µm removes microzooplankton but not viruses; filtration < 30 kDa removes both microzooplankton and viruses. (**b**) Illustration of the typical regression lines which result from plotting phytoplankton growth after 24 hour incubation under in situ light and temperature (µ apparent) versus the fraction of natural water. (**c**) Explanation for the determination of viral lysis rates (V) and microzooplankton grazing rates (G) using regression analysis. Figure adapted from Baudoux et al. (2006).

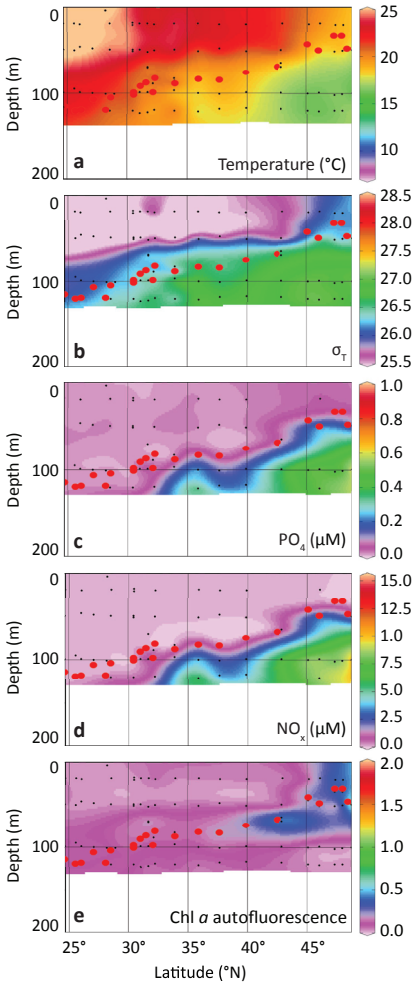

Figure S2. Latitudinal and depth distribution of (**a**) temperature, (**b**) sigma-t (σ_T), (**c**) inorganic phosphorus, (**d**) NO_x (nitrate + nitrite) and (**e**) Chl *a* autofluorescence measured during MEDEA. Black dots indicate sampling points and red dots the sampling depths for modified dilution assays. Figure panels were prepared using Ocean Data View (ODV version 4.6.5, Schlitzer, 2002).

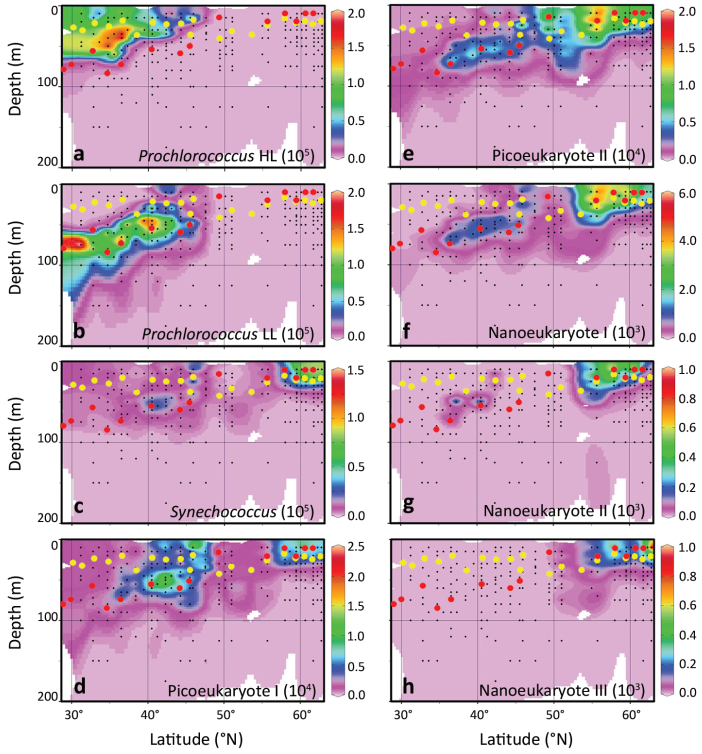

Figure S3. Biogeographical distributions of main phytoplankton groups across the Northeast Atlantic Ocean. (**a**) Prochlorococcus, high-light adapted phenotypes (0.4-0.8 µm Ø) (cells ml^{-1}). (**b**) Prochlorococcus, low-light adapted phenotypes (0.4-1.0 µm Ø) (cells ml^{-1}). (**c**) Synechococcus spp. (0.8-1.5 µm Ø) (cells ml^{-1}). (**d-e**) photosynthetic picoeukaryotes, group I (0.8-2.0 µm Ø) and group II (1-2 µm Ø) (cells ml^{-1}). (**f-h**) photosynthetic nanoeukaryotes, group I (2-5 µm Ø), group II (3-8 µm Ø), group III (5-10 µm Ø) (cells ml^{-1}). Data were obtained by flow cytometry during the STRATIPHYT cruise. Black dots indicate sampling points, yellow dots indicate mixed layer depth (Z_m), and red dots the sampling depths for modified dilution assays. Graphs were prepared with Ocean Data View (ODV version 4.6.5, Schlitzer, 2002).

Chapter 5

Flow cytometric enumeration of marine viral populations at low abundances

Kristina D. A. Mojica[1], Claire Evans[1, 2], and Corina P. D. Brussaard[1,3]

[1]Department of Biological Oceanography, NIOZ - Royal Netherlands Institute for Sea Research, NL 1790 Den Burg, Texel, The Netherlands
[2] Present address: [2]National Oceanography Centre, European Way, Southampton, SO14 3ZH, UK
[3]Aquatic Microbiology, Institute for Biodiversity and Ecosystem Dynamics, University of Amsterdam, P.O. Box 94248, 1090 GE Amsterdam, The Netherlands

Aquatic Microbial Ecology (2014) 71: 203-209

Abstract

Flow cytometric enumeration has advanced our ability to analyze aquatic virus samples and thereby our understanding of the ecological role viruses play in the oceans. However, low virus abundances are underestimated using the current flow cytometry (FCM) protocol. Our results revealed that low dilutions (<30-fold) not only decreased the total virus count but also limited the ability to differentiate between virus clusters. Here we report a simple and efficient method optimization for improving virus counts and optical resolution at low abundances. Raising the pH of the Tris-EDTA (TE) buffer to 8.2 successfully countered the effect of insufficient buffering capacity at low dilutions, which is caused by the higher proportion of acidic glutaraldehyde fixative in the final sample. The higher buffer pH did not interfere with virus enumeration at higher dilutions. We therefore recommend amendment of the standard FCM aquatic virus enumeration protocol using a TE buffer with pH 8.2 as a simple and efficient improvement.

Introduction

Viruses are abundant, ubiquitous and essential components of aquatic systems playing key roles in the mortality of microbes, biogeochemical cycling, structuring host community composition and genetic exchange between microbes (Sullivan et al. 2006; Suttle 2007; Brussaard et al. 2008b). Natural virus populations have been found to be highly dynamic, changing rapidly in abundance and diversity over a broad range of environments (Suttle and Chan 1994; Brussaard et al. 2008a; Winget and Wommack 2009). Therefore, aquatic viral ecology necessitates rapid and reliable methods for enumerating viruses.

The advent of flow cytometry (FCM) has vastly advanced our understanding of aquatic viral ecology (Brussaard 2004). Traditionally, viruses have been counted using culture-based methods (Cottrell and Suttle 1995; Suttle and Chan 1995), transmission electron microscopy (Bergh et al. 1989; Wommack et al. 1992; Bratbak et al. 1993), and epifluorescence microscopy (Hara et al. 1991; Hennes and Suttle 1995; Noble and Fuhrman 1998) in combination with nucleic-acid-specific staining. However, these methods are limited either by the availability of a host system, cost or time (Marie et al. 1999; Brussaard 2004; Duhamel and Jacquet 2006). FCM brought about immense improvements in the speed and accuracy of both the detection and enumeration of viruses in natural systems (Brussaard et al. 2000; Brussaard 2004). Rapid counting not only allows the analysis of more samples per time unit, but also improves detection of stained viruses with low fluorescence compared to epifluorescence microscopy by reducing the potential time for fading (Brussaard 2000). These improvements to the speed and accuracy of counting viruses using FCM, combined with the ability to discriminate different virus clusters (Brussaard et al. 2010) has increased the popularity of this method.

Low virus abundances (i.e., $\leq 10^6$ ml^{-1}) which can be found in the deep ocean, extreme oligotrophic waters, or resulting from experimental design such as the viral production assay (Weinbauer et al. 2010), which reduces virus concentrations in order to permit the detection of the newly produced phage from infected bacteria, demand low dilutions in a buffer solution to obtain an optimal event rate (i.e., 200 - 800 events/second) (Brussaard et al. 2010). However, studies have shown that low dilution factors for virus samples can substantially underestimate the total virus concentration (Brussaard 2004). In order to overcome this limitation, the current study set out to (1) identify the factor responsible for the decline in viral abundance and the nucleic acid-specific staining signal at low dilution factors, and (2) improve

the existing flow cytometric analysis method for the accurate enumeration of viruses present in natural samples at low abundances.

Material and Methods

Samples and FCM

FCM was used to measure the viral abundance in natural samples. Two geographical locations, i.e., the North Atlantic Ocean (STRATIPHYT summer 2009 cruise, samples obtained from 125-175 m, Stns 13 - 15, in the waters located between 42.3 - 44.3°N and 12.7°W) and the Southern Ocean (GEOTRACES austral spring 2008 cruise, samples obtained from 50 m in the central Weddell Sea at 66.2°S and 30.9°W) were used as model systems. These locations were chosen based on the abundance of viruses at these sites; being around 10^6 ml^{-1} but sufficient to remain within the limits of measurement (i.e., 100 - 1100 events per second) at a 50-fold dilution (Marie et al. 1999; Brussaard 2004). As the viral abundance of these samples were not sufficient to test the influence of TE buffer pH on viral abundance at high dilution factors (i.e., 200 and 1000-fold), natural virus communities from the Southern North Sea were used. Additionally, the effect of TE buffer pH 8.2 versus 8.0 was tested on natural virus communities originating from less saline locations, i.e., two estuaries, Wadden Sea and Baltic Sea, and two local freshwater ponds with very different pH values. In order to test these latter communities at a 10-fold dilution, natural samples were diluted (x100) using virus-free ultrafiltrate water from the same location prior to fixation (attained from tangential flow diafiltration using 30 kDa VivaFlow 200 cartridge, Sartorius Stedim Biotech, Germany).

The method presented by Brussaard (2004) for counting viruses using flow cytometry was used as a standard. Briefly, samples were fixed with 25% glutaraldehyde (EM-grade, Sigma-Aldrich, Netherlands) at a final concentration of 0.5% for 15-30 min at 4°C and subsequently flash frozen and stored at -80°C until analysis. In addition, formaldehyde (1% and 2% final concentration) fixation was also tested for a loss of virus counts at low dilution factors. Formaldehyde has been used for flow cytometric analysis and epifluorescence microscopy of natural virus samples and reported to show comparable counts to glutaraldehyde (Robinson et al. 1999; Patel et al. 2007).

In addition to diluting thawed samples in the standard TE buffer (pH 8.0, 10 mM Tris-HCL, 1 mM EDTA; Roche, Germany), TBE (x1, 89 mM Tris, 89 mM Boric

Acid, 2 mM EDTA) and TAE (x1, 40 mM Tris, 20 mM Acetic Acid, 1 mM EDTA) buffers were also tested. These buffers are recommended alongside TE buffer by the manufacturer of SYBR Green I (Life Technologies, Netherlands) and have not been tested previously. Other dilution solutions which have been tested (i.e., Tris, PBS, dH_20, and seawater) have shown that TE buffer provided the highest virus counts and green fluorescence signal (Brussaard 2004). After dilution in buffer solution, samples were stained with the nucleic acid-specific green fluorescence dye SYBR Green I at a final concentration of 5 x 10^{-5} the commercial stock concentration (Life Technologies, Netherlands) and heated at 80°C for 10 min in the dark. Cooled samples (5 min., room temperature) were analyzed using a 15 mW bench-top Becton-Dickinson FACSCalibur flow cytometer equipped with an air-cooled 488 nm Argon laser and MilliQ-water (18 MΩ) as sheath fluid. The discriminator was set on green fluorescence, with the threshold at the lowest company-set level. The maximum voltage, at which no electronic or laser noise was detected, was used for the green fluorescence channel photo-mulitplier according to the recommendations of Brussaard et al. (2010). Samples were analyzed for 1 minute at a medium flow rate (~40 μL min^{-1}), after which the listmode files were analyzed using CYTOWIN (Vaulot 1989); http://www.sb-roscoff.fr/Phyto/index.php?option=com_content&task=view&id=72&Itemid=123). Virus counts were corrected for blanks consisting of TE buffer and SYBR Green I prepared and analyzed in an identical manner to the samples. TE blanks were not found to be significantly different from blanks consisting of virus-free seawater samples generated by 30 kDa ultrafiltrate (2 sample t-test; d.f. = 6; n.s.).

Treatments

Natural virus samples were subjected to different levels of sample dilution, salinity, pH of TE buffer (Table 1), as well as type of fixative and type of buffer solution. The influence of salinity, which will vary according to the proportion of seawater present in the final sample as a consequence of the level of dilution with buffer, was tested. North Atlantic seawater ultrafiltrate (salinity 36.0) attained from tangential flow diafiltration (30 kDa VivaFlow 200, Sartorius Stedim Biotech, Germany) was subjected to slow evaporation using moderate heat until a maximum salinity of 41 was obtained. A range of salinities (Table 1) was then achieved by subsequent addition of increasing amounts of sterile ultrapure MilliQ-water (18 MΩ), while maintaining the ratios for constituent ions. Salinity was monitored using a digital conductivity meter (GMH 3430, Greisinger, Germany). The ultrafiltrate saline

solutions were then used to dilute North Atlantic virus samples 5-fold, after which the samples were 10-fold diluted in TE buffer at 3 different pH levels (7.8, 7.9, and 8.1). The result was a final dilution factor of 50, with the salinity impact of a factor 10 dilution.

Table 1. Treatments investigated for effect on virus enumeration by flow cytometry.

Treatment	Levels
Dilution	10x, 15x, 20x, 30x, 50x
Salinity	26, 28, 30, 32, 34, 36, 38, 40
pH of TE buffer	7.8, 7.9, 8.0, 8.1, 8.2, 8.3, 8.4, 8.5

The staining efficiency of SYBR Green I has been shown to be affected by pH, with significant drops in sensitivity occurring when pH is greater than 8.3 or less than 7.5 (Life Technologies, technical specifications). In order to test the effect of buffer pH on viral abundances measured at low dilutions, a range of pH was created by the addition of either 0.1 M NaOH (J.T. Baker, Sweden) or 0.1 M HCl (J.T. Baker, Sweden) to a working stock buffer solution. In addition, stepwise additions of 0.1 M HCl to glutaraldehyde-fixed North Atlantic samples at higher dilution (x50 dilution in TE buffer at pH 8.0) were performed to verify the direct effect of pH, independent of the increase in glutaraldehyde. A laboratory pH meter (827 pH lab with pH probe (6.0258.010); Metrohm Applikon, Netherlands) was used to monitor pH. Total alkalinity was determined on a fixed volume sample of unfiltered seawater poisoned with mercury chloride (Sigma-Aldrich, Netherlands) (0.05% final concentration of saturated mercury chloride). Potentiometric titration of seawater was performed employing an open cell and computer controlled titration instrument (Titrino DMP 785, Metrohm Applikon, Netherlands) and 0.1 M HCL + 0.6 M NaCl (Vstep of 0.05 ml). Total alkalinity was then calculated using the simple Gran and non-linear least-squares method (Dickson et al. 2003).

Statistical Analysis

Statistical analyses of different treatments were performed using R Statistical Software (R Development Core Team 2012). Assumptions for ANOVA were verified by the Shapiro-Wilk test for normality and the Barlett's test for constancy of variance. If significant ($P < 0.01$) deviations were found, the Box-Cox transformation coefficient was utilized to find the optimal transformation.

In the cases where lambda equaled 1, indicating that no transformations would improve data, non-parametric Kruskal-Wallis analysis was employed. During ANOVA, all variables were initially included in the model with their interaction terms and when necessary the model was trimmed to remove any non-significant terms and interactions. When applicable, post-hoc analysis using Tukey's pairwise comparisons was performed. A probability of $\alpha < 0.01$ was used to conclude that the treatment levels differed significantly in the effect on the measured value. In the case where the effect of salinity (8 levels) and TE buffer pH (3 levels) were considered together, a factorial ANOVA model was fitted to data. Assumptions of equal variance for 2-sample Student's t-tests were verified by Fisher's F test. When significant ($P < 0.01$) deviations were found, nonparametric Wilcoxon rank-sum test was utilized.

Results and Discussion

In order to optimize the staining of the viruses and avoid coincidence of particles during flow cytometric analysis, samples are diluted using TE buffer (Brussaard 2004). However, the enumeration of marine viruses in aquatic systems by FCM has been reported to be limited by a reduced efficiency in counts when the dilution in TE buffer is below 20-fold (Brussaard 2004).

Three virus groups (V1-V3, Fig. 1) were differentiated based on green fluorescent and side scatter properties using bivariate scatter plots (Brussaard et al. 2010). We found that the dilution factor (i.e., 10-50x) of natural virus samples from the North Atlantic in TE buffer at the standard pH 8.0 had a significant effect on the measured abundance of total viruses (one-way ANOVA; $P < 0.0001$; Fig 2A) and V1 group viruses (one-way ANOVA; $P < 0.0001$; Fig 2B). Viral abundances dropped by 23, 13 and 5% for total virus counts and 66, 49, and 19% for the V1 cluster when diluted 10, 15 and 20-fold, respectively.

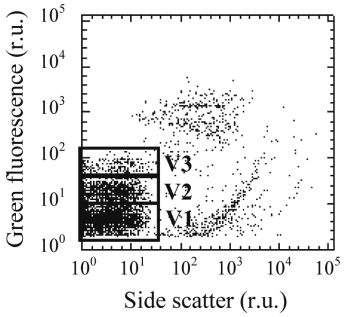

Figure 1. Bivariate scatter plot of green fluorescent verses side scatter illustrating the V1, V2, and V3 virus groups, which together make up total viruses. Virus sample was obtained from the North Atlantic 2009 summer STRATIPHYT cruise (Station 6, 60 m) and diluted x100 in TE buffer of pH 8.0).

Two constituents of a sample which could potentially account for the reduction in viral abundance at lower dilution are the increased proportion of the seawater and the fixative. Salinity, simulating the increasing proportion of seawater sample, did not significantly (factorial ANOVA) impact total virus or V1 counts. However, the pH of the TE buffer used for diluting samples was found to have a significant effect on the V1 group and total virus counts (both $P < 0.0001$). Addition of glutaraldehyde (0.5% final concentration) to a 30 kDa ultrafiltrate seawater sample and diluting 10-fold in TE buffer at pH 8.0 demonstrated that the reduction in virus counts at low dilution was due to the increased proportion of glutaraldehyde in the sample leading to a reduction in the pH, which was not sufficiently buffered against when using TE buffer at pH 8.0. The final sample pH was found to be 6.85, which fell out of the optimal range of 7.5-8.0 reported by Brussaard (2004) and the optimum pH of 8.0 recommended by manufacturer of SYBR Green I (Life Technologies, technical specifications). Stepwise additions of HCl to glutaraldehyde-fixed North Atlantic samples at a higher dilution (x50 dilution in TE buffer at pH 8.0) showed that the general patterns for the decline of total and V1 virus abundance could be reproduced without increasing the proportion of glutaraldehyde; supporting the assumption that pH was the main cause for the underestimation of counts at low dilutions.

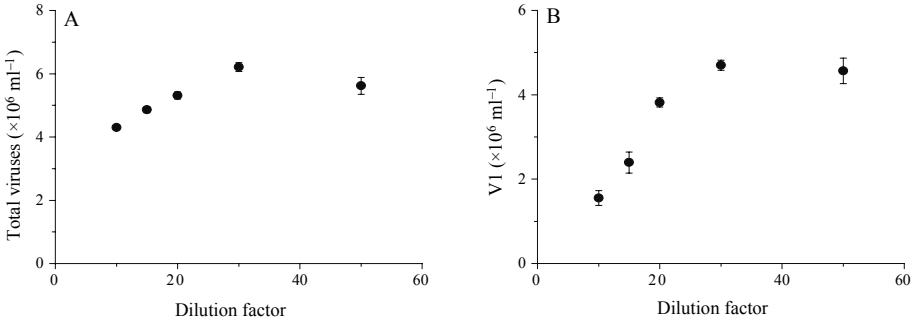

Figure 2. Total virus (A) and V1 (B) abundance enumerated over a dilution range of 10 - 50x using TE buffer pH of 8.0. Error bars represent standard deviations (N = 3).

Adjusting the pH of TE buffer used for dilution lead to improved total virus enumeration and differentiation between the different virus clusters for the North Atlantic Ocean and Southern Ocean virus communities (Fig. 3). At 10-fold dilutions, a pH of 8.2 showed the optimal balance between counts and staining signature. Raising the TE buffer pH from 8.0 to 8.2 at low dilutions resulted in an increase in the green fluorescence intensity of virus particles and subsequently increased the proportion of viruses that could be detected. The degree to which pH affected viral abundance, however, varied across the different sample locations, i.e., the 10-fold diluted North Atlantic virus samples had a proportionality higher reduction of total virus and V1 abundance at lower pH values compared to the Southern Ocean samples (Fig. 3A and 3B). Increasing the TE buffer pH to 8.2 when diluting 10-fold improved V1 and total virus counts by 28% and 31% in Southern Ocean samples and 78% and 69% in North Atlantic Ocean samples, respectively, when compared to TE pH 8.0. The abundance of V2 and V3 groups of the North Atlantic samples remained relatively stable, with a small increase occurring in TE buffer pH 8.2 (Fig. 3C and 3D). However, the relative importance of V1 - V3 in Southern Ocean and North Atlantic samples remained comparable between TE pH 8.2 and 8.0, and as a consequence, there was little effect on the average green fluorescence. These results were not affected by the use of a different FACSCalibur flow cytometers, as measurements for this experiment were performed simultaneously on two separate FACSCaliburs and gave good correlations between counts (0.96 for the Southern Ocean and 0.93 for the North Atlantic samples).

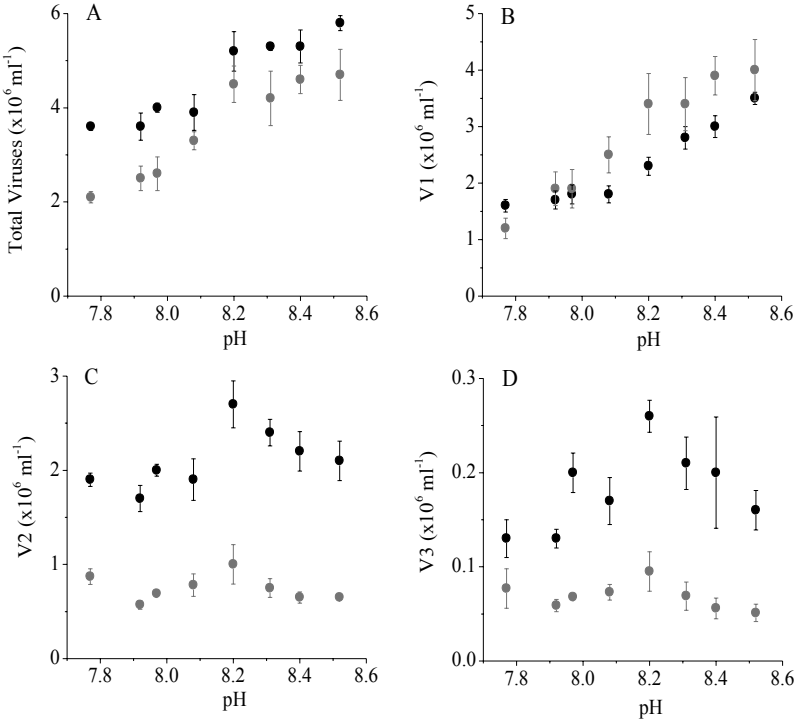

Figure 3. Virus abundance enumerated at a 10-fold dilution using TE buffer at different pH levels. (A) Total virus abundance, (B) V1 virus abundance, (C) V2 virus abundance, and (D) V3 virus abundance in Southern Ocean (black circles) and North Atlantic (grey circles) seawater. Error bars represent standard deviations (N = 4).

When using TE buffer at pH 8.2, the dilution factor (i.e., 10 - 50x) no longer had a significant effect on the viral abundance (Kruskal-Wallis; d.f. = 8; n.s.), demonstrating the effectiveness of pH 8.2 to alleviate the underestimation of virus counts at low dilutions. In order to verify that increased buffer pH did not affect viral counts at higher dilutions, and would therefore be applicable as a general method improvement, natural virus samples were diluted in TE buffer pH 8.0 and 8.2 at a 50-fold dilution for North Atlantic samples and both 200- and 1000-fold for North Sea samples. At these high dilution factors, no significant differences (2 sample t-test; d.f. = 8) were found in V1 or total viral abundance measured between samples diluted in TE buffer pH 8.0 and 8.2 for either location.

The effect of TE buffer pH 8.2 versus 8.0 was further tested on natural virus communities from different low salinity environments, i.e., two estuaries (Wadden Sea and Baltic Sea) and two freshwater ponds (Table 2). Increasing the pH of TE buffer to 8.2 had a relatively low (8%) but significant (2-sample t-test; $\alpha = 0.01$; N

= 4) positive effect on the viral abundance measured in a 10-fold diluted sample from the Baltic Sea. However, no significant effect of TE buffer pH was found for the other locations tested (2-sample t-test; α = 0.01; N = 4). The lack of effect for the Wadden Sea estuary was surprising considering that the alkalinity and pH of this water nearly matched that of the North Atlantic sample. The differences in the effect of pH 8.2 on viral abundance between samples are most likely dependent on variation in the staining sensitivity of the viral communities at these different locations.

Table 2. The effect of TE buffer pH 8.2 (compared to 8.0) on total virus abundance (107 ml-1) in samples from various environments measured at a 10-fold dilution. Talk: total alkalinity (Meq l-1). Significant values in bold. Pond samples originate from Texel, Netherlands

Sample	Salinity	pH	TAlk	%Change
North Atlantic	35.7	7.87	2.37	**69**
Southern Ocean	34.3	8.09	2.41	**31**
Wadden Sea[a]	25.3	7.87	2.36	0
Baltic Sea[b]	5.7	8.15	1.59	**8**
NIOZ pond[a]	0.3	9.59	1.34	1
Den Hoorn pond[a]	0.4	7.94	2.17	0

[a] Samples were pre-diluted using virus-free sample to allow for 10-fold dilution. Salinity, pH and alkalinity are reported for undiluted sample.
[b] Viral production sample (Weinbauer et al. 2010) originating from a Baltic Sea mesocosm experiment.
* indicates significance

The use of formaldehyde (i.e., 1 and 2% final concentration) as a fixative was tested as an alternative to glutaraldehyde for both North Atlantic and Wadden Sea samples, however no significant improvements were found (2-sample t-test; α = 0.01; N = 3). Considering that commercially available formaldehyde (37%) has a pH range of 2.8 - 4.0, it presented the same methodological issues as glutaraldehyde (25%; pH range 3.0 - 4.0) when measuring at low dilutions in TE buffer pH 8.0. Moreover, the use of alternative buffer solutions (TAE and TBE, recommended in addition to TE by the manufacturer of SYBR Green I) did not lead to significant improvements in counts at low dilutions compared to dilution using TE buffer.

In summary, increasing the pH of TE buffer has the potential to significantly improve the efficiency of virus counts in aquatic systems when diluted down to 10-fold. TE buffer with a pH of 8.2 was found to be optimal, as it leads to significantly higher viral abundance (total and V1) as compared to lower pH values, while providing the highest V2 and V3 counts. The beneficial effect of increased pH is not ubiquitous or consistent across all aquatic systems and does not appear to be

dependent on sample pH or alkalinity, indicating that the magnitude of effect is dependent on the viral communities present in the sample. TE buffer at pH 8.2 did not have a significant negative effect on viral abundance in unaffected samples and was not found to affect the virus abundances at higher dilutions and thus can be adopted for general use. While maintaining the best and most commonly used method for fixation and analysis, the modification in the pH of TE buffer is a simple and effective method to achieve vital improvement on viral enumeration at low dilutions. Increasing the accuracy and precision of virus counts in systems with low abundances has the potential to expand (or even open) the field of marine viral ecology which is currently limited by the inability to measure viruses at low numerical abundances.

Acknowledgments

We thank Katharine J. Crawfurd for providing us with the viral production sample from the Baltic Sea mesocosm. This research was supported by the Earth and Life Sciences Foundation (ALW), which is subsided by the Netherlands Organization for Sea Research (NWO).

References

Bergh O, Borsheim KY, Bratbak G, Heldal M (1989) High abundance of viruses found in aquatic environments. Nature 340:467-468

Bratbak G, Egge JK, Heldal M (1993) Viral Mortality of the Marine Alga Emiliania-Huxleyi (Haptophyceae) and Termination of Algal Blooms. Mar Ecol-Prog Ser 93:39-48

Brussaard CPD (2004) Optimization of procedures for counting viruses by flow cytometry. Applied and Environmental Microbiology 70:1506-1513

Brussaard CPD, Payet JP, Winter C, Weinbauer M (2010) Quantification of aquatic viruses by flow cytometry. In: Wilhelm SW, Weinbauer MG, Suttle CA (eds) Manual of Aquatic Viral Ecology. ASLO

Brussaard CPD, Timmermans KR, Uitz J, Veldhuis MJW (2008a) Virioplankton dynamics and virally induced phytoplankton lysis versus microzooplankton grazing southeast of the Kerguelen (Southern Ocean). Deep-Sea Res Pt Ii 55:752-765

Brussaard CPD, Wilhelm SW, Thingstad TF, Weinbauer MG, Bratbak G, Heldal M, Kimmance SA, Middelboe M, Nagasaki K, Paul JH, Schroeder DC, Suttle CA, Vaque D, Wommack KE (2008b) Global-scale processes with a nanoscale drive: the role of marine viruses. The ISME Journal 2:575-578

Cottrell MT, Suttle CA (1995) Dynamics of a lytic virus infecting the photosynthetic marine picoflagellate *Micromonas pusilla*. Limnology and Oceanography 40:730-739

Dickson AG, Afghan JD, Anderson GC (2003) Reference materials for oceanic CO2 analysis: a method for the certification of total alkalinity. Mar Chem 80:185-197

Duhamel S, Jacquet S (2006) Flow cytometric analysis of bacteria- and virus-like particles in lake sediments. Journal of Microbiological Methods 64:316-332

Hara S, Terauchi K, Koike I (1991) Abundance of Viruses in Marine Waters - Assessment by Epifluorescence and Transmission Electron-Microscopy. Applied and Environmental Microbiology 57:2731-2734

Hennes KP, Suttle CA (1995) Direct Counts of Viruses in Natural-Waters and Laboratory Cultures by Epifluorescence Microscopy. Limnology and Oceanography 40:1050-1055

Marie D, Brussaard CPD, Thyrhaug R, Bratbak G, Vaulot D (1999) Enumeration of marine viruses in culture and natural samples by flow cytometry. Applied and Environmental Microbiology 65:45-52

Noble RT, Fuhrman JA (1998) Use of SYBR Green I for rapid epifluorescence counts of marine viruses and bacteria. Aquatic Microbial Ecology 14:113-118

Patel A, Noble RT, Steele JA, Schwalbach MS, Hewson I, Fuhrman JA (2007) Virus and prokaryote enumeration from planktonic aquatic environments by epifluorescence microscopy with SYBR Green I. Nature Protocols 2:269-277

R Development Core Team (2012) R: A language and environment for statistical computing. R Foundation for Statistical Computing, Vienna, Austria

Robinson JP, Darzynkiewicz Z, Dean PN, Orfao A, Rabinovitch P, Stewart CC, Tanke HJ, Wheeless LL (eds) (1999) Current Protocols in Cytometry. John Wiley & Sons, Inc., New York

Sullivan MB, Lindell D, Lee JA, Thompson LR, Bielawski JP, Chisholm SW (2006) Prevalence and evolution of core photosystem II genes in marine cyanobacterial viruses and their hosts. Plos Biology 4:1344-1357

Suttle CA (2007) Marine viruses - major players in the global ecosystem. Nat Rev 5:801-812

Suttle CA, Chan AM (1994) Dynamics and distribution of cyanophages and their effect on marine *Synechococcus* Spp. Applied and Environmental Microbiology 60:3167-3174

Suttle CA, Chan AM (1995) Viruses infecting the marine Prymnesiophyte *Chrysochromulina* spp.: isolation, preliminary characterization and natural abundance. Mar Ecol-Prog Ser 118:275-282

Vaulot D (1989) CYTOPC: Processing software for flow cytometric data. Signal and Noise 2:8

Weinbauer MG, Rowe JM, Wilhelm SW (2010) Determining rates of virus production in aquatic systems by the virus reduction approach. Manual of Aquatic Viral Ecology

Winget DM, Wommack KE (2009) Diel and daily fluctuations in virioplankton production in coastal ecosystems. Environ Microbiol 11:2904-2914

Wommack KE, Hill RT, Kessel M, Russekcohen E, Colwell RR (1992) Distribution of Viruses in the Chesapeake Bay. Applied and Environmental Microbiology 58:2965-2970

Chapter 6

Heterotrophic prokaryotic growth and loss rates along a latitudinal gradient in the Northeast Atlantic Ocean

Kristina D. A. Mojica[1], and Corina P. D. Brussaard[1,2]

[1]Department of Biological Oceanography, Royal Netherlands Institute for Sea Research (NIOZ), P.O. Box 59, 1790 AB Den Burg, Texel, The Netherlands
[2]Department of Aquatic Microbiology, Institute for Biodiversity and Ecosystem Dynamics (IBED), University of Amsterdam, P.O. Box 94248, 1090 GE Amsterdam, The Netherlands

Abstract

The production and mortality of prokaryotes were assessed over a latitudinal gradient in the North Atlantic Ocean during summer stratification. Heterotrophic production was uncoupled from phytoplankton biomass and closely tied to nutrient availability suggesting nutrient limitation played an important role in regulating host production dynamics. Viruses were the dominate mortality factor regulating prokaryotic losses in the surface waters of the Northeast Atlantic Ocean. Wherein, lytic viral production was the favored life strategy for prokaryotic viruses in the mixed layer, independent of system trophic status, with rates ranging from 0.9 to 57.0 $x10^9$ viruses l^{-1} d^{-1}. Lytic VP in the surface waters was correlated to heterotrophic production and the nitrogen to phosphorus ratio. Lysogeny was important only within the deep chlorophyll maximum layer of oligotrophic stations wherein prophage induction decreased hyperbolically from 16.0 to 0.2 $x10^9$ viruses l^{-1} d^{-1} with latitude and Chl *a*. Our results suggest that inorganic nutrient limitation is an important factor regulating heterotrophic prokaryotic production, viral life strategy selection and lytic viral production in the North Atlantic Ocean. Moreover, the ratio of total mortality to heterotrophic production decreased over the latitudinal gradient signifying a gradual change from a system regulated by high turnover in regions of strong stratification to net heterotrophic production with reduced stratification.

Introduction

Prokaryotic viruses are abundant, diverse and pervasive components of marine systems (Suttle 2005; Angly et al. 2006). Viral lysis of microbes shunts matter and energy towards the particulate and dissolved organic matter pools and away from higher trophic levels and thus influences the structure of microbial food webs (Fuhrman 1999; Wilhelm and Suttle 1999). In addition, viral lysis releases cellular material rich in phosphorus and nitrogen compounds, providing substrate for heterotrophic prokaryotes, enhancing respiration and nutrient regeneration and stimulating primary production (Middelboe et al. 1996; Gobler et al. 1997; Middelboe and Jorgensen 2006; Sheik et al. 2014). The viral shunt thus plays an integral role in biogeochemical cycles of the ocean (Fuhrman 1999; Wilhelm and Suttle 1999; Brussaard et al. 2008).

Viral replication in prokaryotes largely occurs by either lytic or lysogenic infection, and the relative importance of these varies throughout the ocean (Payet and Suttle 2013). In the lytic cycle, viral replication proceeds immediately after infection and terminates with the lysis of the host, releasing viral progeny and host cell content into the surrounding water. Conversely, during lysogenic infection, the genetic material of temperate phages (prophage) is stably incorporated into the host genome, and the host continues to live and reproduce normally, transmitting the prophage vertically to daughter cells during each subsequent cell division. Hosts of temperate phages may benefit from association with lysogens, through protection against infection from homologous phages and through advantageous traits encoded in viral genomes (Chibani-Chennoufi et al. 2004; Weinbauer 2004; Gama et al. 2013). The few studies that have examined both viral life strategies, suggest that the relative importance of lysogenic and lytic infection is related to trophic status of the system, which has lead to the theory that lysogeny represents a survival strategy under conditions of low host productivity and abundance (Payet and Suttle 2013; Mojica and Brussaard 2014).

Bottom up resource availability of dissolved organic carbon (DOC) is thought to be the primary factor regulating the activity of heterotrophic prokaryotes in much of the world's oceans (Kirchman 1990; Carlson and Ducklow 1996; Church et al. 2000). Although DOC regulates heterotrophic prokaryotic activity, studies indicate that in oligotrophic regions heterotrophic prokaryotic growth can be limited by N and/or P (Cotner et al. 1997; Rivkin and Anderson 1997; Mills et al. 2008). Therefore, heterotrophic prokaryotic biomass and activity may be related to the nutrient supply and thus to water column stability (Gasol et al. 2009).

The North Atlantic Ocean is key to ocean circulation and stores about 23% of the global ocean anthropogenic CO_2 (Sabine et al. 2004). The northeastern basin provides a meridional gradient in stratification, with permanent stratification in the subtropics and seasonal stratification in the temperate zones (Talley et al. 2011; Jurado et al. 2012a). Vertical stratification suppresses turbulence and reduces the mixed layer depth, and restricts the flow of nutrients from depth. Strong and prolonged stratification often leads to oligotrophication of surface waters as nutrient become depleted due to utilization (Behrenfeld et al. 2006; Huisman et al. 2006; Hoegh-Guldberg and Bruno 2010). Moreover, as a consequence of global warming, oligotrophic areas (i.e., defined as areas below 0.07 μg Chl l^{-3}) are expected to expand in the future (Polovina et al. 2008). Therefore, the Northeast Atlantic provides an ideal area to study the relative contribution of lytic and lysogenic viral infection in a system governed by seasonal stratification.
Here we assess (1) viral induced mortality of prokaryotes relative to grazing over a latitudinal gradient across the North Atlantic Ocean during summer stratification, (2) the proportion of lytic and lysogenic viral infection and (3) discuss the results in terms implications for carbon cycling.

Materials and Methods

Sampling and physicochemical parameters

In July-August of 2009, 32 stations were sampled along a latitudinal gradient in the Northeast Atlantic Ocean during the shipboard expedition of STRATIPHYT which took place onboard othe R/V Pelagia (Fig. 1). Along the transect, the water column was stratified with relatively consistent and shallow mixed layer (ML) depths ranging from 18 - 46 m (Jurado et al. 2012b). Water samples for dissolved inorganic nutrients, bacterial and viral abundances were collected from at least 10 separate depths at each station using 24 plastic samplers (General Oceanics type Go-Flow, 10 liter) mounted on an ultra-clean (trace-metal free) system consisting of a fully titanium sampler frame equipped with CTD (Seabird 9+; standard conductivity, temperature and pressure sensors) and auxiliary sensors for chlorophyll autofluorescence (Chelsea Aquatracka Mk III), light transmission (Wet-Labs C-star) and photosynthetic active radiation (PAR; Satlantic). Samples were collected inside a 6 m clean container. Data from the chlorophyll autofluorescence sensor were calibrated against HPLC data according to van de Poll et al. (2013) (van

de Poll et al. 2013). At 16 stations along the cruise transect (Fig. 1), samples for heterotrophic prokaryote production, virus mediated mortality and protist grazing of prokaryotes were collected from the mixed layer (ML) and, where present, the deep-chlorophyll maximum (DCM; defined by the presence of a subsurface peak in the vertical profile of Chl *a* autofluorescence).

Methods and data for temperature eddy diffusivity (K_T), euphotic depth (Z_{eu}), and dissolved inorganic nutrients have been discussed previously (Jurado et al. 2012b; Mojica et al. 2015). In short, K_T (referred to here as the vertical mixing coefficient) was derived from temperature and conductivity microstructure profiles measured using a SCAMP (Self Contained Autonomous Microprofiler), deployed at 14 stations and down to 100 m depth. For the additional stations and depths, data were interpolated using the spatial kriging function 'krig' executed in R using the 'fields' package (Furrer et al. 2012). Interpolated K_T values were bounded below by the minimum value measured; the upper values were left unbounded. This resulted in estimated K_T values which preserved the qualitative pattern and range of values reported by Jurado et al. (Jurado et al. 2012b). Brunt-Väisälä frequency (N^2), was used to quantify the strength of stratification and was determined from CTD data processed with SBE Seabird software according to the Fofonoff adiabatic leveling method (Bray and Fofonoff 1981).

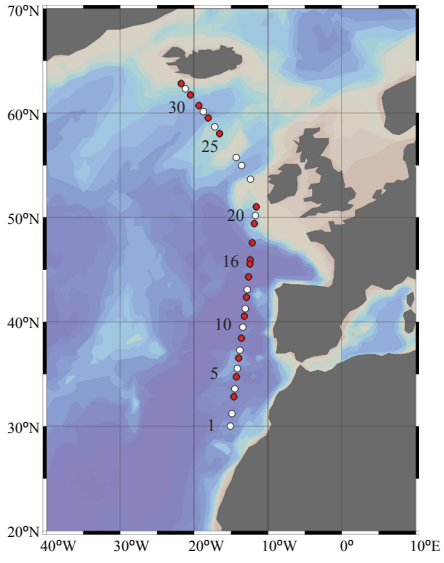

Figure 1. North-south gradient across the Northeast Atlantic Ocean. Bathymetric map depicting stations sampled during the summer STRATIPHYT. Mortality assays to determine viral lysis and microzooplankton grazing rates were performed at stations indicated by the red. Figure was prepared using Ocean Data View version 4 (Schlitzer 2002).

Samples for dissolved inorganic phosphate (PO_4^{3-}), ammonium (NH_4^+), nitrate (NO_3^-), and nitrite (NO_2^-) were gently filtered through 0.2 µm pore size polysulfone Acrodisk filters (32 mm, Pall Inc.), after which samples were stored at -20°C until analysis. Dissolved inorganic nutrients were analyzed onboard using a Bran+Luebbe Quaatro AutoAnalyzer for dissolved orthophosphate (PO_4^{3-}) (Murphy and Riley 1962), inorganic nitrogen (nitrate + nitrite: NO_x) (Grasshoff 1983) and ammonium (NH_4^+) (Koroleff 1969; Helder and de Vries 1979). Detection limits were 0.10 µM for NO_x, 0.028 µM for PO_4^{3-} and 0.09 µM for NH_4^+. The ratio of nitrogen to phosphorus (N:P) was then calculated as the sum of NO_x and NH_4^+ divided by PO_4^{3-}. For the individual nutrients, the flux at the euphotic zone depth ($Z_{eu}N$) was calculated according to $\varphi(Z_{eu}) = -K_T(z)(\partial N/\partial z)|_{Zeu}$, where N represents the individual nutrient and z stands for depth. Z_{eu} was calculated based on the light attenuation coefficient (K_d) and was defined as the depth at which irradiance was 0.1% of the surface value.

Microbial abundances

Prokaryotes and viruses were enumerated using Becton-Dickinson FACSCalibur flow cytometer (FCM) equipped with an air-cooled Argon laser with an excitation wavelength of 488 nm (15 mW) according to Marie et al. (1999), with modifications according to Mojica et al. (2014). Briefly, samples were fixed with 25% glutaraldehyde (EM-grade, Sigma-Aldrich, Netherlands) at a final concentration of 0.5% for 15 - 30 min at 4°C, flash frozen and stored at -80°C until analysis. Thawed samples were diluted using TE buffer, pH 8.2 (10 mM Tris-HCL, 1 mM EDTA; Roche, Germany). Prokaryote samples were stained in the dark at room temperature for 15 min using SYBR Green I at a final concentration of 1×10^{-4} of the commercial stock. Virus samples were stained by heating in the dark at 80°C for 10 min in the presence of the nucleic acid-specific green fluorescence dye SYBR Green I at a final concentration of 0.5×10^{-4} of the commercial stock concentration (Life Technologies, Netherlands). Trigger for analysis was set on green fluorescence and the obtained list-mode files were analyzed using the freeware CYTOWIN (Vaulot 1989).

Heterotrophic nanoflagellates (HNF) were enumerated by epifluorescence microscopy. Briefly, 20 ml of seawater was fixed to a 1% final concentration (10% working stock, Sigma Aldrich) and filtered onto 0.2 µm black polycarbonate filter (25 mm, Whatman). Samples were then stained using 4'6-diamidino-2-phenylindole dihydrochloride (DAPI) (5 mg ml^{-1}, Sigma-Aldrich) at a final concentration of 1 µg ml^{-1} and stored at -20°C. A minimum of 75 fields and 100 HNF in total were then

counted using a Zeiss Axiophot epifluorescence microscope equipped with BP 365, FT395 and LP397 excitation filters.

Viral mediated mortality

Viral production (VP) was determined according to Winget et al. (2005). At *in situ* temperature and under low light conditions, a 600 ml whole seawater sample was reduced to approximately 100 ml by recirculation over a 0.22 µm-pore-size polyether sulfone membrane (PES) tangential flow filter (Vivaflow 50; Sartorius stedim biotech) at a filtrate discharge rate of 40 ml min^{-1}. Five hundred milliliters of virus-free water (generated by 30-kDa ultrafiltration Vivaflow 200, PES membrane; Sartorius stedim biotech) was then added and the washing procedure was repeated an additional 2 times. On the final flush, the volume was reduced a final time to approximately 50 ml and the filter was slowly back-flushed to obtain the 50 ml volume remaining in the system. The sample was then topped up with virus-free water (500 ml) and aliquoted into six 50 ml polycarbonate Greiner tubes. Triplicate samples were used to determine lytic VP, and triplicates for prophage induction using Mytomycin C (Sigma-Aldrich; 1 µg ml^{-1} final concentration) (Paul and Weinbauer 2010). Untreated whole seawater was also aliquoted into three 50 ml polycarbonate tubes in order to provide an estimate of PP_{net}. One milliliter subsamples for viral and prokaryotic abundance were taken at the start of the incubation (T_0), after which the samples were incubated in darkness at *in situ* temperature and sub-sampled every 3 h for a total of 12 - 24 h.

Production rate of new viruses was determined for each replicate from the slope of a first-order regression of viral concentration over time (Wilhelm et al. 2002). Prophage induction was calculated as the difference between virus counts in unamended samples (lytic VP) and virus counts in those to which Mitomycin C was added. The *in situ* VP rate was determined by correcting the experimental VP rate by the prokaryotic loss factor (Winget et al. 2005). Estimates for daily virus-mediated mortality (VMM) expressed in cells l^{-1} d^{-1} were calculated by dividing lytic VP by a burst size of 20 (Parada et al. 2006). Estimates of VMM, in terms of organic carbon released by viral lysis, were obtained by multiplying the VMM by the oceanic bacterial carbon conversion factor of 12.4 fg $cell^{-1}$ (Fukuda et al. 1998).

Protist mediated mortality

Protistian grazing rates of prokaryotes were determined using fluorescently labeled natural bacteria (FLP) according to the procedure described by Sherr and Sherr

(1987). One liter natural whole water samples (polycarbonate bottles) were given FLP at approximately 10% of the natural concentration (FLP stock contained 5 x 10^7 ml^{-1}, stored at -20°C until use). Immediately after addition, a 20 ml subsample (T_0) was then taken and fixed with 10% glutaraldehyde (1% final concentration; EM-grade, Sigma-Aldrich, Netherlands). The sample was then filtered onto a 0.2 µm pore-size black polycarbonate filter (25 mm, Whatman) and stored at -20°C until analysis. The incubation bottles were closed such that no air was trapped inside, mounted on a slow rotating (0.5 rpm) plankton wheel, and incubated under *in situ* light and temperature. After 24 h incubation, a 20 ml subsample was taken and treated as previously described. The estimation of grazing rates (d^{-1}) were determined as the natural log of the abundance of FLP in the T_{24} sample divided by the abundance of FLP in the T_0 sample. Protist mediated mortality (PMM) was calculated as $PMM = PA_0 \times (e^{rt}-1)$, where PA_0 is the abundance of protists and r equals the grazing rate obtained from FLP experiments.

Heterotrophic prokaryotic production

Heterotrophic prokaryotic production was determined from leucine incorporation rates (PP_L) according to Simon and Azam (1989). Ten-milliliter seawater samples were taken in triplicate. One sample was used as a control to which 0.5 ml formaldehyde (37%; Sigma-Aldrich) was added in order to kill the prokaryotes. Thirty µl [3H]leucine (specific activity, 139 Ci $mmol^{-1}$; Amersham) was added to each sample, equivalent to 50 microCurie per vial, and incubated in the dark at *in situ* temperature for 2 h. Samples were then fixed with 0.5 ml formaldehyde (37%; Sigma-Aldrich) and filtered onto 0.2 µm polycarbonate filters (25 mm, Whatman). Filters were washed twice by addition of 5% chilled trichloroacetic acid (TCA) for 5 min and then transferred to scintillation vials and stored at -80°C until analysis. Prior to analysis, 8 ml of scintillation cocktail (Filter-Count LCS cocktail; PerkinElmer) was added and left for 6 h. Samples were analyzed on a LKB WALLAC 1211 Rackbeta liquid scintillation counter. PP_L in terms of organic carbon produced was calculated assuming a carbon to protein ration of 0.86 and an isotope dilution factor of 2 (Simon and Azam 1989). Heterotrophic prokaryotic biomass production was converted to cell concentrations by dividing by the average carbon content of oceanic bacteria of 12.4 fg C $cell^{-1}$ (Fukuda et al. 1998).

PP_L is presumed to measure 'gross production' as the incubation period is short relative to prokaryotic growth and mortality (i.e., a day or longer) (Kirchman 2001). However, taking into account that generally no steps are taken to exclude

mortality, it is likely that losses are incorporated into the PP_L measurements. Heterotrophic prokaryotic production has been shown to be reduced up to 2-fold in the presence of viruses compared to incubations without viruses (Middelboe 2000). Net prokaryotic production (PP_{net}) determined by the increase in prokaryote abundance in unamended seawater over time was higher than the PP_L in more than half of the total paired samples (Table S1). One possibility is that PP_L could have been underestimated, as incubations were carried out in the dark, due to significant contributions of photoheterotrophs (i.e., aerobic anoxygenic phototrophs (AAP) or proteorhodopsin (PR) containing bacteria to prokaryotic abundance (Michelou et al. 2007; Campbell et al. 2008; Gomez-Consarnau et al. 2010). However, in all cases, rates of VMM and PMM were higher than PP_L (Table S1) and therefore it is more likely that PP_L represented net production. In order to account for this we calculated gross production (PP_{gross}) by correcting for losses due to viral lysis and grazing (assuming the rate of mortality in the samples was equivalent to those measured by the mortality assays and a 30% growth efficiency for grazing, i.e., 30% of carbon grazed was retained on filter) (Fenchel and Finlay 1983; Straile 1997). Therefore, $PP_{gross} = PP_L +$ lytic VMM+ [(0.3) x PMM]. Total available carbon (TAC) was then calculated as the sum of prokaryotic standing stock (PA) and production, i.e., PP_L for minimal TAC (TAC_{min}) and PP_{gross} for maximal TAC (TAC_{max}).

Statistical analysis

Statistical analysis was performed using the R statistical software (R Development Core Team 2012). Potential relationships between microbial abundances, production, mortality and environmental parameters were examined by Spearman rank correlation coefficients. Probability values were adjusted with Holm correction of multiple hypothesis testing using the corr.p function of psych (Revelle 2014). Analysis was performed on data as a whole (n = 25), but also separately according to depth layers; ML (n = 20) and DCM (n = 5).

Table 1. Location, physicochemical characteristics and Chl a autofluorescence of water sampled in the North Atlantic for heterotrophic prokaryotic production, viral production and grazing experiments. Abbreviations for depth layer are mixed layer (ML) and deep chlorophyll maximum (DCM).

Station	Latitude (°N)	Longitude (°E)	Depth (m)	Depth Layer	Z_{eu} (m)	Temperature (°C)	Salinity	NO_3^- (µM)	PO_4^{3-} (µM)	NH_4^+ (µM)	Chl *a* (µg l^{-1})
3	32.825	-14.589	15	ML	138	22.8	36.9	0.05	0.00	0.08	0.03
			60	DCM		18.1	36.5	0.07	0.00	0.06	0.24
5	34.720	-14.258	15	ML	119	22.3	36.7	0.00	0.01	0.10	0.04
			85	DCM		16.1	36.3	0.00	0.03	0.16	0.28
7	36.526	-13.934	15	ML	84	20.6	36.2	0.00	0.00	0.06	0.04
9	38.424	-13.586	15	ML	111	21.1	36.4	0.04	0.02	0.06	0.05
			75	DCM		14.9	36.1	1.32	0.13	0.18	0.29
11	40.528	-13.191	15	ML	96	19.8	36.0	0.00	0.01	0.06	0.06
13	42.337	-12.884	15	ML	99	18.7	35.8	0.05	0.03	0.00	0.04
			47	DCM		14.7	35.8	0.09	0.05	0.00	0.55
15	44.283	-12.605	15	ML	122	18.4	35.8	0.05	0.03	0.06	0.05
			60	DCM		14.4	35.8	2.05	0.17	0.07	0.62
16	45.917	-12.363	10	ML	86	16.9	35.6	0.10	0.04	0.04	0.51
18	47.569	-12.110	25	ML	88	16.6	35.7	0.07	0.05	0.11	0.46
19	49.382	-11.829	15	ML	115	15.8	35.5	1.15	0.12	0.31	0.22
19	49.382	-11.829	30	ML		15.7	35.5	1.29	0.16	0.39	0.30
21	51.000	-11.567	15	ML	115	15.9	35.5	1.15	0.15	0.39	0.23
25	58.002	-16.516	10	ML	43	13.5	35.3	1.18	0.11	0.09	1.45
27	59.499	-18.067	20	ML	41	14.0	35.2	2.08	0.18	0.19	1.09
29	60.684	-19.339	10	ML	49	13.1	35.3	2.00	0.19	0.17	0.94
30	61.715	-20.489	15	ML	48	13.1	35.2	1.38	0.15	0.33	1.08
32	62.800	-21.736	10	ML	38	12.8	35.3	1.52	0.14	0.64	1.21

Results

Study site

Temperature, salinity and density showed clear vertical and latitudinal gradients (Table 1, Fig. S1A-C). In accordance with strong vertical stratification, the upper water column was characterized by low K_T and relatively high N^2 (Fig. S1D, E and Table S2). Moreover, the southern region (30 - 45°N; stations 3 - 15) was classified as oligotrophic based on ML concentrations of $NO_3^- \leq 0.13$ µM and $PO_4^{3-} \leq 0.03$ µM (van de Poll et al. 2013), and Chl $a \leq 0.07$ µg l^{-1} (Polovina et al. 2008). In the northern half (46 - 63°N; stations 16 - 32), inorganic nutrient concentrations within the ML were on average 1.4±0.8 µM NO_3^- and 0.14±0.06 µM PO_4^{3-}, with highest concentrations north of 58°N (stations 25 - 32). In the ML, significant correlations were found between N:P and NH_4^+, NO_2^- (positive) and $Z_{eu}PO_4$ (negative; Table S3). Chl *a* in the ML was in turn positively correlated to N:P (and NH_4^+, NO_2^-

and negatively with $Z_{eu}PO_4$; Table S3) and average Chl *a* concentration increased to a maxima of 1.1±0.3 μg l^{-1} in the north (Table 1 and Fig. S1J). In the DCM (oligotrophic southern stations), K_T increased significantly with latitude (positively related to NO_3^- and PO_4^{3-}), and N^2 was negatively related to NO_2^-, $Z_{eu}NO_3$ and N:P (Table S4. Fig. S1D). N:P in the DCM was positively associated with NO_2^- and $Z_{eu}NO_3$. Chl *a* in the DCM increased significantly with latitude (positively related to K_T, NO_3^- and PO_4^{3-}) from 0.24 at station 3 to 0.62 μg l^{-1} at station 15 (Table 1 and S4, Fig. S1J).

Microbial abundances

Prokaryotic abundance (PA) in the ML was on average 6.4±1.5 x10^8 prokaryote l^{-1} until 58°N, above which concentrations increased to 22±0.8 x10^8 l^{-1} (Fig. 2A). Similar to their numerically dominate hosts, viral abundances (VA) were also lowest in the ML of oligotrophic south (average 8.0±2.9 x10^9 l^{-1}; Fig. 2B), however, VA increased earlier (~45°N) and remained relatively stable until 63°N with an average abundance of 24±0.9 x10^9 l^{-1}. The average virus to prokaryote ratio (VPR) in the ML increased from 13±5 in the most southern section of the transect to 26±9 midway through before declining again to 14±7 in the most northern stations (Table 2). HNF abundances in the ML were lowest in the most southern stations (< 40°N, averaging 3.5±1.0 x 10^5 l^{-1}). Highest abundances of 16 x10^5 were found near the DCM of stations 11 - 18 (40 - 47°N). North of this region, HNF in the ML averaged 9.6±2.3 x10^5 l^{-1}.

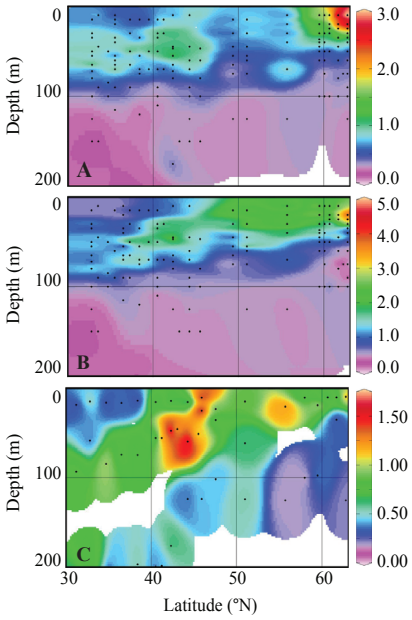

Figure 2. Biogeographical distributions of (**A**) prokaryotes (x10^{9} l^{-1}), (**B**) viruses (x10^{10} l^{-1}), and (**C**) heterotrophic nanoflagellates (x10^{6} l^{-1}) across the Northeast Atlantic Ocean obtained during the STRATIPHYT cruise. Black dots indicate sampling points. Graphs were prepared with Ocean Data View version 4 (Schlitzer 2002).

PA in the ML was significantly correlated to Chl *a* (Table S5). The positive correlation to NO_2^- and negative correlation to $Z_{eu}PO_4$ was most likely an indirect effect due to the high correlation of these variables with Chl *a* (Table S3 and S4). Viral abundance (VA) was tightly associated to their numerically dominate hosts (PA) (Table S5 and S6). However contrary to PA, VA in the ML was positively correlated to latitude and negatively with temperature and salinity (Table S5). VPR in the ML was inversely correlated to Chl *a*, explaining the relationship with $Z_{eu}PO_4$, NH_4^+ and N:P that were each associated to Chl *a* (Table S3 and S5).

Table 2. Heterotrophic nanoflagellates (HNF) abundance, prokaryotic abundance (PA), viral abundance (VA) and virus to prokaryote ratio (VPR) in stratified waters along a south-north transect in the Northeast Atlantic. Abbreviations for depth layer are mixed layer (ML) and deep chlorophyll maximum (DCM). n.d. = not determined.

Station	Latitude (°N)	Longitude (°E)	Depth (m)	Depth Layer	HNF ($x10^5$ l^{-1})	PA ($x10^8$ l^{-1})	VA ($x10^9$ l^{-1})	VPR
3	32.825	-14.589	15	ML	5.2	7.2	5.6	8
			60	DCM	3.8	11.2	10.5	9
5	34.720	-14.258	15	ML	3.0	7.7	7.4	10
			85	DCM	9.7	7.8	13.3	17
7	36.526	-13.934	15	ML	3.5	6.7	7.6	11
9	38.424	-13.586	15	ML	3.0	4.4	7.4	17
			75	DCM	8.0	5.5	12.8	23
11	40.528	-13.191	15	ML	8.4	8.2	14.1	17
13	42.337	-12.884	15	ML	6.9	3.0	12.7	43
			47	DCM	16.0	12.2	21.3	18
15	44.283	-12.605	15	ML	5.8	9.0	16.5	18
			60	DCM	15.8	9.9	14.7	15
16	45.917	-12.363	10	ML	14.2	17.2	35.1	20
18	47.569	-12.110	25	ML	8.8	10.6	27.6	26
19	49.382	-11.829	15	ML	n.d.	5.7	31.1	55
19	49.382	-11.829	30	ML	n.d.	5.5	14.9	27
21	51.000	-11.567	15	ML	8.6	8.4	25.5	30
25	58.002	-16.516	10	ML	7.5	18.7	23.5	13
27	59.499	-18.067	20	ML	9.7	15.7	25.5	16
29	60.684	-19.339	10	ML	6.6	12.9	16.5	13
30	61.715	-20.489	15	ML	n.d.	28.1	28.4	10
32	62.800	-21.736	10	ML	11.7	31.9	3.9	7

Within the DCM in the oligotrophic southern region, PA, VA and HNF abundances were higher compared to the upper ML, with 8.6±2.1 $x10^8$ prokaryotes l^{-1}, 13±0.4 $x10^9$ viruses l^{-1} and 6.5±2.3 $x10^5$ HNF l^{-1} (Fig. 2). As for the ML, VA in the DCM was also positively correlated to PA. PA and VA were positively associated with the $Z_{eu}PO_4$ and negatively with NH_4^+ (Table S6). VPR in the DCM was similar to the ratios in the ML (2-sample *t* test; $\alpha = 0.05$, $p = 0.17$). However, VPR in the DCM was positively related to N^2 and inversely related to $Z_{eu}NO_3$ and N:P (Table S6). HNF abundance was not found to have a significant correlation to any of the environmental or biological parameters measured (Table S5 and S6).

Heterotrophic prokaryotic production

In the ML, PP_L averaged 1.0±0.4 $x10^8$ cells l^{-1} d^{-1} or 1.3 ± 0.5 µgC l^{-1} d^{-1} south of 45°N (Stn 3 - 15) and increased 2-fold (2.4±1.4 $x10^8$ cells l^{-1} d^{-1}) in the north (Table

S1). PP_L varied significantly with latitude and was positively associated with PO_4^{3-} concentrations (Table S5). PP_{gross} in the ML averaged 5.8±2.0 x 10^8 cells l^{-1} d^{-1} (or 7.2 µg C l^{-1} d^{-1}) for the southern stations and was 1.4-fold higher in the northern region (8.4±4.8 x 10^8 cells l^{-1} d^{-1} or 10.4±6.0 µg C l^{-1} d^{-1}) (Table S1). PP_{gross} was significantly correlated to N:P (Table S5). In the DCM, PP_L and PP_{gross} were not significantly different from the surface waters of the same region and were on average 1.3±0.6 x10^8 and 8.4±5.0 x10^8 cells l^{-1} d^{-1}, respectively (Table S1). Within this layer, PP_L and PP_{gross} were significantly correlated to PA, $Z_{eu}PO_4$ and to each other, and negatively to NH_4^+ (Table S6).

Prokaryotic mortality

Lytic VP in the ML increased from 0.6±0.4 x10^{10} viruses l^{-1} d^{-1} in the oligotrophic south to 1.4±1.7 x10^{10} viruses l^{-1} d^{-1} in the north, corresponding to a greater than 2-fold increase in VMM from 3.2±1.9 to 7.0±8.7 x10^8 cell lysed l^{-1} d^{-1} (Fig. 3A, Table 3). Lytic VP was positively correlated to PP_{gross} and N:P (Table S5). Mitomycin C inducible prophages were only detected in a few ML samples (i.e., Stn 11, 15, 19 and 25) and rates varied from 0.1 to 1.0 x10^{10} viruses l^{-1} d^{-1} (Fig. 3B). The prophage induction in the ML was, nonetheless, significantly correlated to $Z_{eu}NO_3$ (Table S5). On average, PPM in the ML increased 1.6-fold between the southern oligotrophic region (2.2±1.0 x10^8) and the north (3.6±3.5 x10^8 cells l^{-1} d^{-1}) (Table 3), which was largely due to differences in PA (Fig. 2A) and not the actual HNF grazing rates (i.e., 0.4±0.2 d^{-1} in the south to 0.3±0.2 d^{-1} in the north; Fig. 3C). The HNF grazing rate in the ML was positively correlated to temperature and inversely to latitude, PP_L and VA (with PP_L and VA positively related to latitude; Table S5).

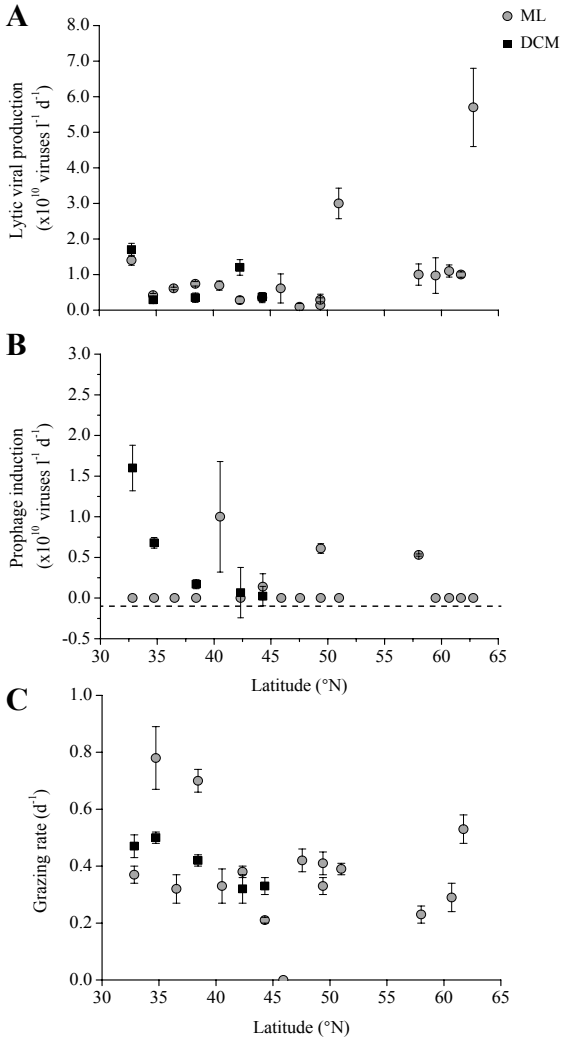

Figure 3. Average mortality rates of prokaryotes by (**A**) lytic viral production, (**B**) inducible prophages and (**C**) grazing measured over the Northeast Atlantic during the STRATIPHYT cruise. Error bars represent standard error (N = 3).

Lytic VP and VMM did not significantly vary between the ML and DCM of oligotrophic regions, i.e., 0.8±0.6 x10^{10} viruses l^{-1} d^{-1} and VMM of 3.8±3.1 x10^{8} cells lysed l^{-1} d^{-1}, respectively (Fig. 3A, Table 3). In the DCM, lytic VP was not only correlated to PP_{gross} but also to PP_{L}, PA, and VA. Inducible prophages were detected within all DCM samples and were found to be significantly related to latitude and Chl *a*, whereby the rates declined hyperbolically from 16.0 to 0.2 x10^{9} viruses l^{-1} d^{-1} with

increasing latitude and Chl *a* concentrations (Fig. 3B, Table S6). HNF grazing rates in the DCM (average of 0.4±0.1 d^{-1}) were also comparable to rates in the ML, however the resulting PMM in the DCM (3.1±0.8 x10^8 cell l^{-1} d^{-1}) were higher (comparable to the ML losses in the north; Table 3). HNF grazing rates in the DCM were inversely correlated to lytic VP, VA and PA, whereby PA was directly linked to VA. PPM was positively tied to VPR and N^2 (and factors associated to these 2 factors; Table S6).

Table 3. Prokaryotic standing stock (SS; µg l^{-1}), production (PP_{gross}) and loss rates (virus mediated, VMM, and grazing mediated, PMM, mortality) in organic carbon (µg l^{-1} d^{-1}) and in terms of percentage of total available carbon (TAC_{max}; determined as the sum of SS and PP_{gross}). Total mortality is abbreviated as TM. n.d. = not determined.

Station	Depth Layer	SS	PP_{gross}	VMM	PMM	TM:PP_{gross}	TAC_{max}	% TAC_{lysed}	% TAC_{grazed}
3	ML	9.0	11.2	8.6	2.8	1.0	20.1	42.5	13.7
	DCM	13.9	16.6	10.4	5.2	0.9	30.6	34.0	17.0
5	ML	9.6	7.1	2.6	5.2	1.1	16.6	15.5	31.1
	DCM	9.7	5.6	1.8	3.8	1.0	15.3	11.9	24.9
7	ML	8.3	n.d.	3.8	2.3	n.d.	n.d.	n.d.	n.d.
9	ML	5.4	7.6	4.6	2.7	1.0	13.0	35.1	21.0
	DCM	6.8	4.6	2.1	2.4	1.0	11.4	18.8	20.5
11	ML	10.2	7.6	4.2	2.8	0.9	17.8	23.9	15.9
13	ML	3.7	4.2	1.7	1.2	0.7	7.9	22.1	14.8
	DCM	15.1	12.0	7.2	4.2	1.0	27.1	26.6	15.3
15	ML	11.2	5.5	2.2	2.1	0.8	16.7	13.0	12.5
	DCM	12.2	6.1	2.3	3.4	0.9	18.3	12.5	18.7
16	ML	21.4	7.1	3.8	0.0	0.5	28.5	13.3	0.0
18	ML	13.2	6.8	0.6	4.5	0.8	20.0	2.9	22.6
19	ML	7.0	3.9	0.9	2.4	0.8	10.9	8.0	21.7
19	ML	6.8	4.7	1.8	1.9	0.8	11.5	15.7	16.8
21	ML	10.4	21.5	18.7	3.3	1.0	31.9	58.6	10.5
25	ML	23.2	13.5	6.5	4.7	0.8	36.7	17.6	12.8
27	ML	19.4	11.3	6.0	n.d.	n.d.	30.8	19.6	0.0
29	ML	15.9	14.4	7.1	4.0	0.8	30.3	23.2	13.1
30	ML	34.8	n.d.	6.5	14.4	n.d.	n.d.	n.d.	n.d.
32	ML	39.5	n.d.	35.5	n.d.	n.d.	n.d.	n.d.	n.d.

Averaged overall, PMM was nearly 2-fold lower at 2.8 x10^8 cells l^{-1} d^{-1} compared to that of VMM at 5.2 x10^8 cells l^{-1} d^{-1} (Table 3). Comparing mortality factors as a function of latitude revealed that VMM was, in most cases, the dominant regulating factor (Fig. 4). Total mortality (TM) (viral lysis plus grazing) ranged from 0.2 to 2.9 x10^9 cells l^{-1} d^{-1}, and was on average slightly lower than PP_{gross} (i.e, average TM:PP_{gross} of ~0.9; Fig. 5A). However, the discrepancy between TM and

PP_{gross} increased significantly with latitude in the ML (Fig. 5B; Table S5), indicating net heterotrophic production in the surface waters at higher latitudes.

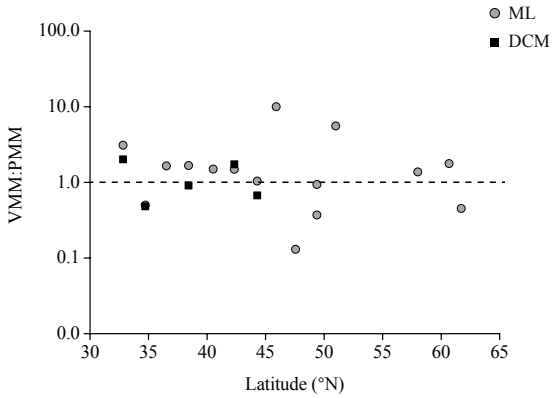

Figure 4. The contribution of viral lysis to prokaryote mortality. Ratio of viral-mediated mortality (VMM) to protist-mediated mortality (PMM) as function of latitude. Rates were determined using FLP and virus reduction experiments performed during the STRATIPHYT cruise. Dotted line indicates a 1:1 relationship of viral lysis to grazing.

TAC in the ML ranged from a minimum of 5 - 27 (TAC_{min}) to a maximum of 8 - 37 μg C l^{-1} d^{-1} (TAC_{max}). On average TAC_{max} was 1.5 times higher than TAC_{min}. TAC_{max} increased 1.6-fold between the oligotrophic south and the north, corresponding to average values increasing from 15.3±4.3 to 25.1±9.7 μg C l^{-1}. TAC concentrations in the DCM of oligotrophic stations were slightly higher with TAC_{max} of 20.6±8.1 μg C l^{-1} (Table 3). The percentage of TAC_{min} lost (i.e., viral lysis plus grazing), sometimes exceeded 100% (up to 203%), which is due to the lack of consideration of production which can be grazed and lysed during measurement. Therefore, the usage of TAC_{min} can lead to unrealistic losses in total available carbon. Using TAC_{max}, the percentage lost ranged from 13 - 69% with an average of 39%. The percentage of TAC_{max} lysed was highest in the ML of the southern oligotrophic region, i.e., 25±11 as compared to 20±17% in the north. In contrast, TAC_{max} grazed in the ML decreased from 18±7 in south to 12±9 in the north. TAC_{max} lysed and grazed in the DCM were comparable to the ML of the same region, i.e., 21±10 and 19±4 %.

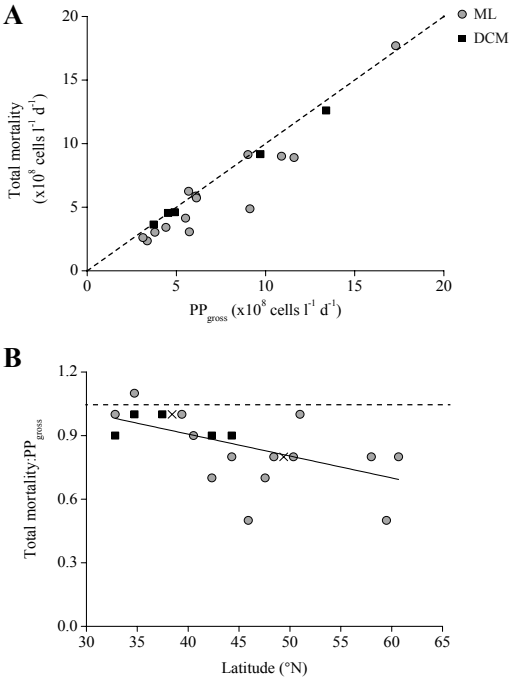

Figure 5. The relationship between total mortality and gross growth of heterotrophic prokaryotes measured over the Northeast Atlantic during the STRATIPHYT cruise. (**A**) Relationship between the total mortality (grazing + viral lysis) and PP_{gross} (in cells l^{-1} d^{-1}), and (**B**) Ratio of total mortality to PP_{gross} of heterotrophic prokaryotes as function of latitude. Dotted lines indicate a 1:1 relationship, and the solid line is a linear regression through the data. Crosses mark the center of overlapping points which are then plotted on either side of the mark..

Discussion

The strong positive correlation between VA and PA has been reported previously for the North Atlantic Ocean and confers with evidence that the majority of viruses in the ocean infect the numerically dominant prokaryotic hosts (Suttle 2007). Viruses are dependent on their host to provide the necessary energy, resources and machinery required for viral replication. Consequently, factors regulating the abundance and physiology of their hosts, as well as their production and removal are also important in governing virus dynamics (Mojica and Brussaard 2014). VA was positively correlated with PP_L, suggesting that host physiology and generation time may have been important factor regulating virus abundance during our study period (Proctor et al. 1993; Moebus 1996; Middelboe 2000). In fact, lytic VP in both the ML and DCM were significantly correlated to heterotrophic prokaryotic

production. Furthermore, lytic VP in the ML was positively correlated to N:P which may suggest that the availability of the inorganic nutrients affected viral production, most likely via nutrient-limited host physiology (Moebus 1996; Motegi and Nagata 2007).

Indeed, heterotrophic prokaryotic production was uncoupled from phytoplankton biomass (Chl *a*) and instead linked to nutrient availability (i.e., PP_L to PO_4^{3-} and PP_{gross} to N:P). Several studies indicated that in oligotrophic regions of the North Atlantic Ocean heterotrophic prokaryotes can be limited by the availability of inorganic nutrients (Cotner et al. 1997; Rivkin and Anderson 1997; Mills et al. 2008). The dominance and relatively high abundance (up to 2 $x10^8$ cells l^{-1}) of pico-sized phytoplankton present during our study period (Mojica et al. 2015) could have efficiently competed for inorganic nutrients and thereby increased the potential for limitation. Alternatively, the nutrient limitation of phytoplankton can affect both the quantity and quality of DOM released, and thus the efficiency with which it can be utilized (Obernosterer and Herndl 1995; Gardes et al. 2012). In the marine environment, trends in prevalence of lysogeny across different systems suggests that it may represent a survival strategy to endure conditions of low host productivity and abundance (Williamson et al. 2002; Weinbauer et al. 2003; Payet and Suttle 2013). We found no direct correlation between lysogeny, inorganic nutrient concentrations, PA or heterotrophic prokaryotic production. However, correlations presented here were to total community abundance and production, and thus correlations may be obscured if induction sensitive host-phage systems were not dominant members of the prokaryotic community. Inducible prophages were only detected at 4 stations within the ML of our study period, with a positive correlation to $Z_{eu}NO_3$. The reason for this connection remains unclear due the lack of association in the ML between $Z_{eu}NO_3$ and other variables measured. An alternative explanation for the lack of inducible prophages in the surface ML may be prolonged exposure to high levels of solar radiation (particularly UV), which can induce lysogens and result in a reduced phophage yield from Mitomycin C addition (Wilcox and Fuhrman 1994; Weinbauer and Suttle 1999). In contrast, inducible prophages were detected within the DCM of every southern station tested and was negatively correlated to Chl *a* (this study). Chl *a* is an indication of phytoplankton biomass but is not necessarily indicative of numerical abundance (as small phytoplankton contribute relatively less to biomass compared to larger phytoplankton). Pico-sized *Prochlorococcus* spp. were dominant in the DCM (93%), with abundances decreasing with latitude (Mojica et al. 2015). Consequently,

competition for inorganic nutrients between autotrophic and heterotrophic prokaryotes may have pushed nutrient limitation to a point at which lytic viral production could no longer be effectively sustained and consequently triggered a switch to lysogenic infection. This hypothesis is supported by evidence that inorganic nutrients may at times be an important factor modulating lysogeny in natural heterotrophic populations (Williamson et al. 2002; Motegi and Nagata 2007). However, further research is required to better understand the role that inorganic nutrient availability plays in regulating viral life strategy selection in natural heteroptrophic prokaryotic host populations.

In general, heterotrophic production, abundances and mortality in the ML was higher for the northern region than the south. However, PMM did not increase uniformly with PP_L and VMM, implying that grazing pressure was reduced in the north. Indeed, correlation analysis showed a significant inverse relationship between HNF grazing rates and latitude and a positive correlation to temperature. This supports evidence that warming will increase bacterial losses due to protist grazing (Sarmento et al. 2010). Alternatively top-down control of protists may have been higher in the northern region (Rychert et al. 2014). Strong top-down control of bacterivores could also explain the lack of correlation between HNF and other measured parameters. Accordingly, predation of protist would relax competition between HNF and viruses for bacterial prey, which would account for the negative correlations of HNF grazing rate with VA, and PMM with VBR. This suggests that viral-induced mortality may also have played a regulatory role by controlling prokaryotic prey density and/or by infecting HNF (Garza and Suttle 1995; Nagasaki et al. 1995; Massana et al. 2007). More research is needed specifically studying the different forcing factors for HNF distribution and activity before decisive conclusions can be drawn. In any case, the lower grazing losses in the northern region do clarify the lack of correlation found between PP_L and PP_{gross} in the ML. Following the hypothesis for a regulatory role of viral-induced mortality in controlling prokaryotic prey density (as indicated through the inverse correlation of HNF grazing with VA and lytic VP), would also explain the higher PA in the DCM despite comparable PP_L between the DCM and the ML. The counter argument that organic resources in the DCM are limited is argued against by the higher phytoplankton abundance and Chl *a* concentration in the DCM compared to the ML.

Contribution to total mortality and consequences for carbon cycling

Overall, VMM was the dominant loss factor regulating prokaryotic populations in the surface waters of the Northeast Atlantic Ocean along a latitudinal gradient in stratification during the summer of 2009. Averaged over all stations and depths, 25% of the TAC was cycled back into the water column by viral activity compared to 14% entering the food web by grazing, emphasizing the role of viruses as important drivers for carbon cycling in the Northeast Atlantic. Moreover, VMM and PMM varied with trophic status, i.e., both were higher in the north compared to the oligotrophic southern region (2.1 and 1.6-fold, respectively). However, the ratio of TM to PP_{gross} decreased over the latitudinal gradient (due to the reduced grazing pressure in the north), thereby representing a gradual change from a system regulated by high turnover in regions of strong stratification to net heterotrophic production with reduced stratification.

Several studies predict that global warming will result in stronger temperature stratification in the North Atlantic Ocean (Sarmiento 2004; Polovina et al. 2008) and thus reduce total availability of photosynthetic carbon at higher latitudes. Our results indicate that in summer this may also lead to a reduction in heterotrophic prokaryote production at these higher latitudes, i.e., as the system moves away from net heterotrophic production towards a steady-state situation where production is balanced by loss. The relative contributions of the different pathways (i.e., grazing versus viral lysis) is likely to remain consistent, with viral lysis cycling more of the organic carbon back into the water column than is being transferred to higher trophic levels by grazers.

Acknowledgements

The STRATIPHYT project was supported by the division for Earth and Life Sciences Foundation (ALW), with financial aid from the Netherlands Organization for Scientific Research (NWO) (Grant number 839.08.420). We thank the captains and shipboard crews of R/V Pelagia and scientific crews during the cruises, with special thanks to Tea de Vries. We acknowledge the support of NIOZ-Marine Research Facilities (MRF) on-shore and on-board.

Reference

Angly FE, Felts B, Breitbart M, Salamon P, Edwards RA, Carlson C, Chan AM, Haynes M, Kelley S, Liu H, Mahaffy JM, Mueller JE, Nulton J, Olson R, Parsons R, Rayhawk S, Suttle CA, Rohwer F (2006) The marine viromes of four oceanic regions. PLOS Biology 4: e368. doi: 10.1371/journal.pbio.0040368

Behrenfeld MJ, O 'Malley RT, Siegel DA, McClain CR, Sarmiento JL, Feldman GC, Milligan AJ, Falkowski PG, Letelier RM, Boss ES (2006) Climate-driven trends in contemporary ocean productivity. Nature 444:752-755

Bray NA, Fofonoff NP (1981) Available potential energy for mode eddies. Journal of Physical Oceanography 11:30-47

Brussaard CPD, Wilhelm SW, Thingstad TF, Weinbauer MG, Bratbak G, Heldal M, Kimmance SA, Middelboe M, Nagasaki K, Paul JH, Schroeder DC, Suttle CA, Vaque D, Wommack KE (2008) Global-scale processes with a nanoscale drive: the role of marine viruses. The ISME Journal 2:575-578

Campbell BJ, Waidner LA, Cottrell MT, Kirchman DL (2008) Abundant proteorhodopsin genes in the North Atlantic Ocean. Environmental Microbiology 10:99-109

Carlson CA, Ducklow HW (1996) Growth of bacterioplankton and consumption of dissolved organic carbon in the Sargasso Sea. Aquatic Microbial Ecology 10:69-85

Chibani-Chennoufi S, Bruttin A, Dillmann ML, Brussow H (2004) Phage-host interaction: an ecological perspective. Journal of Bacteriology 186:3677-3686

Church MJ, Hutchins DA, Ducklow HW (2000) Limitation of bacterial growth by dissolved organic matter and iron in the Southern Ocean. Applied and Environmental Microbiology 66:455-466

Cotner JB, Ammerman JW, Peele ER, Bentzen E (1997) Phosphorus-limited bacterioplankton growth in the Sargasso Sea. Aquatic Microbial Ecology 13:141-149

Fenchel T, Finlay BJ (1983) Respiration rates in heterotrophic, free-living protozoa. Microbial Ecology 9:99-122

Fuhrman JA (1999) Marine viruses and their biogeochemical and ecological effects. Nature 399:541-548

Fukuda R, Ogawa H, Nagata T, Koike I (1998) Direct determination of carbon and nitrogen contents of natural bacterial assemblages in marine environments. Applied and Environmental Microbiology 64:3352-3358

Furrer R, Nychka D, Sain S (2012) fields: Tools for spatial data. R package version 6.7

Gama JA, Reis AM, Domingues I, Mendes-Soares H, Matos AM, Dionisio F (2013) Temperate bacterial viruses as double-edged swords in bacterial warfare. PLOS One 8:e59043. doi: 10.1371/journal.pone.0059043

Gardes A, Ramaye Y, Grossart HP, Passow U, Ullrich MS (2012) Effects of *Marinobacter adhaerens* HP15 on polymer exudation by *Thalassiosira weissflogii* at different N:P ratios. Marine Ecology Progress Series 461:1-14

Garza DR, Suttle CA (1995) Large double-stranded DNA viruses which cause the lysis of a marine heterotrophic nanoflagellate (*Bodo* sp) occur in natural marine viral communities. Aquatic Microbial Ecology 9:203-210

Gasol JM, Vazquez-Dominguez E, Vaque D, Agusti S, Duarte CM (2009) Bacterial activity and diffusive nutrient supply in the oligotrophic Central Atlantic Ocean. Aquatic Microbial Ecology 56:1-12

Gobler CJ, Hutchins DA, Fisher NS, Cosper EM, Sanudo-Wilhelmy SA (1997) Release and bioavailability of C, N, P, Se, and Fe following viral lysis of a marine chrysophyte. Limnology and Oceanography 42:1492-1504

Gomez-Consarnau L, Akram N, Lindell K, Pedersen A, Neutze R, Milton DL, Gonzalez JM, Pinhassi J (2010) Proteorhodopsin phototrophy promotes survival of marine bacteria during starvation. PLOS Biology 8: E1000358. doi: 10.1371/journal.pbio.1000358

Grasshoff K (1983) Determination of nitrate. In: Grasshoff K, Erhardt M, Kremeling K (eds) Methods of Seawater Analysis. Verlag Chemie, Weinheim, Germany

Helder W, de Vries RTP (1979) An automatic phenol-hypochlorite method for the determination of ammonia in sea and brackish water. Netherlands Journal of Sea Research 13:154-160

Hoegh-Guldberg O, Bruno JF (2010) The impact of climate change on the world's marine ecosystems. Science 328:1523-1528

Huisman J, Thi NNP, Karl DM, Sommeijer B (2006) Reduced mixing generates oscillations and chaos in the oceanic deep chlorophyll maximum. Nature 439:322-325

Jurado E, Dijkstra HA, van der Woerd HJ (2012a) Microstructure observations during the spring 2011 STRATIPHYT-II cruise in the northeast Atlantic. Ocean Science 8:945-957

Jurado E, van der Woerd HJ, Dijkstra HA (2012) Microstructure measurements along a quasi-meridional transect in the northeastern Atlantic Ocean. Journal of Geophysical Research 117: C04016. doi: 10.1029/2011JC007137

Kirchman D (2001) Measuring bacterial biomass production and growth rates from leucine incorporation in natural aquatic environments. In: Paul JH (ed) Methods in Microbiology, vol. 30. Academic Press, San Diego

Kirchman DL (1990) Limitation of bacterial growth by dissolved organic matter in the subarctic Pacific. Marine Ecology Progress Series 62:47-54

Koroleff F (1969) Direct determination of ammonia in natural waters as indophenol blue. Coun. Meet. int. Coun. Explor. Sea **C.M.-ICES/C:** 9

Marie D, Brussaard CPD, Thyrhaug R, Bratbak G, Vaulot D (1999) Enumeration of marine viruses in culture and natural samples by flow cytometry. Applied and Environmental Microbiology 65:45-52

Massana R, del Campo J, Dinter C, Sommaruga R (2007) Crash of a population of the marine heterotrophic flagellate *Cafeteria roenbergensis* by viral infection. Environmental Microbiology 9:2660-2669

Michelou VK, Cottrell MT, Kirchman DL (2007) Light-stimulated bacterial production and amino acid assimilation by cyanobacteria and other microbes in the North Atlantic Ocean. Applied and Environmental Microbiology 73:5539-5546

Middelboe M (2000) Bacterial growth rate and marine virus-host dynamics. Microbial Ecology 40:114-124

Middelboe M, Jørgensen NOG (2006) Viral lysis of bacteria: an important source of dissolved amino acids and cell wall compounds. Journal of the Marine Biological Association of the United Kingdom 86:605-612

Middelboe M, Jørgensen NOG, Kroer N (1996) Effects of viruses on nutrient turnover and growth efficiency of noninfected marine bacterioplankton. Applied and Environmental Microbiology 62:1991-1997

Mills MM, Moore CM, Langlois R, Milne A, Achterberg E, Nachtigall K, Lochte K, Geider RJ, La Roche J (2008) Nitrogen and phosphorus co-limitation of bacterial productivity and growth in the oligotrophic subtropical North Atlantic. Limnology and Oceanography 53:824-834

Moebus K (1996) Marine bacteriophage reproduction under nutrient-limited growth of host bacteria. I. Investigations with six phage-host systems. Marine Ecology Progress Series 144:1-12

Mojica KDA, Brussaard CPD (2014) Factors affecting virus dynamics and microbial host-virus interactions in marine environments. FEMS Microbiology Ecology 89:495-515

Mojica KDA, Evans C, Brussaard CPD (2014) Flow cytometric enumeration of marine viral populations at low abundances. Aquatic Microbial Ecology 71:203-209

Mojica KDA, van de Poll WH, Kehoe M, Huisman J, Timmermans KR, Buma AGJ, van der Woerd HJ, Hahn-Woernle L, Dijkstra HA, Brussaard CPD (2015). Phytoplankton community structure in relation to vertical stratification along a north-south gradient in the Northeast Atlantic Ocean. Limnology and Oceanography (*in press*). doi: 10.1002/lno.10113

Motegi C, Nagata T (2007) Enhancement of viral production by addition of nitrogen or nitrogen plus carbon in subtropical surface waters of the South Pacific. Aquatic Microbial Ecology 48:27-34

Murphy J, Riley JP (1962) A modified single solution method for the determination of phosphate in natural waters. Analytica Chimica Acta 27:31-36

Nagasaki K, Ando M, Imai I, Itakura S, Ishida Y (1995) Virus-like particles in unicellular apochlorotic microorganisms in the coastal water of Japan. Fisheries Science 61:235-239

Obernosterer I, Herndl GJ (1995) Phytoplankton extracellular release and bacterial growth: dependence on the inorganic N:P Ratio. Marine Ecology Progress Series 116:247-257

Parada V, Herndl GJ, Weinbauer MG (2006) Viral burst size of heterotrophic prokaryotes in aquatic systems. Journal of the Marine Biological Association of the United Kingdom 86:613-621

Paul JH, Weinbauer M (2010) Detection of lysogeny in marine environments. In: Wilhelm SW, Weinbauer M, Suttle CA (eds) Manual of Aquatic Viral Ecology. ASLO

Payet JP, Suttle CA (2013) To kill or not to kill: the balance between lytic and lysogenic viral infection is driven by trophic status. Limnology and Oceanography 58:465-474

Polovina JJ, Howell EA, Abecassis M (2008) Ocean's least productive waters are expanding. Geophysical Research Letters 35: L03618. doi: 10.1029/2007GL031745

Proctor LM, Okubo A, Fuhrman JA (1993) Calibrating estimates of phage-induced mortality in marine bacteria: ultrastructural studies of marine bacteriophage development from one-step growth experiments. Microbial Ecology 25:161-182

R Development Core Team (2012) R: A language and environment for statistical computing. R Foundation for Statistical Computing: Vienna, Austria, ISBN 3-900051-07-0, http://www.R-project.org

Revelle W (2014) psych: Procedures for Psychological, Psychometric, and Personality Research.

Rivkin RB, Anderson MR (1997) Inorganic nutrient limitation of oceanic bacterioplankton. Limnology and Oceanography 42:730-740

Rychert K, Nawacka B, Majchrowski R, Zapadka T (2014) Latitudinal pattern of abundance and composition of ciliate communities in the surface waters of the Atlantic Ocean. Oceanological and Hydrobiological Studies 43:436-441

Sabine CL, Feely RA, Gruber N, Key RM, Lee K, Bullister JL, Wanninkhof R, Wong CS, Wallace DWR, Tilbrook B, Millero FJ, Peng TH, Kozyr A, Ono T, Rios AF (2004) The oceanic sink for anthropogenic CO_2. Science 305:367-371

Sarmento H, Montoya JM, Vazquez-Dominguez E, Vaque D, Gasol JM (2010) Warming effects on marine microbial food web processes: how far can we go when it comes to predictions? Philosophical Transactions of the Royal Scociety B 365:2137-2149

Sarmiento JL (2004) Response of ocean ecosystems to climate warming. Global Biogeochemical Cycles 18: GB3003. doi: 10.1029/2003GB002134

Schlitzer R (2002) Interactive analysis and visualization of geoscience data with Ocean Data View. Computers and Geoscience 28:1211-1218

Sheik AR, Brussaard CPD, Lavik G, Lam P, Musat N, Krupke A, Littmann S, Strous M, Kuypers MMM (2014) Responses of the coastal bacterial community to viral infection of the algae *Phaeocystis globosa*. The ISME Journal 8:212-225

Sherr BF, Sherr EB, Fallon RD (1987) Use of monodispersed, fluorescently labeled bacteria to estimate *In situ* protozoan bacterivory. Applied and Environmental Microbiology 53:958-965

Simon M, Azam F (1989) Protein content and protein synthesis rates of planktonic marine bacteria. Marine Ecology Progress Series 51:201-213

Straile D (1997) Gross growth efficiencies of protozoan and metazoan zooplankton and their dependence on food concentration, predator-prey weight ratio, and taxonomic group. Limnology and Oceanography 42:1375-1385

Suttle CA (2005) Viruses in the sea. Nature 437:356-361

Suttle CA (2007) Marine viruses - major players in the global ecosystem. Nature Reviews 5:801-812

Talley L, Pickard G, Emery W, Swift J (2011) Typical distribution of water characteristics. Descriptive Physical Oceanography. Elsevier Ltd., London

van de Poll WH, Kulk G, Timmermans KR, Brussaard CPD, van der Woerd HJ, Kehoe MJ, Mojica KDA, Visser RJW, Rozeman PD, Buma AGJ (2013) Phytoplankton chlorophyll *a* biomass, composition, and productivity along a temperature and stratification gradient in the northeast Atlantic Ocean. Biogeosciences 10:4227-4240

Vaulot D (1989) CYTOPC: Processing software for flow cytometric data. Signal and Noise 2:8

Weinbauer MG (2004) Ecology of prokaryotic viruses. FEMS Microbiology Reviews 28:127-181

Weinbauer MG, Brettar I, Hofle MG (2003) Lysogeny and virus-induced mortality of bacterioplankton in surface, deep, and anoxic marine waters. Limnology and Oceanography 48:1457-1465

Weinbauer MG, Suttle CA (1999) Lysogeny and prophage induction in coastal and offshore bacterial communities. Aquatic Microbial Ecology 18:217-225

Wilcox RM, Fuhrman JA (1994) Bacterial viruses in coastal seawater: lytic rather than lysogenic production. Marine Ecology Progress Series 114:35-45

Wilhelm SW, Brigden SM, Suttle CA (2002) A dilution technique for the direct measurement of viral production: a comparison in stratified and tidally mixed coastal waters. Microbial Ecology 43:168-173

Wilhelm SW, Suttle CA (1999) Viruses and nutrient cycles in the sea - viruses play critical roles in the structure and function of aquatic food webs. Bioscience 49:781-788

Williamson SJ, Houchin LA, McDaniel L, Paul JH (2002) Seasonal variation in lysogeny as depicted by prophage induction in Tampa Bay, Florida. Applied and Environmental Microbiology 68:4307-4314

Winget DM, Williamson KE, Helton RR, Wommack KE (2005a) Tangential flow diafiltration: an improved technique for estimation of virioplankton production. Aquatic Microbial Ecology 41:221-232

Supporting information

Table S1. Prokaryotic production (PP) determined by leucine incorporation (PP_L) and net production from whole water incubations (PPnet) with rates of viral mediated mortality (VMM) and protist mediated mortality (PMM). PP_{gross} is PP_L corrected for losses (assuming a 30% growth efficiency for grazing). All units are in $x10^8$ cells l^{-1} d^{-1}. n.d. = not determined.

Station	Depth Layer	PP_L	PP_{net}	VMM	PMM	PP_{gross}
3	ML	0.6	0.1	6.9	2.2	9.0
	DCM	2.1	0.2	8.4	4.2	13.4
5	ML	0.7	5.4	2.1	4.2	5.7
	DCM	0.9	0.1	1.5	3.1	4.5
7	ML	n.d.	5.4	3.1	1.9	n.d.
9	ML	0.9	0.3	3.7	2.2	6.1
	DCM	0.7	2.6	1.7	1.9	3.7
11	ML	1.1	1.3	3.4	2.3	6.1
13	ML	1.3	2.0	1.4	0.9	3.4
	DCM	1.5	1.2	5.8	3.4	9.7
15	ML	1.5	5.3	1.7	1.7	4.4
	DCM	1.1	0.8	1.8	2.8	4.9
16	ML	2.7	2.5	3.1	0.0	5.7
18	ML	2.5	4.8	0.5	3.7	5.5
19	ML	1.1	9.4	0.7	1.9	3.1
19	ML	1.2	4.8	1.5	1.6	3.8
21	ML	0.4	1.0	15.0	2.7	17.3
25	ML	3.0	7.8	5.2	3.8	10.9
27	ML	4.3	0.2	4.9	n.d.	9.1
29	ML	3.7	2.1	5.7	3.2	11.6
30	ML	n.d.	4.5	5.2	11.6	n.d.
32	ML	n.d.	0.6	28.7	n.d.	n.d.

Table S2. Brunt-Väisälä frequency (N^2), vertical mixing coefficient (K_T) and nutrient flux of PO_4^{3-} and NO_3^- at the depth of the euphotic zone for water sampled in the North Atlantic for heterotrophic prokaryotic production, viral production and grazing experiments. Abbreviations for depth layer are mixed layer (ML) and deep chlorophyll maximum (DCM). NA indicates that data were not available.

Station	Latitude (°N)	Longitude (°E)	Depth (m)	Depth Layer	N^2 ($x10^{-5}$ rad^2 s^{-1})	$LogK_T$ (m^{-2} s^{-1})	$Z_{eu}PO_4$ (mmol m^{-2} d^{-1})	$Z_{eu}NO_3$ (mmol m^{-2} d^{-1})
3	32.825	-14.589	15	ML	NA	-1.8	-0.013	-0.013
			60	DCM	NA	-4.7		
5	34.720	-14.258	15	ML	4.7	-2.5	-0.003	0.148
			85	DCM	14.2	-5.0		
7	36.526	-13.934	15	ML	6.6	-3.4	0.012	0.017
9	38.424	-13.586	15	ML	3.2	-3.2	0.002	0.011
			75	DCM	NA	-5.1		
11	40.528	-13.191	15	ML	2.5	-3.1	0.008	0.011
13	42.337	-12.884	15	ML	1.1	-3.0	0.003	0.018
			47	DCM	22.0	-4.8		
15	44.283	-12.605	15	ML	4.8	-2.6	-0.025	-0.149
			60	DCM	12.9	-4.7		
16	45.917	-12.363	10	ML	NA	-2.7	0.064	0.890
18	47.569	-12.110	25	ML	NA	-3.1	0.068	0.755
19	49.382	-11.829	15	ML	4.8	-2.6	0.003	0.401
19	49.382	-11.829	30	ML	2.5	-3.7	0.003	0.401
21	51.000	-11.567	15	ML	NA	-2.5	0.090	1.217
25	58.002	-16.516	10	ML	NA	-2.8	0.208	4.094
27	59.499	-18.067	20	ML	4.0	-3.8	0.064	0.487
29	60.684	-19.339	10	ML	4.4	-2.8	2.015	34.966
30	61.715	-20.489	15	ML	NA	-3.3	0.159	1.163
32	62.800	-21.736	10	ML	2.1	-4.1	0.024	0.199

Table S3. Spearman rank correlation coefficients (above the diagonal) and p-values (below the diagonal) of physicochemical paramters and Chl *a* for the ML samples. Abbreviations are for latitude (Lat), temperature (Temp), vertical mixing coefficient (K_T), Brunt-Väisälä frequency (N^2) and nutrient flux into the euphotic zone (Z_{eu}*). n.s. indicates non-significance at $\alpha = 0.05$.

	Lat	Temp	Salinity	K_T	N^2	$Z_{eu}PO_4$	$Z_{eu}NO_3$	PO_4^{3-}	NH_4^+	NO_2^-	NO_3^-	N:P	Chl *a*
Lat		-1.00	-0.94	n.s.	n.s.	n.s.	n.s.	0.89	n.s.	n.s.	0.84	n.s.	n.s.
Temp	0.00		0.94	n.s.	n.s.	n.s.	n.s.	-0.89	n.s.	n.s.	-0.84	n.s.	n.s.
Salinity	0.00	0.00		n.s.	n.s.	n.s.	n.s.	-0.94	n.s.	n.s.	-0.90	n.s.	n.s.
K_T	1.00	1.00	1.00		n.s.	n.s.	n.s.	n.s.	n.s.	n.s.	n.s.	n.s.	n.s.
N^2	1.00	1.00	1.00	0.09		n.s.	n.s.	n.s.	n.s.	n.s.	n.s.	n.s.	n.s.
$Z_{eu}PO_4$	1.00	1.00	1.00	1.00	1.00		n.s.	n.s.	-0.94	-0.99	n.s.	-0.83	-1.00
$Z_{eu}NO_3$	1.00	1.00	1.00	1.00	1.00	1.00		n.s.	n.s.	n.s.	n.s.	n.s.	n.s.
PO_4^{3-}	0.00	0.00	0.00	1.00	1.00	1.00	1.00		n.s.	n.s.	0.99	n.s.	n.s.
NH_4^+	1.00	1.00	1.00	1.00	1.00	0.00	1.00	1.00		0.89	n.s.	0.94	0.94
NO_2^-	1.00	1.00	1.00	1.00	1.00	0.00	1.00	1.00	0.00		n.s.	0.75	0.99
NO_3^-	0.00	0.00	0.00	1.00	1.00	1.00	0.14	0.00	1.00	1.00		n.s.	n.s.
N:P	1.00	1.00	1.00	1.00	1.00	0.00	1.00	1.00	0.00	0.03	1.00		0.83
Chl *a*	1.00	1.00	1.00	1.00	1.00	0.00	1.00	1.00	0.00	0.00	1.00	0.00	

Table S4. Spearman rank correlation coefficients (above the diagonal) and p-values (below the diagonal) of physicochemical paramters and Chl *a* for the DCM samples. Abbreviations are for latitude (Lat), temperature (Temp), vertical mixing coefficient (K_T), Brunt-Väisälä frequency (N^2) and nutrient flux into the euphotic zone (Z_{eu}*). n.s. indicates non-significance at $\alpha = 0.05$.

	Lat	Temp	Salinity	K_T	N^2	$Z_{eu}PO_4$	$Z_{eu}NO_3$	PO_4^{3-}	NH_4^+	NO_2^-	NO_3^-	N:P	Chl *a*
Lat		-1.00	-1.00	1.00	n.s.	n.s.	n.s.	1.00	n.s.	n.s.	1.00	n.s.	1.00
Temp	0.00		1.00	-1.00	n.s.	n.s.	n.s.	-1.00	n.s.	n.s.	-1.00	n.s.	-1.00
Salinity	0.00	0.00		-1.00	n.s.	n.s.	n.s.	-1.00	n.s.	n.s.	-1.00	n.s.	-1.00
K_T	0.00	0.00	0.00		n.s.	n.s.	n.s.	1.00	n.s.	n.s.	1.00	n.s.	1.00
N^2	1.00	1.00	1.00	1.00		n.s.	-1.00	n.s.	n.s.	-1.00	n.s.	-1.00	n.s.
$Z_{eu}PO_4$	1.00	1.00	1.00	1.00	1.00		n.s.	n.s.	-1.00	n.s.	n.s.	n.s.	n.s.
$Z_{eu}NO_3$	1.00	1.00	1.00	1.00	0.00	1.00		n.s.	n.s.	1.00	n.s.	1.00	n.s.
PO_4^{3-}	0.00	0.00	0.00	0.00	1.00	1.00	1.00		n.s.	n.s.	1.00	n.s.	1.00
NH_4^+	1.00	1.00	1.00	1.00	1.00	0.00	1.00	1.00		n.s.	n.s.	n.s.	n.s.
NO_2^-	1.00	1.00	1.00	1.00	0.00	1.00	0.00	1.00	1.00		n.s.	1.00	n.s.
NO_3^-	0.00	0.00	0.00	0.00	1.00	1.00	1.00	0.00	1.00	1.00		n.s.	1.00
N:P	1.00	1.00	1.00	1.00	0.00	1.00	0.00	1.00	1.00	0.00	1.00		n.s.
Chl *a*	0.00	0.00	0.00	0.00	1.00	1.00	1.00	0.00	1.00	1.00	0.00	1.00	

Table S5. Spearman rank correlation coefficients (above the diagonal) and p-vlaues (below diagonal) for abundances and mortality rates of microbial populations with biological and environmental parameters in the ML. Abbreviations are for vertical mixing coefficient (K_T), Brunt-Väisälä frequency (N^2), nutrient flux into the euphotic zone (Z_{eu}*), prokaryote (PA), viral (VA), virus to prokaryote ratio (VPR), heterotrophic nanaoflagellate abundance (HNF), prokaryotic production determined by leucine incorporation (PP_L) and with correction for loses (PP_{gross}), viral production (VP), protist mediated mortality (PMM), and the ratio of total mortality (TM) to PP_{gross}. n.s. indicates non-significance at $\alpha = 0.05$

	PA	VA	VPR	HNF	PP_L	PP_{gross}	Lytic VP	Prophage induction	Grazing rate	PMM	TM:PP_{gross}
Latitude	n.s.	0.93	n.s.	n.s.	1.00	n.s.	n.s.	n.s.	-0.89	n.s.	-0.81
Temperature	n.s.	-0.93	n.s.	n.s.	-1.00	n.s.	n.s.	n.s.	0.89	n.s.	0.81
Salinity	n.s.	-0.78	n.s.	n.s.	-0.94	n.s.	n.s.	n.s.	n.s.	n.s.	0.90
K_T	n.s.	n.s.	n.s.	n.s.	n.s.	n.s.	n.s.	n.s.	n.s.	n.s.	n.s.
N^2	n.s.	n.s.	n.s.	n.s.	n.s.	n.s.	n.s.	n.s.	n.s.	n.s.	n.s.
$Z_{eu}PO_4$	-0.77	n.s.	0.77	n.s.	n.s.	n.s.	n.s.	n.s.	n.s.	-0.89	n.s.
$Z_{eu}NO_3$	n.s.	n.s.	n.s.	n.s.	n.s.	n.s.	n.s.	0.85	n.s.	n.s.	n.s.
PO_4^{3-}	n.s.	n.s.	n.s.	n.s.	0.89	n.s.	n.s.	n.s.	n.s.	n.s.	-0.84
NH_4^+	n.s.	n.s.	-0.88	n.s.	n.s.	n.s.	n.s.	n.s.	n.s.	0.88	n.s.
NO_2^-	0.75	n.s.	n.s.	n.s.	n.s.	n.s.	n.s.	n.s.	n.s.	0.84	n.s.
NO_3^-	n.s.	n.s.	n.s.	n.s.	0.84	n.s.	n.s.	n.s.	n.s.	n.s.	-0.79
N:P	n.s.	n.s.	-0.94	n.s.	n.s.	0.77	0.83	n.s.	n.s.	0.89	n.s.
Chl *a*	0.77	n.s.	-0.77	n.s.	n.s.	n.s.	n.s.	n.s.	n.s.	0.89	n.s.
PA		0.75	n.s.	n.s.	n.s.	n.s.	n.s.	n.s.	n.s.	n.s.	n.s.
VA	0.03		n.s.	n.s.	0.93	n.s.	n.s.	n.s.	-0.99	n.s.	n.s.
VBR	1.00	1.00		n.s.	n.s.	n.s.	n.s.	n.s.	n.s.	-0.94	-0.75
HNF	1.00	1.00	1.00		n.s.	n.s.	n.s.	n.s.	n.s.	n.s.	n.s.
PP_L	1.00	0.00	1.00	1.00		n.s.	n.s.	n.s.	-0.89	n.s.	-0.81
PP_{gross}	1.00	1.00	1.00	1.00	1.00		0.94	n.s.	n.s.	n.s.	n.s.
Lytic VP	1.00	1.00	0.34	1.00	1.00	0.00		n.s.	n.s.	n.s.	n.s.
Prophage induction	1.00	1.00	1.00	1.00	1.00	1.00	1.00		n.s.	n.s.	n.s.
Grazing rate	0.09	0.00	1.00	1.00	0.00	1.00	1.00	1.00		n.s.	n.s.
PMM	1.00	1.00	0.00	1.00	1.00	0.34	1.00	1.00	1.00		n.s.
TM:PP_{gross}	1.00	0.42	0.03	0.75	0.00	1.00	1.00	1.00	0.50	0.14	

Table S6. Spearman rank correlation coefficients (above the diagonal) and p-vlaues (below diagonal) for abundances and mortality rates of microbial populations with biological and environmental parameters in the DCM. Abbreviations are for vertical mixing coefficient (K_T), Brunt-Väisälä frequency (N^2), nutrient flux into the euphotic zone (Z_{eu}*), prokaryote (PA), viral (VA), virus to prokaryote ratio (VPR), heterotrophic nanaoflagellate abundance (HNF), prokaryotic production determined by leucine incorporation (PP_L) and with correction for loses (PP_{gross}), viral production (VP), protist mediated mortality (PMM), and the ratio of total mortality (TM) to PP_{gross}. n.s. indicates non-significance at $\alpha = 0.05$ and NA indicates insufficient data

	PA	VA	VPR	HNF	PP_L	PP_{gross}	Lytic VP	Prophage induction	Grazing rate	PMM	TM:PP_{gross}
Latitude	n.s.	n.s.	n.s.	n.s.	n.s.	n.s.	n.s.	-1.00	n.s.	n.s.	n.s.
Temperature	n.s.	n.s.	n.s.	n.s.	n.s.	n.s.	n.s.	1.00	n.s.	n.s.	n.s.
Salinity	n.s.	n.s.	n.s.	n.s.	n.s.	n.s.	n.s.	1.00	n.s.	n.s.	n.s.
K_T	n.s.	n.s.	n.s.	n.s.	n.s.	n.s.	n.s.	-1.00	n.s.	n.s.	n.s.
N^2	n.s.	n.s.	1.00	n.s.	n.s.	n.s.	n.s.	n.s.	n.s.	1.00	n.s.
$Z_{eu}PO_4$	1.00	1.00	n.s.	n.s.	1.00	1.00	1.00	n.s.	-1.00	n.s.	n.s.
$Z_{eu}NO_3$	n.s.	n.s.	-1.00	n.s.	n.s.	n.s.	n.s.	n.s.	n.s.	-1.00	n.s.
PO_4^{3-}	n.s.	n.s.	n.s.	n.s.	n.s.	n.s.	n.s.	-1.00	n.s.	n.s.	n.s.
NH_4^+	-1.00	-1.00	n.s.	n.s.	-1.00	-1.00	-1.00	n.s.	1.00	n.s.	n.s.
NO_2^-	n.s.	n.s.	-1.00	n.s.	n.s.	n.s.	n.s.	n.s.	n.s.	-1.00	n.s.
NO_3^-	n.s.	n.s.	n.s.	n.s.	n.s.	n.s.	n.s.	-1.00	n.s.	n.s.	n.s.
N:P	n.s.	n.s.	-1.00	n.s.	n.s.	n.s.	n.s.	n.s.	n.s.	-1.00	n.s.
Chl *a*	n.s.	n.s.	n.s.	n.s.	n.s.	n.s.	n.s.	-1.00	n.s.	n.s.	n.s.
PA		1.00	n.s.	n.s.	1.00	1.00	1.00	n.s.	-1.00	n.s.	n.s.
VA	0.00		n.s.	n.s.	1.00	1.00	1.00	n.s.	-1.00	n.s.	n.s.
VBR	1.00	1.00		n.s.	n.s.	n.s.	n.s.	n.s.	n.s.	1.00	n.s.
HNF	1.00	1.00	1.00		n.s.	n.s.	n.s.	n.s.	n.s.	n.s.	NA
PP_L	0.00	0.00	1.00	1.00		1.00	1.00	n.s.	-1.00	n.s.	n.s.
PP_{gross}	0.00	0.00	1.00	1.00	0.00		1.00	n.s.	-1.00	n.s.	n.s.
Lytic VP	0.00	0.00	1.00	1.00	0.00	0.00		n.s.	-1.00	n.s.	n.s.
Prophage induction	1.00	1.00	1.00	1.00	1.00	1.00	1.00		n.s.	n.s.	n.s.
Grazing rate	0.00	0.00	1.00	1.00	0.00	0.00	0.00	1.00		n.s.	n.s.
PMM	1.00	1.00	0.00	1.00	1.00	1.00	1.00	1.00	1.00		n.s.
TM:PP_{gross}	1.00	1.00	1.00	NA	1.00	1.00	1.00	1.00	1.00	1.00	

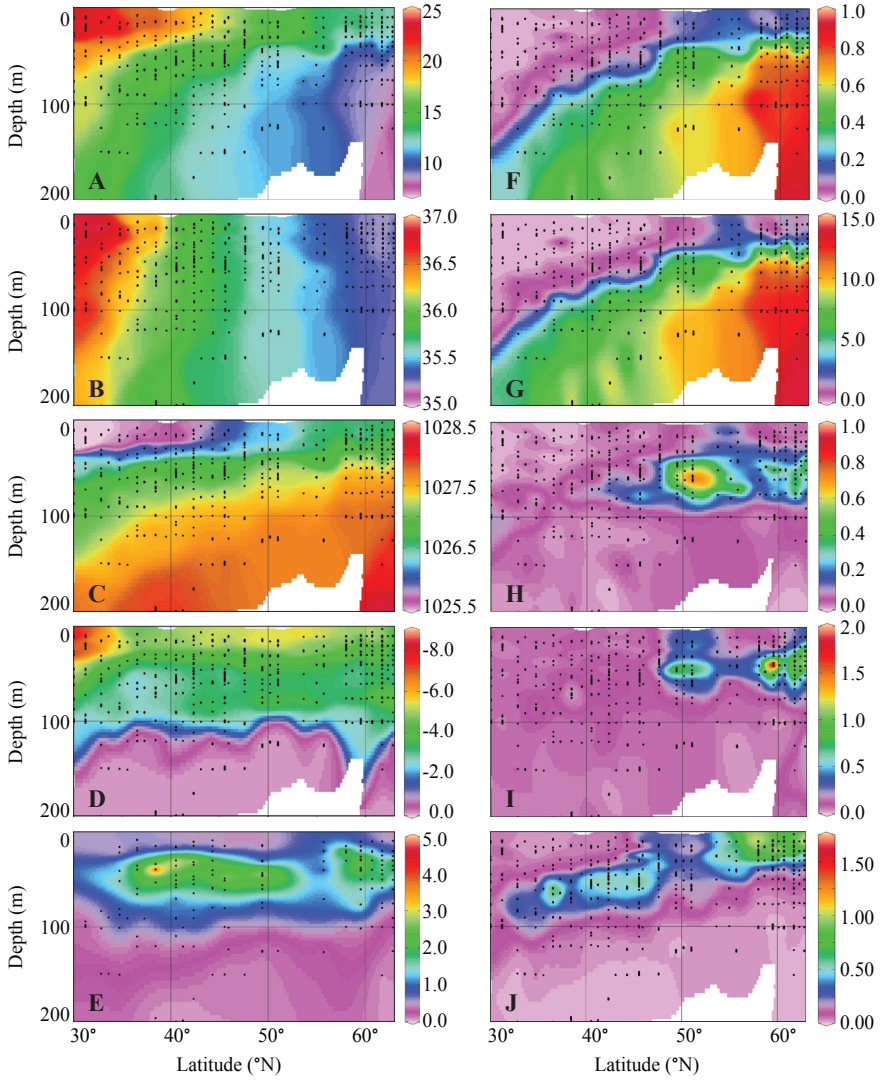

Figure S1. Latitudinal and depth distribution of (**A**) temperature (°C), (**B**) salinity, (**C**) density (kg m^{-3}), (**D**) $\log(K_T)$ (m^2 s^{-1}), (**E**) Brunt-Väisälä frequency, N^2 ($x10^{-4}$ rad^2 s^{-2}), (**F**) inorganic phosphate (µM), (**G**) nitrate (µM), (**H**) nitrite (µM), (**I**) ammonia (µM) and (**J**) Chl *a* autofluorescence (µg Chl *a* l^{-1}) measured during STRATIPHYT. Black dots indicate sampling points. Figure panels were prepared using Ocean Data View version 4 (Schlitzer 2002).

Chapter 7

The viral shunt in a stratified Northeast Atlantic Ocean

Kristina D. A. Mojica[1], and Corina P. D. Brussaard[1,2]

[1]Department of Biological Oceanography, Royal Netherlands Institute for Sea Research (NIOZ), P.O. Box 59, 1790 AB Den Burg, Texel, The Netherlands
[2]Department of Aquatic Microbiology, Institute for Biodiversity and Ecosystem Dynamics (IBED), University of Amsterdam, P.O. Box 94248, 1090 GE Amsterdam, The Netherlands

Abstract

The flux of photosynthetic carbon (C) through the viral shunt affects nutrient cycling, system respiration, and food web dynamics. Yet, little is known about large-scale biogeographical patterns in the functioning of the viral shunt in marine systems. In the summer of 2009, we examined both the production and loss rates (i.e., grazing and viral lysis) of autotrophic as well as prokaryotic microbial populations along a north-south latitudinal gradient in the Northeast Atlantic Ocean. The upper water column located between 30 and 63°N was characterized by a strong temperature-induced vertical stratification, with oligotrophic regions extending to 45°N. Here we present the flow of C through the different components of the microbial food web in order to consider how these latitudinal changes affected the overall role of the viral shunt. Our results demonstrate that 33 and 80% of the photosynthetically fixed C moved through the viral shunt into the dead particulate and dissolved matter pool in the north and south, respectively, indicating a more prominent role of viruses in marine nutrient cycles than theorized previously by Wilhelm and Suttle in 1999. The flux of C was reduced 2-fold in the north, as a consequence of lower viral-induced morality of both phytoplankton and bacteria. Our results suggest that future shifts in the regional climate of the ocean surface layer are likely to increase the role of the viral shunt in marine microbial food webs, which may reduce the transfer of matter and energy up the food chain and thus affect the capacity of the North Atlantic to act as a long-term sink for CO_2.

Introduction

Viruses are the smallest and most abundant biological entities on Earth. Perhaps nowhere is their importance better illustrated than in the world's oceans. A single milliliter of surface seawater contains on average 10^6 viruses and most of these viruses infect the numerically dominant hosts, i.e., microbial prokaryotes (bacteria and archaea) and photoautotrophic eukaryotes (Suttle 2007). Viral lysis of microbes diverts energy and biomass away from the classical food web towards microbial-mediated recycling and the dissolved organic matter (DOM) pool (Middelboe and Lyck 2002; Lønborg et al. 2013; Buchan et al. 2014). In this manner, the 'viral shunt' reduces the transfer of carbon and nutrients to higher trophic levels, while at the same time enhancing the recycling of potentially growth-limiting nutrients (Fuhrman 1999; Wilhelm and Suttle 1999). Through the use of theoretical models and poorly constrained rates, it was estimated that between 6 and 26% of the photosynthetically fixed carbon (PFC) is shunted to the DOM pool by the activity of viruses. However, until recently, our ability to confirm these figures and thus understand the true magnitude for the role of viruses in marine biogeochemical cycles has been restricted by a lack of quantitative measurements of viral lysis in marine phytoplankton populations (Weitz and Wilhelm 2012).

During the summer shipboard expedition of STRATIPHYT (Changes in vertical stratification and its impacts on phytoplankton communities) (Figure 1), the production and loss rates (i.e., grazing and viral lysis) of both autotrophic and prokaryotic microbial populations were examined along a latitudinal gradient in the Northeast Atlantic Ocean. This provided the possibility to model the flux of organic carbon (C) through the marine food web using measured values obtained from the same water. The Northeast Atlantic Ocean was characterized by a strong temperature-induced vertical stratification resulting in oligotrophic conditions in the upper 50 - 100 m at latitudes south of 45°N, whereas towards the north, nutrient limitation slightly relaxed in the upper 50 m surface layer (Mojica et al. 2015b). Dual measurements of viral lysis and grazing rates were obtained for all phytoplankton groups, except for *Prochlorococcus* HL which was largely absent from the sampled depths (Mojica et al. 2015a). Overall, rates of virus-induced mortality and grazing of phytoplankton were comparable. However, the relative share of viral lysis was highest at low and mid latitudes while phytoplankton mortality was dominated by microzooplankton grazing at higher latitudes (> 56°N). Total phytoplankton mortality (virus plus grazer-mediated) was comparable to the gross growth rates,

demonstrating high turnover rates of phytoplankton populations (Mojica et al. 2015a). For heterotrophic prokaryote populations, viral lysis was the dominate mortality factor (Mojica and Brussaard submitted).

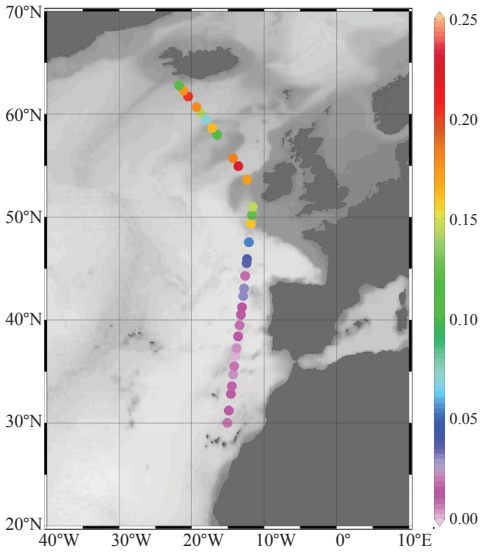

Figure 1. Bathymetric map of the Northeast Atlantic Ocean depicting station locations and PO_4 concentrations (μM) in the surface mixed layer during the summer 2009 (17 July – 9 August), using Ocean Data View (Schlitzer 2002).

Here we present the flux of C through the different components of the microbial food web along a stratified latitudinal gradient in order to consider (1) the effect of trophic state, on the overall relevance of the viral shunt, and (2) compare our results to the more theorized steady state model by Wilhelm and Suttle (1999).

Methods

Phytoplankton (< 20 μm diameter), prokaryotes and viruses were enumerated using a Becton-Dickinson FACSCalibur flow cytometer (FCM) equipped with an air-cooled Argon laser with an excitation wavelength of 488 nm (15 mW). Phytoplankton were enumerated according to Marie et al. (2005) and bacteria and viruses according to Marie et al. (1999) and Brussaard *et al.* (2010), respectively, with modifications according to Mojica et al. (2014). Phytoplankton were

differentiated based on their auto-fluorescence properties using bivariate scatter plots of either orange (i.e., phycoerythrin, present in prokaryotic *Synechococcus* spp.) or red fluorescence (i.e., chlorophyll *a*, present in all phytoplankton) against side scatter. Average cell size for phytoplankton subpopulations were determined by size-fractionation of whole water by sequential gravity filtration. Viruses and prokaryotes were discriminated using the nucleic acid-specific SYBR Green I and side scatter characteristics. Phytoplankton community composition and abundances were described previously by Mojica et al. (2015b).

Phytoplankton growth and loss rates used to calculate organic C-flux originate from Mojica et al. (in review), with the exception of mesozooplankton grazing (this study). Briefly, growth, viral lysis and microzooplankton (< 200 µm) grazing rates of the different photoautotrophic groups were determined using the modified dilution assay (Kimmance and Brussaard 2010). Experiments were conducted onboard, using water samples obtained from those depths where Chl *a* autofluorescence was maximal. The microzooplankton grazing rate (M_G) was estimated from the regression coefficient of the apparent growth rate versus fraction of natural seawater for the 0.45 µm series (i.e., removing grazers). The combined rate of viral-induced lysis and microzooplankton grazing (M_{V+G}) was estimated from a similar regression of the 30 kDa series (i.e, viruses and grazer removed). Viral lysis rate (M_V) was then determined as the difference between the combined mortality rate and the microzooplankton grazing rate. Phytoplankton gross growth rate (μ_{gross}, in the absence of mortality) was derived from the y-intercept of the 30 kDa series regression, and phytoplankton gross production (P_{gross}, cells l^{-1} d^{-1}) was calculated as $P_{gross} = P_0 \times (e^{\mu t})$, where P_0 is phytoplankton abundance, t is time (d) and µ is μ_{gross}. Phytoplankton net growth rate (μ_{net}, d^{-1}) was defined as the difference between μ_{gross} and total mortality rate, and phytoplankton net production (P_{net}, cells l^{-1} d^{-1}) calculated according to the previous equation, where µ is μ_{net}. Total mortality rate in cells (TMM), was then calculated by subtracting P_{net} from P_{gross}. Virus mediated mortality (VMM) and grazing mediated mortality (GMM) was calculated as $VMM = (M_V/M_{V+G})*TMM$ and $GMM = (M_G/M_{V+G})*TMM$, respectively. To convert P_{gross} to gross primary production (C l^{-1} d^{-1}), cells were converted to C using conversion factors of 237 fg C μm^{-3} (Worden et al. 2004) and 196.5 fg C μm^{-3} (Garrison et al. 2000) for pico- and nano-sized phytoplankton, respectively, assuming spherical diameters equivalent to the average cell size determined from size fractionation. To obtain total photosynthetically fixed carbon (PFC), we added 20% for respiration (Langdon 1993, Lopez-Sandoval et al. 2014) and a standard 20% for excretion

(Teira et al. 2003). However, in order to maintain steady-state in the model with respect to net production in the north, excretion was increased to 28%.
Mesozooplankton were collected using a 300 µm vertical net with a 0.35 m^2 opening and grazing rates were determined using the gut fluorescence approach in combination with HPLC pigment analysis (Baars and Oosterhuis 1984). Mesozooplankton were dominated by copepods (95±7% of total counts), with *Acartia clausii* and *Calanus finmarchicus* comprising 49% and 26% of the community, respectively. Mesozooplankton grazing of phytoplankton was considered negligible (< 0.1%) in the south and on average 0.64±0.5% of Chl *a* in the north. To convert to C, a C:Chl *a* ratio of 50 was applied (Brown et al. 1999), this value was shown to give good agreement between carbon estimated from HPLC and FCM analysis (Mojica et al. 2015b). Due to dominance of pico-sized phytoplankton (95% of total), low net primary production and low mesozooplankton grazing rates, sinking was assumed negligible (Jackson 2001; Richardson and Jackson 2007) Although there is evidence of viral-induced mortality for marine zooplankton (Garza and Suttle 1995; Nagasaki et al. 1995; Drake and Dobbs 2005; Massana et al. 2007), actual rates of loss are still largely unknown (current estimates are < 5% of production for copepods) and therefore are not included in the model. The remaining mesozooplankton production was assumed to be ingested by higher trophic levels with 20% of the ingested carbon being transferred to the DOC pool (Jumars et al. 1989) (Table 1).
Heterotrophic prokaryotic abundance, viral mediated mortality and grazing data are reported in Mojica et al. (submitted). In short, heterotrophic prokaryotic production was determined from leucine incorporation rates according to Simon and Azam (1989) and corrected for loss due to viral lysis and grazing (Mojica et al. submitted; assuming the rate of mortality in the samples was equivalent to those measured by the mortality assays and 30% of carbon grazed was retained on filter). Protistian grazing rates of prokaryotes were determined using fluorescently labeled natural prokaryotes (FLP) according to the procedure described by Sherr and Sherr (1987). Protist mediated mortality (PMM) was calculated as $PMM = PA_0 \times (e^{rt}-1)$ where PA is prokaryote abundance, t is time (d), and r is the grazing rate obtained from FLP experiments. Viral production (VP) was determined according to Winget et al. (2005). Lytic viral mediated mortality (VMM) was calculated by dividing lytic virus production by a burst size of according to estimates for oligotrophic regions of the ocean (Parada et al. 2006). A conversion factor of 12.4 fg C $cell^{-1}$ was used for heterotrophic bacteria (Fukuda et al. 1998). In order to maintain steady-state in the model with respect to heterotrophic prokaryotic production, net C production was

balanced as loss through excretion (Stoderegger and Herndl 1998, 2001), which were 4 and 16% for the south and north, respectively.

For the zooplankton, literature values were used for the growth efficiencies and fraction of C shunted to dead particulate and dissolved matter (P/DOC) pool (Table 1). Alternative modes of grazer-associated release include "sloppy feeding", excretion, and egestion and dissolution of fecal pellets. It is estimated that around 50% of the food ingested by microzooplankton is lost to respiration, which is consistent with a growth efficiency of around 30% (Calbet and Landry 2004). Twenty percent of the carbon intake by microzooplankton was considered to be partitioned to the P/DOC pool due to the combination of direct excretion (max 9%; Taylor et al. 1985) and rapid dissolution of small fecal pellets (Turner 2002; Buck et al. 2005), while sloppy feeding by microzooplankton was considered negligible (Møller et al. 2003; Møller 2005; Saba et al. 2011). We assume that all available microzooplankton biomass is grazed by mesozooplankton, with 24% of ingested C lost to DOC (3% by sloppy feeding, 12% excretion and 9% fecal pellet DOC released within in the euphotic zone; Møller et al. 2003; Urban-Rich et al. 2004; Møller 2005; Saba et al. 2011) and mesozooplankton gross growth efficiency was 0.25 (Straile 1997).

Table 1. Measured variables and model parameters applied in steady state C-flux model presented in Figure 2 and 3.

Variables			
α	Phytoplankton C production		
α_V	Phytoplankton C lysed		
α_{G1}	Phytoplankton C grazed by microzooplankton		
α_{G2}	Phytoplankton C grazed by mesozooplankton		
β	Bacterial C production		
β_V	Bacterial C lysed		
β_G	Bacterial C grazed by microzooplankton		
γ	Microzooplankton C production		
γ_G	Microzooplankton C grazed		
ζ	Mesozooplankton C production		
η	Higher trophic level C production		
P/DOC	Dissolved organic carbon from all sources and particulate cell debris C resulting from viral lysis		
Parameters			**References**
α_E	Phytoplankton C lost to excretion*	0.2	(Teira et al. 2003)
β_E	Bacterial C lost to excretion*	0.04	(Stoderegger and Herndl 1998; Stoderegger and Herndl 2001; Kawasaki and Benner 2006)
GGE_γ	Gross growth rate efficiency of microzooplankton	0.3	(Straile 1997; Calbet and Landry 2004)
φ_1	Fraction of C cycled to the P/DOC pool from microzooplankton activity	0.2	(Taylor et al. 1985; Turner 2002; Buck et al. 2005)
GGE_ζ	Gross growth rate efficiency of mesozooplankton	0.25	(Straile 1997)
φ_2	Fraction of C cycled to P/DOC pool from excretion, pellet dissolution and sloppy feeding of mesozooplankton	0.24	(Møller et al. 2003; Urban-Rich et al. 2004; Møller 2005; Saba et al. 2011)
GGE_η	Gross growth rate efficiency of higher trophic levels	0.15	(Houde 1989)
φ_3	Fraction of C cycled to P/DOC pool from higher trophic levels	0.2	(Jumars et al. 1989)

* to force steady state values differ in northern region

Results

The upper surface waters of the Northeast Atlantic Ocean along the meridional transect between 30 - 63°N were characterized by strong temperature-induced vertical stratification. The southern half of the transect (< 45°N) was distinguished by oligotrophic surface waters (i.e., Chl *a* < 0.7 µg l^{-1} and NO_3^- ≤ 0.13 and PO_4^{3-} ≤ 0.03 µM; Polovina et al. 2008; van de Poll et al. 2013) (Figure 1). In the northern half (46 - 63°N). In the north, inorganic nutrients and Chl *a* concentrations increased within the ML to average 1.30±0.60 µM, 0.14±0.04 µM and 1.1±0.3 µg $l^{-1}$for NO_3^-,

PO_4^{3-} and Chl *a*, respectively. Consequently, the distribution and composition of microbial communities varied between these two regions (Mojica et al. 2015b; Mojica and Brussaard submitted) and accordingly regions are presented separately here.

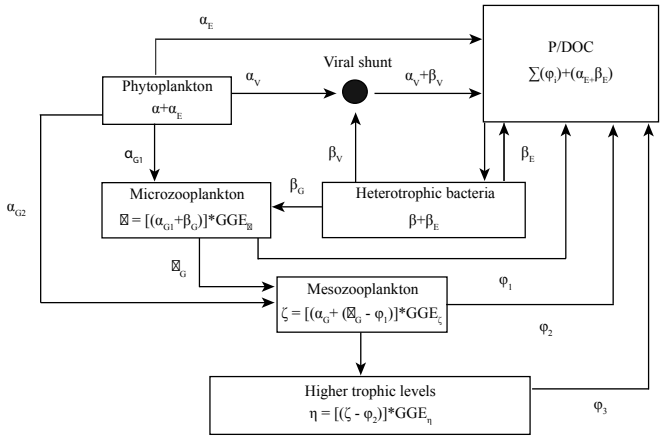

Figure 2. Flow diagram of steady state carbon flux model through a pelagic food web. See Table 1 for more explanation of variables, parameters and symbols. Carbon lost to respiration is included but not explicitly illustrated.

PFC in the oligotrophic south averaged 10.6 µg C l^{-1} d^{-1}, while in the north PFC was about 4-fold higher (47.2 µg C l^{-1} d^{-1}) as a result of 2-fold higher total phytoplankton biomass (larger contribution of nanoeukaryotic phytoplankton (Figure 2 and 3) (Mojica et al. 2015b). Viral lysis was the dominate loss factor for phytoplankton C in the south with an average 3.7 µg C l^{-1} d^{-1} being shunted into the P/DOM pool compared to 2.7 µg C l^{-1} d^{-1} being grazed (Table 1, Figure 3a). In the north, microzooplankton grazing C-flux was higher than viral lysis, accounting for 11.5 µg C l^{-1} d^{-1} of PFC loss compared to 9.9 µg C l^{-1} d^{-1} being lysed (Figure 3b). Heterotrophic prokaryotic production was 9.0 µg C l^{-1} d^{-1} in the south, with 4.8 µg C l^{-1} d^{-1} lost to viral lysis and 3.8 µg C l^{-1} d^{-1} being grazed by microzooplankton. In the north, production was only slightly higher at 10.4 µg C l^{-1} d^{-1} and viral lysis remained the dominate loss factor, with 5.7 µC l^{-1} d^{-1} being shunted to the P/DOC pool compared to 3.0 µg C l^{-1} d^{-1} being transferred to microzooplankton.

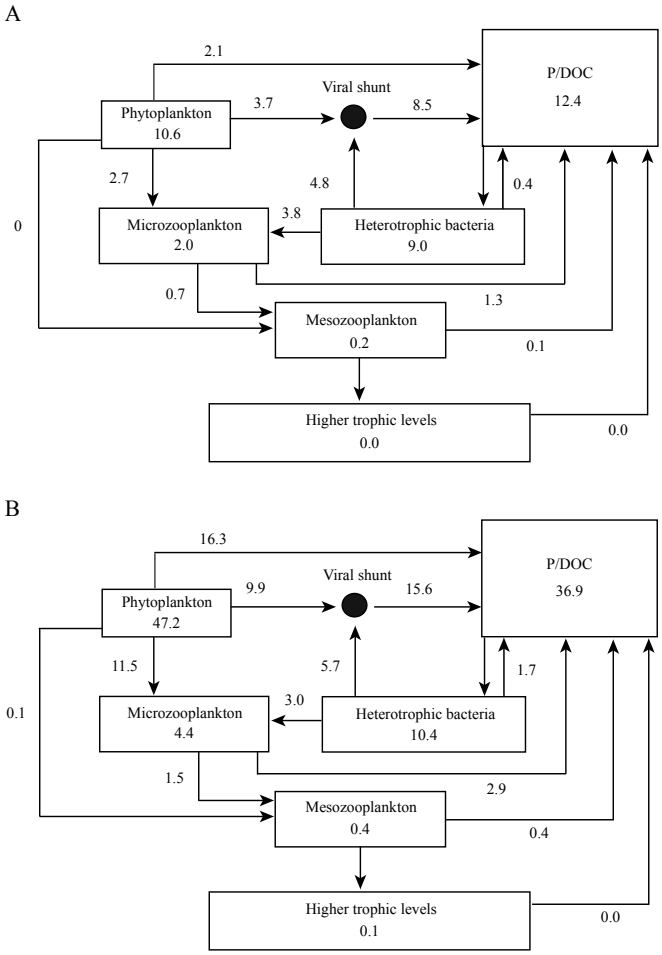

Figure 3. Carbon flow (μg C l^{-1} d^{-1}) through a pelagic food web in steady state for both the (**A**) southern (30 - 45°N) and (**B**) northern region (45 - 63°N) region of the Northeast Atlantic Ocean during the summer STRATIPHYT cruise. See Table 1 for explanation of variables, parameters and symbols, and Figure 2 for equations. Carbon lost to respiration is included but not explicitly illustrated.

Total microzooplankton production and the contribution by microzooplankton to the P/DOM pool was ~ 2-fold higher in the south compared to the north (i.e., 2.0 and 1.3 μg C l^{-1} d^{-1} compared to 4.4 and 2.9 μg C l^{-1} d^{-1}) (Figure 3a and b). DOC release by mesozooplankton was 0.1 and 0.4 μg C l^{-1} d^{-1} for the south and north, respectively. The P/DOC contribution from higher trophic levels was then 0.04 (taken as zero) and 0.06 (taken as 0.1) μg C l^{-1} d^{-1} for the south and north respectively, assuming all zooplankton production was consumed.

Discussion

The steady state assumption of our model was supported in the southern region, with 100% and 95% of the phytoplankton and prokaryotic heterotrophic cellular production being lost through the combined mortality of grazing and viral lysis (Figure 3a; excluding respiration and excretion). However, the north demonstrated a net production of 14% and 16% for phytoplankton and bacteria, respectively, when steady state was not enforced via increasing excretion. Nevertheless, values of excretion remained within the range reported in literature (Stoderegger and Herndl 1998; Stoderegger and Herndl 2001; Kawasaki and Benner 2006) and confer with evidence that rates increase with productivity (Baines and Pace 1991). The ratios of prokaryotic heterotrophic production to primary production (HP:PP) in our study (0.85 and 0.22 for south and north, respectively) are relatively high (Ducklow 1999). However, they are comparable to HP:PP reported for the North Atlantic by Hoppe et al. (2002) (0.01 - 0.83), who found also the highest values in subtropical regions. HP:PP is dependent upon the conversion efficiency and the degree of recycling and therefore can theoretically exceed 1.0 when recycling is intense (Ducklow et al. 2002). The source of dissolved and dead particulate dead matter, whether through passive diffusion across phytoplankton cell membranes, actively excreted, released from sloppy feeding, diffused from fecal pellets or released from viral lysis, affects both the chemical composition and bioavailability (Middelboe and Jorgensen 2006; Kirchman et al. 2013; Lønborg et al. 2013). Taking into considering dominance of viral lysis as a loss factor for both heterotrophic and autotrophic production within the oligotrophic region (thus prokaryotic C-demand is not restricted to excretion and DOC released from grazing activity) and recent evidence for a diverse array of enzymatic capabilities within bacteria in subtrophic regions (Arnosti et al. 2011), together may help explain why open ocean areas can have bacterial carbon demands that exceed primary production estimates. Furthermore, the steady-state model does not account for excretion by standing stock populations which would also be utilized to support the bacterial carbon demand.

The recognition for the importance of the 'viral shunt' to nutrient cycles and energy flow in the ocean was supported through the use of (mostly) theoretical models (Fuhrman 1992; Wilhelm and Suttle 1999). Simultaneous measurements of growth and loss rate rates for phytoplankton as well as heterotrophic bacteria provide an ideal dataset to further substantiate the role of the viral shunt in marine systems.

Our study confirms the relevance of the viral shunt for diverting energy and biomass away from the classical grazer-mediated food web towards microbial-mediated recycling and the dissolved organic matter pool (Figure 4). More importantly, our data show that the percentage of PFC in stratified waters which was recycled back to the P/DOC pool by viral lysis, 33 and 80% (Figure 4), was substantially higher than the previous estimates of 6 - 26% (Wilhelm and Suttle 1999). These former estimates consisted of a 2 - 10% contribution of PFC from the viral-induced mortality of phytoplankton and 3 - 15% from heterotrophic bacteria. Our data show higher values for both groups, i.e., 35 and 45% for the southern and 21 and 12% for the northern phytoplankton and heterotrophic prokaryotes, respectively (Figure 4), with the strongest increase in flux of PFC from phytoplankton lysis. Considering that the mortality of zooplankton due to viral infection was not accounted for here (Garza and Suttle 1995; Nagasaki et al. 1995; Drake and Dobbs 2005; Massana et al. 2007), these values likely still represent an underestimate. Overall, our results indicate that during summer stratification in the northeastern Atlantic Ocean the viral shunt plays a significant role in marine food web dynamics, particularly in the oligotrophic region.

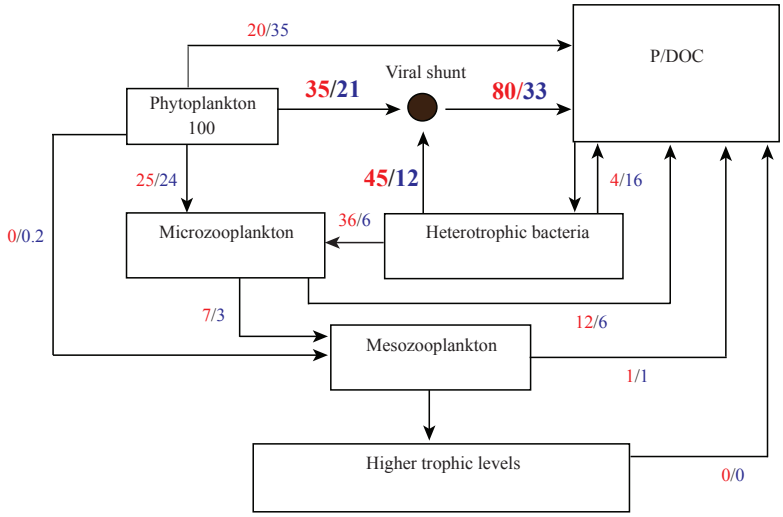

Figure 4. The C-flux for the pelagic food web for both the oligotrophic south (red) and the northern region (blue) of the Northeast Atlantic Ocean cruise transect. Fluxes are indicated as percentage of total photosynthetically fixed carbon (100%). The percentage of photosynthetically fixed carbon flowing through the viral shunt is indicated in large bold print. All carbon is assumed to be eventually respired, with negligible loss due to export. This steady state model also assumes that all carbon in the P/DOC pool is bioavailable to heterotrophic prokaryotes.

Due to deep water formation, the North Atlantic is key to ocean circulation and global climate (Sabine et al. 2004). Several studies predict that global warming will result in a stronger temperature-induced vertical stratification and subsequent oligotrophication in the North Atlantic Ocean (Sarmiento 2004; Polovina et al. 2008). Consequently, changes in phytoplankton community structure are anticipated, e.g. enhanced dominance of smaller-sized phytoplankton (Mojica et al. in press) and northward expansion of (sub)tropical photoautotrophs such as the cyanobacterium *Prochlorococcus* spp. (expanding up to 50°N in the year 2100; Flombaum et al. 2013). The C-flux model presented here indicates that this will enhance the role of the microbial loop due to an amplified viral shunt, increased microzooplankton grazing on heterotrophic prokaryotes and tighter coupling between P/DOC and heterotrophic production. The partitioning of photosynthetic C through the different pathways (i.e., grazing versus cell lysis) has important implications for ecosystem function as each pathway differentially affects the structure and functioning of pelagic microbial food webs. Grazing transfers matter to higher trophic levels, thereby increasing the overall efficiency and carrying capacity of the ecosystem. In addition, the production of fecal pellets by mesozooplankton in the open ocean is responsible for much of the carbon transported out of the euphotic zone into the deeper ocean (Ducklow et al. 2001). A more prominent role of the viral shunt in the northern North Atlantic Ocean would thus markedly reduce biological C-export into the ocean's interior in one of the key areas of global C-sequestration, and reduce the potential for it to function as a long-term sink for anthropogenic carbon dioxide.

Acknowledgements

The STRATIPHYT project (Grant number 839.08.420) was supported by the division for Earth and Life Sciences Foundation (ALW), with financial aid from the Netherlands Organization for Scientific Research (NWO). We thank the captains and shipboard crews of R/V Pelagia and scientific crew during the cruise, with special thanks to Swier Oosterhuis. We acknowledge the support of NIOZ-Marine Research Facilities (MRF) on-shore and on-board.

References

Arnosti C, Steen AD, Ziervogel K, Ghobrial S, Jeffrey WH (2011) Latitudinal gradients in degradation of marine dissolved organic carbon. PLOS One 6: e28900. doi: 10.1371/journal.pone.0028900

Baars MA, Oosterhuis SS (1984) Diurnal feeding rhythms in North Sea copepods measured by gut fluorescence, digestive enzyme activity and grazing on labeled food. Netherlands Journal of Sea Research 18:97-119

Baines SB, Pace ML (1991) The production of dissolved organic-matter by phytoplankton and its importance to bacteria: patterns across marine and fresh water systems. Limnology and Oceanography 36:1078-1090

Brown SL, Landry MR, Barber RT, Campbell L, Garrison DL, Gowing MM (1999) Picophytoplankton dynamics and production in the Arabian Sea during the 1995 Southwest Monsoon. Deep-Sea Research, Part II 46:1745-1768

Brussaard CPD, Payet JP, Winter C, Weinbauer M (2010) Quantification of aquatic viruses by flow cytometry. In: Wilhelm SW, Weinbauer MG, Suttle CA (eds) Manual of Aquatic Viral Ecology. ASLO

Buchan A, LeCleir GR, Gulvik CA, Gonzalez JM (2014) Master recyclers: features and functions of bacteria associated with phytoplankton blooms. Nature Reviews Microbiololgy 12:686-698

Buck KR, Marin R, Chavez FP (2005) Heterotrophic dinoflagellate fecal pellet production: grazing of large, chain-forming diatoms during upwelling events in Monterey Bay, California. Aquatic Microbial Ecology 40:293-298

Calbet A, Landry MR (2004) Phytoplankton growth, microzooplankton grazing, and carbon cycling in marine systems. Limnology and Oceanography 49:51-57

Drake LA, Dobbs FC (2005) Do viruses affect fecundity and survival of the copepod *Acartia tonsa* Dana? Journal of Plankton Research 27:167-174

Ducklow HW (1999) The bacterial component of the oceanic euphotic zone. FEMS Microbiology Ecology 30:1-10

Ducklow HW, Kirchman DL, Anderson TR (2002) The magnitude of spring bacterial production in the North Atlantic Ocean. Limnology and Oceanography 47:1684-1693

Ducklow HW, Steinberg DK, Buesseler KO (2001) Upper ocean carbon export and the biological pump. Oceanography 14:50-58

Flombaum P, Gallegos JL, Gordillo RA, Rincon J, Zabala LL, Jiao N, Karl DM, Li WKW, Lomas MW, Veneziano D, Vera CS, Vrugt JA, Martiny AC (2013) Present and future global distributions of the marine cyanobacteria *Prochlorococcus* and *Synechococcus*. Proceedings of the National Academy of Sciences of the United States of America 110:9824-9829

Fuhrman JA (1992) Bacterioplankton roles in cyling of organic matter: the microbial food web. In: Falkowski PG, Woodhead AD (eds) Primary Productivity and Biogeochemical Cycles in the Sea. Plenum Press, New York, NY

Fuhrman JA (1999) Marine viruses and their biogeochemical and ecological effects. Nature 399:541-548

Fukuda R, Ogawa H, Nagata T, Koike I (1998) Direct determination of carbon and nitrogen contents of natural bacterial assemblages in marine environments. Applied and Environmental Microbiology 64:3352-3358

Garrison DL, Gowing MM, Hughes MP, Campbell L, Caron DA, Dennett MR, Shalapyonok A, Olson RJ, Landry MR, Brown SL, Liu HB, Azam F, Steward GF, Ducklow HW, Smith DC (2000) Microbial food web structure in the Arabian Sea: a US JGOFS study. Deep-Sea Research, Part II 47:1387-1422

Garza DR, Suttle CA (1995) Large double-stranded DNA viruses which cause the lysis of a marine heterotrophic nanoflagellate (*Bodo* sp) occur in natural marine viral communities. Aquatic Microbial Ecology 9:203-210

Hoppe HG, Gocke K, Koppe R, Begler C (2002) Bacterial growth and primary production along a north-south transect of the Atlantic Ocean. Nature 416:168-171

Houde ED (1989) Comparative growth, mortality, and energetics of marine fish larvae: temperature and implied latitudinal effects. Fishery Bulletin 87:471-495

Jackson GA (2001) Effect of coagulation on a model planktonic food web. Deep-Sea Research Part I 48:95-123

Jumars PA, Penry DL, Baross JA, Perry MJ, Frost BW (1989) Closing the microbial loop: dissolved carbon pathway to heterotrophic bacteria from incomplete ingestion, digestion and absorption in animals. Deep-Sea Research 36:483-495

Kawasaki N, Benner R (2006) Bacterial release of dissolved organic matter during cell growth and decline: molecular origin and composition. Limnology and Oceanography 51:2170-2180

Kimmance SA, Brussaard CPD (2010) Estimation of viral-induced phytoplankton mortality using the modified dilution method. In: Wilhelm SW, Weinbauer M, Suttle CA (eds) Manual of Aquatic Viral Ecology. ASLO

Kirchman DL, Lancelot C, Fasham M, Legendre L, Radach G, Scott M (2013) Dissolved organic matter in biogeochemical models of the ocean. In: Evans GT, Fasham MJR (eds) Towards a Model of Ocean Biogeochemical Processes. Springer Berlin Heidelberg

Langdon C (1993) The significance of respiration in production measurements based on oxygen. ICES Marine Science Symposium 197:69-78

Lønborg C, Middelboe M, Brussaard CPD (2013) Viral lysis of *Micromonas pusilla*: impacts on dissolved organic matter production and composition. Biogeochemistry 116:231-240

López-Sandoval DC, Rodríguez-Ramos T, Cermeño P, Sobrino C, Marañón E (2014) Photosynthesis and respiration in marine phytoplankton: Relationship with cell size, taxonomic affiliation, and growth phase. Journal of Experimental Marine Biology and Ecology 457:151-159

Marie D, Brussaard CPD, Thyrhaug R, Bratbak G, Vaulot D (1999) Enumeration of marine viruses in culture and natural samples by flow cytometry. Applied and Environmental Microbiology 65:45-52

Marie D, Simon N, Vaulot D (2005) Phytoplankton cell counting by flow cytometry. In: Andersen RA (ed) Algal Culturing Techniques. Elsevier Academic Press: Burlington, MA

Massana R, del Campo J, Dinter C, Sommaruga R (2007) Crash of a population of the marine heterotrophic flagellate *Cafeteria roenbergensis* by viral infection. Environmental Microbiology 9:2660-2669

Middelboe M, Jørgensen NOG (2006) Viral lysis of bacteria: an important source of dissolved amino acids and cell wall compounds. Journal of the Marine Biological Association of the United Kingdom 86:605-612

Middelboe M, Lyck PG (2002) Regeneration of dissolved organic matter by viral lysis in marine microbial communities. Aquatic Microbial Ecology 27:187-194

Mojica KDA, Evans C, Brussaard CPD (2014) Flow cytometric enumeration of marine viral populations at low abundances. Aquatic Microbial Ecology 71:203-209

Mojica KDA, Huisman J, Wilhelm SW, Brussaard CPD (2015a) Latitudinal variation in virus-induced mortality of phytoplankton across the North Atlantic Ocean. The ISME Journal, *in press*

Mojica KDA, van de Poll WH, Kehoe M, Huisman J, Timmermans KR, Buma AGJ, van der Woerd HJ, Hahn-Woernle L, Dijkstra HA, Brussaard CPD (2015b). Phytoplankton community structure in relation to vertical stratification along a north-south gradient in the Northeast Atlantic Ocean. Limnology and Oceanography (*in press*). doi: 10.1002/lno.10113

Møller EF (2005) Sloppy feeding in marine copepods: prey-size-dependent production of dissolved organic carbon. Journal of Plankton Research 27:27-35

Møller EF, Thor P, Nielsen TG (2003) Production of DOC by *Calanus finmarchicus*, *C. glacialis* and *C. hyperboreus* through sloppy feeding and leakage from fecal pellets. Marine Ecology Progress Series 262:185-191

Nagasaki K, Ando M, Imai I, Itakura S, Ishida Y (1995) Virus-like particles in unicellular apochlorotic microorganisms in the coastal water of Japan. Fisheries Science 61:235-239

Parada V, Herndl GJ, Weinbauer MG (2006) Viral burst size of heterotrophic prokaryotes in aquatic systems. Journal of the Marine Biological Association of the United Kingdom 86:613-621

Polovina JJ, Howell EA, Abecassis M (2008) Ocean's least productive waters are expanding. Geophysical Research Letters 35:L03618. doi: 10.1029/2007GL031745

Richardson TL, Jackson GA (2007) Small phytoplankton and carbon export from the surface ocean. Science 315:838-840

Saba GK, Steinberg DK, Bronk DA (2011) The relative importance of sloppy feeding, excretion, and fecal pellet leaching in the release of dissolved carbon and nitrogen by *Acartia tonsa* copepods. Journal of Experimental Marine Biology and Ecology 404:47-56

Sabine CL, Feely RA, Gruber N, Key RM, Lee K, Bullister JL, Wanninkhof R, Wong CS, Wallace DWR, Tilbrook B, Millero FJ, Peng TH, Kozyr A, Ono T, Rios AF (2004) The oceanic sink for anthropogenic CO_2. Science 305:367-371

Sarmiento JL (2004) Response of ocean ecosystems to climate warming. Global Biogeochemical Cycles 18:GB3003. doi: 10.1029/2003GB002134

Schlitzer R (2002) Interactive analysis and visualization of geoscience data with Ocean Data View. Computers and Geosciences 28:1211-1218

Sherr BF, Sherr EB, Fallon RD (1987) Use of monodispersed, fluorescently labeled bacteria to estimate *in situ* protozoan bacterivory. Applied and Environmental Microbiology 53:958-965

Simon M, Azam F (1989) Protein content and protein synthesis rates of planktonic marine bacteria. Marine Ecology Progress Series 51:201-213

Stoderegger K, Herndl GJ (1998) Production and release of bacterial capsular material and its subsequent utilization by marine bacterioplankton. Limnology and Oceanography 43:877-884

Stoderegger KE, Herndl GJ (2001) Visualization of the exopolysaccharide bacterial capsule and its distribution in oceanic environments. Aquatic Microbial Ecology 26:195-199

Straile D (1997) Gross growth efficiencies of protozoan and metazoan zooplankton and their dependence on food concentration, predator-prey weight ratio, and taxonomic group. Limnology and Oceanography 42:1375-1385

Suttle CA (2007) Marine viruses - major players in the global ecosystem. Nature Reviews 5:801-812

Taylor GT, Iturriaga R, Sullivan CW (1985) Interactions of bactivorous grazers and heterotrophic bacteria with dissolved organic matter. Marine Ecology Progress Series 23:129-141

Teira E, Pazo MJ, Quevedo M, Fuentes MV, Niell FX, Fernandez E (2003) Rates of dissolved organic carbon production and bacterial activity in the eastern North Atlantic Subtropical Gyre during summer. Marine Ecology Progress Series 249:53-67

Turner JT (2002) Zooplankton fecal pellets, marine snow and sinking phytoplankton blooms. Aquatic Microbial Ecology 27:57-102

Urban-Rich J, McCarty JT, Shailer M (2004) Effects of food concentration and diet on chromophoric dissolved organic matter accumulation and fluorescent composition during grazing experiments with the copepod *Calanus finmarchicus*. ICES Journal of Marine Science 61:542-551

van de Poll WH, Kulk G, Timmermans KR, Brussaard CPD, van der Woerd HJ, Kehoe MJ, Mojica KDA, Visser RJW, Rozeman PD, Buma AGJ (2013) Phytoplankton chlorophyll *a* biomass, composition, and productivity along a temperature and stratification gradient in the northeast Atlantic Ocean. Biogeosciences 10:4227-4240

Weitz JS, Wilhelm SW (2012) Ocean viruses and their effects on microbial communities and biogeochemical cycles. F1000 Biology Reports 4: 17

Wilhelm SW, Suttle CA (1999) Viruses and nutrient cycles in the sea - Viruses play critical roles in the structure and function of aquatic food webs. Bioscience 49:781-788

Winget DM, Williamson KE, Helton RR, Wommack KE (2005) Tangential flow diafiltration: and improved technique for estimation of virioplankton production. Aquatic Microbial Ecology 41:221-232

Worden AZ, Nolan JK, Palenik B (2004) Assessing the dynamics and ecology of marine picophytoplankton: The importance of the eukaryotic component. Limnology and Oceanography 49:168-179

Chapter 8

General Discussion

Over the last few decades, mathematical models have played an essential role in elucidating and evaluating the consequences of increasing concentrations of atmospheric CO_2 on global climate (Meehl et al. 2007, Gruber and Doney 2009). Due to this success, models are increasingly used for making quantitative predictions with direct consequences for climate policy. Modeling the effect of global climate change on marine biogeochemistry and ecology is demanding due to the complexity of interactions among biological, physical, and chemical variables. Additionally, marine biogeochemical/ecological modeling is currently restricted by the scarcity of data required to formulate and parameterize key processes and/or to evaluate the model predictions (Gruber and Doney 2009).

Biogeochemical and ecological processes in the surface ocean are ultimately regulated by the rate at which carbon is fixed photosynthetically into organic matter by phytoplankton, which is distributed heterogeneously in the ocean by variations in the availability of light and nutrients. Vertical stratification of the water column suppresses turbulence and reduces mixing depth, affecting the availability of light and nutrients to phytoplankton in the surface water (Mahadevan et al. 2012). Ocean-climate models agree that warming of the surface oceans will strengthen surface stratification and decrease winter mixing, leading to an earlier onset and increasing the duration of seasonal stratification (Sarmiento 2004, Saenko et al. 2011, Collins et al. 2013). These changes will eventually impact the growth, spatial distribution and species composition of phytoplankton communities (Follows and Dutkiewicz 2001, Jöhnk et al. 2008, Dutkiewicz et al. 2013). The incorporation of the vertical turbulence structure of the water column, with parameters such as Brunt-Väisälä frequency (N^2) and mixing depth, is likely to improve existing models by refining differentiation between different phytoplankton functional types (Chapter 3; Huisman et al. 2004, Jäger et al. 2008, Ryabov et al. 2010). The combination of pigment analysis (HPLC-Chemtax) and flow cytometry permits phytoplankton community structure to be examined from both size and taxonomic perspectives (Chapter 3; Veldhuis and Kraay 2004, Suzuki et al. 2005, Cassar et al. 2015). However, it is recommended here to further complement this by size-fractionated HPLC analysis in order to better discriminate affects on size class distribution within specific taxonomic groups (Chapter 3). Moreover, models focusing exclusively on bottom-up (i.e. resource availability) control may fail to capture a substantial proportion of the variability in the structure and distribution of phytoplankton communities (Chapter 3). This is due to the considerable top-down (i.e., grazing and viral lysis) control of phytoplankton communities, which

can also be distributed heterogeneously across ocean basins and may be regulated by processes related to the vertical stratification of the water column (Chapter 4; Behrenfeld and Boss 2014).

Biogeochemical and ecological models have traditionally credited grazers as the main loss factor for net primary production in the euphotic zone (i.e. sunlit surface layers), with a small fraction lost to sinking (Gruber and Doney 2009, Ducklow et al. 2010). However, studies indicated that viruses can be a significant factor regulating primary production (Suttle et al. 1990) and phytoplankton bloom dynamics (Castberg et al. 2001, Brussaard et al. 2005, Ruardij et al. 2005, Baudoux et al. 2006). To my knowledge, Chapter 4 represents the largest data set of viral lysis rates of different marine phytoplankton groups and in addition provides simultaneous measurements of microzooplankton grazing. The data reveal that for all phytoplankton groups, (determined by flow cytometry) the losses from viral lysis rival microzooplankton grazing (Chapter 4; Baudoux et al. 2006, Tsai et al. 2012). Moreover, rates of viral-induced mortality can vary significantly over latitudinal scales and across different phytoplankton groups (Chapter 4). In the oligotrophic Northeast Atlantic Ocean, viral lysis was found to be the dominate loss factor for phytoplankton during summer, while microzooplankton grazing dominated at higher latitudes (Chapter 4). The switch in mortality type was related to water column stability through the vertical mixing coefficient (K_T). However, it most likely represents an interplay between physical and biological processes that in turn regulate the formation of transparent exopolymer particles (TEP) and subsequently led to the (temporarily) inactivation of viral infectivity at higher latitudes (Chapters 2 and 4).

Bacterial turnover of dissolved organic matter (DOM) and the associated remineralization of nutrients close the major biogeochemical cycles of these elements in the ocean (Falkowski et al. 2008). The DOM-bacteria pathway of the microbial loop represents a major mechanism by which primary production is respired to CO_2 (Kirchman et al. 2013). Availability of dissolved organic carbon (DOC) is thought to be the primary factor regulating the abundance and activity of heterotrophic prokaryotes in much of the world's oceans (Carlson and Ducklow 1996, Church et al. 2000). However, in oligotrophic regions of the North Atlantic, inorganic nutrient limitation of heterotrophic prokaryotic populations may also be a significant factor regulating bacterial production (Chapter 6; Cotner et al. 1997, Rivkin and Anderson 1997, Mills et al. 2008). Due to the reliance of viruses on their hosts to provide the energy required for replication, inorganic nutrient limitation

may then also effect viral infection dynamics. Viral lysis was shown to be the dominate mortality factor for prokaryotes in the Northeast Atlantic during summer stratification (Chapter 6), wherein lytic infection was the favored life strategy in the surface mixed layer (ML). Data show that lytic viral production rates in the ML were tied to inorganic nutrients most likely through nutrient limited host physiology. In contrast, inducible prophages were detected within the deep chlorophyll maximum (DCM) layer of every oligotrophic station. Lysogeny is thought to represent a survival strategy to persevere conditions of low host productivity and abundance (Williamson et al. 2002, Weinbauer et al. 2003, Payet and Suttle 2013). However, no direct correlation was found between lysogeny, inorganic nutrient concentrations, and heterotrophic prokaryotic production or abundance (Chapter 6). It could be that the host groups (species) that underwent induction of prophage are not dominant, which would obscure the correlations made to total heterotrophic abundance and production such as those presented here. Quantitative analysis of the heterotrophic prokaryotic community composition may shed more light on alterations occurring during viral infections and may also clarify members involved in prophage induction. The induction of prophages within the DCM was negatively correlated to chlorophyll *a*. Pico-sized *Prochlorococcus* spp. were dominant in the DCM (93%), with abundances decreasing with latitude (Mojica et al. 2015). These autotrophic prokaryotic counterparts could have effectively competed with heterotrophic prokaryotes and pushed nutrient limitation to a point at which lytic viral production could no longer be effectively sustained and consequently triggered a switch to lysogenic infection. This hypothesis is supported by evidence that inorganic nutrients may at times be an important factor modulating lysogeny in natural heterotrophic populations (Williamson et al. 2002, Motegi and Nagata 2007). Overall, these results support prokaryotic host physiology and growth as important factors regulating virus abundance in aquatic environments (Chapters 2 and 6; Proctor et al. 1993, Moebus 1996, Middelboe 2000).

The incorporation of virus-induced morality rates of the different microbial populations at rates which rival or exceed those of zooplankton grazing has important implications for biogeochemical and ecological models (Chapter 7). First, the flux of photosynthetically fixed carbon (PFC) through the viral shunt is much higher (up to 80%) than previously thought (up to 26%) for steady state ecosystems such as those found under oligotrophic conditions (Chapter 7; Wilhelm and Suttle 1999). Consequently, less PFC is available to be transferred to higher trophic levels via the classical grazer food chain, decreasing the overall efficiency

and carrying capacity of the ecosystem (Fuhrman 1999, Wilhelm and Suttle 1999). Secondly, the different sources of dissolved and particulate dead matter, whether through passive diffusion across phytoplankton cell membranes, actively excreted, released from sloppy feeding, diffused from fecal pellets or released from viral lysis, vary in their chemical composition and bioavailability (Middelboe and Jorgensen 2006, Kirchman et al. 2013, Lønborg et al. 2013). The dominance of viral lysis as a loss factor for both autotrophic and heterotrophic prokaryotic production in the oligotrophic region suggests that bacterial C-demand is not restricted to excretion and DOC released from grazing activity. Furthermore, recent evidence has demonstrated that bacteria within subtrophic regions posses a diverse array of enzymatic weaponry to hydrolyze high molecular weight organic substrates (Arnosti et al. 2011). Together these results may explain consistent reports of net heterotrophy (i.e., bacterial carbon demand exceed phytoplankton carbon fixation) in subtropical regions of the Northeast Atlantic Ocean (Agusti et al. 2001, Duarte et al. 2001, Serret et al. 2001, Gonzalez et al. 2002, Hoppe et al. 2002, Moran et al. 2004).

The data presented in this thesis indicate that climate change-induced alterations in the timing and strength of seasonal stratification will reinforce or shift the ecosystem towards a more viral-lysis dominated system. Increased carbon recycling at the expense of trophic transfer will have cascading effects on the overall structure and functioning of pelagic microbial food webs, reducing productivity and biological carbon export into the ocean's interior (Weinbauer et al. 2011). As the North Atlantic is one of the key areas of global carbon sequestration, such alterations could have global implications for the potential for the ocean to function as a long-term sink for anthropogenic carbon dioxide.

References

Agusti S, Duarte CM, Vaque D, Hein M, Gasol JM, Vidal M (2001) Food-web structure and elemental (C, N and P) fluxes in the eastern tropical North Atlantic. Deep-Sea Research, Part II 48:2295-2321

Arnosti C, Steen AD, Ziervogel K, Ghobrial S, Jeffrey WH (2011) Latitudinal gradients in degradation of marine dissolved organic carbon. PLOS One 6: e28900. doi: 10.1371/journal.pone.0028900

Baudoux AC, Noordeloos AAM, Veldhuis MJW, Brussaard CPD (2006) Virally induced mortality of *Phaeocystis globosa* during two spring blooms in temperate coastal waters. Aquatic Microbial Ecology 44:207-217

Behrenfeld MJ, Boss ES (2014) Resurrecting the ecological underpinnings of ocean plankton blooms. Annual Review of Marine Science 6:167-194

Brussaard CPD, Kuipers B, Veldhuis MJW (2005) A mesocosm study of *Phaeocystis globosa* population dynamics. I. Regulatory role of viruses in bloom control. Harmful Algae 4:859-874

Carlson CA, Ducklow HW (1996) Growth of bacterioplankton and consumption of dissolved organic carbon in the Sargasso Sea. Aquatic Microbial Ecology 10:69-85

Cassar N, Wright SW, Thomson PG, Trull TW, Westwood Kj, de Salas M, Davidson A, Pearce I, Davies DM, Matear RJ (2015) The relation of mixed-layer net community production to phytoplankton community composition in the Southern Ocean. Global Biogeochemical Cycles 29:446-462

Castberg T, Larsen A, Sandaa RA, Brussaard CPD, Egge JK, Heldal M, Thyrhaug R, van Hannen EJ, Bratbak G (2001) Microbial population dynamics and diversity during a bloom of the marine coccolithophorid *Emiliania huxleyi* (Haptophyta). Marine Ecology Progress Series 221:39-46

Church MJ, Hutchins DA, Ducklow HW (2000) Limitation of bacterial growth by dissolved organic matter and iron in the Southern Ocean. Applied and Environmental Microbiology 66:455-466

Collins M, Knutti R, Arblaster J, Dufresne J-L, Fichefet T, Friedlingstein P, Gao X, Gutowski WJ, Johns T, Krinner G, Shongwe M, Tebaldi C, Weaver AJ, Wehner M (2013) Long-term climate change: projections, commitments and irreversibility. In: Stocker TF, Qin D, Plattner G-K, Tignor M, Allen SK, Boschung J, Nauels A, Xia Y, Bex V, Midgley PM (eds) Climate Change 2013: The Physical Science Basis Contribution of Working Group I to the Fifth Assessment Report of the Intergovernmenal Panel on Climate Change. Cambridge University Press, Cambridge, United Kingdom and New York, NY, USA

Cotner JB, Ammerman JW, Peele ER, Bentzen E (1997) Phosphorus-limited bacterioplankton growth in the Sargasso Sea. Aquatic Microbial Ecology 13:141-149

Duarte MC, Agusti S, Aristegui J, Gonzalez N, Anadon R (2001) Evidence for a heterotrophic subtropical northeast Atlantic. Limnology and Oceanography 46:425-428

Ducklow HW, Moran XAG, Murray AE (2010) Bacteria in the greenhouse: marine microbes and climate change. In: Mitchell R, Gu J (eds) Environmental Microbiology. Wiley-Blackwell, New York

Dutkiewicz S, Scott JR, Follows MJ (2013) Winners and losers: ecological and biogeochemical changes in a warming ocean. Global Biogeochemical Cycles 27:463-477

Falkowski PG, Fenchel T, Delong EF (2008) The microbial engines that drive Earth's biogeochemical cycles. Science 320:1034-1039

Follows MJ, Dutkiewicz SW (2001) Meteorological modulation of the North Atlantic spring bloom. Deep-Sea Research, Part II 49:321-344

Fuhrman JA (1999) Marine viruses and their biogeochemical and ecological effects. Nature 399:541-548

Gonzalez N, Anadon R, Maranon E (2002) Large-scale variability of planktonic net community metabolism in the Atlantic Ocean: importance of temporal changes in oligotrophic subtropical waters. Marine Ecology Progress Series 233:21-30

Gruber N, Doney S (2009) Ocean biogeochemistry and ecology, modeling of. In: Steele JH, Turekian KK, Thorpe SA (eds) Encyclopedia of Ocean Sciences. Academic Press, Oxford

Hoppe HG, Gocke K, Koppe R, Begler C (2002) Bacterial growth and primary production along a north-south transect of the Atlantic Ocean. Nature 416:168-171

Huisman J, Sharples J, Stroom JM, Visser PM, Kardinaal WEA, Verspagen JMH, Sommeijer B (2004) Changes in turbulent mixing shift competition for light between phytoplankton species. Ecology 85:2960-2970

Jäger CG, Diehl S, Schmidt GM (2008) Influence of water-column depth and mixing on phytoplankton biomass, community composition, and nutrients. Limnology and Oceanography 53:2361-2373

Jöhnk KD, Huisman J, Sharples J, Sommeijer B, Visser PM, Stroom JM (2008) Summer heatwaves promote blooms of harmful cyanobacteria. Global Change Biology 14:495-512

Kirchman DL, Lancelot C, Fasham M, Legendre L, Radach G, Scott M (2013) Dissolved organic matter in biogeochemical models of the ocean. In: Evans GT, Fasham MJR (eds) Towards a Model of Ocean Biogeochemical Processes. Springer, Berlin Heidelberg

Lønborg C, Middelboe M, Brussaard CPD (2013) Viral lysis of *Micromonas pusilla*: impacts on dissolved organic matter production and composition. Biogeochemistry 116:231-240

Mahadevan A, D 'Asaro E, Lee C, Perry MJ (2012) Eddy-driven stratification initiates North Atlantic spring phytoplankton blooms. Science 337:54-58

Meehl GA, Stocker TF, Collins WD, Friedlingstein P, Gaye AT, Gregory JM, Kitoh A, Knutti R, Murphy JM, Noda A, Raper SCB, Watterson IG, Weaver AJ, Zhao Z-C (2007) Global climate projections. In: Solomon S, Qin D, Manning M, Chen Z, Marquis M, Averyt KB, Tignor M, Miller HL (eds) Climate Change 2007: The Physical Science Basis Contribution of Working Group I to the Fourth Assessment Report of the Intergovernmental Panel on Climate Change. Cambridge University Press, Cambridge, United Kingdom and New York, NY, USA

Middelboe M (2000) Bacterial growth rate and marine virus-host dynamics. Microbial Ecology 40:114-124

Middelboe M, Jørgensen NOG (2006) Viral lysis of bacteria: an important source of dissolved amino acids and cell wall compounds. Journal of the Marine Biological Association of the United Kingdom 86:605-612

Mills MM, Moore CM, Langlois R, Milne A, Achterberg E, Nachtigall K, Lochte K, Geider RJ, La Roche J (2008) Nitrogen and phosphorus co-limitation of bacterial productivity and growth in the oligotrophic subtropical North Atlantic. Limnology and Oceanography 53:824-834

Moebus K (1996) Marine bacteriophage reproduction under nutrient-limited growth of host bacteria. I. Investigations with six phage-host systems. Marine Ecology Progress Series 144:1-12

Mojica KDA, van de Poll WH, Kehoe M, Huisman J, Timmermans KR, Buma AGJ, van der Woerd HJ, Hahn-Woernle L, Dijkstra HA, Brussaard CPD (2015b). Phytoplankton community structure in relation to vertical stratification along a north-south gradient in the Northeast Atlantic Ocean. Limnology and Oceanography (*in press*). doi: 10.1002/lno.10113

Moran XAG, Fernandez E, Perez V (2004) Size-fractionated primary production, bacterial production and net community production in subtropical and tropical domains of the oligotrophic NE Atlantic in autumn. Marine Ecology Progress Series 274:17-29

Motegi C, Nagata T (2007) Enhancement of viral production by addition of nitrogen or nitrogen plus carbon in subtropical surface waters of the South Pacific. Aquatic Microbial Ecology 48:27-34

Payet JP, Suttle CA (2013) To kill or not to kill: the balance between lytic and lysogenic viral infection is driven by trophic status. Limnology and Oceanography 58:465-474

Proctor LM, Okubo A, Fuhrman JA (1993) Calibrating estimates of phage-induced mortality in marine bacteria: ultrastructural studies of marine bacteriophage development from one-step growth experiments. Microbial Ecology 25:161-182

Rivkin RB, Anderson MR (1997) Inorganic nutrient limitation of oceanic bacterioplankton. Limnology and Oceanography 42:730-740

Ruardij P, Veldhuis MJW, Brussaard CPD (2005) Modeling the bloom dynamics of the polymorphic phytoplankter *Phaeocystis globosa*: impact of grazers and viruses. Harmful Algae 4:941-963

Ryabov AB, Rudolf L, Blasius B (2010) Vertical distribution and composition of phytoplankton under the influence of an upper mixed layer. Journal of Theoretical Biology 263:120-133

Saenko OA, Yang XY, England MH, Lee WG (2011) Subduction and transport in the Indian and Pacific Oceans in a 2 X CO_2 Climate. Journal of Climate 24:1821-1838

Sarmiento JL (2004) Response of ocean ecosystems to climate warming. Global Biogeochemical Cycles 18:GB3003. doi: 10.1029/2003GB002134

Serret P, Robinson C, Fernandez E, Teira E, Tilstone G (2001) Latitudinal variation of the balance between plankton photosynthesis and respiration in the eastern Atlantic Ocean. Limnology and Oceanography 46:1642-1652

Suttle CA, Chan AM, Cottrell MT (1990) Infection of phytoplankton by viruses and reduction of primary productivity. Nature 347:467-469

Suzuki K, Hinuma A, Saito H, Kiyosawa H, Liu HB, Saino T, Tsuda A (2005) Responses of phytoplankton and heterotrophic bacteria in the northwest subarctic Pacific to *in situ* iron fertilization as estimated by HPLC pigment analysis and flow cytometry. Progress in Oceanography 64:167-187

Tsai AY, Gong GC, Sanders RW, Chiang KP, Huang JK, Chan YF (2012) Viral lysis and nanoflagellate grazing as factors controlling diel variations of *Synechococcus* spp. summer abundance in coastal waters of Taiwan. Aquatic Microbial Ecology 66:159-167

Veldhuis MJW, Kraay GW (2004) Phytoplankton in the subtropical Atlantic Ocean: towards a better assessment of biomass and composition. Deep-Sea Research, Part I 51:507-530

Weinbauer MG, Brettar I, Hofle MG (2003) Lysogeny and virus-induced mortality of bacterioplankton in surface, deep, and anoxic marine waters. Limnology and Oceanography 48:1457-1465

Weinbauer MG, Chen F, Wilhelm SW (2011) Virus-mediated redistribution and partitioning of carbon in the global oceans. In: Jiao N, Azam F, Sanders S (eds) Microbial Carbon Pump In the Ocean. The American Association for the Advancement of Science, Washington DC

Wilhelm SW, Suttle CA (1999) Viruses and nutrient cycles in the sea - viruses play critical roles in the structure and function of aquatic food webs. Bioscience 49:781-788

Williamson SJ, Houchin LA, McDaniel L, Paul JH (2002) Seasonal variation in lysogeny as depicted by prophage induction in Tampa Bay, Florida. Applied and Environmental Microbiology 68:4307-4314

Summary

Marine microorganisms represent the largest reservoir of living organic carbon in the ocean and collectively manage the pools and fluxes of nutrients and energy. Climate-induced increases in sea surface temperature and associated modifications to vertical stratification are affecting the structure and production of autotrophic and heterotrophic microorganisms in ocean surface waters. However, little is known about how future alterations will affect the mortality of marine microbes. The various modes of mortality influence the cycling of biogeochemical elements very differently. This in turn affects the production to respiration ratio of the ocean and thus the efficiency with which photosynthetic organic carbon is transferred to higher trophic levels or exported to the deep ocean (via the biological pump). The Atlantic Ocean provides a meridional gradient in stratification, is essential to global circulation and acts as a major sink for anthropogenic carbon dioxide. The Northeast Atlantic thus provides an ideal model system for the current study which aims to investigate the influence that vertical stratification has on the source of mortality (i.e., viral lysis versus grazing).

After a general introduction, this thesis begins by providing a comprehensive overview of what is currently known about how environmental factors in the marine environment affect virus-host interactions. Abiotic and biotic variables can influence the infectivity and survival of marine viruses, and regulate the physiology, production and distribution of the host. Ultimately, these aspects govern the efficiency with which viruses can replicate and thus propagate through the marine environment (Chapter 2). The review illustrates that at this moment in time, our ability to identify general ecologically functional patterns important in governing virus dynamics over broad oceanic scales is restricted by the availability of information regarding both the effect of individual environmental factors and by the scarcity of reported rates.

In order to better understand the importance of vertical mixing and physicochemical features in structuring phytoplankton (unicellular algae) host populations, a high-resolution mesoscale description of the phytoplankton community along a meridional gradient in the Northeast Atlantic Ocean was conducted during the spring and summer (Chapter 3). Vertical stratification was identified as a key factor governing the distribution and separation of different phytoplankton taxa and size classes, indicating that incorporation of vertical turbulence structure of the water column will improve biogeochemical and ecological modeling studies. The data support predictions that climate-change induced increases in ocean surface temperature and expansion of oligotrophic (nutrient-limited) areas will

increase the contribution of pico-sized (< 2 μm) eukaryotic phytoplankton (while decreasing the abundance of cryptophytes and diatoms), and expand the geographic range of *Prochlorococcus* spp. northward (leading to alterations in phylogeography within unicellular cyanobacterial populations). This will likely result in large-scale biogeographical changes in virus distributions, including an expansion of the V3 viruses associated with picocyanobacterial hosts (Chapter 4).

More importantly, simultaneous measurements of viral lysis and microzooplankton grazing rates conducted along the latitudinal transect during summer (Chapter 4) show that (i) viral lysis was responsible for half of the total mortality occurring in all phytoplankton groups, (ii) average virus-mediated lysis rates were higher for eukaryotic phytoplankton than for the prokaryotic cyanobacteria *Prochlorococcus* spp. and *Synechococcus* spp., (iii) overall the total phytoplankton mortality rate (viral lysis plus microzooplankton grazing) was comparable to phytoplankton gross growth rate, signifying high turnover rates of marine phytoplankton populations, and finally (iv) viral lysis rates were reduced in the north (> 58°N), resulting in grazing-dominated phytoplankton mortality.

A method optimization for the enumeration of samples with low viral abundance (pH modification of the TE-buffer used for the dilutions) substantially improved total virus counts in North Atlantic samples compared to those obtained using the standard method (Chapter 5). This method was applied to enumerate field samples which utilized a virus reduction approach to investigate the viral life strategy and magnitude of infection in heterotrophic prokaryotic populations (Chapter 6). Compared to grazing, viruses were the dominant mortality factor regulating prokaryotic losses in the surface waters of the Northeast Atlantic Ocean during summer. Lytic infection (virus replication and host lysis proceeds immediately after infection) was the favored life strategy in the surface mixed layer, while lysogeny (virus incorporated into host genome where it remains until triggered into lytic cycle upon stimulation by an environmental factor) was only relevant within the deep chlorophyll maximum layer of oligotrophic southern stations. The data revealed a close to steady state situation and rapid turnover in the south and net heterotrophic production in the north, suggesting that alterations in stratification will also affect heterotrophic prokaryote production.

Implementing measured production and loss rates of autotrophic (Chapter 4) and heterotrophic (Chapter 6) organisms into a steady state carbon-flux model demonstrates that 80% of the photosynthetically fixed carbon flowed through the viral shunt in the oligotrophic south, which is more than 2-fold higher than the

northern region. These results illustrate that viruses play a more prominent role in stratified (steady state) marine ecosystems than thought previously.

Overall, this thesis reveals that viral lysis is an important factor regulating the biomass and productivity of marine microbial populations during summer stratification in the Northeast Atlantic Ocean. Moreover, the data support the hypothesis laid out in this thesis that alterations in microbial communities due to global warming-induced changes in vertical stratification will affect mortality processes and the distribution of predators (e.g. mortality agents). The partitioning of photosynthetic carbon through the separate mortality pathways has important implications for ecosystem functioning as each pathway affects the structure and activity of the pelagic food web in different ways. Grazing transfers biomass to higher trophic levels, thus increases the overall efficiency and carrying capacity of the ecosystem. On the other hand, viral activity stimulates recycling via heterotrophic prokaryotes by shunting biomass to the dissolved organic matter pool, and therefore enhances the availability of inorganic nutrients in the oligotrophic surface waters of the ocean. In conclusion, the data presented in this thesis indicate that climate change-induced alterations in the timing and strength of seasonal stratification at the higher latitudes will shift the ecosystem towards a more viral-lysis dominated system. A more prominent future role of viral lysis in the northern region of the North Atlantic Ocean would thus markedly reduce biological carbon export into the ocean's interior in one of the key areas of global carbon sequestration, reducing the potential for the ocean to serve as a long-term sink for anthropogenic carbon dioxide.

Samenvatting

Mariene micro-organismen vertegenwoordigen het grootste reservoir van organische koolstof in de oceaan en hebben een sturende rol in de kringloop van nutriënten en de stromingen van materie en energie. Klimaatverandering leidt tot opwarming van de bovenste waterlagen (oppervlaktewateren) in zeeën en oceanen, waarbij de resulterende veranderingen in verticale gelaagdheid (stratificatie) van de bovenste waterlaag de structuur en productie van auto- en heterotrofe micro-organismen beïnvloeden. Er is nog maar weinig bekend over de wijze waarop deze toekomstige veranderingen de sterfte (mortaliteit) van mariene micro-organismen beïnvloeden. De verschillende modi van sterfte werken anders door op de cycli van biochemische elementen. Dit heeft weer gevolgen voor de verhouding tussen de productie en respiratie van de oceaan en daarmee dus de efficiëntie waarmee fotosynthetisch vastgelegd organisch koolstof naar hogere trofische niveaus (plek in de voedselketen), of naar de diepzee wordt getransporteerd. De Atlantische Oceaan heeft een noord-zuid gradiënt in stratificatie, is essentieel voor de wereldwijde oceaan circulatie en dient als voornaamste afvoer voor antropogeen koolstofdioxide. Het noordoostelijk deel van de Atlantische Oceaan vormt daarom een ideaal modelsysteem voor de huidige studie, die als doel heeft om de invloed van verticale stratificatie op de sterfte (virale lysis of begrazing) en de onderlinge verhouding van de verschillende wijzen van mortaliteit te onderzoeken.

Het onderzoek in dit proefschrift begint met een uitgebreid overzicht van de huidige kennis van omgevingsfactoren die virus-gastheer interacties in het mariene milieu beïnvloeden. Abiotische en biotische variabelen kunnen invloed uitoefenen op en overleving van mariene virussen en kunnen de fysiologie, productie en de (geografische) verspreiding van de gastheer reguleren. Uiteindelijk reguleren deze aspecten het succes waarmee virussen zich repliceren en verspreiden in het mariene milieu (Hoofdstuk 2). Het review artikel maakt duidelijk dat op dit moment ons vermogen om algemene ecologisch functionele patronen te herkennen die belangrijk zijn in het aansturen van de virus populatiedynamiek op oceanische schaal, wordt belet door de schaarste aan informatie betreffende de individuele omgevingsfactoren en de intensiteit van hun effect.

Om beter te begrijpen wat het belang is van verticale menging en de fysisch-chemische eigenschappen van het zeewater op het structureren van eencellige algen (fytoplankton) gastheerpopulaties, werd over een noord-zuid transect en met hoge resolutie de fytoplanktongemeenschap in de Noordoost Atlantische Oceaan tijdens de lente en zomer in kaart gebracht (Hoofdstuk 3). Verticale stratificatie werd geïdentificeerd als een belangrijke factor die de vertikale en geografische

verspreidingvan verschillende fytoplankton taxa en grootteklassen bepaalt, wat aangeeft dat toevoeging van de verticale turbulentiestructuur van de waterkolom de biochemische en ecologische modelstudies zal verbeteren. De data ondersteunen de voorspellingen dat (1) klimaatverandering-gerelateerde toename in temperatuur en de uitbreiding van oligotrofe (nutrient-gelimiteerde) gebieden in de oceaan de bijdrage van eukaryote picofytoplankton (<2 μm diameter) vergroot, terwijl het aantal cryptofyten en diatomeeën afneemt; en (2) dat het verspreidingsgebied van *Prochlorococcus* spp. noordelijk uitbreid (wat leidt tot veranderingen in de geografische verspreiding van de verschillende populaties van deze eencellige cyanobacteriën). Dit zal waarschijnlijk resulteren in biogeografische veranderingen in virusverspreiding op grote schaal, inclusief een expansie van de V3-virussen die geassocieerd zijn met eencellige cyanobacterie gastheren (Hoofdstuk 4).

Belangrijker nog, simultane metingen van sterftesnelheden door virale lysis en microzoöplankton begrazing, uitgevoerd langs een noord-zuid transect gedurende de zomer (Hoofdstuk 4), laten zien dat (i) virale lysis verantwoordelijk was voor de helft van de mortaliteit in alle fytoplankton groepen, (ii) de gemiddelde sterftesnelheid door virale lysis hoger was voor eukaryote fytoplankton dan voor de prokaryote cyanobacteriën *Prochlorococcus* spp. en *Synechococcus* spp., (iii) omzettingssnelheden van fytoplankton populaties hoog zijn aangezien algeheel de totale sterftesnelheid voor fytoplankton (virale lysis plus begrazing) vergelijkbaar was met de bruto groeisnelheid, en tot slot (iv) de afgenomen virale lysis snelheden in het noorden (58°N) resulteerden in begrazing-gedomineerde algensterfte. Deze resultaten impliceren dat door het opwarmen van de oceaan het ecosysteem op hogere breedtegraden kan verschuiven naar een systeem waarin virale lysis domineert.

Door een methode te optimaliseren voor monsters met kleine concentraties virussen (bijstellen van de pH van de TE-buffer in de verdunningen) verbeterde het aantal getelde virussen in monsters in de Noord-Atlantische Oceaan aanzienlijk in vergelijking met de standaard methode (Hoofdstuk 5). Deze methode was ontwikkeld om virale lysis van de heterotrofe prokaryoten beter te kunnen bestuderen (Hoofdstuk 6). In vergelijking met begrazing was virale lysis de overwegende sterftefactor voor heterotrofe prokaryoten in de oppervlaktewateren van de Noordoost Atlantische Oceaan gedurende de zomer. Lytische infectie (virus vermenigvuldiging en lysis gastheer vindt plaats direct na infectie) was de preferente levensstrategie in de gemixte oppervlakte laag, terwijl lysogenische infectie (uitgestelde lysis door inbouw in gastheer genoom) alleen relevant was in

het chlorofyl-maximum (diepere laag in zuidelijke oligotrofe stations). De data laten een noord-zuid gradiënt zien met een nagenoeg stabiel evenwicht (steady state) met hoge omzetting in het zuiden en netto heterotrofe productie in het noorden. Dit impliceert dat veranderingen in stratificatie dus ook effect zullen hebben op de heterotrofe prokaryote productie.

Het implementeren van de gemeten productie- en verliessnelheden van autotrofe (Hoofdstuk 4) en heterotrofe (Hoofdstuk 5) organismen in een steady-state koolstofmodel laat zien dat in het oligotrofe zuiden 80% van de door fotosynthese vastgelegde koolstof via de virale route ('viral shunt') stroomt, wat meer dan twee keer zoveel is dan in de noordelijke regio. Deze resultaten tonen aan dat virussen een prominentere rol spelen in gestratificeerde (steady-state) mariene ecosystemen dan eerder gedacht.

Algeheel laat dit proefschrift zien dat sterfte door virale lysis een belangrijke factor is in het reguleren van biomassa en productiviteit van mariene microbiële populaties gedurende stratificatie in de zomer in de Noordoost Atlantische Oceaan. Bovendien ondersteunen de data de hypothese die was uiteengezet in dit proefschrift, namelijk dat aanpassingen in microbiële gemeenschappen door veranderingen in verticale stratificatie ten gevolge van wereldwijde opwarming effect hebben op de sterfteprocessen en verspreiding van virussen en predatoren. De verdeling van de vastgelegde koolstof via de verschillende routes van sterfte heeft belangrijke implicaties voor het functioneren van het ecosysteem, omdat elke route de structuur en activiteit van het pelagisch voedselweb op verschillende wijze beïnvloedt. Begrazing transporteert biomassa naar hogere trofische niveauswaarbij als zodanig de algehele efficiëntie en draagkracht van het ecosysteem wordt verhoogd. Anderzijds stimuleert virale activiteit recycling door biomassa naar het reservoir van opgelost organisch koolstof te transporteren alwaar omzetting hiervan door heterotrofe prokaryoten de beschikbaarheid van anorganische nutriënten in oligotrofe oppervlaktewateren van de oceaan vergroot. Ter afsluiting, de data in dit proefschrift tonen aan dat deviaties in de timing en de sterkte van seizoensstratificatie door klimaatverandering het ecosysteem op hogere breedtegraden zal verschuiven naar een systeem waarin lysis door virussen de dominante verliesfactor is. Een toekomstig prominentere rol van sterfte door virale lysis in de noordelijke regio van de Noord Atlantische Oceaan zou dus de export van biologisch koolstof naar de diepzee aanzienlijk verminderen en daarbij zal ook het potentieel van dit belangrijke gebied voor koolstofopslag als langdurige put voor antropogeen koolstofdioxide afnemen.

Acknowledgements

The path that has led me here has been a long and arduous one, filled with many trials and tribulations. However, I am exceedingly grateful and truly blessed that I have never walked the road alone.

To my brother, Michael Mojica, it is your dreams that have brought me to this path and this thesis is for the both of us. Thank you for being the light in the darkness. For sharing your dreams, aspirations, and love for science and nature with me. Thank you for never judging me when I was lost and never giving up on me as I tried to find my way. You are and will always be my biggest inspiration. I love you with all my heart, I am so lucky to have you as my big brother.

To my parents, Kurt and Janey Dustin, for without them I would not exist and with them all this has been possible. Thank you for believing in me when there was no reason to, for opening your door and your hearts and giving me all the opportunities that life can bring. I can never express my eternal gratitude and love I have for you both. You are truly the best thing that has ever happened to me.

I would like to express my sincere gratitude to my advisor Prof. dr. Corina Brussaard. Thank you very much for granting me this PhD position, but more importantly for your continued support as a supervisor and as a friend. As a supervisor, I am grateful for your patience, encouragement and immense knowledge which you have given me over the years. Your desire to understand the reasons "for why I am the way I am", was refreshing and I am thankful for the mutual understanding and friendship which has only grown from that moment.

I would also like to thank the entire STRATIPHYT team: Klaas Timmermans, Henk Dijkstra, Anita Buma, Hans van der Woerd, Willem van de Poll, Elena Jurado, Lisa Hahn-Woernle, Michael Keohe and Corina Brussaard. With special thanks to Jef Huisman, for his advice regarding statistical analysis and financial support through the OPTIMUM project. And I would like to thank all my students who helped with experiments in the lab and during the cruises, with special thanks to Tea de Vries.

I have received advice and support from many people at the NIOZ over the years for which I am grateful. Special thanks to the technical staff of the BIO department: Anna Noordeloos, Harry Witte, Kirsten Kooijman-Scholten, Robin van de Ven, Richard Doggen, Swier Oosterhuis, Santiago Gonzalez, Govert van Noort, Jan

Hegeman and Judith Bleijswijk. And special thanks to the shipboard crew and captains of the R/V Pelagia: Klaas Kikkert, John Ellen, Corky Burkhard, Pieter Kuijt, Freddy Hiemstra and Sjaak Maas.

And finally, to those who have kept me sane!

First and foremost, thanks to all my besties around the world (in order of the years), Danielle (Bazemore) Alley, Nicole (Becker) Rakes, Adrienne Neale and Anouk Goedknegt. I love you ladies so much! Thank you for always being there no matter how close or how far. I look forward to sharing many more years and even more bottles of wine with you in the future.

Douwe Maat – thanks for all your support whether it be an understanding shoulder, one to lean on, a hand to lend or a brain to bounce ideas off. All the friends I have made on Texel – there are far too many to list! But particular thanks to my first friend Jolanda Evers! You are a beautiful and unique lady and I am so glad that we got to know one another. I love you lady and look forward to many years of knowing you in the future. Dorien Verheyen – thanks for being you and letting me be me. Here is to dancing and singing in the streets. Love you girl! And to the boys: Andreas Wasser, Dennis Mosk and Freek van den Heuvel thank you for being there for me and watching out for me throughout the years. You guys were like my Texel brothers from another mother. And to Nate Prado - Thanks for being my best friend and my biggest cheerleader, no matter how near or how far life takes us.

The JugBros for keeping music in my ears throughout all these years and for just being a great group of guys.

The football crew! I can't tell you how immensely grateful I was for all the games in the park. Thanks for putting up with my enthusiasm and giving me an outlet for all that steam.

Like I said when I began, I am truly blessed by the people in my life, I am so lucky to have so many wonderful people around me.

Thank you. Bedankt. And of course Big Hugs!! ☺